Exploring diversity in iron resistance to obtain yeasts of biotechnological interest

Tesi Doctoral

Raquel Sorribes Dauden

Octubre 2023

Directors:

Dra. Mª Teresa Martínez Pastor i Dr. Sergi Puig Todolí

Departament de Bioquímica i Biologia Molecular

Programa de doctorat en Biomedicina i Biotecnologia

Departament de Bioquímica i Biologia Molecular

iata
Instituto de Agroquímica y Tecnología de Alimentos

VNIVERSITAT DE VALÈNCIA

CSIC
Consejo Superior de Investigaciones Científicas

Els directors de tesi:

MARÍA TERESA MARTÍNEZ PASTOR, Doctora en Ciències Químiques i Professora Titular en el Departament de Bioquímica i Biologia Molecular de la Universitat de València;

SERGI PUIG TODOLÍ, Doctor en Ciències Químiques i Científic Titular de l'Institut d'Agroquímica i Tecnologia dels Aliments (IATA) del Consell Superior d'Investigacions Científiques (CSIC);

I la tutora acadèmica:

MARÍA TERESA DONATO MARTIN, Professora Contractada Doctora en el Departament de Bioquímica i Biologia Molecular de la Universitat de València

INFORMEN:

Que Raquel Sorribes Dauden, graduada en Bioquímica i Ciències Biomèdiques per la Universitat de València ha realizat sota la seua direcció el treball de Tesi Doctoral que porta per títol "Exploring diversity in iron resistance to obtain yeasts of biotechnological interest". Revisat el present treball, expressen la seua conformitat per a la presentació del mateix per considerar que reuneix els requisits necessaris per a ser sotmés a discussió davant el Tribunal corresponent, per a optar al títol de Doctora en Biomedicina i Biotecnologia per la Universitat de València.

En Burjassot, 25 d'octubre de 2023

Directora: Dra. Mª Teresa Martínez Pastor

MARIA TERESA| MARTINEZ| PASTOR

Firmado digitalmente por MARIA TERESA| MARTINEZ|PASTOR
Fecha: 2023.10.25 16:41:32 +02'00'

Director: Dr. Sergi Puig Todolí

Firmado por PUIG TODOLI SERGI - DNI ***0878** el día 26/10/2023 con un certificado emitido por AC Sector Público

Tutora: Mª Teresa Donato Martín

MARIA TERESA| DONATO| MARTIN

Firmado digitalmente por MARIA TERESA| DONATO|MARTIN
Fecha: 2023.10.26 14:40:24 +02'00'

Aquest treball s'ha dut a terme al Departament de Bioquímica i Biologia Molecular de la Universitat de València i al Departament de Biotecnologia d'Aliments del IATA (CSIC). He rebut un contracte predoctoral cofinançat per la Conselleria d'Educació, Investigació, Cultura i Esport de la Generalitat Valenciana i el Fons Social Europeu (ACIF/2018/077). A més, se'm va concedir finançament per a una estada breu en el grup "Functional Biology Lab" de la Universitat KU Leuven (Bèlgica, Europa) finançat per la Conselleria d'Educació, Investigació, Cultura i Esport de la Generalitat Valenciana i el Fons Social Europeu (BEFPI/2021/089). El "Ministerio de Ciencia e Innovación de España / Agencia Estatal de Investigación (MCIN/ AEI/10.13039/501100011033/)" junt amb el "Fondo Europeo de Desarrollo Regional (FEDER). Una manera de hacer Europa" va fer possible el desenvolupament d'aquesta tesi a través de la concessió dels projectes "BIO2017-87828-C2-1-P" i "PID2020-116940RB-I00".

A aquelles que pensen i fan la ciencia en comú.

Ningú inventa, construeix o programa en solitari, senzillament perquè la complexitat de la tasca és tal que resultaria impossible.

Margarita Padilla

AGRAÏMENTS

En primer lloc, m'agradaria agrair als meus directors de tesi, Maite i Sergi, per donar-me l'oportunitat de poder realitzar-la en el CuFe Lab. Sense dubte la seua direcció ha sigut clau per a empentar aquesta tesi cap al final, per a la meua formació científica i a escala personal. També voldria agrair a Peris la predisposició per a col·laborar i ensenyar-me, així com el suport constant al llarg d'aquesta etapa. D'altra banda, voldria agrair a altres IPs de la tercera planta: José Manuel, Amparo, Eladio, Andrew i Carmela que, d'alguna manera o altra heu tingut un paper en fer possible aquesta tesi.

A totes les que formeu o heu format part del CuFe Lab us done les gràcies per tot el suport, l'aprenentatge, la companyonia i els moments més disfrutons. Les persones que formen part d'un laboratori són el factor més determinant al llarg d'aquest camí i no hauria sigut igual sense les rialles i el bon rotllo a l'hora d'ajudar i donar suport. Anto, Lucía, Ana, i Pilar, incorporar-me al CuFe Lab va ser tot un gust amb vosaltres de companyes i us agraïsc moltíssim tot el que he aprés de i amb vosaltres, tant a escala personal com professional. També he d'agrair a les que heu vingut o tornat després de mi: Helen, Sara i Amparo; el vostre suport i comprensió al llarg d'aquest últim any ha sigut fonamental, així com la companyia i l'espai per a poder xerrar de tot i de res. Tania, en menys d'un mes seràs també doctora i tancaràs aquesta etapa per encetar-ne una de nova. Espere que després de tots aquests anys, haja valgut la pena i t'aporte coses bones. Elena, que després dels teus primers sis mesos només amb mi en el lab, continues escoltant les meues historietes i tonteries, agafant els tramvies amb mi i sent una excel·lent companya: no té preu. Espere que cap de les tres oblidem aquell dia extra a Cork, ni l'olor dels llençols, ni l'habitació de les maletes, ni la calor del *hostel*. D'altra banda, no m'oblide de totes aquelles que heu passat pel 302 com a alumnat col·laborador, TFGs, TFMs, pràctiques externes, etc. Us desitge bona sort en les noves etapes.

Però, les simbiosis en aquest llarg camí van més enllà de les companyes del 302 i sense adonar-te'n, el teu espai de treball acaba ocupant quasi tota la tercera planta. Les companyes i companys del 303, 307 i 309 sou una peça fonamental d'aquesta tesi, així com totes les converses dels esmorzars i dinars i les quedades fora de l'IATA que hem compartit. Als que ja fa un temps que us n'anàreu de l'IATA: Dolo, Sebas, Ying, Sara, Laura, María, Miguel i Javi; moltes gràcies pel vostre llegat i la passió per la ciència que heu transmés. A totes les persones que heu vingut a l'IATA per a estades i heu acabat sent persones molt importants per a nosaltres: David, Vasni, Dani, Sofi mucha suerte en vuestros caminos, deseo de corazón que alguna vez se crucen con el mio. A Judit, Antonio i Ana Cris, moltes gràcies per la vostra ajuda i calidesa, he aprés molt de vosaltres. Gràcies a Laura per totes les converses sobre les múltiples problemàtiques de l'stacker i de la vida, també per la iniciació al món de les fermentacions. María, Alba C., Alba G. i Regino... quin grupet!! Sempre disposades a passar-ho bé i gaudir de la vida. Sou molt bona gent, sempre em quedaré amb el vostre caliu i us desitge lo millor. Sonia i Ric: no em fareu mai del *team roco*, però sempre he agraït el vostre entusiasme amb la vida, la vostra bondat i, per descomptat, la vostra passió pel menjar. Lainy, sempre recordaré les converses sobre Jersey Shore i altres deliris televisius que tant ens han unit en els dinars. Romain: molta sort amb aquesta aventureta! No tinc molt clar si per a la pròxima etapa necessitaré el passaport, però ara sé que sempre podré preguntar-te a tu, Andrés i, fer tot *lo* contrari al que em respongues xD, trobaré a faltar les teues idees peculiars. No em puc oblidar d'una de les persones fonamentals de la tercera planta: Vicky. No hi ha ningú que haja passat per la tercera planta que no sàpiga de tu. T'interesses per tot el món i sempre estàs pendent de nosaltres. Aquesta etapa no seria res sense tu, moltes gràcies per fer tanta companyia. Per acabar amb la tercera planta de l'IATA, voldria desitjar molts ànims i sort a la nova fornada que està començant ara mateix: Lourdes, Juan Carlos, Irene, Ana, Paula, Flor i Sandra.

Aprofite també per a agrair a tot el personal de l'IATA més enllà del SBYBI: administració, direcció, personal de cafeteria, personal de la porteria, personal dels serveis generals, netejadores, l'equip d'informàtica, l'equip de divulgació,

persones que em somriuen pels corredors i altres que contribuïu tant a l'excel·lència d'aquest centre.

D'altra banda, aquesta tesi no hauria sigut possible sense les companyes i companys del departament de bioquímica que em van acollir amb els braços oberts en uns dels anys més complicats del segle XXI. Marina, Sara, Sheila, Paco, Marta, Lian i Sam. Us dec tant... Ha sigut un plaer tenir-vos al costat dins i fora del departament. Vau alleugerir aquell fatídic any i heu omplert el meu cor d'alegria en cada quedada des d'aquell moment. A més, heu fet posible seguir connectada amb el departament després de marxar i conéixer a altra gent meravellosa com Dani, Lluís i Gemma.

També voldria agrair a altres membres del departament de bioquímica amb qui he compartit els moments de docència. En especial, als tècnics de laboratori Juan Ramón Diosdado i Mª Ángeles Tornero, sense els quals, senzillament, no existiria el departament: no tindria cap sentit. Per deixar-me aprendre de la seua dedicació a la docència i la seua paciència en les pràctiques d'immuno i bioquímica, el meu agraïment profund a Lola Peñarrubia, Imma Quilis, Patricia Casinos i Maria Jesus García. Per a acabar amb el departament de bioquímica, agrair també a Ayelén, César, Marta i Pedro Carrasco per la companyia tot el període que vam compartir i per acollir-me als seus dinars i sopars de lab com una més.

I would also thank the members of the Joris Winderickx lab (Cathy, Joëlle, Els, Marie-Anne, Joke, Tien-Yang, Alejandro and Ludo) for welcoming me and helping me. Especially to Mara who, in spite of having just gone through a very hard time, did not hesitate to help me in any way she could. També a Marina que, em va mostrar tots els racons de Lovaina amb encant.

M'agradaria, també, agrair a Aleksandra Elbakian, la persona darrere de Scihub. Aleksandra va recollir el llegat de la lluita per l'accés en obert del coneixement científic dels anys 90 per crear aquest immens repositori, convertint-se en una de les principals responsables que no entenguem la ciència sense l'"Open Access".

I, finalment, agrair de tot cor a aquelles persones, amiguis i família, que em coneixen de lluny i que tant m'han sentit queixar-me i garolar de tot. Us estime!

ABSTRACT

Iron (Fe) is a transition metal that is essential for almost all forms of life because it is indispensable for many key biological processes, such as cellular respiration and biosynthesis of cellular components. However, in excess, Fe can also participate in Fenton reactions, which produce reactive oxygen species. Thus, organisms have developed sophisticated molecular mechanisms to keep Fe levels into a narrow range. In this work, we expand our knowledge on the diverse strategies that budding yeasts of the *Saccharomyces* genus have developed to adapt to high Fe conditions in order to obtain yeasts of biotechnological interest. Firstly, we analyzed the suitability of 3 different Fe salts to perform analyses of iron-resistance in yeast cells: $(NH_4)_2Fe(SO_4)_2$, $FeSO_4$ and $FeCl_3$, prepared with or without acid addition. Our results indicate that $(NH_4)_2Fe(SO_4)_2$ and $FeSO_4$ are adequate sources of Fe for yeast cells, but the use of acid is recommended in stocks to fully avoid the generation of precipitate. We also explored the evolutionary conservation of the Fe^{2+}/Mn^{2+} vacuolar importer Ccc1/VIT1, which is the main player in the response of *S. cerevisiae* to Fe overload. Interestingly, we found that members of the Ccc1/VIT1 family are present in fungi, plants, protists and prokaryotes. The key Ccc1/VIT1 residues involved in Fe transport are well conserved. However, considerable variations in the domain architecture occur in a species-specific manner, especially in the amino-terminal (Nt) domain and the metal-binding domain. On the other hand, we studied the potential of *CCC1* up-regulation as a biotechnological tool to obtain Fe-enriched yeasts. Our analysis showed that, although *CCC1* overexpression is toxic, it can be rescued by the deletion of Ccc1 Nt domain. Our results suggested that NtΔCcc1 protein has a partial loss-of-function, which is not related to protein stability but probably to the fine-tuning of its localization in the vacuolar membrane. The most interesting outcome is that *NtΔCCC1*-overexpressing cells accumulate higher amounts of Fe per volume of medium than wild-type cells, which could facilitate the development

of a potential tool to extract Fe from media. Lastly, we took advantage of the huge amount of available isolates and sequenced genomes from the *Saccharomyces* genus to explore the Fe resistance of strains representative of the main populations. We found that species evolutionarily closer to *S. cerevisiae* were more resistant to high Fe levels than the more distant species. Remarkably, we noticed that there are two groups of Fe-sensitive strains: (i) strains that overaccumulate Fe and (ii) strains highly sensible to the acquired Fe, pointing out to diverse mechanisms of response to Fe overload. In summary, in this thesis work we have deepened our knowledge on how *Saccharomyces* cells respond to Fe excess, setting up new bases to allow the development of yeast-based biotechnological tools for Fe extraction and biofortification.

TABLE OF CONTENTS

ABBREVIATIONS

ABBREVIATIONS

Aco1: Aconitase 1

AREs: Adenosine and uridine-rich elements

At: *Arabidopsis thaliana*

AUC: Area under the curve

BLOSUM: Blocks substitution matrix

BPS: Bathophenanthroline disulfonic acid disodium

bZIP: Basic leucine zipper

CBC: CCAAT-binding core complex

CNV: Copy number variation

CRD: Cysteine-rich domains

CS: Consistency score

DCYTB1: Duodenal cytochrome b reductase 1

DIC: Differential interference contrast

DMT1: Divalent metal transporter 1

dNTPs: Deoxyribonucleotides

DW: Dry weight

Eg: *Eucalyptus grandis*

Fa: Fractional area

FAS / $(NH_4)_2Fe(SO_4)_2 \cdot 6H_2O$: Ferrous ammonium sulfate

FC: Fold change

$Fe(OH)_3$: Ferric hydroxide

Fe: Iron

Fe^{2+}: Ferrous iron

Fe^{3+}: Ferric iron

$FeCl_3$: Ferric chloride

$FePO_4 \cdot 2H_2O$: Ferric phosphate dihydrate

FeREs: Iron response elements

$FeSO_4$: Ferrous sulfate

FPN-1: Ferroportin 1

FTN: Ferritin

Fz: Ferrozine

GCAT: Growth curve analysis tool

GOE: Great oxygenation event

H: Helix

Hap: Heme activator protein

HCP1: Heme carrier protein 1

HGT: Horizontal gene transfer

HH: Hereditary haemochromatosis

HOT: Horizontal operon transfer

ID: Iron deficiency

IDA: Iron deficiency anemia

IREs: Iron responsive elements

IRP1/2: Iron regulatory proteins 1 and 2

ISC: Iron sulfur clusters

KAPA: 7-keto-8-aminopelargonic acid

LIP: the labile iron pool

MAFFT: Multiple alignment using fast Fourier transform

MAPK: Mitogen activated protein kinase

MBD: Metal-binding domain

MFS: Major facilitator superfamily

MIC: Minimal inhibitory concentration

ML: Maximum-likelihood

mtDNA: Mitochondrial DNA

NIC: Non-inhibitory concentration

NJ: Neighbor-joining

NRAMP: Natural resistance-associated macrophage protein

Nt: Amino-terminal

NTBI: Non transferrin bound iron

OD: Optical density

PC: Principal components

PCA: Principal components analysis

Pu: Purine

Py: Pyrimidine

RIA: Reductive iron assimilation

RNR: Ribonucleotide reductase

ROS: Reactive oxygen species

SC: synthetic complete

SNPs: Single nucleotide polymorphisms

TbpA: Transferrin binding protein A

TCA: Tricarboxylic acid

TF: Transferrin

TFR1: Transferrin receptor

TMD: Transmembrane domain

TTP: Tristetraprolin

TZF: Tandem zinc fingers

UTR: Untranslated region

VIT: Vacuolar iron transporter

VTL: Vacuolar iron transporter-like

YAP: Yeast activator protein

YREs: Yap response elements

RESUM EN VALENCIÀ

RESUM EN VALENCIÀ

El ferro és un metall de transició essencial per a pràcticament tots els éssers vius amb l'excepció d'alguns grups de bacteris. És crucial per a molts processos biològics claus com la respiració cel·lular i el transport d'oxigen, la biosíntesi de components cel·lulars, la fotosíntesi i la coloració de flors (Momonoi et al., 2009; Connorton et al., 2017; Puig et al., 2017; Ramos-Alonso et al., 2019; Donker et al., 2021). Les seues formes predominants són l'ió ferrós, Fe^{2+} i l'ió fèrric, Fe^{3+}. A causa del seu potencial redox, són dos estats fàcilment intercanviables permetent que el ferro participe en múltiples activitats bioquímiques d'oxidoreducció i en múltiples reaccions de transferència d'electrons. A més, el ferro pot unir oxigen, nitrogen i àtoms de sofre, normalment presents en cadenes laterals d'aminoàcids o com a petites molècules inorgàniques (Sanvinsens and Puig, 2011; Kosman, 2013). Totes les propietats abans esmentades fan del ferro un cofactor redox ideal present en múltiples enzims que es poden classificar en tres grups de metal·loproteïnes segons continguen: i) centres de ferro-sofre (ISC), ii) grups hemo, i iii) complexes oxo-diferro.

El ferro és el quart element de la taula periòdica més abundant en l'escorça terrestre, per tant, no és sorprenent que els processos en els quals el ferro té un paper fonamental siguen nombrosos. No obstant això, el Gran Esdeveniment d'Oxigenació (GOE) va disminuir dràsticament la quantitat de ferro biodisponible a la superfície de la Terra a causa de la presència massiva d'oxigen. Quan hi ha oxigen, el ferro tendeix a formar hidròxids que fan que no estiga biodisponible a pH fisiològic (Kaplan and Kaplan, 2009; Wade et al., 2021). Aquest canvi en la disponibilitat de Fe^{2+} va forçar l'evolució de la vida complexa a través d'una adaptació a un entorn pobre en ferro (Dupont et al., 2006). No obstant això, l'excés de ferro és tòxic, ja que pot participar en les reaccions de tipus Fenton, que condueixen a la producció d'espècies reactives d'oxigen (ROS) que danyen els components cel·lulars, a més, de ser tòxic en

condicions anaeròbiques. Així, pel que fa a la rellevància del ferro en biologia, els nivells d'aquest metall han de ser estrictament regulats. De fet, els organismes han desenvolupat diverses estratègies per a adaptar-se als canvis de concentració de ferro.

En humans, una dieta baixa en ferro o altres circumstàncies específiques pot provocar deficiència de ferro (ID), és a dir, un desequilibri entre la demanda i les reserves de ferro. Per exemple, les demandes de ferro augmenten a causa del ràpid creixement del fetus durant l'embaràs, així com el ràpid creixement en la infància o l'adolescència, especialment en les joves amb menstruació. A més, la inflamació, les cirurgies o medicaments poden reduir l'absorció intestinal de ferro i als països del Sud global és freqüent que les infeccions causen pèrdues de sang, reduint les reserves de ferro. La ID quan és severa pot provocar anèmia (IDA) que afecta 1.2 mil milions de persones a tot el món, i s'associa amb un desenvolupament cognitiu i motor pobre en xiquets, augment de morbiditat i mortalitat en dones i xiquets, i una disminució de la capacitat física i de treball en adults (Camaschella, 2019; Bathla and Arora, 2022; Hess et al., 2023). Les estratègies comunament recomanades per superar l'ID són: i) diversificar la dieta, reduint aquells aliments que interfereixen amb l'absorció de ferro i augmentant la presència d'aquells que afavoreixen la seua absorció; ii) la utilització de suplements orals de ferro; iii) la fortificació d'aliments; i iv) la biofortificació d'aliments. No obstant això, les tres primeres estratègies presenten problemes, sobretot els suplements orals que causen molèsties i efectes secundaris com nàusees, vòmits, estrenyiment o diarrea (Moretti et al., 2015; Nair et al., 2015; Camaschella, 2019; Mkambula et al., 2020). A banda, la biofortificació resulta molt interessant ja que té múltiples avantatges: i) després de la inversió econòmica inicial en el desenvolupament de mètodes, no hi ha un augment de preus; ii) diversos nutrients poden ser enriquits simultàniament; iii) és el mètode més sostenible entre altres intervencions; i iv) té un impacte menor en les propietats organolèptiques dels aliments. Hi ha diversos exemples de biofortificació d'aliments derivats de plantes com l'arròs, el blat o la mandioca (Ofori et al., 2022). Un altre exemple és el llevat *Saccharomyces cerevisiae,* microorganisme àmpliament utilitzat en la fermentació d'aliments i com a

complement nutricional, i del qual també s'ha testat la seua utilitat per a l'enriquiment en ferro (Pas et al., 2007; de Llanos et al., 2016; Nowosad et al., 2021). Curiosament, el ferro derivat de llevats biofortificats està unit a metal·loproteïnes, cosa que el fa més biodisponible i fàcilment absorbible. De fet, estudis amb rosegadors van mostrar que promou una recuperació més ràpida de la deficiència de ferro en comparació amb la suplementació oral amb sals inorgàniques (Pirman and Oresnik, 2012; Kyyaly et al., 2015; Sabatier et al., 2017). Per tant, *S. cerevisiae* es pot utilitzar tant com a eina com a aliment per a la biofortificació del ferro.

En *S. cerevisiae*, la resposta a la deficiència de ferro està regulada pels factors transcripcionals Aft1 i Aft2, que reconeixen una seqüència curta, PyPuCACCCPu (Py: pirimidina i Pu: purina), present en el promotor de gens de reguló de ferro i comunament coneguda com FeRE (*Iron Response Element*) (Rutherford et al., 2003). Aquests factors transcripcionals són importats al nucli independentment de l'estat de ferro cel·lular (Ueta et al., 2003) però, sota condicions de suficiència, són exportats del nucli pel receptor d'exportació nuclear Msn5 (Yamaguchi-Iwai et al., 1995). Com a resultat, s'acumulen al nucli només sota condicions d'escassetat de ferro. L'activació de la transcripció no depén del ferro citosòlic, sinó que respon indirectament a la síntesi d'ISC que es produeix en els mitocondris (Chen, O. S. et al., 2004). Una molècula intermèdia de la síntesi d'ISC és exportada del mitocondri i transformada en un centre $[2Fe–2S]^{2+}$, al que s'uniran les glutarredoxines de monotiol Grx3/4 i la proteïna Fra2 (Kumanovics et al., 2008; Li, H. et al., 2009). Aquest complex transfereix els ISC a Aft1/2, afavorint el seu alliberament de les seues dianes i la seua exportació al citosol, disminuint la transcripció dels gens de reguló de ferro (Ueta et al., 2012; Poor et al., 2014; Li, H. and Outten, 2019). Tot i que aquests factors transcripcionals són paràlogs i tenen funcions superposades, Aft2 té un paper més predominant en la mobilització del ferro intracel·lular i Aft1 en la captació externa de ferro (Courel et al., 2005; Gonçalves, I. R. et al., 2014). El grup de gens activats per Aft1/2 són coneguts com el reguló de ferro i codifica proteïnes implicades en: (i) captació de ferro (*FRE1-4, FET3, FTR1, ARN1-4, FIT1-3*), (ii) mobilització de reserves de ferro (*FET5, FTH1, FRE6, SMF3*), (iii) importació de ferro mitocondrial (*MRS4*), (v)

remodelació del metabolisme del ferro (*CTH1* i *CTH2*), i (vi) captació de biotina i àcid 7-keto-8-aminopelargonic (KAPA) (Shakoury-Elizeh et al., 2004; Ramos-Alonso et al., 2020).

D'altra banda, com que no hi ha un mecanisme regulat d'excreció de ferro, els nivells de ferro citosòlic depenen de l'adquisició del medi, l'emmagatzematge en el vacúol i la divisió cel·lular. Quan els nivells extracel·lulars de ferro són alts, el reguló de ferro es desactiva donant lloc a una reducció en l'adquisició de ferro i en la mobilització d'aquest des del vacúol. A més, s'indueix la resposta transcripcional a l'excés de ferro, sent *CCC1,* que codifica un importador de manganés i ferro localitzat a la membrana vacuolar, el gen més important (Lapinskas et al., 1996; Li, L. et al., 2001). La deleció de *CCC1* redueix notablement el creixement en excés de ferro tant en condicions aeròbiques com anaeròbiques (Li, L. et al., 2001). Recentment, la resolució de l'estructura cristal·lina de l'ortòleg de Ccc1 en *Eucalyptus grandis, Eg*VIT1 (*Vacuolar Iron Transporter 1*) va fer possible la identificació dels residus conservats necessaris per al transport del metall (Kato et al., 2019). A més, estudis amb endosomes suggereixen que *Eg*VIT1 podria ser un antiportador de H^+ (Kato et al., 2019). El factor transcripcional més conegut de *CCC1* és el membre de la família *Yeast Activator Protein* (YAP), Yap5, que reconeix els *Yap Response Elements* (YREs) del promotor de *CCC1* i d'altres gens a través del seu domini d'unió a l'ADN de tipus cremallera bàsica de leucina (bZIP) (Li, L. et al., 2008). Yap5 està unit constitutivament als YREs de manera independent del ferro, però, posseeix dos dominis rics en cisteïna (CRD) que són capaços d'unir dos ISCs, induint-se així un canvi conformacional que activa la seva funció transcripcional (Rietzschel et al., 2015). Curiosament, l'activació de Yap5 depén de la síntesi dels ISCs als mitocondris en lloc dels nivells de ferro citosòlic (Li, L. et al., 2012). A més, Yap5 activa l'expressió d'altres gens com *GRX4* que codifica una glutarredoxina implicada en la desactivació d'Aft1/2 i *TYW1* que codifica un enzim responsable de la modificació del nucleòsid de wybutosina, present en els ARNt. Com que aquest enzim necessita ISCs per a la seua funció i Grx4 és capaç d'unir-ne, es creu que podrien estar implicades en l'atenuació de la toxicitat del ferro al citosol prevenint la seva lliure circulació (Li, L. et al., 2011). A més de Yap5, l'expressió

de *CCC1* està regulada per Snf1, la quinasa del canvi diàuxic a través dels factors transcripcionals de resposta a l'estrès general Msn2 i Msn4. No obstant això, els resultats suggereixen que encara queden més reguladors per descobrir (Li, L. et al., 2017). A més, la degradació de l'ARNm de *CCC1* està regulada post-transcripcionalment per Cth1/2 sota concentracions baixes de ferro, i l'activitat de transport Ccc1 podria estar influenciada per danys oxidatius (Puig et al., 2005; Li, L. et al., 2010). Per tant, Ccc1 està altament regulat a nivell transcripcional, post-transcripcional i proteic, subratllant el seu important paper en la desintoxicació del ferro. En excés de ferro també hi ha una regulació dels gens implicats en la resposta d'estrés oxidatiu com *TSA1, TRX2, SOD1, YAP1* o *GRX4* (diana també de Yap5) (Lin et al., 2011; Lee, Y. J. et al., 2012; Pimentel et al., 2012). Encara que la majoria dels estudis s'han centrat en els danys oxidatius produïts pel ferro, la toxicitat encara apareix en condicions anaeròbiques, implicant altres mecanismes. Una possibilitat que s'ha assenyalat és l'augment de la taxa de síntesi d'esfingolípids que provoca una alteració en la senyalització mediada per aquests (Lee, Y. J. et al., 2012). D'altra banda, ja que el ferro i el manganés tenen preferències de coordinació similars, aquest metall pot competir amb el manganés en el lloc actiu d'enzims com Sod2 i aquesta metal·lació incorrecta podria conduir a la disfunció o inactivació d'enzims clau (Yang, M. et al., 2006).

A banda de *S. cerevisiae*, el gènere *Saccharomyces* inclou 7 espècies més: *S. paradoxus, S. mikatae, S. jurei, S. kudriavzevii, S. arboricola, S. eubayanus* i *S. uvarum* (Alsammar and Delneri, 2020). Tot i que les soques més estudiades del gènere estan associades amb processos de fermentació, la majoria de les espècies són salvatges. Només *S. cerevisiae, S. uvarum* i amb menor freqüència *S. paradoxus* s'han aïllat d'entorns humanitzats com la cervesa, el vi o la sidra (Alsammar and Delneri, 2020). La majoria de les soques es troben associades a l'ordre Fagales i és possible aïllar diferents espècies del gènere en el mateix hàbitat suggerint que l'adaptació a diferents temperatures ha permés la coexistència d'espècies (Salvadó et al., 2011; Spurley et al., 2022; Peris et al., 2023). A més, diversos estudis han assenyalat l'ADN mitocondrial (ADNmt) com un factor clau en l'especiació relacionat amb l'adaptació a la temperatura (Gonçalves, P. et al., 2011; Li, X. C. et al., 2019;

Peris et al., 2023). Recentment, ha augmentat el nombre d'estudis sobre els mecanismes moleculars responsables de l'adaptació a la disponibilitat de ferro en diferents ambients de soques de *S. cerevisiae* que no són les de referència del laboratori (Lee, H. N. et al., 2013; Martínez-Garay et al., 2016; Eldarov et al., 2018; Balaban et al., 2019). Generalment, s'observa que les soques sensibles tenen un major contingut de ferro intracel·lular que les soques resistents al ferro (Martínez-Garay et al., 2016). Com que no hi ha un mecanisme regulat d'excreció de ferro, probablement aquestes diferències es deuen a la incapacitat de les soques sensibles de limitar la captació de ferro quan es troba a altes concentracions (Martínez-Garay et al., 2016). A més, sembla que l'adaptació a baixes concentracions de ferro condiciona la resposta a l'excés (Martínez-Garay et al., 2016). A causa de la diversitat genètica present en aquest gènere, fins i tot a nivell intraespecífic, l'àmplia disponibilitat de soques aïllades, genomes i dades relatives a la caracterització del creixement en diverses condicions, el gènere *Saccharomyces* presenta una oportunitat extraordinària per a estudiar la divergència de l'homeòstasi del ferro. A més, aquest gènere té una estreta relació amb els humans, ja que aquests llevats participen en el procés de fermentació d'aliments àmpliament consumits. L'exploració d'aquesta diversitat pot permetre'ns obtenir i caracteritzar soques que esdevinguen útils com a eines biotecnològiques per a millorar el contingut de ferro.

L'objectiu principal d'aquesta tesi és augmentar el coneixement sobre els mecanismes moleculars que hi ha darrere de les diverses estratègies d'adaptació a la (bio)disponibilitat de ferro en soques de llevat. Al mateix temps, es vol obtenir soques de llevat amb alteracions en el metabolisme de ferro amb possible aplicació biotecnològica. Aquesta proposta es pot dividir en quatre apartats representats en els següents capítols:

1-Determinar quina és la forma ideal de ferro a usar per l'estudi de la sensibilitat de les soques segons l'estat d'oxidació, la composició de la sal o el pH de la preparació de ferro.

2-Conéixer la conservació, així com la diversificació dels dominis proteics en l'Arbre de la Vida del principal responsable en la desintoxicació de ferro a *S. cerevisiae*, Ccc1 i la seua família de proteïnes.

3-Obtenir una soca de *S. cerevisiae* capaç d'acumular alts nivells de ferro sense pèrdua de viabilitat.

4-Estudiar la diversitat del metabolisme de ferro en soques representatives de les poblacions disponibles del gènere *Saccharomyces.*

La metodologia emprada per a dur a terme l'estudi d'aquests objectius proposats inclou: i) fenotipat en diferents condicions i medis de creixement de soques del gènere *Saccharomyces*; ii) tècniques microbiològiques per a la construcció de soques i plasmidis específics; iii) tècniques per a l'estudi del RNA (RT-qPCR); iv) assaig colorimètric per a la detecció de ferro; v) ferramentes bioinformàtiques per a l'obtenció i l'alineament de seqüencies i la construcció d'arbres filogenètics (MetaphORs, Geneious Prime, IQtree); vi) tècniques moleculars per a l'estudi de l'estabilitat de proteïnes; vii) microscòpia per a l'estudi de la localització subcel·lular; i viii) tècniques d'anàlisi de dades (Heatmaps, Principal Component Analysis i anàlisis estadístiques).

En el capítol 1 hem analitzat com influeix el tipus de sal en el fenotip de resistència al ferro i hem determinat quina font de ferro és millor utilitzar, pel que fa a l'estat redox (Fe^{2+} o Fe^{3+}), la preparació d'estoc (dissolució en 0.1 M HCl, 1 mM H_2SO_4, o H_2O Milli-Q) o la composició de la sal: clorur fèrric, $FeCl_3$; sulfat d'amoni i ferro (II) / FAS, $(NH_4)_2Fe(SO_4)_2 \cdot 6H_2O$; o sulfat ferrós, $FeSO_4 \cdot 7H_2O$. Un grup de soques prèviament caracteritzades com a resistents i sensibles a ferro es va créixer en medi sintètic complet (SC) suplementat amb les sals mencionades preparant l'estoc sense i amb HCl. A partir d'aquests resultats es podria assenyalar que el $FeCl_3$ és la sal més tòxica, ja que la concentració necessària per a l'aturada del creixement de les soques és menor que per a les altres sals estudiades, aparentment perquè la seua naturalesa àcida baixa el pH del medi, fent el ferro més disponible. No obstant això, descartem l'ús d'aquesta sal en medi líquid perquè l'addició de $FeCl_3$ al medi causa augment de la turbidesa per la formació d'un precipitat, probablement derivat del ferro, que interfereix amb la mesura del creixement mitjançant

absorbància. No està clar quin és el compost derivat del ferro responsable de la turbiditat observada. D'acord amb l'equilibri d'hidròlisi del $FeCl_3$, el precipitat podria ser $Fe(OH)_3$ ja que és molt insoluble en aigua i a més, quan la sal s'afegeix directament en aigua d'un estoc preparat amb HCl aquest precipitat desapareix (Stefansson, 2007). Altres possibilitats assenyalen $FePO_4 \cdot 2H_2O$ com la sal precipitada, ja que està ben documentat que el ferro té una forta afinitat pel fosfat i la concentració de fosfat de potassi és de fins a 1000 mg/L en el medi SC utilitzat (Pa Ho, 1976; Pierri et al., 2000; Schroder et al., 2003). Les sals de FAS i $FeSO_4$ no se sotmeten a hidròlisi quan es dissolen en aigua a pH 8, en canvi, té lloc la formació, entre altres espècies, de l'aquo-complex $[Fe(H_2O)_6]^{2+}$ que és molt vulnerable a l'oxidació i podria conduir a la generació de $Fe(OH)_3$ o $FePO_4 \cdot 2H_2O$. Quan es prepara l'estoc amb HCl, hi ha un efecte clar: la terbolesa desapareix i la toxicitat del ferro es produeix a una menor concentració, permetent que aquestes sals s'utilitzen per a l'anàlisi del creixement líquid. És ben sabut que la solubilitat de ferro pot ser augmentada gairebé 6 ordres de magnitud quan el pH canvia de 7 a 2. De fet, baixar el pH extracel·lular és una estratègia estesa entre els organismes per augmentar la captació de ferro (Kaplan and Kaplan, 2009). L'addició d'un àcid, la presència de sulfat d'amoni, $(NH_4)_2SO_4$, o ambdues, redueixen l'oxidació de manera que s'evita la formació del precipitat (Gaensly et al., 2014). Aquests resultats indiquen que: 1) Totes les sals es poden utilitzar per a assajos en medis sòlids, ja que s'observa la mateixa tendència des resposta al ferro en les soques independentment de la sal; 2) el FAS és una sal menys àcida que $FeCl_3$, tot i que encara mostra algunes propietats d'àcid feble; 3) el FAS preparat amb aigua no està disponible per al llevat, ja que es necessiten grans concentracions per a detindre el creixement; 4) l'HCl augmenta la solubilitat de FAS a causa d'una caiguda en el pH, ja que la turbiditat no s'observa; 5) l'ió amoni del FAS és important per a la solubilitat, però no causa una diferència en la toxicitat, ja que els resultats de creixement amb ambdues sals són molt similars; 6) l'augment de la solubilitat de les sals FAS i $FeSO_4$ amb HCl permet l'anàlisi del creixement de les soques en el medi líquid; i 7) la toxicitat observada quan el FAS o el $FeSO_4$ es prepara amb HCl es deu majoritàriament a l'efecte del ferro i no de l'àcid.

En el capítol 2 ens endinsem en l'estudi de la conservació evolutiva de la principal proteïna involucrada en la desintoxicació de ferro en *S. cerevisiae*, Ccc1. En bacteris, arqueobacteris i animals, el ferro s'emmagatzema dins del complex proteic de la ferritina mentre que en fongs i plantes el ferro s'acumula en el vacúol i el tonoplast, respectivament (Arosio et al., 2009). En tots dos casos, no són dipòsits estancs, sinó que constitueixen reservoris de ferro des d'on es pot mobilitzar aquest metall a demanda (Kaplan and Kaplan, 2009; Arosio et al., 2017). D'altra banda, les plantes també tenen ferritines, però aquestes no semblen jugar un paper principal en la desintoxicació com en animals i procariotes (Connorton et al., 2017). Ccc1 és un transportador de Fe^{2+} i Mn^{2+} situat a la membrana vacuolar que importa aquests ions del citosol al vacúol. Aquesta proteïna té un paper fonamental en *S. cerevisiae*, ja que l'eliminació de *CCC1* dóna lloc a un defecte de creixement sever quan hi ha excés de ferro (Lapinskas et al., 1996; Li, L. et al., 2001). Els homòlegs de Ccc1 s'han trobat en plantes (VIT1 i VTLs), diatomees, bacteris i protists i alguns d'ells s'han confirmat com a ortòlegs funcionals a través d'assajos de complementació en mutants *ccc1Δ* de *S. cerevisiae* (Kim, S. A. et al., 2006; Brembu et al., 2011; Bhubhanil et al., 2014; Slavic et al., 2016). Donat el seu important paper en la desintoxicació del ferro, volíem explorar la conservació d'aquesta família de proteïnes. Per tant, es va buscar ortòlegs de Ccc1/VIT1 a través de la base de dades MetaPhORs (Chorostecki et al., 2020). MetaPhOrs és un repositori públic d'ortòlegs i paràlogs que utilitza per a la predicció arbres filogenètics procedents de diverses fonts. Normalment, els repositoris filogenòmics comparteixen informació superposada, però aquesta redundància no implica necessàriament que la informació siga idèntica, ja que normalment s'obté utilitzant diferents paràmetres i fonts. MetaPhORs obté avantatge d'aquesta informació redundant augmentant la robustesa de la predicció de l'ortologia entre dues seqüències (Pryszcz et al., 2011; Chorostecki et al., 2020). Els resultats mostren que la família Ccc1/VIT1 està àmpliament distribuïda al llarg de l'Arbre de la Vida amb l'excepció notable dels metazous. Curiosament, té una àmplia representació en els regnes d'arqueobacteris i bacteris on la ferritina és la principal proteïna implicada en la desintoxicació del ferro. El 2019, Kato i col·laboradors (Kato et al., 2019) van publicar l'estructura cristal·lina del transportador VIT1 de la planta *Eucalyptus grandis* (*Eg*), que

consistia en una estructura dimèrica amb cada oligòmer compost per dos dominis: un domini transmembrana (*Transmembrane domain*, TMD) que estaria implicat en el transport de ferro a través de la membrana i el domini d'unió al metall (*Metal binding domain*, MBD) que podria ser un domini que facilitaria l'entrada del ferro. En aquest treball es van identificar aminoàcids essencials i es va proposar un mecanisme de transport que ens va permetre ampliar aquesta informació a les seqüències d'ortòlegs obtingudes. Pel que fa a les seqüències que hem analitzat, la similitud d'aminoàcids és baixa al llarg de la seqüència, però l'estructura general i els dominis principals es conserven notablement. Una elevada variació es troba en el domini amino-terminal (Nt): està absent en el Grup II, consisteix en un domini ric en prolina i serina en els fongs (Grup VI-VIII), és una seqüència bàsica curta en les plantes (Grup III i V) i protistes (Grup IV) o, com ocorre en els bacteris i arqueobacteris del Grup I, es tracta d'un domini similar a la ferritina/eritrina (Andrews, S. C., 2010; Ruangkiattikul et al., 2012). El MBD també constitueix una font de notable diversitat: per exemple, les plantes no només posseeixen les ben conegudes proteïnes VIT1 similars a l'estructura d'*Eg*VIT1 (Grup V) sinó que també posseeixen proteïnes VTL (Grup III) que destaquen per manca de MBD (Gollhofer et al., 2014). El grup II (principalment Archaea) i el grup IA també manquen de MBD, però no el Grup IB, el que suggereix que la diversitat de dominis proteics va aparèixer en aquests procariotes. La presència de més d'un homòleg i l'alta diversitat de dominis assenyalen una història evolutiva complexa, potser implicant transferència horitzontal des de bacteris i arqueobacteris durant l'origen de l'últim ancestre eucariota comú. Curiosament, les proteïnes del grup I-III normalment es localitzen a la membrana plasmàtica. Aquest és el cas dels bacteris *Agrobacterium tumefaciens*, on l'ortòleg de Ccc1 s'anomena *Membrane-bound ferritin A* (MbfA) i actua com un exportador de ferro (Bhubhanil et al., 2014). Un altre exemple el constitueixen alguns VTL de soia localitzats a la membrana del simbiosoma del nòdul que exporten ferro al rizobi per subministrar l'alta demanda de Fe per a la fixació de nitrogen (Liu et al., 2020). Al contrari, les proteïnes del grup V-VIII es troben al vacúol/tonoplast, per tant, potser la divergència de seqüència també s'associa amb la localització i la subfuncionalització. De fet, la topologia dels arbres no canvia quan no s'inclouen les seqüències MBD. La baixa conservació

d'aquests dos dominis suggereix que no són essencials i podrien servir com a dominis auxiliars adaptats a les necessitats de cada organisme (Bhubhanil et al., 2014; Kato et al., 2019).

Un cop explorada la diversitat d'arquitectures proteiques de la família Ccc1/Vit1, i delimitada la divergència dels dominis, en el capítol 3 es va estudiar la sobreexpressió de *CCC1* com a potencial eina per a obtenir llevats enriquits amb ferro. Sorprenentment, s'observa que la sobreexpressió de *CCC1* esdevé molt tòxica per a la cèl·lula en condicions normals. Es van utilitzar diferents promotors per a augmentar l'expressió de *CCC1*: i) el promotor del gen *TEF2*, que indueix una alta expressió de forma constitutiva; ii) el promotor regulable *GAL1*, que activa l'expressió en presència de galactosa, i iii) el promotor reprimible *MET25*, que permet l'expressió a nivells baixos en absència de metionina en el medi. Tot i que la sobreexpressió és tòxica en els tres casos, la toxicitat és notablement més baixa quan *CCC1* està sota el control del promotor *MET25*, perquè aquest promotor activa l'expressió en menor grau. El principal factor de transcripció que indueix l'expressió de *CCC1* és Yap5, tot i que els factors transcripcionals Msn2/4 regulats per la quinasa Snf1 també són responsables de la seua expressió de manera dependent del ferro (Li, L. et al., 2017). Es creu que la quinasa Snf1 també actua sobre altres factors de transcripció que encara no s'han identificat i que altres reguladors poden estar implicats en la regulació de *CCC1* (Li, L. et al., 2017). A més, el terminador del gen *CYC1* substitueix l'extrem 3'UTR de *CCC1* en les tres construccions esmentades anteriorment, eliminant la regulació post-transcripcional de *CCC1* per part de Cth2 en deficiència de ferro (Puig et al., 2005). Definitivament, sembla que el promotor i terminador de *CCC1* són essencials per a una funció adequada de la proteïna Ccc1 i el desacoblament de la regulació per concentració de ferro és perjudicial en condicions en que no hi ha un excés. D'altra banda, s'observa que la toxicitat per sobreexpressió de *CCC1* es pot atribuir, en part, a la baixa disponibilitat de ferro, ja que el reguló de ferro està activat en condicions normals i la deleció d'*AFT1* suprimeix totalment el creixement de les cèl·lules. A més, eliminar el transport d'alta afinitat de ferro (*FTR1* i *FET3*) és perjudicial per a les cèl·lules i, per contra, l'addició de ferro rescata el fenotip tòxic. D'altra banda, les cèl·lules sobreexpressants també

acumulen grans quantitats de ferro total reforçant la idea que la captació del metall està augmentada perquè el ferro intracel·lular no està disponible. A més, diversos estudis han establert una relació entre els reservoris de ferro del vacúol i el mitocondri de manera que un augment en el transport vacuolar de ferro condueix a una disminució dels depòsits mitocondrials i al contrari (Li, L. and Kaplan, 2004; Li, L. et al., 2010; Lin et al., 2011). Per exemple, la sobreexpressió de *CCC1* evita l'acumulació de ferro mitocondrial i limita el dany del ISC en fenotips d'excés de ferro, afavorint la desactivació del reguló de ferro (Chen, Opal S. and Kaplan, Jerry, 2000; Chen, O. S. et al., 2004; Li, L. et al., 2010; Li, L. et al., 2012). D'altra banda, estudis de transport en endosomes han demostrat que *Eg*VIT actua com un antiportador de protons i aquesta funció podria estar conservada en *S. cerevisiae* (Cockrell, A. et al., 2014; Slavic et al., 2016; Kato et al., 2019). En conseqüència, la sobreexpressió de *CCC1* podria desequilibrar el gradient de protons a través de la membrana vacuolar, de manera similar al que ocorre quan hi ha un mal funcionament de la H^+-ATPasa vacuolar, V-ATPasa. La pèrdua de funció V-ATPasa condueix a l'activació del reguló de ferro a causa d'estrés oxidatiu crònic (Milgrom et al., 2007; Diab and Kane, 2013). Es creu que una de les raons podria ser l'acumulació de nutrients al citosol, ja que el vacúol constitueix un rebost de diversos nutrients, com aminoàcids i altres metalls, a més del ferro. Especialment, s'ha demostrat que l'acumulació de cisteïna citosòlica causa danys als components de la ruta de síntesi de ISC, limitant l'activitat enzimàtica i causant l'activació del reguló de ferro (Hughes et al., 2020). Aquesta alteració de la regulació de l'homeòstasi del ferro i la disfunció mitocondrial han estat relacionades amb un fenotip d'envelliment (Chen, K. L. et al., 2020; Hughes et al., 2020). Com es menciona en el capítol 2, el domini Nt té una elevada variabilitat específica d'espècie. A més, en *S. cerevisiae*, diversos estudis proteòmics han revelat que determinats residus de serina i lisina són fosforilats i ubiqüitinats, respectivament (Albuquerque et al., 2008; Swaney et al., 2013). La deleció del domini Nt sembla ser una mutació de pèrdua parcial de funció, ja que a concentracions elevades de ferro el creixement d'aquest mutant està molt deteriorat i l'activació del reguló de ferro és més baixa que quan la versió completa està present. D'altra banda, quan les cèl·lules s'incuben en un lleuger excés de ferro, les que expressen la versió completa acumulen vuit vegades

més ferro que les WT, mentre que l'augment en les cèl·lules que sobreexpressen *NtΔ-CCC1* és només de 4 vegades més. No obstant això, quan el total de ferro es calcula per volum, vam observar que les cèl·lules que expressaven la versió completa no milloraven la capacitat de les cèl·lules WT per treure ferro del medi, principalment a causa del seu baix creixement. En canvi, els llevats amb Ccc1 sense l'extrem Nt extreien el doble de ferro que la resta de les cèl·lules assajades sense un defecte de creixement, convertint-se en una eina interessant per a l'extracció de ferro del medi. Per exemple, per eliminar el ferro del vi, ja que de vegades causa un gust desagradable, color rovellat i una disminució en l'estabilitat dels productes alimentaris (Tsuji et al., 2012). Observem que aquesta pèrdua parcial de funció no es deu a una menor estabilitat de la proteïna, ja que la vida mitjana de la proteïna NtΔCcc1 etiquetada amb GFP és similar a la versió completa. Però, sembla que l'absència del domini Nt altera lleugerament la distribució del transportador tot i que encara es localitza a la membrana vacuolar. D'altra banda, el fet que el domini Nt continga residus de serina, que són fosforilats, podria suggerir la existència d'una regulació post-traduccional necessària per a l'activació completa del transportador, com ocorre, per exemple, en el cas del transportador de cadmi *Yeast Cadmium Factor 1*, Ycf1 (Khandelwal et al., 2022). A més, no es pot descartar que el domini Nt estiga subjecte a altres regulacions, ja que s'ha demostrat que Ccc1 augmenta la seua activitat en resposta a la producció de ROS, suggerint que aquesta proteïna està regulada a nivell post-traduccional, tot i que el mecanisme específic roman per definir (Li, L. et al., 2010). Cal fer més estudis per a determinar la funció del domini Nt, no obstant, la sobreexpressió de *NtΔCCC1* permet acumular nivells més alts de ferro amb un defecte de creixement mínim proporcionant una eina biotecnològica interessant per a l'extracció d'aquest metall del medi i, alhora, una nova estratègia per a obtenir llevats enriquits amb ferro.

En el capítol 4, s'amplia l'estudi sobre l'adaptació a diferents disponibilitats de ferro en *S. cerevisiae*, a soques representatives de les poblacions del gènere *Saccharomyces*. De la nostra anàlisi destaca la diferència observada en la tolerància al ferro segons l'espècie, és a dir, les espècies més pròximes filogenèticament a *S. cerevisiae*, com *S. paradoxus*, *S. mikatae*, *S. jurei* o *S.*

arboricola, són més resistents a altes concentracions de ferro que les més distants (*S. kudriavzevii, S. uvarum* i *S. eubayanus)*. És ben sabut que la temperatura ha estat un factor de pressió de selecció molt rellevant i que va tenir un paper clau en el procés d'especiació d'aquest gènere (Gonçalves, P. et al., 2011; Peris et al., 2023). Una possibilitat és que l'adaptació a la temperatura haja condicionat l'homeòstasi del ferro, per exemple de manera que les temperatures altes requerisquen una major demanda de ferro. De fet, l'ADNmt que codifica principalment gens implicats en la respiració cel·lular, procés amb altes demandes de ferro, ha estat assenyalat com un punt calent d'evolució vinculat a l'adaptació a la temperatura (Li, X. C. et al., 2019). Una altra possibilitat és que les espècies de *Saccharomyces* s'han vist obligades a adoptar estratègies per adaptar-se a les diferents disponibilitats de ferro per coexistir en hàbitats deficients de ferro com fulles caigudes o troncs de roure. D'altra banda, *S. mikatae* i *S. jurei* es van comportar de manera similar en resposta a l'excés de ferro, així com *S. uvarum* i *S. eubayanus*, probablement perquè són les espècies germanes menys divergents del gènere d'acord amb estudis previs (Peris et al., 2023). En canvi, les espècies *S. cerevisiae* i *S. paradoxus* presenten una alta variabilitat fenotípica intraespecífica. La soca resistent al ferro Sc3 és Kyokai 6, que pertany a la població de Sake; Sc7 i Sc8 són YJM978 i CECT11032, totes dues de la població de *Wine/European,* aïllades d'ambient clínic i most de raïm, respectivament (Peter et al., 2018). Aquestes tres soques són d'entorns relacionats amb l'ésser humà, però segons altres estudis, no sembla que hi haja una correlació entre la resistència al ferro i pertànyer a ambients humanitzats, ja que altres soques de sake estretament relacionades amb Kyokai 6 no són tan resistents com aquesta i una situació similar ocorre en altres soques víniques i clíniques (Martínez-Garay et al., 2016). No obstant això, el nombre de soques relacionades amb l'ésser humà en aquest estudi es reduït i totes pertanyen a la mateixa espècie, per tant, no es pot establir cap relació entre la resistència al ferro i l'entorn humà. A banda d'estudiar el comportament de les soques front a l'excés, també es va determinar la quantitat total de ferro que adquireixen del medi a les 24 hores. S'escull un temps llarg ja que segons estudis previs, quan els llevats es troben en l'etapa post-exponencial, es produeix una manca de sincronització entre la captació de ferro i la divisió cel·lular. Així, les cèl·lules quan es divideixen a una

velocitat menor o no es divideixen continuen important Fe a través d'aquesta via quan són incubades durant molt de temps (Haurie et al., 2003; Park et al., 2013). No obstant, en l'espècie *S. cerevisiae* es coneix que les soques resistents al ferro són capaces de limitar l'adquisició, al contrari de les sensibles que acumulen grans quantitats de ferro (Martínez-Garay et al., 2016). En l'estudi actual amb les espècies del gènere *Saccharomyces*, s'observen dos patrons ben diferenciats en les soques sensibles al ferro: i) soques que acumulen grans quantitats de ferro, i ii) soques que han augmentat la sensibilitat al ferro interioritzat. Les espècies de *Saccharomyces* són incapaces d'exportar ferro i, d'acord amb la teoria d'"evitació o segrest" respecte a la tolerància als metalls suggerida per Jennings (1993), el primer grup sembla ser incapaç d'evitar l'entrada de ferro, mentre que el segon grup sembla tenir defectes en la maquinària de desintoxicació. Com es mostra a Martínez-Garay et al., (2016), les soques sensibles al ferro estan aparentment adaptades a entorns de baixa disponibilitat, ja que són resistents a la deficiència del ferro. D'altra banda, una estratègia comunament observada per fer front a l'escassetat de ferro en soques naturals de *S. cerevisiae* és augmentar la captació de ferro (Lee, H. N. et al., 2013; Eldarov et al., 2018). Indirectament, la desregulació d'Aft1 s'ha utilitzat com a mètode per augmentar l'entrada de ferro en soques de llevat bio-enginyeritzat (Ramos-Alonso et al., 2018; Gambacorta et al., 2022). A més, en el capítol 4 s'observa que les soques sensibles al ferro que acumulen grans quantitats d'aquest, tenen una alta activació de les dianes de Yap5 (*TYW1*, *CCC1* i *GRX4*) després de l'addició de ferro, que correlacionarien amb l'acumulació elevada de ferro observada. Tot i que són capaços d'apagar l'expressió de *FET4* quan s'afegeix ferro, presenten l'expressió d'aquest gen en condicions normals com si perceberen deficiència de ferro. No obstant això, també hem observat un grup de soques molt sensibles, però amb nivells de ferro intracel·lulars similars a les resistents. Per tant, aquestes soques són capaces d'aturar la importació de ferro, però no podrien desintoxicar el ferro adequadament. De fet, tenen una activació menor de *TYW1* i *CCC1*. Pel que fa a la conservació de la família Ccc1/Vit1, en el gènere *Saccharomyces,* d'acord amb l'estudi realitzat en el capítol 2, la majoria dels canvis es troben en el domini Nt. No obstant això, la toxicitat de la sobreexpressió de *CCC1* fa difícil discernir la conseqüència de les mutacions.

Una possibilitat interessant d'abordar aquesta anàlisi seria utilitzar CRISPR, que permetria mantenir el fons genètic de les soques sense sobreexpressió (DiCarlo et al., 2013). A més, també podem buscar divergència en altres proteïnes implicades en l'homeòstasi del ferro, estudiant si la taxa d'evolució és més alta en aquests gens i si de fet han estat sota pressió selectiva (Yang, Z., 2007). No obstant això, eventualment pot ser necessari comprovar si aquesta selecció té una relació amb el ferro o la temperatura. En el nostre treball, observem que els llevats sensibles estan més oxidats que els resistents a baixes concentracions de ferro, però només veiem un augment en els nivells de RNA missatger en *TRX2*, en contrast amb altres treballs que també van detectar l'augment de *SOD1, TSA1* o *YAP1* (Lin et al., 2011; Pimentel et al., 2012). No obstant això, en Lin et al., (2011) es va demostrar que l'eliminació del gen *YAP1* o la sobreexpressió d'altres gens de resposta oxidativa no tenen un efecte notable sobre la toxicitat del ferro que ocorre fins i tot en condicions anaeròbiques. Per tant, potser hi ha altres conseqüències derivades de l'excés de ferro, com serien els defectes en la senyalització d'esfingolípids o en la metal·lació de proteïnes (Yang, M. et al., 2006; Lee, Y. J. et al., 2012).

Des del punt de vista biotecnològic, les soques resistents al ferro descrites ací semblen menys interessants, ja que aparentment la resistència al ferro s'aconsegueix limitant l'acumulació d'aquest. Les soques sensibles que adquireixen nivells de ferro comparables als de les resistents tampoc no són apropiades, sinó que les més convenients serien les soques sensibles que acumulen quantitats de ferro elevades. No obstant això, com que un excés de ferro és perjudicial per a la cèl·lula, és crucial aconseguir un equilibri entre la viabilitat cel·lular i l'acumulació de ferro, com en el cas de la soca que expressa *CCC1* sense l'extrem Nt. D'altra banda, es coneix que la tolerància al coure està relacionada amb l'augment del nombre de còpies del gen *CUP1*, que codifica una metal·lotioneïna que segresta el coure al citosol (Adamo et al., 2012). Pel que fa a la tolerància al ferro, s'espera que aquest paper siga executat per *TYW1* i *GRX4*. No obstant això, també s'ha demostrat que la reducció de la senyalització d'esfingolípids o l'augment de la resposta oxidativa als danys i la mitofàgia són requisits per a la tolerància al ferro (Lee, Y. J. et al., 2012; Ramos-Alonso et al., 2018; Balaban et al., 2019; Kocaefe-Ozsen et

al., 2022). Per tant, l'ús del llevat com a eina per a la desintoxicació del ferro o la biofortificació depén de: i) l'augment de la captació, ii) l'augment del transport vacuolar i iii) l'augment de la tolerància del ferro intracel·lular.

En aquest treball de tesi, hem llançat llum sobre l'elecció de la millor sal per a caracteritzar la resposta a l'excés de ferro, hem estudiat la conservació d'un mecanisme per a la desintoxicació del ferro en procariotes, plantes, fongs i protistes, hem desenvolupat una eina per a l'extracció de ferro del medi i hem analitzat la idoneïtat de l'ús de soques de *Saccharomyces* per a la biofortificació.

INTRODUCTION

1. RELEVANCE OF IRON IN BIOLOGY

Iron is a transition metal that is essential for almost all forms of life with the exception of some groups in the Bacteria domain. Iron is indispensable for many key biological processes such as cellular respiration and oxygen transport, biosynthesis of cellular components, photosynthesis, and flower coloring (Momonoi et al., 2009; Connorton et al., 2017; Puig et al., 2017; Ramos-Alonso et al., 2018; Donker et al., 2021). Similar to other transition metals, iron exists in a wide range of oxidation states, from −II to +VII; however, its most predominant forms are Fe^{2+} (ferrous iron) and Fe^{3+} (ferric iron). Due to the redox potential of the pair Fe^{2+}/Fe^{3+}, both states are easily interchangeable which allows iron to participate in multiple oxidoreductase biochemical activities and in multiple electron transfer reactions. Furthermore, iron can reversely bind oxygen, nitrogen, and sulfur atoms usually present in amino acid side chains or as small inorganic molecules (Sanvinsens and Puig, 2011; Kosman, 2013). All the above-mentioned properties make iron an ideal redox cofactor present in multiple enzymes, which can be classified into three different groups of ferroproteins: i) iron-sulfur clusters-, ii) heme-, and iii) oxo-diiron-containing proteins.

1.1. Iron-sulfur clusters-containing proteins

Iron-sulfur clusters (ISC) are small inorganic complexes of iron and sulfide which participate as cofactors in many essential biochemical reactions. These molecules can be found forming different structures from the simple [Fe-S], [2Fe-2S], or [4Fe-4S] in the largest group of ferredoxins to the complex [7Fe-7S] or [8Fe-8S] in bacterial nitrogenases. Moreover, interconversions between clusters have also been reported (Brzóska et al., 2006). Such cluster diversity exists because the coordination geometry of the cluster adapts the redox potential to the enzymatic needs (Capozzi et al., 1998). ISCs are thought to be among the earliest catalysts in the evolution of biomolecules and to have a pivotal role in the origin of life. Almost all species among the Tree of Life depend on ISCs for viability and have a large amount of ISC-containing proteins (Lill and Freibert, 2020). Although their synthesis can be reproduced *in vitro*, these molecules are highly unstable under an aerobic atmosphere, which conditions

the need to compartmentalize and enzymatically direct it. This extraordinarily complex enzymatic pathway is deeply conserved in Eukaryotes and has been object of exhaustive research during the last decades (Braymer and Lill, 2017). One of the most studied ISC-containing proteins is the metazoan aconitase 1 (Aco1), a tricarboxylic acid (TCA) cycle enzyme that contains a [4Fe-4S] cluster and catalyzes the conversion of citrate to isocitrate. Moreover, this protein is also involved in the response to low iron, acting as a sensor of iron levels (Koleini et al., 2021). In a similar way, [2Fe-2S] clusters have a pivotal role in iron sensing in the baker's yeast *Saccharomyces cerevisiae* which will be deeply discussed in the next sections. Other examples are complexes I-III of mitochondrial electron transport chain, DNA polymerases and helicases, and enzymes involved in tRNA post-transcriptional modification (Lill and Freibert, 2020).

1.2. Heme-containing proteins

Heme is a prosthetic group consistent of a porfirin IX ring and Fe^{2+} and is present in several proteins involved in oxygen transport, diatomic gas sensing (e.g. CO and NO), regulation of protein stability, circadian rhythm, tumorigenesis, electron transfer and many others. The heme group is also considered a nutrient, as it is in fact a major source of dietary iron for many microbes and animals, being more bioabsorbable than non-heme iron (Chambers et al., 2021). The redox activity of the heme ring can render it toxic, thus its synthesis and degradation imply a large number of enzymes, is finely regulated and requires compartmentalization (Piel et al., 2019). Interesting examples of heme-containing proteins are hemoglobin and myoglobin (involved in oxygen transport and storage, respectively), the mitochondrial yeast cytochrome c peroxidase (catalyzes the reduction of hydrogen peroxide to water), horseradish peroxidase (catalyzes the oxidation of various organic substrates by hydrogen peroxide and is widely used in biochemistry techniques), peroxidases involved in prostaglandin synthesis, the human P450 called CYP3A4 (responsible for xenobiotic detoxification) and nitric oxide synthase (catalyzes the oxidation of L-arginine to L-citrulline and nitric oxide) (Poulos, 2014).

1.3. Oxo-diiron-containing proteins

Oxo-diiron-containing proteins are metalloproteins that have active sites consisting in two non-heme iron ions with a bridging oxygen atom interacting with each iron. These proteins belong to the ferritin superfamily and share a common structural fold consisting in a 4 α-helix bundle that provides the residues involved in the coordination of the diiron site. It is commonly believed that these oxo-diiron bridges are self-assembled (Caldas Nogueira et al., 2021). The most known examples are ferritin, which uses the oxo-bridged diiron centers to store iron and prevent it from oxidative damage, and ribonucleotide reductase (RNR) that catalyzes the reduction of ribonucleotides to deoxyribonucleotides (Arosio et al., 2009; Puig et al., 2017). Other examples are hemerythrins, which function as oxygen transporters; hemerythrin-like proteins involved in iron and oxygen sensing, iron-sulfur center repair machinery, or nitric oxygen reductase and catalase activity (Andrews, S. C., 2010).

Iron is the fourth most abundant metal element in the Earth's crust, thus it is not surprising that processes in which iron has a pivotal role are highly conserved, suggesting that life development was linked to iron. Indeed, Archaea and Bacteria domains have a highly enriched iron-proteome (Dupont et al., 2010). However, the Great Oxygenation Event (GOE) dramatically decreased the amount of bioavailable iron at Earth's surface due to the massive oxygen production. When oxygen is present, iron tends to form hydroxides which make iron poorly available at physiological pH (Kaplan and Kaplan, 2009; Wade et al., 2021). This change in Fe^{2+} availability forced the evolution of complex life through an adaptation to an iron-depleted environment (Dupont et al., 2006). Generally, organisms respond to iron-depletion increasing iron uptake from the environment, mobilizing iron stores and remodeling metabolism to prioritize iron-consuming pathways that are essential. However, iron overload is toxic, since it is a redox active metal that can participate in Fenton's reactions, which lead to reactive oxygen species (ROS) production that damage cellular components. Moreover, iron can be also toxic in anaerobiotic conditions through enzyme mismetallation and impaired sphingolipid signaling (Winterbourn, 1995; Yang, M. et al., 2006; Lee, Y. J. et

al., 2012). Thus, regarding iron relevance in biology, the levels of this metal have to be tightly regulated. Indeed, organisms have developed multiple strategies to adapt to iron concentration changes. The response to iron deprivation and overload in humans and *S. cerevisiae* will be discussed in the following sections.

2. IMPLICATIONS OF LOW IRON BIOAVAILABILITY

2.1. Iron metabolism in humans

In humans, most of the iron present in the body, approximately 65%, is contained in the heme-group of hemoglobin in erythrocytes. Only an 8% of the required iron comes from the diet, while the rest comes from iron recycled by macrophages from senescent cells, especially erythrocytes, and the release of stored iron in hepatocytes (Koleini et al., 2021). Dietary iron is absorbed in the intestine tract both as heme, which has high bioavailability, and non-heme iron, mostly present as Fe^{3+}. Heme iron is suggested to be transported across enterocytes by heme carrier protein 1, HCP1, and Fe^{2+} iron is enzymatically released at the cytosol (Latunde-Dada et al., 2006), (Figure 1). Conversely, non-heme iron, previously to its absorption in enterocytes, has to be reduced by cell surface ferrireductases, being the most known the duodenal cytochrome b reductase 1, DCYTB1 (Choi et al., 2012), (Figure 1). Then, Fe^{2+} ion is transported through the divalent metal transporter 1, DMT1 (Mackenzie et al., 2006), (Figure 1). Ferroportin 1 (FPN-1) allows iron to be released into the blood stream, where it is bound to transferrin protein (TF) and distributed across tissues. Iron enters the cell through endocytosis mediated by the transferrin receptor, TFR1, and it is released at the lysosome, from where it will be either distributed or stored in ferritin (FTN) depending on the cellular requirements (Luck and Mason, 2012), (Figure 1). When body iron levels are low, FPN1 favors iron export to the blood stream; however, when there is an iron overload, hepatocytes secret hepcidine, a small hormone peptide that favors FPN1 degradation or inhibition. Thus, iron remains in enterocytes until they become sloughed off or in hepatocytes, which constitute an iron reservoir (Koleini et al.,

2021). Conversely, there is no iron excretion system, thus iron is passively lost thought skin desquamation, blood losses or enterocyte sloughing. Besides hepcidine, iron levels can also be regulated by hypoxia and inflammation (Koleini et al., 2021).

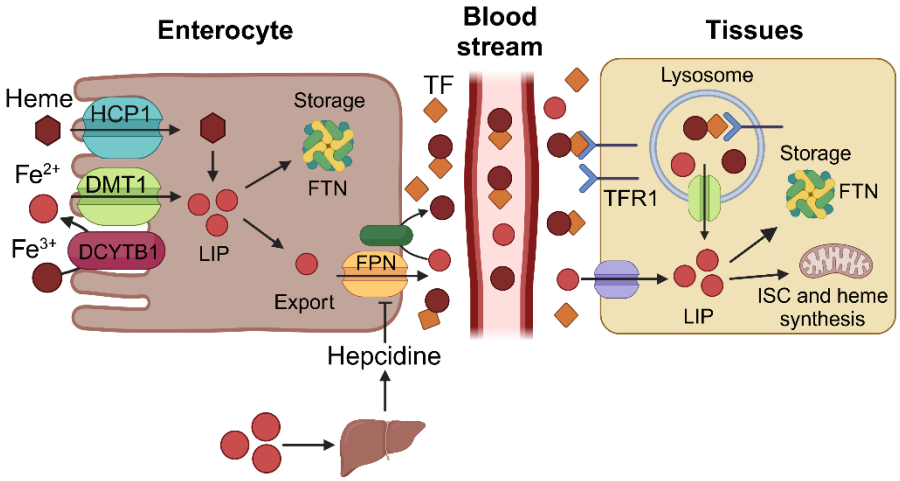

FIGURE 1. SYSTEMIC IRON HOMEOSTASIS IN HUMANS. Heme-bound iron is absorbed into duodenal enterocytes, possibly via HCP1 (Heme carrier protein 1) and Fe^{2+} is released from porphyrin ring. Fe^{2+} is directly transported through DMT1 (Divalent metal transporter 1) or previously reduced from Fe^{3+} by DCYTB1 (Duodenal cytochrome b reductase 1) ferrireductases. Once inside the cell, Fe^{2+} forms part of the labile iron pool (LIP) which can be stored in ferritin (FTN) or exported via ferroportin (FPN). Exported Fe^{2+} is oxidized to Fe^{3+} and bound to transferrin (TF) in the blood stream. Once in tissues, iron bound TF is recognized by transferrin receptor 1 (TFR1), endocyted and directed to lysosome. Inside lysosomes Fe^{3+} is relieved from TF, reduced and exported to cytosol via DMT1. Iron can again, be used for storage or transported into the mitochondria for iron/sulfur clusters (ISC) and heme synthesis. Alternatively, iron can enter cells from blood in Fe^{2+} state through other transporters.

At cellular scale, in low iron conditions the regulation mainly occurs at the post-transcriptional level, mediated by iron regulatory protein 1 and 2 (IRP1/2), and depends on ISC synthesis at mitochondria. IRP1 and IRP2 recognize iron responsive elements (IREs) present in certain mRNAs favoring iron mobilization and rationing (Figure 2). IREs present at the 3′ untranslated region or 3'UTR of transcripts such as TFR1 induce stabilization while localized at 5'UTR inhibit translation, as it happens, for example, with FPN-1 and FTN mRNAs (Figure 2). IRP1 is the apoprotein of the TCA cycle enzyme Aco1, which acquires the ability to bind IREs when the ratio of ISC synthesis

decreases and cannot bind them. IRP2 is constitutively activated but it is ubiquitinated and proteasome-degraded in the presence of iron (Wilkinson and Pantopoulos, 2014). Upon severe iron starvation, an mRNA-binding protein called tristetraprolin (TTP) is induced and promotes the degradation of transcripts encoding proteins involved in a number of iron-consuming processes, prioritizing the most essential ones (Bayeva et al., 2012), (Figure 2).

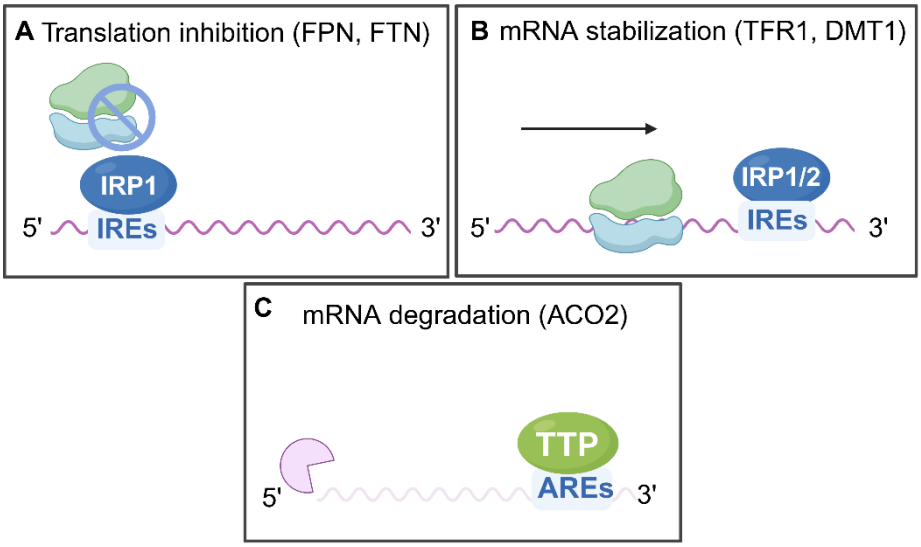

FIGURE 2. RESPONSE TO IRON DEFICIENCY AT CELLULAR LEVEL IN HUMANS. **A)** IRP1 bind IREs at 5'UTR to avoid translation of certain mRNAs like FPN or TFN favoring iron mobilization. **B)** IRP1/2 recognize IREs at 3'UTR of mRNAs like TFR1 and DMT1 which facilitates iron acquisition. **C)** In severe deficiency, TTP activates mRNA degradation of non-essential iron-consuming genes via recognition of AREs. IRP1/2: Iron regulatory proteins 1/2, IREs: Iron responsive elements, UTR: Untranslated region, FPN: Ferroportin, TFN: Transferrin, TFR1: Transferrin receptor 1, DMT1: Divalent metal transporter 1, TTP: Tristetraprolin.

2.2. Iron deficiency consequences in humans

As described above, the body is well adapted to optimize iron uptake and recycling as well as minimizing losses depending on body requirements. However, a diet low in iron or other specific circumstances can lead to an imbalance between iron demand and supplies, which is known as iron deficiency (ID). For example, iron demands increase due to the rapid growth of

the fetus during pregnancy as well as rapid growth in childhood or adolescence, especially in young menstruating women. Moreover, inflammation, surgeries or drugs can reduce intestinal iron absorption and, in countries from the global South is frequent that infections cause blood losses, leading to iron depletion. In very rare cases, iron deficiency has a genetic origin. Iron deficiency can lead to anemia (IDA), indeed, it is the cause of 60 % of anemia cases. IDA affects >1.2 billion individuals worldwide, and is associated with poor cognitive and motor development in children, increased morbidity and mortality in women and children, poor birth outcomes, and decreased physical and working capacities in adults (Camaschella, 2019; Bathla and Arora, 2022; Hess et al., 2023).

A commonly recommended strategy to overcome ID is a dietary diversification, including the reduction of those foods that interfere with iron absorption, like phytates and polyphenols derived from vegetables or tannins from tea and coffee, and increasing the presence of those favoring iron absorption like vitamin C. However, this strategy does not always work since it requires changing dietary patterns, obtaining accurate food composition data and an economic investment on more quality food (Nair et al., 2015). On the other hand, oral iron supplementation through inorganic and organic salts such as iron sulfate, fumarate, and gluconate remains a mainstay of therapy. However, absorption of non-heme iron is lower and requires high doses which can lead to ROS-mediated toxicity or inhibition of iron absorption on intestinal mucosa due to systemic regulation, as well as common adverse effects, such as nausea, vomiting, constipation, or diarrhea. Although medical research has adjusted the doses to improve these treatments, alternative methods are still needed (Moretti et al., 2015; Camaschella, 2019). Another strategy consists on food fortification, that is, the addition of selected nutrients to food, regardless they were naturally present or not, in such a manner that nutrient levels approach those recommended by health institutions. Common examples of fortified processed foods include iodized salts, iron and folic acid-fortified wheat, or milk fortified with vitamin D and calcium, which have reduced the prevalence of some diseases associated with nutrient deficiencies. However, food fortification can increase prices with a consequent reduction in the number of consumers, especially in developing countries (Mkambula et al., 2020). One

promising solution to the above-mentioned problems relies on food biofortification, which is a biotechnological approach focused on increasing not only nutrient levels but also their bioavailability, and it occurs before food processing, contrary to general food fortification. Biofortification has multiple advantages: (i) after the initial economic investment on method development, there is not an increase in prices; (ii) several nutrients can be enriched simultaneously; (iii) it is the most sustainable method among other interventions; and (iv) it has a minor impact in organoleptic food properties. However, it fails to restore iron levels in highly deficient populations in a short period of time (Gani et al., 2018). There are several examples of biofortification in plant-derived food, like rice, wheat or cassava (Ofori et al., 2022). However, since *S. cerevisiae* is a widely used microorganism, both for food fermentation and as a nutritional complement itself, as it possesses high protein and vitamin value, several research efforts have been directed towards iron-enrichment of this yeast (Pas et al., 2007; de Llanos et al., 2016; Nowosad et al., 2021). Also, the iron derived from iron-enriched yeasts is bound to metalloproteins, which makes it more bioavailable and easily absorbed. Indeed, studies with rodents showed that it promotes a faster recovery from iron deficiency compared to oral supplementation with inorganic salts (Pirman and Oresnik, 2012; Kyyaly et al., 2015). Moreover, a recent study in humans by Sabatier et al. (2017), showed that iron absorption from iron-enriched yeast added to fresh cheese was in the range of 72–82%. Thus, *S. cerevisiae* can be used both as a tool and as a food for iron biofortification.

2.3. The role of iron-depletion in infection

Iron has also a pivotal role during infection since it is essential for both the host and the pathogen. Multicellular hosts have developed sophisticated mechanisms to deprive invading pathogens of iron. On the one hand, iron is not free in the body. Most iron is bound to hemoglobin in erythrocytes, protected inside cells in the ferritin complexes, or bound to TF and lactoferrin in the blood current and mucosa, respectively (Koleini et al., 2021). On the other hand, when an infection takes place, the host engages a response commonly known as innate nutrient immunity, consisting in reducing the iron that is available to both extra- and intra-cellular pathogens. These mechanisms are present in

vertebrates, invertebrates and plants (Hood and Skaar, 2012). Conversely, pathogens have also got mechanisms to overcome host iron deprivation, such as the production of siderophores, which are small organic molecules present in bacteria, plants and fungi that chelate iron with an extreme affinity, and are considered key determinates of virulence (Kramer et al., 2020; Martínez-Pastor and Puig, 2020). Furthermore, some pathogens possess heme, hemoglobin or transferrin receptors and are able to get iron directly from these sources. Genes encoding iron transporters or receptors used to be grouped in clusters forming virulence islands which can be transferred via horizontal gene transfer (HGT) (Barber and Elde, 2015). As part of the innate immune response, mammals also possess the protein lipocalin 2 which acts as a bacteriostatic agent by sequestering iron chelators (Flo et al., 2004). For all these reasons, iron metabolism is a promising source of new antimicrobial targets (Stelitano et al., 2023). Thus, iron has an important relevance on the virulence of microorganisms and has constrained both host and pathogen evolution. Indeed, hominids TF sequence presents a strong positive selection against recognition by TF binding protein A (TbpA) from infectious microorganisms (Barber and Elde, 2015). Another interesting example is the occurrence of sickle cell anemia, which consists in an anomaly in blood cell morphology due to a point mutation in the β-globin gene. Heterozygous carriers are asymptomatic and present protection from malaria meanwhile homozygous carriers develop severe anemia (Aidoo et al., 2002). Furthermore, recent studies have demonstrated that *Plasmodium falciparum* transmission stages were more prevalent in heterozygous individuals highlighting the narrow relationship between host-pathogen evolution and iron (Ngou et al., 2023).

2.4. Iron deficiency and agronomics

Iron limitation is also an agronomic problem since it affects crop yield and quality. This is important because, despite economic losses, plants are the gateway to the food chain and influence iron levels of other organisms. As depicted for humans, plants have a sophisticated system to overcome iron deficiency, based as well in increasing iron uptake, favoring iron redistribution and remodeling of metabolism. Due to the abundant consumption of plant-based foods world-wide, plants such as maize, rice, wheat, legumes and

cassava are promising tools for iron biofortification, together with yeast (Connorton et al., 2017).

3. IRON TOXICITY AND DETOXIFICATION

The same extraordinary ability of iron to easily alternate between its two most abundant redox states Fe^{2+} and Fe^{3+} can turn it toxic. It is well known that Fe^{2+} ion can engage in Fenton reactions leading to ROS formation. The most common example of Fenton reaction is the Haber-Weiss cycle which implies the participation of Fe^{2+} and the mostly innocuous ROS hydrogen peroxide (H_2O_2), an abundant molecule in the cell (Winterbourn, 1995). ROS generation can oxidize cellular components as lipids, proteins, DNA and RNA molecules, inducing oxidative stress to the cells (Dixon and Stockwell, 2014). One important thing to take into account is that organisms, generally, do not have a regulated mechanism to export iron, thus strategies to overcome iron overload basically imply iron buffering and storage, as well as avoidance of iron uptake.

3.1. Strategies for iron detoxification in eukaryotes

Due to its potential toxicity, either as Fe^{2+}, ISC or heme, iron is not generally free in the cytosol but protein-bounded or organelle-stored. As mentioned above, iron ions and complexes are not able to cross the plasma membrane but rely on transporters (Kaplan and Kaplan, 2009). In eukaryotes, once in the cytosol, iron forms the so-called LIP, which is associated with proteins and delivered either to the mitochondria by iron-chaperones, where ISC and heme synthesis takes place, or stored in the ferritin complex and/or in the vacuole/plastid (Philpott et al., 2023), (Figure 1). Ferritin is a hollow spherical protein that can accommodate large amounts of Fe^{3+} in a safe and compact way, while at the same time allowing easy access to the iron when needed. Besides cytosolic ferritin, other mitochondrial and chloroplast isoforms exist in animals and plants. Ferritin tridimensional structure is widely conserved, even in prokaryotes, although the amino acid sequence can vary a lot (Arosio et al., 2009). In animals, on the other hand, iron is commonly bound to TF when present in the bloodstream, and only in certain circumstances can be detected

as free ions (Dresow et al., 2008). At systemic level, hepatocytes secret hepcidine, which reduces or avoids iron export to the blood stream through FPN1 (Figure 1). Thus, iron remains in enterocytes until they become sloughed or in hepatocytes, which constitute an iron reservoir (Koleini et al., 2021). Intriguingly, ferritin is absent in the fungi kingdom, where vacuoles are used for iron storage instead. Moreover, even though plants possess different ferritin isoforms, it is thought that the main iron storage function is carried out by the plastid in plants (Briat et al., 2010).

3.2. Consequences of iron overload in humans

Although the mechanisms described above protect organisms from iron toxicity, when iron is present in excess, homeostasis can get imbalanced. In humans, iron overload is diagnosed when TF saturation exceeds a threshold making it unable to bind more iron and causing the appearance of free iron, known as non-transferrin bound iron, NTBI (Dresow et al., 2008). Iron excess is accumulated in liver, cardiac and exocrine glands where it can lead to a function impairment. One of the most common causes of iron overload in humans is primary hereditary haemochromatosis (HH), which is caused by mutations in different iron homeostasis genes, mostly affecting the hepcidine-iron sensing axis, and is characterized by an excessive iron uptake (Adams et al., 2023). Inherited syndromes such as α- and β-thalassemia, sickle cell anemia and others are associated with defective erythropoiesis, which treatment used to consist in blood transfusions. This could lead to extra iron acquisition, increased by the low iron signal caused by the defective erythropoiesis (Porter et al., 2016). Another source of iron overload can be dietary intake, occurring in patients with anemia due to overuse of iron supplements (Camaschella, 2019). On the other hand, a growing body of evidence has related intracellular iron accumulation with aging. Iron accumulation at mitochondria is accompanied by mitochondrial dysfunction and ROS production, which could lead to ferroptosis, an iron-dependent mechanism of regulated cell death implying lipid peroxidation and different from apoptosis and necrosis (Dixon et al., 2012; Chen, K. L. et al., 2020; Hughes et al., 2020). Ferroptosis plays a key role in neurodegenerative conditions such as Alzheimer, Parkinson or Huntington diseases (ferrosenescence) as well as in

cancer and metastasis. It has become a topic of interest, and several studies pointed out iron chelators and ferroptosis inducers as promising treatments for neurodegeneration and cancer, respectively (Sfera et al., 2018; Tian et al., 2022; Zhang, R. et al., 2023).

4. IRON DEPLETION RESPONSE IN *SACCHAROMYCES CEREVISIAE*

In *S. cerevisiae*, the response to iron depletion is regulated by the transcriptional factors Aft1 and Aft2, which recognize a short sequence, PyPuCACCCPu, present in the promoter of iron regulon genes and commonly known as FeREs (Iron response elements) (Rutherford et al., 2003). These transcriptional factors are imported into the nucleus by the nuclear import receptor Pse1 regardless of cellular iron status (Ueta et al., 2003). However, under iron-replete conditions, they are exported from the nucleus by the nuclear export receptor Msn5 (Yamaguchi-Iwai et al., 1995). As a result, Aft1 accumulates in the nucleus only under iron-limited conditions. Transcriptional activation does not depend on cytosolic iron but responds indirectly to ISC synthesis occurring in mitochondria (Chen, O. S. et al., 2004). An unknown intermediate molecule of ISC synthesis, X-S, is transported by Atm1, an ATP-binding cassette transporter, to the cytosol and transformed into a $[2Fe–2S]^{2+}$ cluster, which is bound by the monothiol glutaredoxins Grx3 and Grx4 and Bol2/Fra2 protein (Kumanovics et al., 2008; Li, H. et al., 2009). This complex transfers the $[2Fe–2S]^{2+}$ clusters to Aft1/2, favoring their liberation from their targets and their exportation to the cytosol, decreasing the transcription of the iron regulon genes (Li, H. et al., 2009; Ueta et al., 2012; Poor et al., 2014), (Figure 3). Moreover, Aft1 is also downregulated by the mitogen activated protein kinase (MAPK) Hog1 through phosphorylation in certain serine residues (Martins, T. S. et al., 2018). Although these transcriptional factors are paralogs and have overlapping functions, Aft2 has a predominant role regulating intracellular iron and Aft1 in external iron uptake (Courel et al., 2005; Gonçalves, I. R. et al., 2014). The group of genes activated by Aft1/2 are known

as the iron regulon and encode proteins involved in: (i) iron uptake (*FRE1-4, FET3, FTR1, FET4, ARN1-4, FIT1-3*), (ii) iron mobilization from stores (*FET5, FTH1, FRE6, SMF3*), (iii) iron recycling (*HMX1*), (iv) mitochondrial iron import (*MRS4*), (v) iron metabolism remodeling (*CTH1* and *CTH2*), and (vi) biotin and 7-keto-8-aminopelargonic acid (KAPA) uptake (Shakoury-Elizeh et al., 2004; Ramos-Alonso et al., 2020).

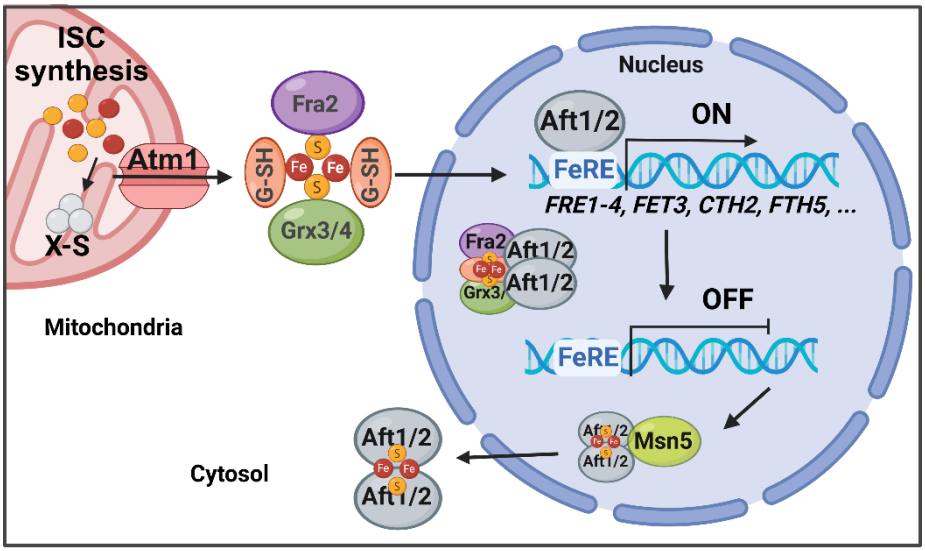

FIGURE 3. DEACTIVATION OF IRON REGULON VIA ISC SYNTHESIS. When ISC synthesis increases at mitochondria, an unknown derived molecule called X-S is exported to cytosol by Atm1. At cytosol, X-S molecule is full processed to $[2Fe–2S]^{2+}$ cluster and bounded by Fra2, Grx3/4 along with two glutathione molecules. This complex enters the nucleus where ISC is transferred to Aft1/2 favoring their dimerization and release from their targets inactivating iron regulon. Finally, Aft1/2 are exported to cytosol by Msn5.

4.1. Iron uptake in *S. cerevisiae*

The principal ways of iron acquisition from the medium in *S. cerevisiae* are: (i) the non-reductive system and (ii) the reductive iron assimilation (RIA) pathway.

The non-reductive system consists on the transport of iron-siderophores complexes through the plasma membrane. Siderophores are small molecules which have a superior affinity for iron and are secreted to the medium by fungi, bacteria and plants. *S. cerevisiae* is unable to synthesize siderophores, but it

can recognize and utilize a wide range of iron-siderophore complexes produced by other organisms and, curiously, more than half of the iron regulon genes are involved in siderophore uptake (Martínez-Pastor and Puig, 2020). Arn1-4 proteins belong to the major facilitator superfamily and are siderophore transporters at the plasma membrane with affinity for specific iron chelates (Figure 4). Moreover, Fit1-3 are secreted serine- and threonine-rich mannoproteins attached to the cell wall which are also involved in siderophores transport (Philpott et al., 2002), (Figure 4).

The RIA system requires a previous step before transport consisting in the reduction of Fe^{3+} to Fe^{2+} by reductases (Philpott, 2006). *S. cerevisiae* possess six different flavocytochrome reductases (Fre1-6) regulated by Aft1/2 in iron depletion conditions: the first four are in the plasma membrane and Fre5 and Fre6 are in the mitochondrial and vacuolar membrane, respectively. There is an additional reductase called Fre7, however it is regulated by copper levels through the transcriptional factor Mac1 and its function is not well characterized (Martins, L. J. et al., 1998; Singh, A. et al., 2007). Although Fre1 and Fre2 are the main responsible for reductase activity of iron and copper ions, they are also able to reduce iron from siderophores, in addition to the siderophores-specific Fre3 and Fre4 reductases (Martins, L. J. et al., 1998; Yun et al., 2001), (Figure 4). Reduced iron is taken up through a high-affinity transport complex that consists of a multicopper ferroxidase (Fet3) and a permease (Ftr1) (Askwith et al., 1994; Wang, T. P. et al., 2003), (Figure 4). Iron oxidation by Fet3 before transport through Ftr1 is essential for the complex function; indeed, Fet3 or Ftr1 monomers are not able to independently reach the plasma membrane and the expression of both genes is coupled. Besides, iron transport via this complex depends on oxygen and copper (Wang, T. P. et al., 2003). On the other side, the low affinity transport system is composed by the membrane transporters Smf1 (not regulated by Aft1/2) and Fet4, which possess low iron specificity and are expressed in iron-replete conditions (Figure 4). Smf1 is a member of the NRAMP family of divalent transporters, which include the mammalian DMT1, and transports primarily manganese into the cytosol (Cohen et al., 2000). Fet4 is a low affinity transporter for iron, copper, zinc and cadmium. Its expression levels are upregulated by low-iron, as well as in hypoxic or anaerobic

conditions, when the Fet3/Ftr1 complex is not able to operate (Hassett et al., 2000; Waters and Eide, 2002).

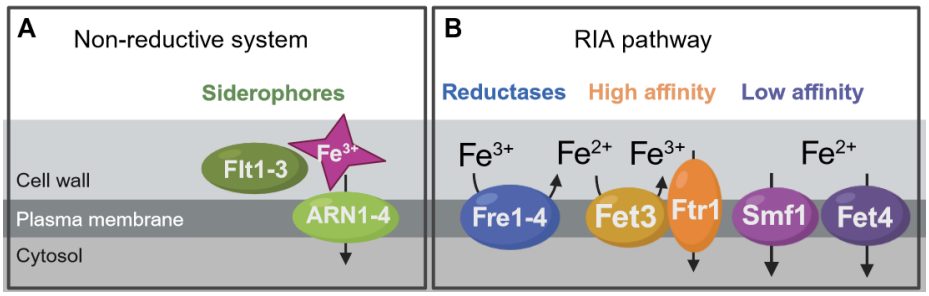

FIGURE 4. IRON UPTAKE PATHWAYS IN *S. CEREVISIAE*. A) Non-reductive pathway is composed by the mannoproteins Fit1-3 which retain siderophores at cell wall and are involved in their transport. Arn1-4 transport iron-bound siderophores. **B)** Fre1-4 reductases are the first step of RIA pathway. Fe^{2+} is transported by the high-affinity complex Fet3/Ftr1 or by the low-affinity transporters Smf1 and Fet4.

4.2. Iron mobilization and recycling

As depicted above, iron detoxification in fungi and plants occurs in the vacuole, which acts as the main iron reservoir. When iron levels decrease, there is an upregulation of *FRE6, FET5, FTH1* and *SMF3* genes by Aft1/2 (Figure 5). In aerobic conditions, Fe^{3+} must be reduced to Fe^{2+} by Fre6 and can then be exported from the vacuole by Fet5/Fth1, the Fet3/Ftr1 complex homologues at the vacuole membrane (Urbanowski and Piper, 1999; Singh, A. et al., 2007). Smf3, as well as Smf1 belongs to the NRAMP family of transporters but the first one is located at the vacuole, where it acts as an additional iron exporter. Although its expression is regulated mainly by Aft2 in iron-depleted conditions, low oxygen levels also upregulate it allowing iron mobilization from the vacuole in anaerobic conditions (Cohen et al., 2000; Jensen and Culotta, 2002). On the other hand, ISC and heme synthesis takes place in mitochondria, essential processes which need iron supply. *MRS4* gene is exclusively upregulated by Aft2 and codifies a mitochondrial iron importer favoring iron import to this organelle (Muhlenhoff et al., 2003; Froschauer et al., 2009), (Figure 5). Finally, Hmx1 is a heme oxygenase located in the membrane of the endoplasmic reticulum where it favors heme recycling and homeostasis (Protchenko and Philpott, 2003), (Figure 5).

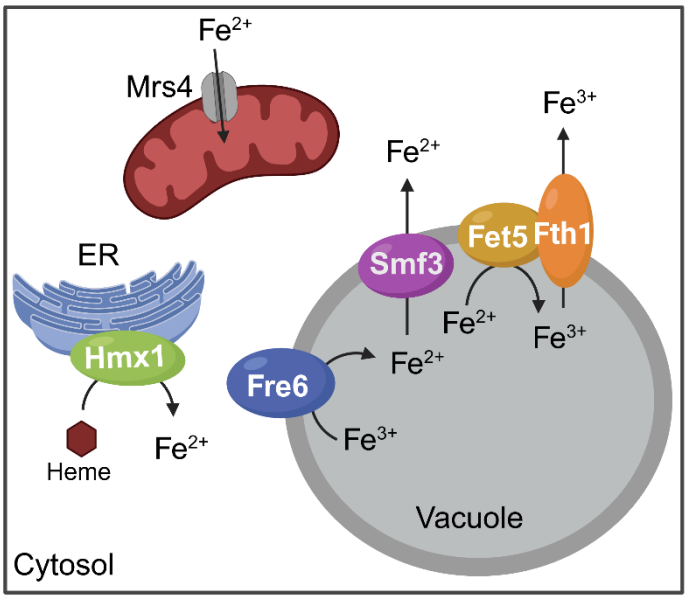

FIGURE 5. IRON MOBILIZATION AND RECYCLING. At cytosol, iron is mobilized from vacuole through the low-affinity transporter Smf3 and the high-affinity complex Fet5/Fth1. Previously, Fe^{3+} has to be reduced by Fre6 to Fe^{2+}. Hmx1 is an heme oxygenase that releases Fe^{2+} from heme-containing proteins. Mrs4 imports Fe^{2+} to mitochondria where ISC and heme synthesis takes place. ER: endoplasmatic reticulum.

4.3. Iron metabolism remodeling

Another important strategy during iron starvation is to limit processes that are iron-consuming but are not strictly necessary. This metabolic remodeling is regulated by Cth1 and Cth2 proteins, which are members of the TTP family and are characterized by the presence of tandem zinc fingers (TZF) motifs able to recognize AREs from the 3'UTR of certain mRNAs (Puig et al., 2005; Prouteau et al., 2008; Puig et al., 2008), (Figure 6A). Both proteins are paralogs and share many targets; however, Cth2 is considered the main acting factor, as it has a wider range of targets and its expression is highly upregulated when the iron deficiency persists, while *CTH1* expression only experiments a slight fluctuation (Puig et al., 2008). Cth2 shuttles between the nucleus and the cytosol; indeed, it possesses a nuclear localization signal embedded in its TZF motif which allows its import to the nucleus. Once in the nucleus, through the TZF motif, it recognizes the AREs of its target mRNAs and binds them co-transcriptionally (Vergara et al., 2011). Then, mRNA-bound Cth2 is exported to

the cytosol where the degradation or translational repression of its target will take place (Pedro-Segura et al., 2008; Vergara et al., 2011; Ramos-Alonso et al., 2019), (Figure 6B). Cth2 targets are mostly implicated in electron transfer chain at mitochondria, but it also regulates TCA cycle components, the biosynthesis of unsaturated fatty acids, ergosterol and sphingolipids, the synthesis of numerous amino acids and cofactors as biotin and lipoic acid. *CCC1* gene, which encodes a vacuolar iron importer, also contains an ARE that is recognized by Cth2, thus limiting iron storage (Puig et al., 2005). Conversely, Cth2 also favors the activity of the RNR enzyme which catalyzes the *de novo* synthesis of deoxyribonucleotides (dNTPs) by degrading *WTM1*, *RNR2* and *RNR4* mRNAs (Sanvinsens and Puig, 2011). Thus, Cth2 performs a pivotal role during iron starvation regarding metabolism, indeed, this protein is highly regulated at both the transcriptional and translational level (Romero et al., 2018).

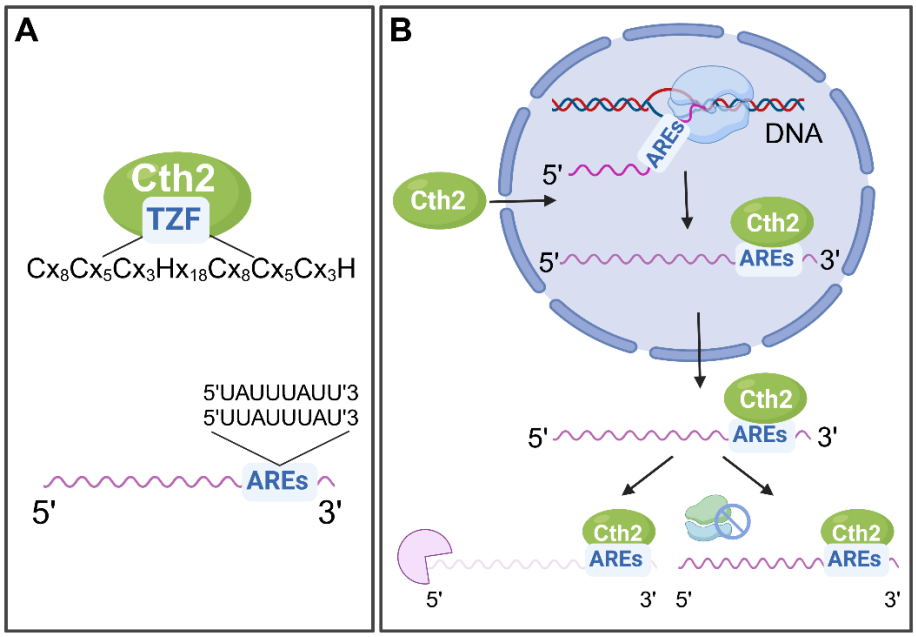

FIGURE 6. MECHANISM OF ACTION OF CTH2. A) Cth2 has a C-terminal domain end characterized by the presence of a cysteine-rich sequence called TZF. This domain is able to recognize uracil- and adenine-rich regions of mRNA 3'UTR known as AREs. TZF and AREs sequence details are depicted. **B)** Cth2 is a shuttle protein that switches between cytosol and nucleus. It binds AREs of nascent transcripts at nucleus. AREs binding allows Cth2 exportation to cytosol where drives their degradation or blockage of their translation.

5. IRON OVERLOAD RESPONSE IN *S. CEREVISIAE*

In the yeast *S. cerevisiae*, there is no mechanism for iron excretion, thus, cytosolic iron levels depend on acquisition from the medium, storage at the vacuole and cellular division. When the extracellular levels of iron are high, the iron regulon is switched off leading to a reduction in iron acquisition and iron mobilization from the vacuole. Moreover, there is an induction of a high-iron transcriptional response, which involves a reduced number of genes compared to low-iron signal. The main player in the response to high iron is *CCC1* (Ca^{2+} sensitive cross-complement 1), a gene encoding a manganese/iron importer located at the vacuolar membrane, responsible for iron storage (Lapinskas et al., 1996; Li, L. et al., 2001). Cells lacking a functional *CCC1* have a severe phenotype in iron excess in both aerobic and anaerobic conditions (Li, L. et al., 2001). Besides, this protein is highly conserved in fungi, plants, protists and prokaryotes but absent in animals (Sorribes-Dauden et al., 2020). Crystal structure resolution of the *Eucalyptus grandis* vacuolar iron transporter 1 (*Eg*VIT1) ortholog made possible the identification of essential and conserved motifs required for metal transport, as well as other species-specific domains (Kato et al., 2019). According to *Eg*VIT1 structure and protein alignments, Ccc1/VIT1 proteins, including yeast Ccc1, possess five transmembrane domains (TMDs), a metal-binding domain (MBD) containing three alpha helixes (H1–H3) between TMD2 and TMD3 that face the cytosol, a cytosolic amino-terminal (Nt) region, and a vacuolar carboxyl terminus (Figure 7). Structure-function data in *Eg*VIT1 also suggest that Ccc1/VIT1 proteins dimerize and function as H^+ antiporters for Fe^{2+} (Cockrell, A. et al., 2014; Slavic et al., 2016; Kato et al., 2019), (Figure 7). The Ccc1/VIT1 cytosolic Nt domain is not conserved among organisms but displays different properties depending on the species (Sorribes-Dauden et al., 2020). *S. cerevisiae* Nt domain possesses serine and lysine residues that have been identified in proteomic studies as phosphorylated and ubiquitylated, respectively, moreover, certain SNPs in this domain are related to low-iron adaptation (Albuquerque et al., 2008; Lee, H. N. et al., 2013; Swaney et al., 2013). Thus, this domain may be dispensable but necessary for fine regulation.

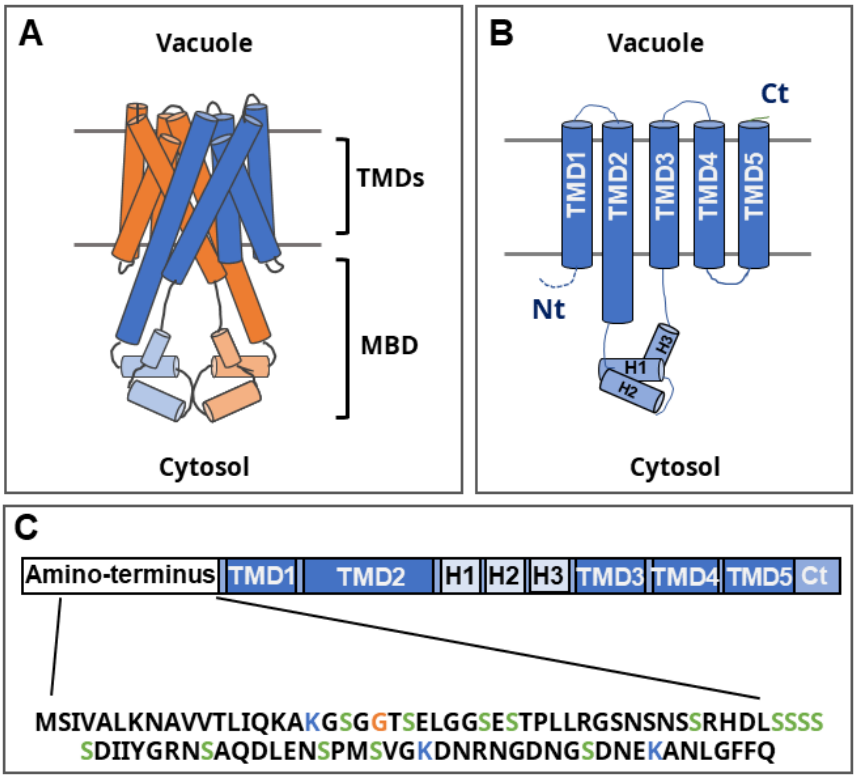

FIGURE 7. SCHEMATIC REPRESENTATION OF CCC1 PROTEIN STRUCTURE. A) Bidimensional drawn of quaternary structure of Ccc1 highlighting main domains (TMDs and MBD). **B)** Membrane topology of Ccc1 showing details of TMDs and helixes (H1-3) of MBD. **C)** Representation of Ccc1 primary structure with amino-terminus sequence. TMDs: Transmembrane domain; MBD: Metal binding domain; H: helix; Nt: Amino-terminus and Ct: Carboxy-terminus. Ubiquitylated lysines, phosphorylated serines and 22th amino acid position are highlighted in blue, green and orange, respectively. Modified from (Sorribes-Dauden et al., 2021; Sorribes-Dauden et al., 2022).

CCC1 most known transcriptional factor is the yeast activator protein (YAP) family member Yap5, which recognizes the Yap response elements (YREs) of *CCC1* and other gene promoters through its amino terminal basic leucine zipper (bZIP) DNA-binding domain (Li, L. et al., 2008), (Figure 8). Yap5 is constitutively bound to YREs in an iron-independent manner, however, it possesses two cysteine-rich domains (CRD) called n-CRD and c-CRD which are able to bind two [2Fe-2S] clusters, thus inducing a conformational change which activates its transcriptional function (Rietzschel et al., 2015). Interestingly, Yap5 activation depends on the synthesis of ISCs at the

mitochondria rather than on cytosolic iron levels. Indeed, defects in ISCs synthesis reduce Yap5 activation regardless of cytosolic iron (Li, L. et al., 2012).

Besides Yap5, *CCC1* expression is regulated by other transcriptional factors in an iron-dependent manner. Indeed, *YAP5* deletion has a less severe phenotype compared to *CCC1* deletion. Recently, Li, L. et al., (2017) have shown that the diauxic shift kinase regulator Snf1 is involved in *CCC1* transcription in a Yap5-independent manner. The general stress response transcriptional factors Msn2 and Msn4 contribute to Snf1-mediated *CCC1* regulation. However, there is still *CCC1* expression in the absence of *MSN2/4*, suggesting that there remain more regulators to be discovered (Li, L. et al., 2017), (Figure 8). Furthermore, *CCC1* mRNA is also regulated at a post-transcriptional level by Cth1/2 under low iron, and Ccc1 transport activity could be influenced by oxidative damage (Puig et al., 2005; Li, L. et al., 2010), (Figure 8). Thus, Ccc1 is highly regulated at transcriptional, post-transcriptional and protein levels, underscoring its important role in iron detoxification. Another mechanism to avoid iron toxicity is mitochondrial storage, as it has been shown that overexpression of the mitochondrial iron importers *MSR3* and *MSR4* decrease iron sensitivity in *ccc1Δ* mutants (Chen, Opal S. and Kaplan, Jerry, 2000; Li, L. et al., 2001; Lin et al., 2011).

Upon iron excess, there is also an upregulation of genes involved in the oxidative stress response such as *TSA1, TRX2*, *SOD1*, *YAP1* or *GRX4* (also a Yap5-target) (Lin et al., 2011; Pimentel et al., 2012). Although most studies focused on the oxidative damage produced by iron, iron toxicity still appears under anaerobic conditions, suggesting that other mechanisms are occurring. Lee et al. (2012) detected an increase in sphingolipid synthesis rate during iron overload in yeast, which induces an impaired signaling cascade transduction responsible for iron toxicity. On the other hand, since iron and manganese possess similar coordination preferences, this metal can compete with manganese in the active site of enzymes such as Sod2 and this mismetallation could lead to dysfunction or inactivation of key enzymes (Yang, M. et al., 2006).

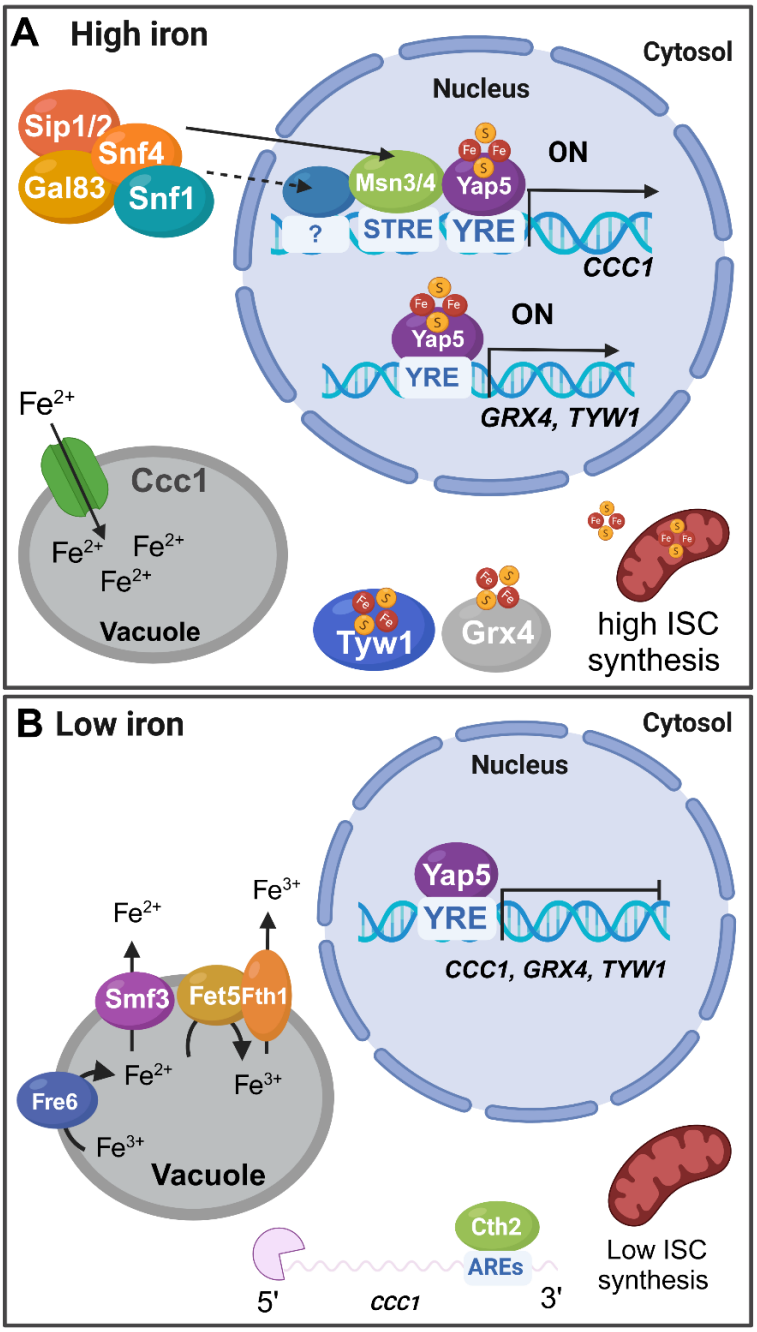

FIGURE 8. REGULATION OF YAP5 TARGETS DEPENDING ON IRON AVAILABILITY. A) Yap5 transcriptional factor is constitutively bound to YREs of its targets in an iron-independent manner, but in high-iron conditions it is able to bind ISC causing a conformational change that fully activates the protein. Yap5 activates

the transcription of *CCC1, GRX4* and *TYW1* among other genes. *CCC1* gene transcription also depends on Msn2/4 transcriptional factors activated by the glucose kinase Snf1, which at the same time would regulate other unknown transcriptional factors. Ccc1 is an iron importer localized at vacuolar membrane. Tyw1 is a ISC-containing protein which, together with the Grx4 glutaredoxin, may be involved in iron buffering at cytosol. **B)** In low iron conditions, the ISC synthesis rate decreases, Yap5 is unable to bind ISC and it is inactivated, although it remains bound to its target YREs. Besides, low ISC synthesis activates iron regulon genes, which causes *CCC1* mRNA degradation through Cth2 and iron mobilization from vacuole.

6. *SACCHAROMYCES* GENUS AND IRON HOMEOSTASIS

6.1. Iron homeostasis divergence in *S. cerevisiae* strains

Iron homeostasis has been deeply studied in the model organism *S. cerevisiae,* as depicted in the above sections, but most studies have been performed in well-stablished laboratory strains. Laboratory strains are usually selected, either deliberately or inadvertently, due to their easy manipulation, they constitute a reduced number group and are genetically isolated from other strains. Thus, these strains have conserved the same genetic background, allowing reproducibility among different research groups which has been useful to decipher fundamental mechanisms and processes. However, laboratory strains usually do not represent the whole species, rather they represent outliers. Laboratory strain traits such as auxotrophies, haploidy or lack of flocculence are mainly absent in nature, and indeed may be deleterious outside the laboratory. On the contrary, wild strains present different genetic backgrounds and are adapted to different iron availabilities and therefore can provide wider insights into the molecular mechanisms of iron homeostasis (Gasch et al., 2016).

Recently, the huge rise of isolated *S. cerevisiae* strains and genome sequences availability due to the fall in sequencing costs have favored the study of the molecular mechanisms behind natural strains adaptation to iron availability in wild environments. Taking into account that iron is a valuable nutrient which is found mostly in the less available state Fe^{3+}, non-laboratory

strains are largely expected to be adapted to low iron environments. Generally, it is observed that iron-sensitive strains have more intracellular iron content than iron-resistant strains (Martínez-Garay et al., 2016). Since there is not an iron excretion mechanism, probably these differences are due to the incapacity of iron-sensitive strains to limit iron uptake in high iron conditions. Curiously, adaptation to iron-limited environments impairs growth in high overload, and vice versa (Martínez-Garay et al., 2016). For example, a work from Lee, H. N. et al., (2013) characterized the iron response of a group of *S. cerevisiae* strains adapted to the nectar of Malaysian bertam palm trees flowers, an iron-limited niche. This group of genetically isolated strains presented a repression of iron uptake genes and an upregulation of high iron-response genes in normal conditions when compared to Wine/European strains. Reciprocal hemizygote analysis revealed the appearance of loss of function alleles in the high iron-response genes *CCC1* and *YAP5*, and a gain of function allele in the transcriptional factor *AFT1*. These genes have been under positive selection and seemed to be responsible for changes in iron sensing, shortening the concentration range to which they respond. Another interesting example is set by the flor yeasts isolated from wineries producing sherry-like wine in Armenia and Crimera. These strains exhibit large deletions of genes involved in iron uptake at a subtelomeric region, together with the deletion of the last 42 amino acids of Aft1. It seems that these deletions allowed an increase in iron uptake but confer a high sensitivity to iron excess (Eldarov et al., 2018). In contrast to lab conditions, siderophores have an important role in iron acquisition in other environments. Siderophores provide an efficient mechanism of iron acquisition and competition among microorganisms. As indicated above, *S. cerevisiae* is unable to synthesize iron siderophores, but it possesses the pathway for uptake and utilization of several siderophores, which allows cheating iron-bound siderophores from other microorganisms (Martínez-Pastor and Puig, 2020). It seems that siderophore biosynthesis was an ancestral treat of certain budding yeasts and has been totally lost in some lineages, while others conserved only the genes implicated in its transport (Krause et al., 2018). The origin of these siderophore biosynthesis pathways has been related in some cases to an operon acquisition from bacteria through horizontal operon transfer (HOT) (Kominek et al., 2019). On the other hand, the limitation of iron acquisition in

iron-resistant strains seems to be conditioned by phosphate uptake, as downregulation of *PHO84*, gene encoding a protein with phosphate-sensing and permease function, favors the reduction of iron uptake. Finally, an increase in the oxidative damage response and the remodeling of carbon metabolism may be also necessary for iron overload tolerance (Balaban et al., 2019; Kocaefe-Ozsen et al., 2022).

6.2. An overview of *Saccharomyces* genus

Saccharomyces genus belongs to the budding yeasts subphylum Saccharomycotina from the Ascomycota phylum. This subphylum is composed of unicellular fungi which lack fruiting bodies, showing highly diverse metabolism, with amino acid sequence divergences comparable to levels observed across plants or animals and ubiquity in nearly every biome of the world on a wide array of substrates. It includes the most known species *S. cerevisiae*, the commensal and opportunistic human pathogen *Candida albicans* or other species of biotechnological interest like *Yarrowia lipolytica* or *Lachanchea thermotolerans* (Shen et al., 2020; Li, Y. et al., 2021). The *Saccharomyces* genus includes 8 species: *S. cerevisiae, S. paradoxus, S. mikatae, S. jurei, S. kudriavzevii, S. arboricola, S. eubayanus* and *S. uvarum* (Figure 9). Although being different species, it is common to find interspecific hybrids involving members of the group in industrial environments, such as the well-known lager-beer yeast *S. pastorianus*, a cross between *S. cerevisiae* and *S. eubayanus* (Alsammar and Delneri, 2020).

All the species share the “Make-Accumulate-Consume” life strategy characteristic of *S. cerevisiae*, consisting in fermenting sugar independently of oxygen availability. It is thought that rapid conversion of sugar into ethanol secures carbon-source and takes advantage of ethanol toxicity for competitors (Merico et al., 2007; Hagman et al., 2013).

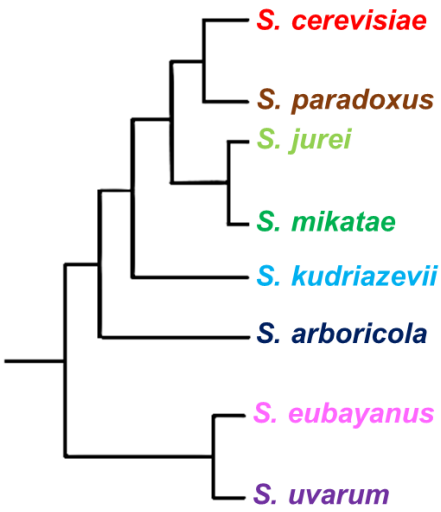

FIGURE 9. SCHEMATIC CLADOGRAM DEPICTING PHYLOGENETIC RELATIONSHIPS AMONG *SACCHAROMYCES* GENUS. Adapted from (Ono et al., 2020).

Generally, metabolic capacities are correlated with the ecological niche where they are present. For example, strains related to beverage fermentation are adapted to nutrient limitation or ethanol production among other stresses (Opulente et al., 2018). In fact, it seems that adaptation to the broad environments across the subphylum was achieved through repeated extensive losses of genes from a more metabolically complex ancestor (Shen et al., 2020).

Although, the most studied strains in the genus are associated with fermentation processes and have genetic marks of domestication, most *Saccharomyces* species are wild. Only *S. cerevisiae, S. uvarum* and at lower frequency *S. paradoxus* have been isolated from humanized environments such as beer, wine or cider (Alsammar and Delneri, 2020). *Saccharomyces* wild strains are generally associated with the plant order Fagales, which includes some of the best-known trees. Most of them have their niche in *Quercus* species, however, *S. uvarum* and *S. eubayanus* which are usually isolated from regions where there are no oak trees, like South America, they are found in *Nothofagus sp*. Actually, it is thought that *Saccharomyces* genus evolution is

closely related to these trees (Alsammar and Delneri, 2020; Peris et al., 2023). Another source of evolution is thought to be environmental temperature: *S. uvarum* and *S. eubayanus* are cryotolerant, and *S. paradoxus* and *S. cerevisiae* are thermoresistant. The other species in the genus also grow better at low temperatures which suggests that it is an ancestral trait. Several studies have pointed out mitochondrial DNA (mtDNA) as a key factor in yeast speciation and in the adaptation to temperature (Gonçalves, P. et al., 2011; Li, X. C. et al., 2019; Peris et al., 2023). Moreover, it is possible to isolate strains form different species of the genus in the same habitat, suggesting that adaptation to different temperatures has allowed the coexistence of species (Salvadó et al., 2011; Spurley et al., 2022; Peris et al., 2023).

Genomes are mostly homozygous, tending to conserve gene synteny, and evolution mainly relies on single nucleotide polymorphisms (SNPs) with the remarkably exemption of domesticated strains (Boynton and Greig, 2014; Peris et al., 2023). Adaptation to human environments has involved chromosomal rearrangements, aneuploidies, polyploidies, HGTs, interspecific hybridizations and introgressions deeply conditioning the evolutionary history of these yeasts (Yue et al., 2017; Giannakou et al., 2020). A typical example are *S. cerevisiae* strains, which are divided into different lineages that correlate with geography, environmental niches and the degree of human association. Domesticated and wild clades fall into two well-delineated sides of the tree and are separated by a large group of mosaics, with some exceptional cases. Subtelomeric regions are considered hotspots of copy number variation (CNV) or HGT acquisition and are related to cell-cell interaction, secondary metabolism and stress responses (Peter et al., 2018).

Saccharomyces species are genetically divergent among species and populations, indeed, the minimum amino acid identity interspecies is comparable to *Homo sapiens* and *Mus musculus* amino acid identity, around 70%. *S. cerevisiae* displays the major phenotypic diversity, although the most genetic divergence is observed among *S. paradoxus* populations, followed by *S. kudriavzevii* and *S. uvarum*. Certainly, *S. mikatae* and *S. cerevisiae* populations are the less genetically divergent. The major genetic distance is registered between *S. kudriavzevii* or *S. arboricola* and the other strains. *S.*

eubayanus and *S. uvarum* strains are the less phenotypically diverse species compared with the other ones and the genetic distance between them is the lowest (Peris et al., 2023). The most divergent haplotypes are found in East Asia strains, which suggest that many *Saccharomyces* lineages originated in this region (Lee, T. J. et al., 2022).

Due to the genetic diversity present in these genus, even at an interspecies level, the wide availability of isolated strains, genomes, and data regarding growth characterization in several conditions, *Saccharomyces* genus presents an extraordinary opportunity to study iron homeostasis divergence. Moreover, this genus has a close relationship with humans as these yeasts participate in the fermentation process of widely-consumed foods. Exploring this diversity may allow us to obtain and characterize strains that become useful as biotechnological tools for improving iron content.

OBJECTIVES

OBJECTIVES

The main objective of this thesis is to increase the knowledge about the molecular mechanisms behind the diverse strategies that yeasts use to adapt to high iron conditions. All together to obtain yeast strains with alterations in iron metabolism of biotechnological interest. Our aim can be split in four objectives depicted in the corresponding chapters:

1- To determine the ideal form of iron to screen for iron sensitivity regarding to oxidation state, salt composition and pH.

2- To decipher the conservation and domain diversification across the Tree of Life of the vacuolar iron transport protein Ccc1, the main player in *S. cerevisiae* iron detoxification.

3- To obtain a *S. cerevisiae* strain able to accumulate high levels of iron weighing a tradeoff.

4- To study the iron metabolism diversity of different populations of the *Saccharomyces* genus.

RESULTS

CHAPTER 1:
Iron toxicity depends on iron source

Raquel Sorribes-Dauden [1,2], Nicolás García-García[2], María Teresa Martínez-Pastor [1,2,*] and Sergi Puig [2,*]

[1]Departamento de Bioquímica y Biología Molecular, Universitat de València, Burjassot, Valencia, Spain

[2]Departamento de Biotecnología, Instituto de Agroquímica y Tecnología de Alimentos (IATA), Consejo Superior de Investigaciones Científicas (CSIC), Paterna, Valencia, Spain

* Authors to whom correspondence should be addressed.

(Draft. Not submitted)

1. ABSTRACT

Iron participates as a cofactor in several key biological processes like DNA replication and repair, cellular respiration and photosynthesis, rendering it essential for virtually all organisms. At the same time, iron overload is toxic for cells since it can engage in Fenton's reactions leading to reactive oxygen species generation that damage cellular components. Thus, organisms have developed molecular mechanisms for keeping iron levels into a narrow range. The baker's yeast *Saccharomyces cerevisiae*, besides being a model organism for the study of iron homeostasis, it has also been used as a biotechnological tool for metal detoxification and biofortification. Previous studies have analyzed the behavior of different yeast strains upon excess iron, but different iron sources were used, making any comparison difficult. In this study, we analyzed the suitability of three different iron salts prepared with and without acid addition for iron-resistance phenotyping. All the tested iron salts had reduced solubility in water, with $(NH_4)_2Fe(SO_4)_2$ (FAS) being the most soluble, followed by $FeSO_4$ and $FeCl_3$. Despite its solubility can be increased by lowering the pH of the stock preparation, $FeCl_3$ precipitates when added to the growth medium, probably due to the formation of $Fe(OH)_3$, $FePO_4$ or both, which prevents monitoring of growth in liquid medium. A precipitate was also observed when FAS or $FeSO_4$ were added to the growth medium from a stock solution without HCl. Since the concentrations of HCl used did not cause any growth defect but prevented FAS and $FeSO_4$ salts to precipitate, we conclude that both salts prepared with HCl are suitable for iron-resistance phenotyping.

KEYWORDS: yeast, iron toxicity, ferrous ammonium sulfate, ferrous sulfate, ferric chloride, iron bioavailability, pH

2. INTRODUCTION

Iron is an essential metal present as a redox cofactor in many key biological pathways like biosynthesis of the main cellular components (nucleic acids, proteins, lipids), cellular respiration, photosynthesis or oxygen transport (Ramos-Alonso et al., 2020). However, when present in excess, iron becomes toxic since it can favor Fenton reactions that lead to reactive oxygen species (ROS) generation and as a consequence cell damage (Winterbourn, 1995). Consequently, organisms have developed fine-tuned mechanisms to maintain

intracellular iron concentrations at physiological levels. Despite its abundance, in oxidative environments iron tends to react with oxygen forming ferric hydroxides, which are poorly soluble at neutral to alkaline pH, rendering its bioavailability very low. In fact, iron deficiency is the most widespread nutritional disorder that affects humans worldwide and can lead to iron deficiency anemia (IDA) in the most severe cases. IDA affects approximately 25 % of global population and it is related to fatigue, cognitive development impairment, headache or gastrointestinal disorders (Bathla and Arora, 2022).

It has been proved that food biofortification decreases the occurrence of anemia with greater benefits in populations with risk of deficiency (Bouis and Saltzman, 2017; Gani et al., 2018; Olson et al., 2021). Besides, biofortification constitutes the most sustainable strategy to restore iron levels in humans and, unlike iron supplements, it is not related to side effects like gastrointestinal problems, parasite infections, or sickness, and it allows quite higher bioabsorption (von Haehling et al., 2019; Lowe, 2021). Moreover, once the biotechnological tool is developed, biofortification entails low costs and it usually has a small impact on food organoleptic properties. Several works have pointed out that the baker's yeast *Saccharomyces cerevisiae* is an ideal iron carrier (Ofori et al., 2022). This yeast is closely related to human life, since it has been used for food fermentation (e.g. bread, wine and beer) along history. Besides, yeast is used as a nutritional supplement because it is especially rich in proteins, vitamins, amino acids and fiber, making it a food with a high nutritional value (Sun, J. et al., 2022). Moreover, this model organism can be easily used as a tool for the study of biological processes, since a wide range of molecular mechanisms are conserved from yeast to humans (Kaplan and Kaplan, 2009).

In recent years, the number of sequenced genomes of budding yeast strains and other fungi species has experimented a huge rise, allowing the exploration of iron homeostasis alleles that could be of biotechnological interest (Peter et al., 2018; Shen et al., 2020; Opulente et al., 2023; Peris et al., 2023). Several studies have been performed in order to assess the phenotypical diversity and molecular mechanisms that are behind yeast adaptation to iron excess or depletion (Pimentel et al., 2012; Lee, H. N. et al., 2013; Eldarov et

al., 2018; Balaban et al., 2019). However, comparisons of growth behavior in iron excess among these studies are sometimes difficult, since different sources of iron have been used, being ferric chloride, $FeCl_3$ (de Llanos et al., 2016; Eldarov et al., 2018; Ramos-Alonso et al., 2018); ferrous sulfate, $FeSO_4$ (Li, L. et al., 2008; Pimentel et al., 2012; Lee, H. N. et al., 2013); and ferrous ammonium sulfate, $(NH_4)_2Fe(SO_4)_2{\cdot}6H_2O$ or FAS (Li, L. et al., 2010; Bleackley et al., 2011; Hughes et al., 2020) the most commonly used. In the present work, our aim is to study how the type of iron salt influences the iron resistance phenotype of *S. cerevisiae* and to determine which iron source is better to use, regarding iron redox state (Fe^{2+} or Fe^{3+}), stock preparation (dissolution in HCl, H_2SO_4, or H_2O) or salt composition ($FeCl_3$, $(NH_4)_2Fe(SO_4)_2{\cdot}6H_2O$ or $FeSO_4{\cdot}7H_2O$).

3. MATERIALS AND METHODS

3.1. Yeast strains and growth conditions

All the *S. cerevisiae* strains used in this study are listed in Table C1.2. All experiments were performed in synthetic complete (SC) medium unless otherwise is specified. Yeast nitrogen base without amino acids and ammonium sulfate (Condalab, Madrid, Spain) salt composition is depicted in Table C1.1. Solid and liquid SC medium was prepared in distilled water at 2X, autoclaved and, when it is less warm, iron is added. Distilled water is added to the medium once the iron is present to achieve the volume needed to dilute it to 1X. Ferric chloride ($FeCl_3$, Merck-Sigma, Darmstadt, Germany) stock solutions were prepared at 125 mM in Milli-Q water and 0.1 HCl (Phillipsburg, New Jersey, USA). Ferrous ammonium sulfate ($(NH_4)_2Fe(SO_4)_2{\cdot}6H_2O$ or FAS, Merck-Sigma, Darmstadt, Germany) was added to the medium from a 100 mM stock solution prepared with Milli-Q water or 0.1 M HCl. Ferrous sulfate ($FeSO_4$, Merck-Sigma, Darmstadt, Germany) stocks were prepared at 100 mM in Milli-Q water with 1mM H_2SO_4 or 0.1 HCl. Growth was also tested in SC supplemented with the equivalent HCl concentration. For grow spot assays, overnight precultures were adjusted to an OD_{600} of 0.1, 0.01, and 0.001, and

then spotted on SC agar plates with the indicated form and concentrations of iron. Plates were incubated for 3 days at 28 ˚C and then photographed.

TABLE C1.1. YEAST NITROGEN BASE SALT COMPOSITION

Compound	g/L	Compound	g/L
Biotine	0.000002	Niacine	0.0004
Boric acid	0.0005	p-Aminobenzoic acid	0.0002
Calcium chloride	0.1	Potassium iodide	0.0001
Calcium pantothenate	0.0004	Riboflavine	0.0002
Ferric chloride	0.0002	Sodium chloride	0.1
Folic acid	0.000002	Sodium molybdate	0.0002
Inositol	0.002	Thiamine hydrochloride	0.0004
Magnesium sulfate	0.5	Zinc sulfate	0.0004
Manganese sulfate	0.0004	Cupric sulfate	0.00004
Monopotassium phosphate	1		

3.2. pH and absorbance measurements

pH was determined in SC liquid media supplemented with the different iron forms and concentrations used in spot assays, through a Crison Basic 20 pHmeter with HACH 50-12T electrode (Hach Lange Spain, L'Hospitalet de Llobregat, Barcelona). Absorbance was measured using a V-12000 spectrophotometer (VWR, Radnor, Pennsylvania, USA).

4. RESULTS

4.1. Characterization of iron resistance using $FeCl_3$ as a source of iron.

In a previous report, we analyzed the response of a set of *S. cerevisiae* strains from a wide diversity of origins to excess iron and classified them according to their sensitivity to this condition (Martínez-Garay et al., 2016). A representative group of them, listed in Table C1.2, together with the reference strain BY4741, were challenged to different concentrations of ferric chloride ($FeCl_3$). Strains were grown as described in Materials and Methods of this section, and spotted in SC plates with different concentrations of $FeCl_3$, which was added from a stock solution dissolved either in Milli-Q water or 0.1 M HCl. Regardless of how the stock was prepared, sensitive strains (UWOPS03-461.4, CBS5287, YPS128, Sc9) stopped their growth at 5 mM $FeCl_3$, while iron-resistant strains (L246, Kyokai 6, YJM978) kept growing at 7 mM. Finally, no growth was observed at higher iron concentrations for any strain (Figures C1.1A and C1.1B). In parallel, pH and turbidity (A_{600}) were measured in liquid media. We observed a noticeable fall in pH as the iron concentration increased, which was accentuated in the presence of HCl in the stock solution. Surprisingly, iron addition in both cases originated an increase in medium turbidity which increased along with iron concentration, with a greater effect in the stock prepared with water (Figures C1.1C and C1.1D). Such elevated turbidity can interfere with growth analysis in liquid media through absorbance registration, thus, $FeCl_3$ is not a good salt for liquid growth analysis.

TABLE C1.2. *S. CEREVISIAE* STRAINS USED IN THIS WORK. *Classification according to (Peter et al., 2018). ** Classification according to (Martínez-Garay et al., 2016).

Strain	Synonym	Ecological source	Geographical origin	Population*	Iron Phenotype**
BY4741	-	Laboratory	-	NA	Reference
L246	-	Fermentation (Wine)	South America (Chile)	NA	Resistant
UWOPS03-461.4	-	Wild (Nectar bertam palm)	Asia (Malaysia)	19. Malaysia	Sensitive
Kyokai No. 6	CECT10711	Fermentation (Sake)	Asia (Japan)	25. Sake	Resistant
CBS5287	CLIB219-2B	Wild (Grape)	Europe (Russia)	18. Far East Asia	Sensitive
YPS128	-	Wild (Quercus soil)	North America	23.North American oak	Sensitive
YJM978	-	Human (Clinical)	Europe (Italy)	1.Wine/European	Resistant
Sc9	-	Wild (Soil)	Europe (Hungary)	NA	Sensitive

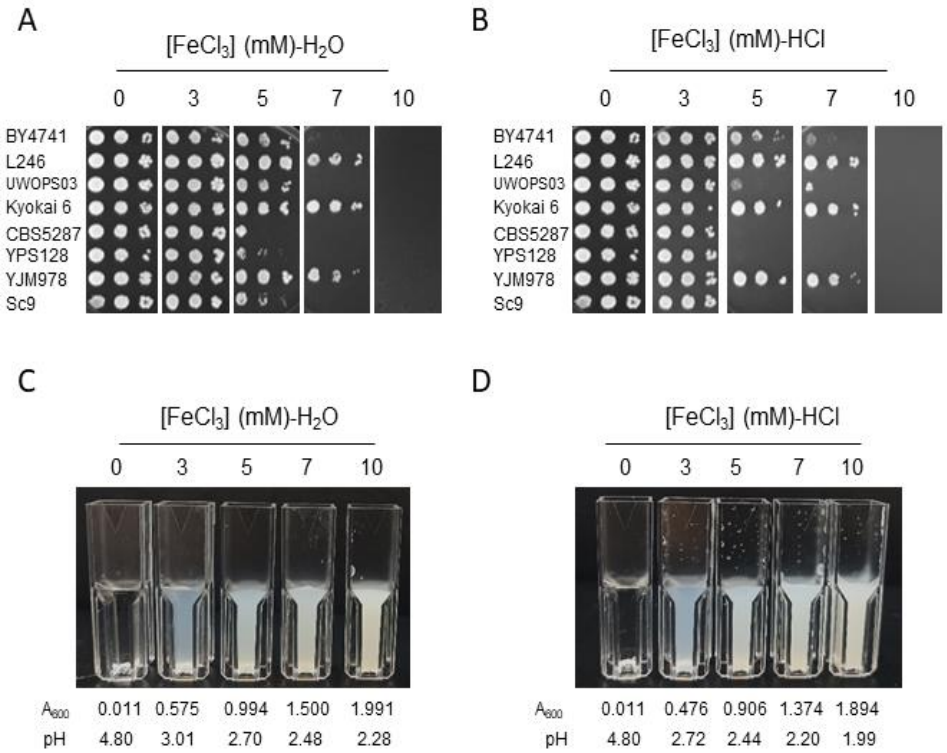

FIGURE C1.1 EFFECT OF $FeCl_3$ ON YEAST GROWTH AND MEDIA. A AND B) Overnight precultures were spotted on SC agar plates with the indicated range of $FeCl_3$ concentrations, from a stock prepared with Milli-Q water or 0.1 M HCl, respectively. **C) AND D)** Representative images of liquid medium supplemented with different $FeCl_3$ concentrations, from stock prepared with Milli-Q water or 0.1 M HCl, respectively. Absorbance and pH measurements of each medium condition are depicted below the photographs. UWOPS03 is the abbreviation for UWOPS03-461.4.

4.2. Characterization of iron resistance using $(NH_4)_2Fe(SO_4)_2$ salt

Strains were spotted in SC solid plates with iron, added in the form of ((NH4)2Fe(SO4)2·6H2O or FAS at different concentrations from a stock solution prepared with Milli-Q water or 0.1 M HCl (Figure C1.2A and C1.2B, respectively). In this case, a quite different effect was observed depending on the solvent used for the preparation of FAS stock. When the stock was prepared with Milli-Q water, only iron concentrations as high as 35 mM started to cause a growth arrest in some iron-sensitive strains. At 50 mM FAS, none of the iron-

sensitive strains were able to grow, but this concentration was still non-toxic for the iron-resistant strains (Figure C1.2A). Iron addition from the water-prepared stock caused a slight decrease in pH, compared to the observations with $FeCl_3$, and also a slight effect on medium turbidity that, nonetheless, could interfere with liquid growth measurements (Figure C1.2C).

On the other hand, HCl addition to the FAS stock solution lowered to 7 mM the concentration at which iron-sensitive strains arrest their growth, and to 15 mM the concentration at which no growth is detected (Figure C1.2B). Moreover, pH decreased at a similar but slower rate than with $FeCl_3$ addition. Conversely, no iron-compound precipitation was not observed, only modest turbidity could be seen at lower concentrations (Figure C1.2D). These results indicate that: (1) FAS is a less acidic salt than $FeCl_3$, although it still shows some weak acid properties that lower pH but to a lesser degree; (2) FAS is not well dissolved in water, which would make iron less available to yeast cells and, as a consequence, an effect on growth is only observed at very high FAS concentrations; and (3) HCl increases FAS solubility due to a drop in pH, since less iron concentration is needed to cause toxicity, and turbidity is not observed.

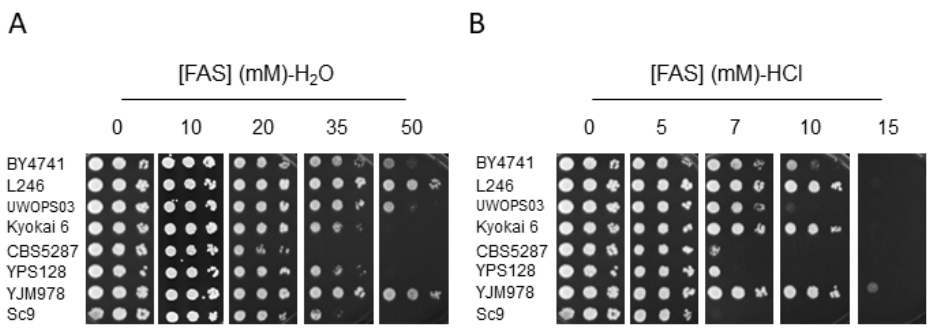

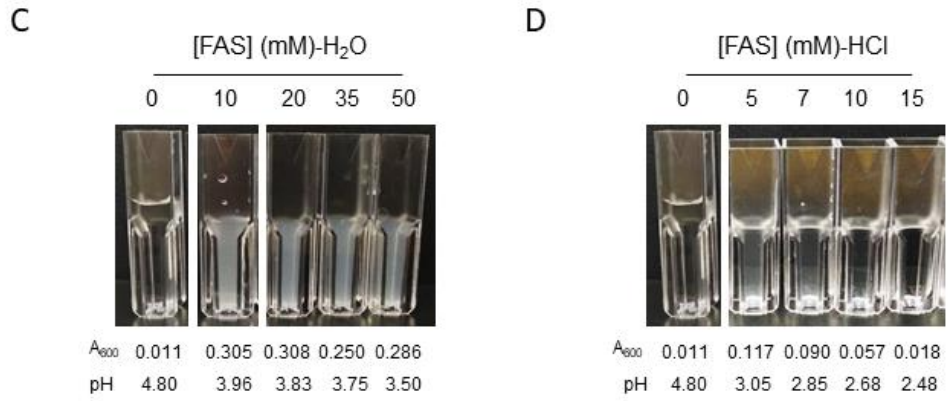

FIGURE C1.2. EFFECT OF FAS ON YEAST GROWTH AND MEDIA. A AND B) Strains were grown as above and spotted on SC plates supplemented with FAS dissolved in Milli-Q water or 0.1 M HCl, respectively. **C AND D)** FAS prepared with Milli-Q water and 0.1 M HCl, respectively, were added to SC liquid medium. Absorbance and pH were determined as above and pictures of the medium were taken.

4.3. Characterization of iron resistance using $FeSO_4$ salt as an iron source

Growth of the strains used in this study was also tested in SC plates supplemented with $FeSO_4$. It was not possible to solubilize $FeSO_4 \cdot 7H_2O$ in Milli-Q water. Therefore, $FeSO_4$ stock was prepared with 1 mM H_2SO_4 or 0.1 M HCl (Figure C1.3). When the stock was prepared with H_2SO_4, results were similar to FAS preparation in Milli-Q water: there was a needed for a higher concentration of iron to cause strains growth arrest (Figure C1.2A and C1.3A). However, absorbance measurements were more similar to the $FeCl_3$ assay: $FeSO_4$ addition to liquid medium led to elevated turbidity, which increased along with iron concentration (Figure C1.3C). Similar to FAS, when HCl was used for stock preparation, iron toxicity appeared at lower concentrations and the drop in pH became more noticeable. Again, HCl addition made turbidity inappreciable, maybe because pH decrease improves iron solubility in a similar way to FAS stock prepared with HCl (Figure C1.3D). Altogether, these results suggest that the ammonium ion in FAS is important for solubility, but it does not cause a difference in toxicity since growth results with both salts were vastly similar. Increasing iron salt solubility with HCl allows the analysis of strains' growth in liquid medium.

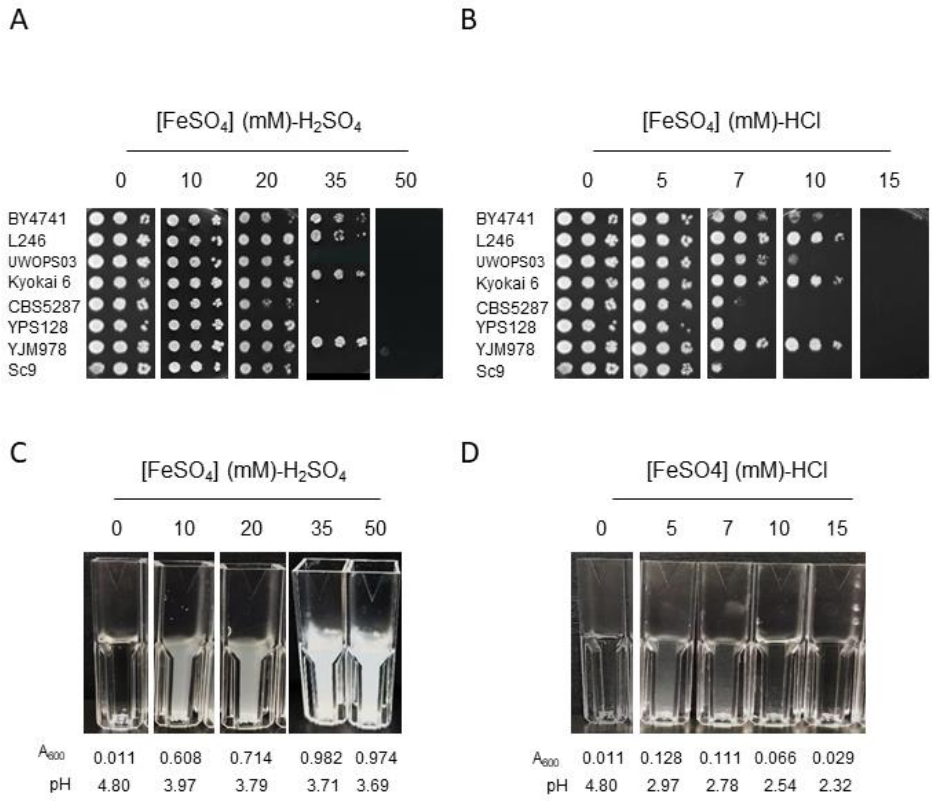

FIGURE C1.3. EFFECT OF $FeSO_4$ ON YEAST GROWTH AND MEDIA. A AND B) Strains' growth on agar plates with $FeSO_4$ addition from a stock dissolved in 1 mM H_2SO_4 and 0.1 M HCl, respectively. **C AND D)** Images, absorbance, and pH measurements of liquid medium supplemented with the stocks used in A and B.

4.4. Characterization of growth in HCl

To distinguish among the effect that iron and HCl addition exert on yeast growth, we cultured the selected strains on SC plates with HCl concentrations equivalent to those previously used in the above experiments. We observed that pH decreased at the same rate as when any iron salt is added from a HCl-prepared stock. Iron phenotype and growth arrest can be studied at 7 mM and 10 mM, respectively, when $FeCl_3$ is used and up to 15 mM in the case of the other salts, since HCl concentrations do not cause any growth defect (Figures C1.4A). Thus, a decrease of pH below 2.5 caused by HCl is not sufficient to explain the observed toxicity, being iron the main responsible (Figures C1.4A,

C1.2D, and C1.3D). Moreover, no turbidity was detected in liquid medium when HCl was added (Figure C1.4B).

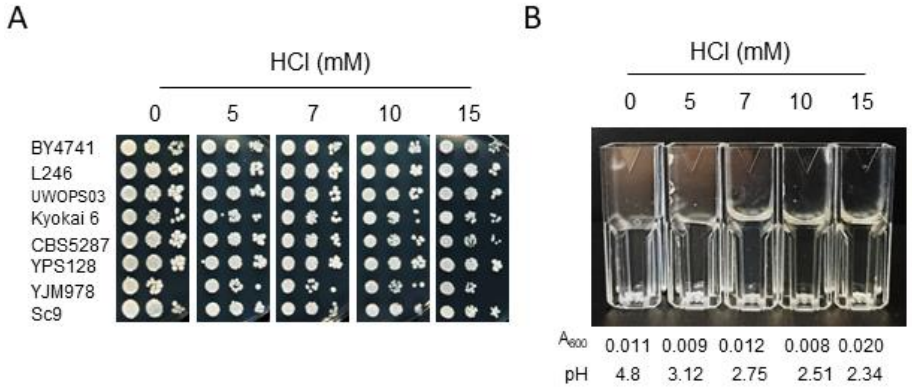

FIGURE C1.4. GROWTH OF *S. CEREVISIAE* STRAINS IN HCL SOLID MEDIUM. A. Growth assays were performed as above in SC agar plates with the indicated range of HCl concentrations. **B.** Representative images, pH, and absorbance measurements of each medium condition are depicted.

4.5. Effect of medium composition in precipitate formation

As we have shown above, when iron is added to the SC medium, especially when it comes from a stock prepared in water, turbidity increases probably due to the formation of a precipitate derived from iron. It is well known that iron in an aqueous solution can interact with OH^- anions and lead to $Fe(OH)_3$ or $Fe(OH)_2$ formation, both poorly soluble and prone to precipitate (Stefansson, 2007). Moreover, iron ions can interact with plenty of ligands and salts present in the medium (Schroder et al., 2003). Thus, in order to avoid the influence of medium composition in precipitate formation, we added iron directly to Milli-Q water. As shown in Figure C1.5A, turbidity was observed when $FeCl_3$ was added from a stock prepared with Milli-Q water, however, it did so to a lower degree compared to SC medium observations, and only at the highest tested concentration. On the contrary, when iron was added from the HCl-prepared stock, there was no precipitate formation unlike what we observed in SC medium (Figure C1.1B and C1.5B). Regarding pH, the fall occurred at the same rate that in SC medium, however, the pH of Milli-Q water was more acidic than SC medium. If the iron salt was changed to FAS or $FeSO_4$, turbidity faintly appeared at the highest concentration when the stock was prepared with water,

and none was observed when HCl was present in the stock. Again, the pH variation resembled that observed in SC medium (Figure C1.5C, C1.5D, C1.5E and C1.5F). Similarly, precipitate was also formed in stock solutions without HCl (Figure C1.5G), confirming that HCl increases the solubility of the three iron salts. When iron was added to water or SC, the decrease in pH necessary to make precipitate disappear was lower than in stocks, where iron was more concentrated. Taken together, these observations suggest that iron precipitation depends on SC medium composition and is closely related to pH.

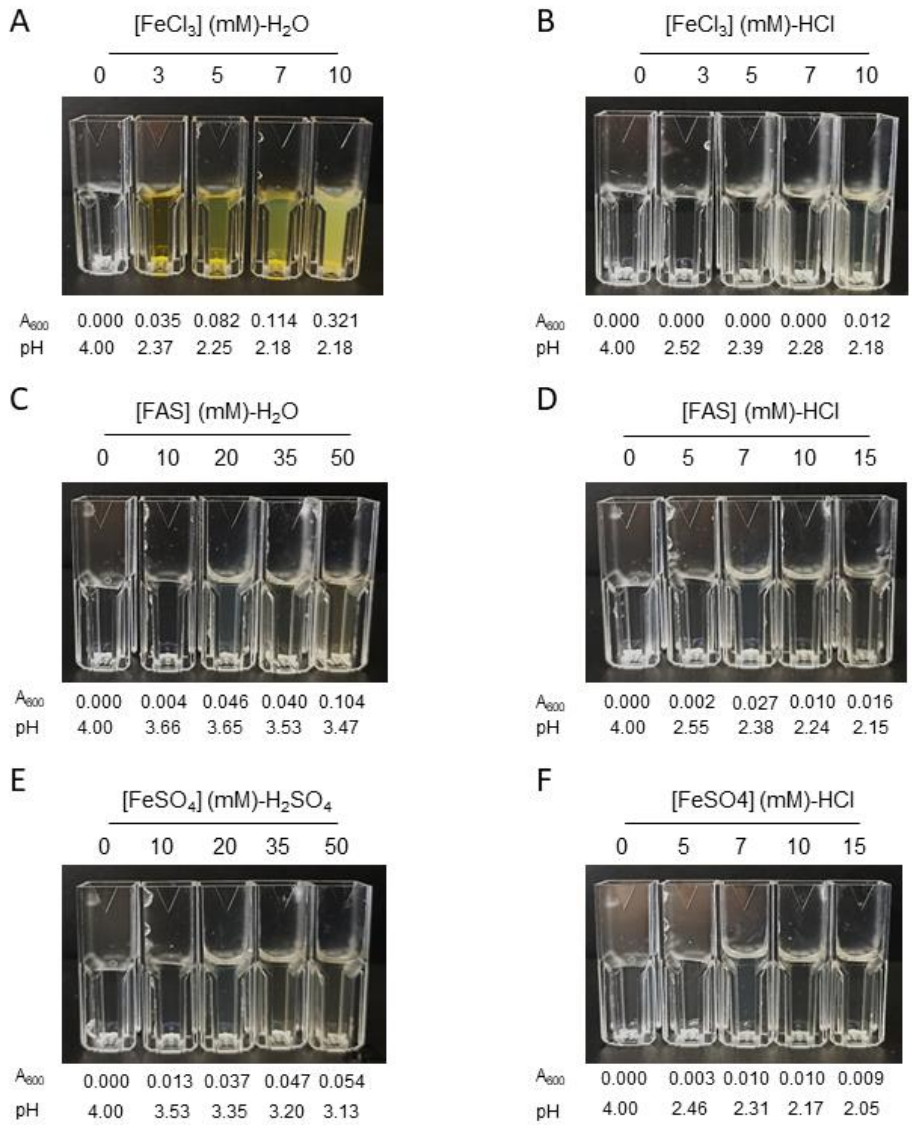

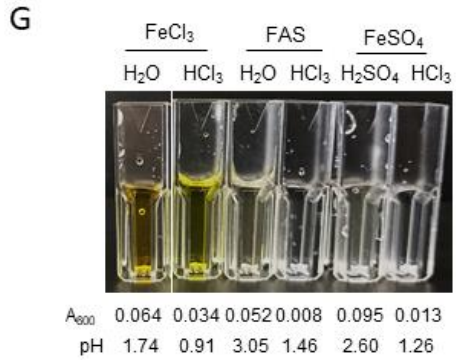

FIGURE C1.5. IRON SOLUBILITY IN MILLI-Q WATER. A-F) Representative images of iron addition to Milli-Q water at indicated concentrations and from different salt preparations. **G)** Representative images of the different salt stocks mentioned above. The absorbance and pH of each solution are also shown under the images.

5. DISCUSSION

In this study, we grew 8 strains that were previously characterized regarding their phenotype in iron excess. We observed the same behavior as previously described for all the salt preparations used here, as compared to the laboratory strain BY4741: L246, Kyokai 6, and YJM978 are iron-resistant strains, whereas UWOPS03-461.4, CBS5287, YPS128, and Sc9 are iron-sensitive strains (Martínez-Garay et al., 2016). Regardless of the salt type, the same tendency was observed for the tested strains, but at a different range of concentrations. $FeCl_3$ resulted more toxic than the other iron salts when the stock was prepared with Milli-Q water and with HCl-addition, since a lower concentration was needed to achieve growth arrest (Figures C1.1-3). $FeCl_3$ is an acidic salt, since when dissolved in an aqueous medium it leads to ferric hydroxide ($Fe(OH)_3$) and HCl production, according to the following acid-base equilibrium:

Equation 1: $FeCl_3 + 3H_2O \leftrightarrow Fe(OH)_3\downarrow + 3\ HCl$

Since HCl is a very strong acid, it is only present in the deprotonated form in water dissolution. Thus, proton liberation decreases pH and makes iron more accessible (Figure C1.1C and C1.1D), (Stefansson, 2007). The same reason could account for the lower concentration required for FAS or $FeSO_4$ to inhibit

growth on solid medium, when the stock is prepared with HCl (Figure C1.2B and C1.3B). It is known that iron solubility can be increased almost 6 orders of magnitude when pH changes from 7 to 2 and, indeed, lowering the extracellular medium pH is a widespread strategy among organisms to increase iron uptake (Kaplan and Kaplan, 2009).

Regarding turbidity in liquid medium, a precipitate was observed in all cases when the stock was prepared with Milli-Q water (Milli-Q water and H_2SO_4 for $FeSO_4$ and added to the SC medium, which would interfere with growth recording based on absorbance measurements (Figure C1.1C, C1.2C, and C1.3C). One possibility is that the iron-derived compound is $Fe(OH)_3$, which is formed in water dissolution according to the equilibrium depicted in Equation 1 and is barely insoluble. This might account when iron is added directly to water, since there is not anything else present (Figure C1.5A). Indeed, when $FeCl_3$ stock is prepared with 0.1 HCl, precipitate is not observed, probably due to a shift to the left in the equilibrium which would lower $Fe(OH)_3$ formation (Figure C1.5B). The higher presence of salts in SC medium could favor $Fe(OH)_3$ precipitation through an increase in ionic strength and would explain why HCl addition in the stock is not enough to avoid precipitation. However, SC medium used in this experiment is more complex, involving trace element-containing salts, such as boric acid, copper sulfate, or potassium iodide, as well as other salts like potassium phosphate monobasic, magnesium sulfate anhydrate, sodium and calcium chloride (see Materials and Methods of this chapter). Since potassium phosphate concentration is up to 1 g/L, and it is well documented that iron has a strong affinity for phosphate, another possibility points out ferric phosphate dihydrate, $FePO_4 \cdot 2H_2O$, salt as a candidate behind the achieved turbidity (Pa Ho, 1976; Pierri et al., 2000; Schroder et al., 2003). Nonetheless, further experiments would be necessary to discern the molecular identity of the precipitate observed when $FeCl_3$ is added to SC medium.

On the contrary, when the used iron form is Fe^{2+} as $FeSO_4$ or FAS at pH <8, the hydrolysis is virtually absent. Instead, the aquo-complex $[Fe(H_2O)_6]^{2+}$ is formed, which can be easily oxidized to form $Fe(OH)_3$. The addition of H_2SO_4 when the $FeSO_4$ stock is prepared with Milli-Q water slightly probably prevents $[Fe(H_2O)_6]^{2+}$ formation, thus diminishing the oxidation of $FeSO_4$, and favoring

its dissolution, which is not possible otherwise (Guimarães et al., 2007; Gaensly et al., 2014). On the contrary, FAS is a double sulfate salt containing both ferrous sulfate, $FeSO_4$, and ammonium sulfate, $(NH_4)_2SO_4$, in equimolar quantities. The presence of the double sulfate makes iron less susceptible to oxidation than $FeSO_4$ itself and there is no need for acid addition to prepare the stock in water (Gaensly et al., 2014), (Figure C1.5C). In both cases, when the stock is prepared in HCl, there is a decrease in pH making oxidation more difficult (Greenwood and Earnshaw, 1997; Guimarães et al., 2007). Fe^{2+} oxidation is also influenced by ligands. Thus, it would not be surprising that this ion is more prone to oxidation in SC medium and could also participate in $FePO_4 \cdot 2H_2O$ formation as proposed for $FeCl_3$ (Greenwood and Earnshaw, 1997). Furthermore, there is huge evidence that points out that iron is more prone to be up taken from the medium by yeasts when it is present as $FeSO_4$ or FAS (Pas et al., 2007; Gaensly et al., 2014).

6. CONCLUSIONS

All salts can be used for spot assays in solid medium since the same tendency is observed regarding iron source. However, if it is necessary to analyze growth in liquid medium, it is better to use $FeSO_4$ or FAS instead of $FeCl_3$ since, in aqueous medium, Fe^{3+} is prone to react with other cations present in the medium, probably leading to $Fe(OH)_3$ and $Fe(PO_4)_3$ formation. Both salts are highly insoluble and may be the responsible for the observed precipitate that don't allow liquid growth recording. Moreover, if Fe^{2+} is used as $FeSO_4$ it is important to lower pH thought acid addition which prevents iron oxidation and thus, precipitation occurrence. FAS is less susceptible to iron oxidation due to the presence of the double sulfate; however, it is better to use along with an acid to make it fully soluble in SC medium. Moreover, HCl at the added concentrations does not cause growth arrest, thus the observed growth inhibition is mainly caused by iron addition. In summary, FAS or $FeSO_4$ salts prepared with HCl seem to be the best option for iron-resistance phenotyping.

Author Contributions: Conceptualization, M.T.M-P. and S.P.; Methodology, R.S-D. and N.G-G. Investigation, R.S-D., and N. G-G. Resources S.P.; Data curation, R.S-D. Writing—original draft preparation, R-S-D., M.T.M-P. and S.P.; Writing—review and editing, R-S-D., M.T.M-P. and S.P. Visualization, R.S-D. Supervision, M.T.M-P. and S.P.; Project administration, S.P.; Funding acquisition, S.P. All authors have read and agreed to the published version of the manuscript.

Funding: This research was supported by grants BIO2017-87828-C2-1-P, PID2020-116940RB-I00, RED2018-102467-T, and CEX2021-001189-S funded by MCIN/AEI/10.13039/501100011033 and, in the case of BIO2017-87828-C2-1-P, by ERDF A way of making Europe. This work has also been supported by a predoctoral fellowship ACIF/2018/077 to R.S-D., both funded by “Generalitat Valenciana” and European Social Fund (ESF).

Institutional Review Board Statement: Not applicable.

Informed Consent Statement: Not applicable.

Data Availability Statement: Not applicable.

Acknowledgments: We thank all the members of the Iron Homeostasis laboratory for technical assistance.

Conflicts of Interest: The authors declare no conflict of interest. The funders had no role in the design of the study; in the collection, analyses, or interpretation of data; in the writing of the manuscript; or in the decision to publish the results.

CHAPTER 2:

Structure and function of the vacuolar Ccc1/VIT1 family of iron transporters and its regulation in fungi

Raquel Sorribes-Daudén[1], David Peris [2,3], María Teresa Martínez-Pastor[1] and Sergi Puig[2*]

[1]Departamento de Bioquímica y Biología Molecular, Universitat de València, Burjassot, Valencia, Spain.

[2]Departamento de Biotecnología, Instituto de Agroquímica y Tecnología de Alimentos (IATA), Consejo Superior de Investigaciones Científicas (CSIC), Paterna, Valencia, Spain.

[3]Department of Biosciences, University of Oslo, Oslo, Norway.

* Authors to whom correspondence should be addressed.

Computational and Structural Biotechnology Journal 18 (2020) 3712–3722

1. ABSTRACT

Iron is an essential micronutrient for most living beings since it participates as a redox active cofactor in many biological processes including cellular respiration, lipid biosynthesis, DNA replication and repair, and ribosome biogenesis and recycling. However, when present in excess, iron can participate in Fenton reactions and generate reactive oxygen species that damage cells at the level of proteins, lipids and nucleic acids. Organisms have developed different molecular strategies to protect themselves against the harmful effects of high concentrations of iron. In the case of fungi and plants, detoxification mainly occurs by importing cytosolic iron into the vacuole through the Ccc1/VIT1 iron transporter. New sequenced genomes and bioinformatic tools are facilitating the functional characterization, evolution and ecological relevance of metabolic pathways and homeostatic networks across the Tree of Life. A thorough sequence analysis shows that Ccc1/VIT1 homologs are widely distributed among organisms with the exception of animals. The recent elucidation of the crystal structure of a Ccc1/VIT1 plant ortholog has enabled the identification of both conserved and species-specific motifs required for its metal transport mechanism. Moreover, recent studies in the yeast *Saccharomyces cerevisiae* have also revealed that multiple transcription factors including Yap5 and Msn2/Msn4 contribute to the expression of *CCC1* in high-iron conditions. Interestingly, Malaysian *S. cerevisiae* strains express a partially functional Ccc1 protein that renders them sensitive to iron. Different regulatory mechanisms have been described for non-Saccharomycetaceae Ccc1 homologs. The characterization of the structure, function and regulation of Ccc1/VIT1 proteins is of high interest in the development of biofortified crops and in the protection against microbial-derived diseases.

2. INTRODUCTION

Iron is an indispensable micronutrient for almost all living organisms since it participates as a cofactor in a wide range of biochemical processes, such as oxygen transport, electron transfer in the respiratory and photosynthetic chains, lipid biosynthesis, DNA replication and repair, as well as ribosome biogenesis and recycling. Although iron is the fourth most abundant element in the Earth's crust, the predominant form of iron is ferric iron (Fe^{3+}), which solubility is very low at physiological pH. Thus, organisms have developed or acquired from other organisms sophisticated mechanisms to overcome poor iron

bioavailability (Andrews, N. C. and Schmidt, 2007; Ganz and Nemeth, 2012; Connorton et al., 2017; Martínez-Pastor and Puig, 2020). The same redox properties that make iron an essential element render it potentially toxic. When in excess, iron can participate in Fenton reactions, leading to reactive oxygen species (ROS) generation that can damage proteins, lipids and nucleic acids in the cell (Eid et al., 2017). Since there is no regulated mechanism for iron excretion, organisms protect themselves from iron toxicity by regulating its acquisition and distribution, and by storing its excess in the less harmful form Fe^{3+}, that can be mobilized when needed.

The most ancient molecule involved in iron detoxification, protection and storage is hypothesized to be ferritin (Arosio et al., 2009). Ferritin is present in mammals, plants, bacteria and archaea, but it is absent in fungi, where iron is stored in the vacuole (Raguzzi et al., 1988). The tertiary structure of this molecule is highly conserved and consists of a multisubunit hollow sphere that can shelter up to 4000 iron atoms in a compact configuration. Ferritin has ferroxidase activity that allows iron to be stored as ferric iron. In animals, iron release from ferritin is mainly promoted in the lysosomes. Then, iron is transported to the cytosol for reutilization, probably via the divalent metal transporter 1, DMT1, and it is exported from the cell through ferroportin. Thus, these vacuole-equivalent organelles act as recycling compartments rather than as a storage site (Kurz et al., 2011). Plant ferritin, phytoferritin, is very similar in sequence and structure to mammalian ferritin, but it is not localized in the cytoplasm, being instead distributed into organelles like plastids and mitochondria. It is thought that plant ferritin provides iron to metabolic processes in these organelles as well as protection from oxidative stress (Briat et al., 2010) Nonetheless, the most important iron storage site in plants, and similarly in fungi, is the vacuole (Sharma et al., 2016). In the budding yeast *Saccharomyces cerevisiae*, extracellular iron can enter vacuoles via steady state endocytosis (Li, L. et al., 2001). In fact, yeast mutants unable to endocytose display growth defects in iron-deficient conditions, an observation that highlights the physiological relevance of endocytosed iron (L. Li et al., 2001). However, the major mechanism for iron detoxification in yeast cells depends on Ccc1 protein, which localizes to the vacuolar membrane and

transports iron from the cytosol into the vacuole, being responsible for ~60% of vacuolar iron accumulation under iron-replete conditions (Li, L. et al., 2001; Cockrell, A. et al., 2014). Spectroscopy studies have shown that, in fermenting yeast cells, vacuolar iron is predominantly found as magnetically mononuclear high-spin Fe^{3+} species, although Fe^{3+} nanoparticles are also present (Cockrell, A. L. et al., 2011; Nishida and Silver, 2012; Holmes-Hampton et al., 2013). Specifically, vacuolar Fe^{3+} associates to low-molecular-mass polyphosphate chains consisting of 6 to 20 phosphate units coordinated to 1-3 metal ions (Nguyen et al., 2019). In response to iron depletion, Fre6 metalloreductase reduces vacuolar Fe^{3+} to Fe^{2+}, and then Fet5-Fth1 high-affinity and Smf3 low-affinity iron transporters export Fe^{2+} to the cytoplasm (Urbanowski and Piper, 1999; Portnoy et al., 2000; Singh, A. et al., 2007). During the shift from fermentation to respiration, yeast cells transiently accumulate iron in mitochondria and vacuoles (Park et al., 2013). Vacuolar pH and the oxidation state determine the form of iron stored in the vacuole (Cockrell, A. L. et al., 2011; Cockrell, A. et al., 2014). A *ccc1Δ* mutant is extremely sensitive to high iron concentrations and displays severe oxidative damage (Li, L. et al., 2001; Cockrell, A. et al., 2014).

Complementation assays with *S. cerevisiae ccc1Δ* mutant strain allowed the identification in *Arabidopsis thaliana* (*At*) of the first plant Ccc1 ortholog, denoted *At*VIT1 (Vacuolar iron transporter) (Kim, S. A. et al., 2006). *At*VIT1 localizes to the tonoplast membranes of the endodermal cells of *Arabidopsis* seeds, and its disruption leads to iron distribution impairment and poor seed growth (Kim, S. A. et al., 2006). The important role of plant VIT1 and its homologs have emerged as attractive targets for the development of iron biofortified crops to improve crop productivity (Zhang, Y. et al., 2012; Narayanan et al., 2015; Connorton et al., 2017). In addition to VIT1 orthologs, plants express the so-called VIT1-like (VTL) genes. In *A. thaliana*, VTL transporters *At*VTL1-5 share high similarity with *At*VIT1, and most of them are iron regulated and complement the *ccc1Δ* yeast mutant (Gollhofer et al., 2014). Besides plants and fungi, Ccc1/VIT1 homologs have been found in other organisms, including bacteria and protists (Brembu et al., 2011; Bhubhanil et al., 2014; Sankari and O'Brian, 2014; Slavic et al., 2016). Interestingly, the

crystal structure of *Eucalyptus grandis* VIT1 (*Eg*VIT1) homolog has been recently elucidated, allowing the comparison between Ccc1/VIT1 orthologs particularly on the residues required for metal transport (Kato et al., 2019). The aim of this mini-review is to explore and discuss the diversity of the Ccc1/VIT1 family of iron transporters, focusing on fungal Ccc1 function and regulation by iron.

3. MATERIALS AND METHODS

3.1. Orthology search

In order to know the distribution of *S. cerevisiae* Ccc1 homologs across the Tree of Life, we retrieved Ccc1 sequences from MetaPhOrs 2.0 database (Pryszcz et al., 2011; Chorostecki et al., 2020). An additional search limited to Metazoa taxa was performed using the tblastn method of BLAST search tool (Altschul et al., 1990), detecting a potential homolog in *Spodoptera litura* (Phylum: Arthropoda; LOC111363577). We did not include this organism because the most likely scenario might be a bacterial sequence contamination during sequencing, since there is no metazoan Ccc1/VIT1 homologs and the *S. litura* sequence was phylogenetically related to four bacterial sequences (*Niastella koreensis, Spirosoma linguale, Mucilaginibacter paludis* and *Flavobacterium psychrophilum*) (Figure C2.1 and Figure C2.S1). 24 additional Ccc1 homolog sequences, not detected by the two previous methods but published, were downloaded using the accession numbers included in Table C2.S1. A total of 745 potential Ccc1 homologs were obtained. Proteins with a consistency score (CS) equal or higher than 0.5 were retained. A CS of 0.5 indicates that 50% or more gene tree predictions agreed to suggest the protein sequence is a homolog of the query protein. Sequences containing errors were also discarded.

3.2. Phylogenetic analysis

A final alignment of 707 amino acid sequences was generated using MAFFT v7.388 (Katoh and Standley, 2013) in Geneious 2019.1.1 (Kearse et al., 2012) with the following parameters: FFT-NS-I x 1000 algorithm, BLOOSUM 62 scoring matrix and gap open penalty 1.53 with offset value 0.123

(https://perisd.github.io/EukCCC1/). An untrimmed sequence was used for phylogenetic reconstruction (Figure C2.1), as the presence/absence of specific domains are phylogenetically informative. Another phylogenetic tree with a previous trimming step with ClipKIT v0.1.2 (Steenwyk et al., 2020) was reconstructed to remove the gaps shown in more than 99% (-g 0.99) of the sequences. A third phylogenetic tree was reconstructed using a trimmed alignment (-g 0.99), but without the MBD region. All trees showed similar topologies. Maximum-likelihood (ML) phylogenetic trees were reconstructed using IQTree v2.0.3 (Minh et al., 2020), under the LG+F+R10 (for the first two alignments) or LG+R10 (for the alignment without MBD) evolutionary protein models estimated by ModelFinder (Kalyaanamoorthy et al., 2017), which is implemented in IQTree. Branch support was assessed with the ultrafast bootstrap and SH-aLRT methods by performing 1000 pseudoreplicates. The resulting unrooted phylogenetic trees were represented in R v3.6.3 (R Development Core Team 2010) parsed using treeio v1.10.0 (Wang, L. G. et al., 2020) and drawn with ggtree v2.0.4 (Yu et al., 2016) packages, using the equal angle layout. More detailed phylogenetic trees were represented with iTOL and they can be accessed following the next link: http://itol.embl.de/shared/Peris_D.

4. Ccc1/VIT1 conservation and distribution across the Tree of Life

To explore the conservation and diversity of the Ccc1/VIT1 family of proteins, Ccc1/VIT1 homologs were retrieved from the MetaPhORs database (Pryszcz et al., 2011; Chorostecki et al., 2020) using the *S. cerevisiae* Ccc1 protein as a query (for further details see Supplementary Information of this chapter). Up to 721 homolog protein sequences were retrieved and 23 public available sequences were manually added (Table C2.S1). Ccc1/VIT1 homologs are widely distributed across the Tree of Life with the exception of Metazoa taxa, where ferritin is the main iron storage protein. Ferritin is also the main iron storage site in Archaea and Bacteria, although these two groups of organisms also contain Ccc1/VIT1 homologs. These Ccc1 protein homologs are functionally related to bacterioferritin, but their main function is the export

of iron out of the cell (Bhubhanil et al., 2014; Sankari and O'Brian, 2014, 2016). We classified the Ccc1/VIT1 homologs in eight different groups according to phylogenetic analysis and protein structure (Figure C2.1 and C2.S1). Archaea and Bacteria are mostly found in groups I and II. Group III includes VTL protein from angiosperm plants (monocots and dicots), Lycopsida class (Gollhofer et al., 2014), and a small divergent group composed by the diatom *Phaeodactylum tricornutum (*Brembu et al., 2011), the algae *Chlamydomonas reinhardtii*, and *Schizosaccharomyces* fission yeasts. Group IV is enriched in protist parasites, such as species *Plasmodium* and *Trypanosoma* (Huang et al., 2014; Slavic et al., 2016). The topology of the tree indicates that *VTL* was transferred from an archaean lineage during the origin of the last common eukaryote ancestor (Williams et al., 2020). A second major clade includes groups V-VIII, which contains plant VIT1-type (Kim, S. A. et al., 2006) and fungi homologs (Figure C2.1 and C2.S1). Group V also contains 21 bacterial sequences and one Rhodophyta algae (*Cyanidioschyzon merolae*). A plausible scenario is an ancestral horizontal gene transfer from bacteria to the ancestor of eukaryotes, where most fungi (groups VI-VIII) and Viridiplantae retained the gene (Figure C2.1 and C2.S1), (Cao, 2019). The presence of more than one homolog in several Archaea and Bacteria species and the high domain diversity in prokaryotes (next section) support a complex evolutionary history for this protein family. In plants, several transpositions and both segmental and tandem duplication events contributed to generate an elevated number of Ccc1/VIT1 proteins with specialized functions (Table C2.S1) (Sharma et al., 2016; Cao, 2019). In a lesser extent, gene expansions have also occurred in some clades of fungi like the genus *Aspergillus* and *Penicillium*, *Glomeromycota* division, and *Mucoromycotina* and *Agaricomycotina* subdivisions.

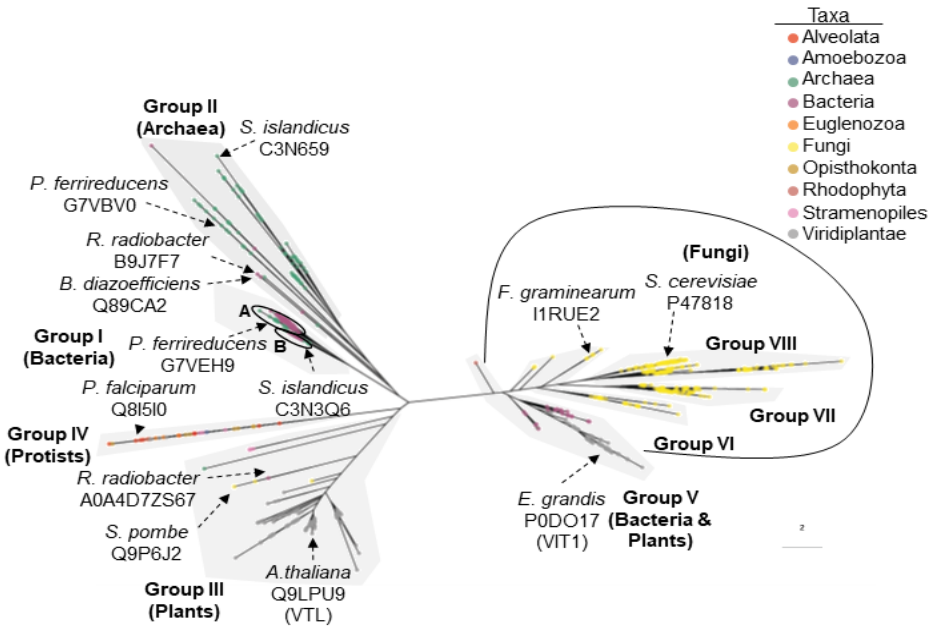

FIGURE C2.1. PHYLOGENETIC TREE RECONSTRUCTION OF THE IRON VACUOLAR TRANSPORTER CCC1/VIT1. A maximum likelihood phylogenetic tree was reconstructed using the complete Ccc1/VIT1 protein alignment. The scale bar represents the number of amino acid substitutions. Sequence names of some published proteins are indicated (more details in Table C2.S1). Tips are colored according to taxa designation, which taxonomic depth is different for simplicity. Most frequent taxa are displayed in each group. *A. thaliana: Arabidopsis thaliana; B. diazoefficiens: Bradyrhizobium diazoefficiens; E. grandis: Eucalyptus grandis; F. graminearum: Fusarium graminearum; P. ferrireducens: Pyrobaculum ferrireducens; P. falciparum: Plasmodium falciparum; R. radiobacter: Rhizobium radiobacter; S. cerevisiae: Saccharomyces cerevisiae; S. islandicus: Sulfolobus islandicus.*

5. CCC1/VIT1 FAMILY STRUCTURE AND FUNCTION

The recently solved crystal structure of the *Eucalyptus grandis Eg*VIT1 protein and its function-structure analysis have allowed the identification of conserved domains and residues within Ccc1/VIT1 proteins that are essential for the mechanism of iron transport (Kato et al., 2019). *Eg*VIT1 possesses five transmembrane domains (TMD1-5), with a cytoplasmic loop containing three alpha helices (H1-3) between TMD2 and TMD3. Its amino-terminal region faces the cytosol, whereas its carboxy-terminal extreme localizes towards the

vacuolar lumen (Figure C2.2). *Eg*VIT1 functions as a dimer and the interface formed by the two protomers constitutes a channel through which the metal ions are translocated. In this cavity, TMD1 and TMD2 provide conserved amino acids with oxygen and sulfur atoms (tyrosine and methionine), as well as carboxylated groups from glutamate and aspartate amino acids, conferring a hydrophilic environment appropriated for metal ion transport (Figure C2.3), (Kato et al., 2019). Indeed, aspartate 43 and methionine 80 are found in almost all Ccc1/VIT1 sequences (Figure C2.3). These two amino acids are present at the entrance of the cavity and are involved in the coordination of the metal ions and in the discrimination between alkaline earth- and transition-metal ions, respectively (Kato et al., 2019). Methionine 80 might also participate in preventing proton leakage to the cytosol (Kato et al., 2019). The other transmembrane segments are disposed around this cavity. The hydrophilic cavity is opened in the cytosolic face, but it is sealed at the opposite side by hydrophobic residues. To deliver iron to the vacuole, glycine and proline residues generate kink motions that release the seal and allow iron entry into the vacuole (Kato et al., 2019). In the same way, glycine residues 44, 69 and 76 of *Eg*VIT1 are present in barely all group sequences (Figure C2.3). Studies in *Arabidopsis* have shown that this highly conserved glycine residue, located within the second TMD, is critical for VIT1 iron transport activity (Mary et al., 2015).

Amino acid sequence similarity is low throughout the different species, but Ccc1/VIT1 domains and structure are mostly maintained. Besides such conservation, some domains are highly variable, such as the metal-binding domain (MBD). The MBD is constituted by the carboxy-terminal region of TMD2 and H1 and H3 helices, with both helices forming the cytoplasmic loop between TMD2 and TMD3 (Figure C2.2). This domain is rich in glutamate residues and it has been proposed to facilitate iron incorporation from siderophores and other iron-containing molecules (Kato et al., 2019). This domain is absent in groups IA, II and III, and seems to be lost independently in these groups. The addition or removal of this region does not affect the topology of the phylogenetic tree of Ccc1/VIT homologs (Figure C2.S1).

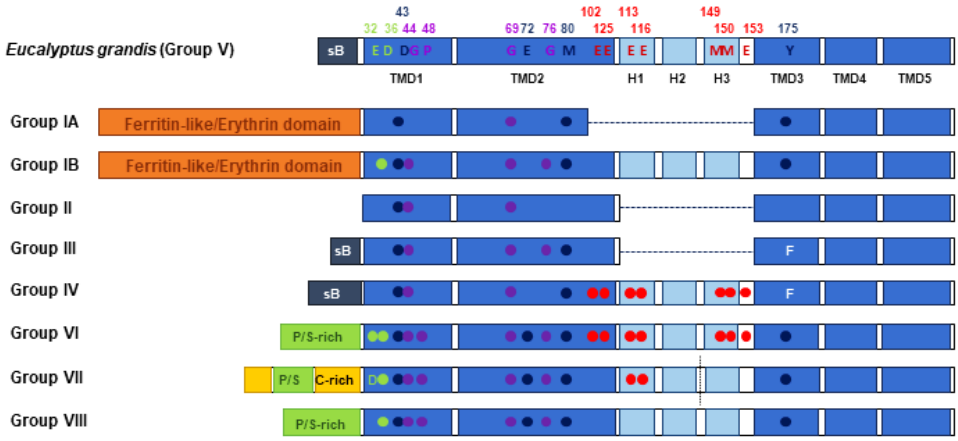

FIGURE C2.2. DOMAIN ORGANIZATION AND AMINO ACID CONSERVATION IN CCC1/VIT1 FAMILY PROTEINS. Schematic representation of the architecture and key amino acids of the consensus sequence of each group. *Eg*VIT1 group V key amino acids are represented by its IUPAC letter and by the following color code: green for amino acids involved in iron transport from the MBD to the hydrophilic cavity; dark blue, amino acids involved in the transport throughout the cavity; purple, residues implicated in the induction of the seal opening; and red, residues within the MBD. White letters are used when other amino acids are conserved for more than two non-group V protein groups, and circles represent conserved amino acids colored as above for non-group V proteins. Dark and light blue rectangles represent the five TMDs and the three helices, respectively. Orange, grey, green and yellow rectangles symbolize Ferritin-like/erythrin domain, short basic (sB), proline/serine-rich (P/S-rich) and cysteine-rich (C-rich) motives, respectively. Group VII sequences contain a unique short amino acid sequence in the MBD, represented by a dashed line. Numbers indicate the amino acid position in *Eg*VIT1 protein. Alignment of 707 amino acid sequences is available in the following link: https://perisd.github.io/EukCCC1/.

Instead, in some proteobacteria there is an amino-terminal ferritin-like or erythrin domain consisting of a four-α-helix bundle containing the Ex6Y, ExxH, Ex6Y and ExxH motifs and forming a di-iron-binding site. This domain has the ability to oxidize Fe^{2+} to Fe^{3+}, as a typical ferroxidase catalytic subunit (Andrews, S. C., 2010; Bhubhanil et al., 2014; Sankari and O'Brian, 2014). Curiously, the MDB also protects against H_2O_2 stress, probably by limiting free iron availability for ROS generation (Ruangkiattikul et al., 2012). Mutations in glutamate residues from the erythrin domain impair iron export and the oxidative stress response (Sankari and O'Brian, 2014). Sequences belonging to group IB contain an MBD-like domain consisting of the erythrin domain

pattern but lacking well-defined third and fourth helices. Plant VTL proteins lack the MBD and differ in sequence from VIT1 homologs. In *A. thaliana*, most VTL transporters localize to the tonoplast and participate in iron homeostasis (Gollhofer et al., 2014). Interestingly, recent studies have shown that VTL1a from *Glycine max,* VTL8 from *Medicago truncatula,* and probably SEN1 from *Lotus japonicum* localize to the symbiosome membrane and deliver iron from the plant to the bacteroid in order to supply iron-demands derived from the symbiosis interaction (Hakoyama et al., 2012; Brear et al., 2020; Liu et al., 2020; Walton et al., 2020).

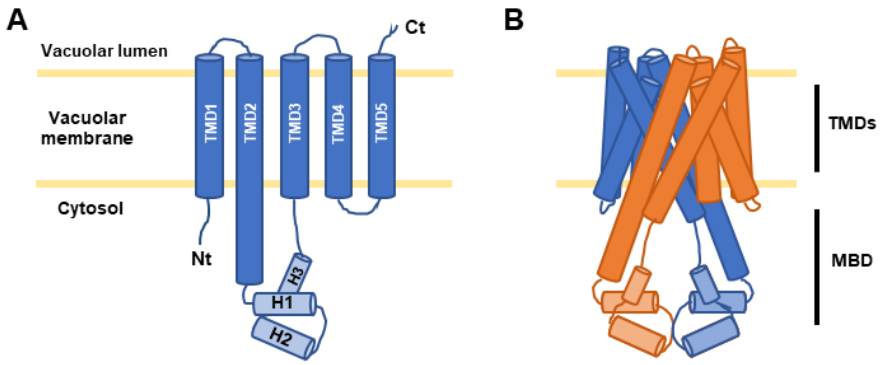

FIGURE C2.3 SCHEMATIC REPRESENTATION OF *EG*VIT1 MEMBRANE TOPOLOGY AND DIMER STRUCTURE. A) Transmembrane domains (TMD1-5) are represented by dark blue cylinders. The helices between TMD2 and TMD3 domains, represented by light blue cylinders, conform the MBD. **B)** An *Eg*VIT1 dimer representation, coloring TMDs and MBD as dark or light colors, respectively. Each protomer is colored in blue or orange. Adapted from (Kato et al., 2019). Ct: carboxyl terminus, H: helix, MBD: metal-binding domain, Nt, amino-terminus, TMD: transmembrane domain.

Genetic and biophysical studies have shown that yeast Ccc1 contributes to manganese homeostasis, suggesting that it could facilitate Mn^{2+} transport from the cytosol to the vacuole (Lapinskas et al., 1996; Cockrell, A. et al., 2014). More recently, liposome transport assays with reconstituted *Eg*VIT1 have demonstrated that, in addition to Fe^{2+}, it also transports Co^{2+} (Kato et al., 2019). Iron transport assays with *Plasmodium falciparum* VIT1 expressed in yeast suggest that Ccc1/VIT1 proteins are selective for Fe^{2+} over other dimetal ions

including Mn^{2+}, Zn^{2+}, Cu^{2+} and Ca^{2+} (Slavic et al., 2016). Liposome transport assays have also shown that *Eg*VIT1 is a H^+-coupled antiporter for metal ions, which provides the vacuolar H^+-ATPase with an important function in metal storage (Kato et al., 2019). Glutamate 72 participates in iron translocation as well as proton movement towards aspartate residue 43 (Kato et al., 2019). Nonetheless, aspartate 43 is absent in groups I-IV, suggesting that this is not the principal residue involved in proton-coupled transport, as it happens in other iron transporters such as those from the natural resistance-associated macrophage protein (NRAMP) family, where a histidine residue instead of a glutamate plays a key role in proton transport (Ehrnstorfer et al., 2017). Tyrosine 175, also involved in iron translocation, is not conserved in groups III and IV, with phenylalanine found instead. In this sense, studies of the crystal structure and protein function of ferroportin have revealed that the benzene ring from phenylalanine also interacts with divalent metals forming a cation-π interaction (Taniguchi et al., 2015). Finally, the kink-inducing residue proline 48 is not found in groups I-IV either (Figure C2.3). Group III-VIII sequences, including *Schizosaccharomyces pombe* and *P. tricornutum*, share high sequence similarity with *Eg*VIT1 and probably a similar mechanism for iron translocation. All these proteins contain a glutamate-rich MBD, but only in certain cases the number of glutamates and their position are strictly conserved (Figure C2.3). Methionine residues 149 and 150 are only present in group VI, and group VII possesses a larger MBD (Figure C2.3). In the case of *P. tricornutum,* it has been suggested that VIT1 would act as a Cd^{2+} transporter since its expression is regulated by this metal (Brembu et al., 2011). VIT1 proteins of group IV, which includes protist human parasites from the *Plasmodium* genus, localize mainly in the endoplasmic reticulum (Slavic et al., 2016). In the case of *Plasmodium* parasites, VIT1 plays a major role in iron detoxification during infection and is considered as a potential target for anti-malaria drugs (Weiner and Kooij, 2016). VIT1 protein sequences within group V share high similarity through the plant kingdom and are responsible for iron accumulation around the provasculature in seeds (Eroglu et al., 2019). However, plant VIT1 homologs have experimented functional divergence. For example, in *Tulipa gesnariana*, iron accumulation into the vacuole by *Tg*VIT1 is responsible for the blue coloration of petals, where it is exclusively expresse

(Momonoi et al., 2009). In rice *Oryza sativa, Os*VIT1 and *Os*VIT2 homologs are exclusively expressed in flag leaves and are involved in iron distribution between source and sink tissues (Zhang, Y. et al., 2012). Disruption of rice VIT genes decreases flag leaves iron content and increases iron accumulation in seeds, becoming a potential strategy of iron biofortification (Zhang, Y. et al., 2012). Although basic residues and amino acids with carboxylate groups are usually present, the amino-terminal region of Ccc1/VIT1 proteins has diverged and seems unique in each species. The amino-terminal region of fungal Ccc1/VIT1 is rich in serine, proline and cysteine residues (Figure C2.3). Interestingly, in *S. cerevisiae*, genome-wide studies have indicated that some of these serine residues are phosphorylated and together with ubiquitinated lysines could represent potential sites to regulate protein function and stability (Albuquerque et al., 2008; Swaney et al., 2013). Overall, these data strongly suggest that the mechanism of metal transport involving a hydrophilic dimer interface, proton antiporter and kink motions to open the luminal face of the transporter is unique and widely conserved across the Ccc1/VIT1 family, whereas other more variable domains may be involved in fine-tuning its functionality, abundance and subcellular localization.

6. REGULATION OF YEAST *CCC1* EXPRESSION BY IRON

As fungi cannot excrete iron, the vacuolar iron importer Ccc1 represents the most important factor implicated in fungal iron resistance. Consistent with its crucial function in cytosolic iron detoxification, the expression of *CCC1* is finely regulated by iron. In response to iron excess, *S. cerevisiae* Yap5, a member of the yeast activator protein (Yap) subfamily of transcriptional factors (Rodrigues-Pousada et al., 2019), activates the expression of *CCC1* (Li, L. et al., 2008; Li, L. and Ward, 2018) (Figure C2.4). Yap5 contains an amino-terminal basic leucine-zipper (bZIP) DNA-binding domain that associates to two Yap response elements (YREs) within the promoter of *CCC1* (Li, L. et al., 2008). Although Yap5 binding to YREs is constitutive and independent of iron levels, the activation of *CCC1* transcription only occurs in the presence of excess iron (Li, L. et al., 2008). Yap5 carboxy-terminal region contains an activation domain, which consists of two cysteine-rich domains (CRDs), n-CRD and c-CRD, with four and three conserved cysteine residues, respectively (Li,

L. et al., 2008). *In vivo* and *in vitro* studies have demonstrated that Yap5 directly binds two [2Fe-2S]-type clusters, which promote a conformational change that could be responsible for transcriptional activation (Rietzschel et al., 2015) (Figure C2.4). The conserved n-CRD domain, with higher affinity for iron than c-CRD, seems to function as a general iron sensor module. Remarkably, Yap5 activation depends specifically on the rate of mitochondrial Fe-S cluster (ISC) biogenesis, but not on cytosolic iron content, since defects in ISC synthesis prevent high-iron *CCC1*-induced expression (Li, L. et al., 2012). In response to high-iron, Yap5 also activates the expression of *TYW1*, which encodes for a cytosolic ISC-containing protein probably implicated in iron buffering, and *GRX4*, which encodes for a monothiol glutaredoxin that limits the transcriptional activity of the low-iron-responsive transcription factors Aft1 and Aft2 (Li, L. et al., 2011; Pimentel et al., 2012).

Yap5 is not the only transcriptional factor that contributes to *CCC1* expression in high-iron conditions, since *yap5Δ* cells partially activate *CCC1* and are less sensitive to iron than *ccc1Δ* mutants. The overexpression of some members of the Yap family induces the expression of *CCC1* in *yap5Δ* cells (Rietzschel et al., 2015). However, the mutagenesis of *CCC1* YREs suggests that other *cis*-regulatory elements and transcription factors beyond the Yap family activate the transcription of *CCC1* (Pimentel et al., 2012). A recent report has shown that the low-glucose sensor Snf1 participates in the regulation of *CCC1* (Li, L. et al., 2017) (Figure C2.4). Cells lacking Snf1 kinase activity or other components of the Snf1 complex, such as Snf4, Sip1, Sip2 and Gal83, show defects in *CCC1* expression under high-iron conditions that lead to iron toxicity (Li, L. et al., 2017). Previous studies have shown that iron deficiency promotes the phosphorylation of Snf1 (Puig et al., 2008), but no evidence for changes in Snf1 phosphorylation stage have been reported in excess iron. The Snf1-dependent expression of *CCC1* is independent of Yap5 and ISC biogenesis, but requires the general stress transcription factors Msn2 and Msn4, which are targets of Snf1 kinase, and other unidentified regulatory factors (Li, L. et al., 2017) (Figure C2.4). Similarly to other stresses, Msn4 protein translocates to the nucleus when cells are exposed to excess iron (Du et al., 2012). The relevance of Msn2 and Msn4 in iron homeostasis is

corroborated by the sensitivity of *msn2Δmsn4Δ* double mutants to both iron deficiency and excess (Li, L. et al., 2017; Ramos-Alonso et al., 2019). Further studies would be necessary to decipher how iron modulates the activity of the Snf1 kinase complex and its downstream effects on iron homeostasis.

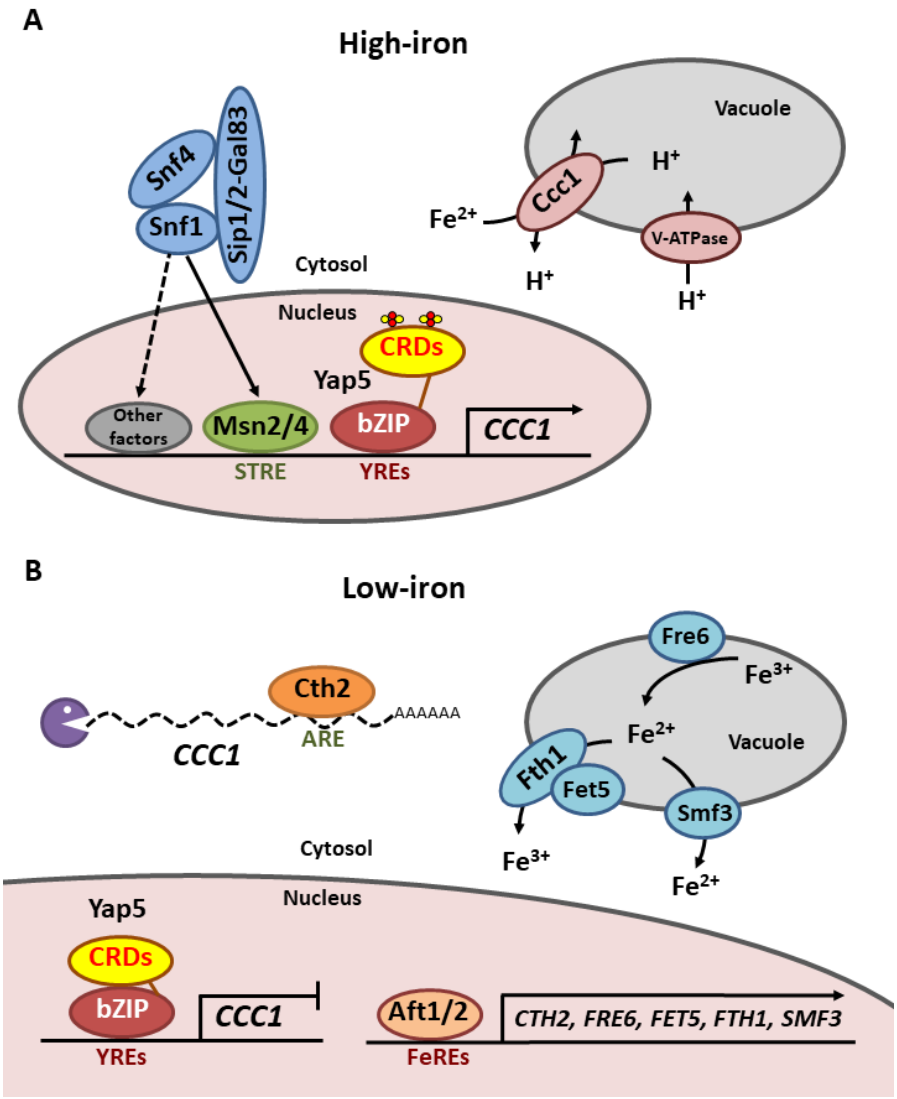

FIGURE C2.4. REGULATION OF *S. CEREVISIAE CCC1* IN RESPONSE TO IRON OVERLOAD AND DEPLETION. A) High-iron conditions. During iron overload, two ISCs associate to the CRDs of DNA-bound Yap5 leading to a conformational change that promotes *CCC1* transcription. *CCC1* expression is also activated by the Snf1 effectors Msn2/Msn4 and other unknown transcriptional factors. Ccc1 facilitates the import of Fe^{2+} into the vacuole while exporting H^+. Therefore, pH and V-ATPase function are tightly connected to cellular iron homeostasis. **B)** Low-iron conditions. During iron depletion,

Aft1/Aft2 activate the iron regulon, including *FRE6, FET5, FTH1* and *SMF3* genes, which encode for the vacuolar iron export machinery, and *CTH2*, which promotes the degradation of *CCC1* mRNA. The decrease in ISC synthesis prevents the activation of Yap5, which is constitutively bound to YREs within *CCC1* promoter. ARE: AU-rich element; bZIP: basic leucine-zipper domain; CRD: cysteine-rich domain; FeRE: iron regulatory element; STRE: stress response element; V-ATPase: vacuolar ATPase; YRE: Yap5 response element.

In response to iron deficiency, Aft1 and Aft2 transcriptional factors activate the expression of a group of genes, known as the iron regulon, that participate in iron uptake, iron mobilization from the vacuole and iron metabolism remodeling (Philpott and Protchenko, 2008; Ramos-Alonso et al., 2020). The Aft1/Aft2-dependent transcriptional activation of the vacuolar *FRE6* metalloreductase and the *FET5*/*FTH1* and *SMF3* vacuolar iron transporters facilitates the efflux of iron from the vacuole when iron is scarce (Martins, L. J. et al., 1998; Urbanowski and Piper, 1999; Portnoy et al., 2000; Rutherford et al., 2001; Singh, A. et al., 2007), whereas another Aft1/Aft2 target, Cth2, limits vacuolar iron storage by promoting the degradation of *CCC1* mRNA (Puig et al., 2005; Li, L. et al., 2008) (Figure C2.4). Therefore, both transcriptional and post-transcriptional mechanisms tightly match the expression of *CCC1* to cellular iron availability.

Multiple connections link vacuolar and mitochondrial iron homeostasis. For instance, the overexpression of *CCC1* suppresses mitochondrial iron overload phenotypes, limits ISC biogenesis and decreases the activity of mitochondrial ISC-dependent enzymes including aconitase (Chen, Opal S. and Kaplan, Jerry, 2000). Moreover, the overexpression of the mitochondrial iron importers *MRS3* or *MRS4* suppresses the sensitivity of *ccc1Δ* cells to iron, whereas their simultaneous deletion increases vacuolar iron transport and diminishes cytosolic iron (Li, L. and Kaplan, 2004; Li, L. et al., 2010). It has been proposed that *mrs3Δmrs4Δ* mutants generate ROS that increase the activity of the vacuolar Ccc1 transporter (Li, L. et al., 2010). Both *ccc1Δ* and *mrs3Δmrs4Δ* mutant cells activate the Aft1/Aft2-dependent low-iron transcriptional response, while cellular iron homeostasis is mostly restored in *ccc1Δmrs3Δmrs4Δ* mutants (Li, L. et al., 2001; Li, L. and Kaplan, 2004; Li, L. et al., 2010). The overexpression of the mitochondrial iron exporters *MMT1* and *MMT2* leads to phenotypes similar to *mrs3Δmrs4Δ* mutants, which are also

rescued by the deletion of *CCC1* (Xu et al., 2014). Altogether, these results indicate that subcellular iron pools including mitochondrial, vacuolar and cytosolic iron are highly interdependent. Several studies have linked vacuolar acidification to iron homeostasis. As indicated above, Ccc1/VIT1 seem to function as H^+/Fe^{2+} antiporters whose activity depends on vacuolar pH (Cockrell, A. et al., 2014; Kato et al., 2019). Moreover, the loss of vacuolar H^+-ATPase activity has been reported to activate the Aft1-dependent low-iron response in iron-repleted cells probably due to oxidative stress, leading to iron homeostasis defects (Milgrom et al., 2007; Diab and Kane, 2013). More recent data have shown that the loss of vacuolar acidification impairs vacuolar cysteine storage, which cause an oxidative damage to mitochondrial ISC biosynthesis components and ISC-containing activities such as aconitase (Chen, K. L. et al., 2020; Hughes et al., 2020). As a consequence, cells develop an age-related mitochondrial dysfunction characterized by the activation of the iron-deficiency and DNA damage responses, which can be rescued by iron supplementation (Chen, K. L. et al., 2020; Hughes et al., 2020).

7. *CCC1* IRON REGULATION IN OTHER FUNGI

Ccc1 function and regulation have been mostly studied in laboratory strains of *S. cerevisiae*, while little is known about its diversity in other strains and related fungal species. For instance, a genetic analysis with the use of reciprocal hemizygotes has shown that *S. cerevisiae CCC1* and *YAP5* alleles from a wild Malaysian population contain a partial loss-of-function that renders these yeast strains sensitive to high iron concentrations (Lee, H. N. et al., 2013). Compared to other available *S. cerevisiae* strain sequences, the Malaysian *CCC1* allele displays a single G22R amino acid change within its fungal-specific amino-terminal domain, which role in Ccc1 function has not been deciphered. Moreover, the Malaysian strains also display a gain-of-function allele for the master low-iron regulatory factor *AFT1* that improves their adaptation to iron deficiency (Lee, H. N. et al., 2013). These observations suggest that *S. cerevisiae* Malaysian strains have specialized to low-iron environments and have lost some of their high-iron resistance attributes. The phenotypic analysis

of other natural and human-domesticated yeast strains, which genome has been deciphered, will be tremendously useful to understand at the molecular level the evolution and adaptation of *S. cerevisiae* iron homeostasis network to particular ecological niches.

Non-Saccharomycetaceae fungi regulate the expression of *CCC1* orthologs through CCAAT-type transcription factors composed of a heterotrimeric CCAAT-binding core complex (CBC), which constitutively associates to CCAAT-consensus promoter sequences, and an iron-sensing Hap-type CBC-regulatory subunit that binds to CBC through a conserved amino-terminal Hap4-like CBC-binding domain (CBC-BD) (Martínez-Pastor and Puig, 2020). *S. cerevisiae* and its closely related pathogen species *Candida glabrata* have specialized their CBC-Hap4 regulatory system in the positive control of respiratory genes. However, a recent study suggests that *C. glabrata* Yap5 also associates to its CBC through a vestigial CBC-BD to activate the expression of *CCC1* and iron-dependent processes in response to high-iron conditions (Thiébaut et al., 2017) (Figure C2.5). *S. cerevisiae* Yap5 also contain a partial CBC-BD, but since a function has not been demonstrated for this region, it has not been represented in Figure 4. Similar to *S. cerevisiae*, *C. glabrata* expresses a Cth2 homolog that promotes *CCC1* mRNA down-regulation in response to iron limitation (Gerwien et al., 2016) (Figure C2.5). The expression of the *S. pombe CCC1*-homolog gene *pcl1*$^{+}$, which deletion confers iron sensitivity, and of genes encoding for non-essential iron-dependent processes is controlled by the Php2/3/5 CBC and its negative regulatory subunit Php4. Php4 lacks a bZIP DNA-binding domain, so during low-iron conditions it associates to CBC through its CBC-BD to repress *pcl1*$^{+}$ and iron-consuming genes expression. In response to high-iron conditions, the monothiol glutaredoxin Grx4 delivers a [2Fe-2S] to Php4 that abrogates its interaction with the CBC and allows *pcl1*$^{+}$ and iron-using genes transcription to proceed (Mercier et al., 2006) (Figure C2.5). Two Php4 cysteine residues (Cx_5C) are critical for iron-sensing and *pcl1*$^{+}$ regulation (Labbe et al., 2013). In the pathogen mold *Aspergillus fumigatus*, there are two homologs of *CCC1* (*cccA* and *cccB*), but only *cccA* is responsible for iron storage into the vacuole and contributes to iron resistance (Gsaller et al., 2012). Remarkably, *A.*

fumigatus CBC and its HapX regulatory factor, which contains a CBC-BD, a bZIP domain and four CRDs, function in response to both iron limitation and excess by activating or repressing iron metabolism genes depending on iron bioavailability (Schrettl et al., 2010; Gsaller et al., 2014; Furukawa et al., 2020). When iron is scarce, HapX represses the transcription of genes participating in iron-consuming pathways and activates genes implicated in siderophore biosynthesis. Strikingly, in response to high-iron conditions, *A. fumigatus* CBC and HapX cooperatively associate to the promoter of the vacuolar *cccA* iron importer and iron-using genes to activate their transcription (Schrettl et al., 2010; Gsaller et al., 2014; Furukawa et al., 2020) (Figure C2.5). HapX association to both CBC and a variable bipartite HapX DNA-recognition site downstream of the CBC-binding motif are necessary for all described HapX functions (Furukawa et al., 2020). Although *A. fumigatus* and other fungi synthesize intracellular siderophores that participate in iron distribution and storage, vacuolar CccA still acts as the principal iron detoxification system (Schrettl et al., 2007; Gsaller et al., 2012). The deletion of *HapX*, which is present in almost all Euascomycetes and Basidiomycetes, attenuates virulence in pathogenic fungi (Schrettl et al., 2010; Furukawa et al., 2020). *Candida albicans* CBC-Hap43 complex also plays a dual role by activating genes that participate in iron uptake and repressing non-essential iron-consuming processes when iron is scarce (Chen, C. et al., 2011; Singh, R. P. et al., 2011). Further studies with *C. albicans* have reinforced the role of Ccc1 as a connector between vacuolar and mitochondrial iron pools previously observed in *S. cerevisiae*. Deletion of the unique *C. albicans* mitochondrial importer, *MRS4,* and its vacuolar iron exporter *SMF3* increase intracellular iron levels, enhance mitochondrial dysfunction, impair filamentous development and adhesion to host epithelial, and consequently reduce virulence (Xu et al., 2012; Xu et al., 2014). Importantly, the simultaneous deletion of *CCC1* rescues all these phenotypes, positioning the Mrs4-Ccc1-Smf3 pathway as an attractive antifungal drug target.

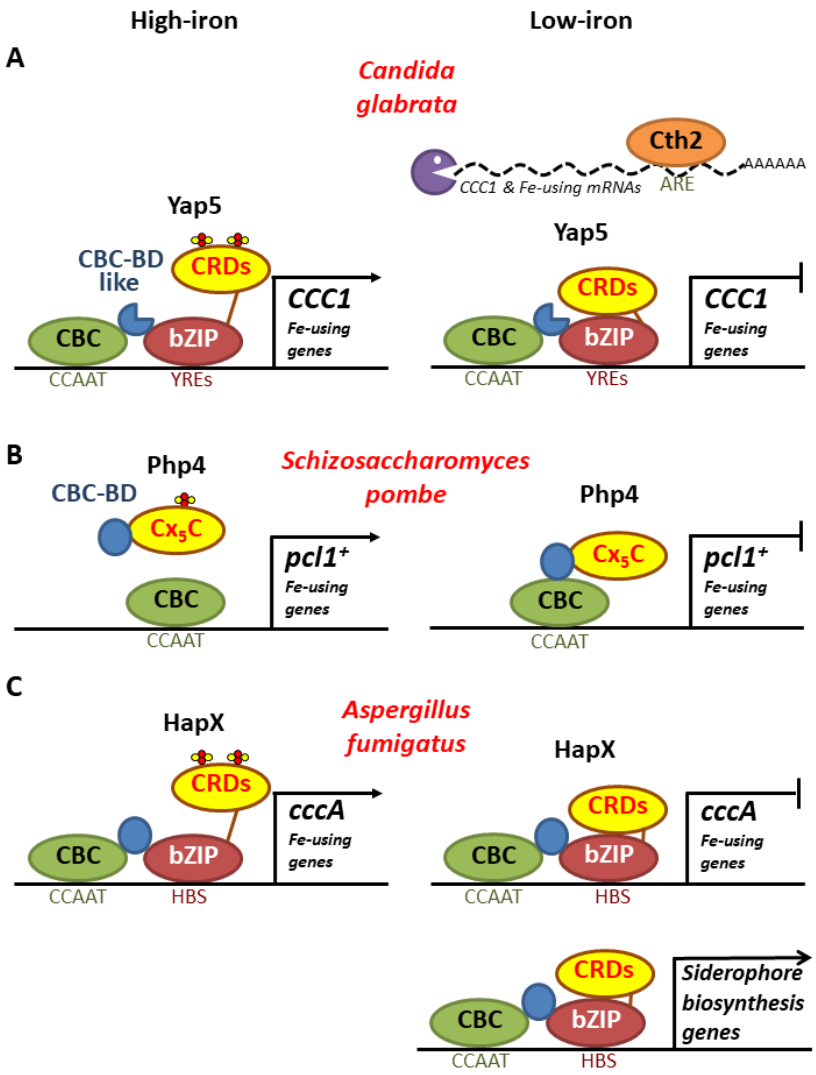

FIGURE C2.5. IRON REGULATION OF *CCC1* AND OTHER GENES ENCODING FOR DISPENSABLE IRON-DEPENDENT PROCESSES IN *C. GLABRATA*, *S. POMBE* AND *A. FUMIGATUS*. A) *C. glabrata*. Although *C. glabrata* possesses a transcription iron overload response similar to *S. cerevisiae*, recent studies have shown that Yap5 associates to CBC through a vestigial CBC-BD to activate the transcription of *CCC1* and multiple genes encoding for iron-using proteins in response to high-iron conditions. **B)** *S. pombe.* Under iron deficiency, the *S. pombe* CBC negative regulatory subunit associates to DNA-bound CBC via its CBC-BD and represses the transcription of the *S. pombe CCC1* homolog gene, *pcl1*+, and iron-consuming processes. Under iron-overload conditions, ISC-binding to a Cx5C motif in Php4 abrogates its interaction with the CBC, allowing the expression of *pcl1*+ and iron-dependent processes. **C)** *A. fumigatus*. In *A. fumigatus*, HapX CBC regulatory subunit exerts both positive and negative effects on CBC activity. During high-iron conditions, ISC-binding to HapX CRDs

triggers a conformational change that promotes the expression of *CccA* and iron-using genes. In response to low-iron conditions, HapX represses the expression of *CccA* and genes encoding for iron-dependent processes, but promotes iron acquisition by activating the expression of genes implicated in iron siderophore biosynthesis. The association of HapX to both CBC, via its CBC-BD, and two bipartite downstream HapX-binding sites (HBS), via its bZIP domain, are required for all HapX functions. ARE: AU-rich element; bZIP: basic leucine-zipper domain; CBC: CCAAT-binding complex; CBC-BD: CBC-binding domain; CRD: cysteine-rich domain; HBS: bipartite HapX-binding site; YRE: Yap5 response element.

8. CONCLUSIONS AND REMARKS

Living organisms have developed sophisticated strategies to deal with iron scarcity at the same time that they protect themselves from high levels of iron. Specifically, prokaryotes and animals synthesize the protein ferritin, which stores iron in a safe and compact but accessible form. Despite ferritin is also present in plants, it plays a secondary role in iron storage. Plants, as well as fungi, mainly detoxify and accumulate excess iron into vacuoles and mobilize it in response to iron limitation. The most studied iron transporters responsible for iron storage into vacuoles are *S. cerevisiae* Ccc1 and *A. thaliana* VIT1 (Li, L. et al., 2001; Kim, S. A. et al., 2006). However, homologs to these proteins can be found in all kingdoms with the exception of Metazoa. The Ccc1/VIT1 family possesses a complex phylogeny that probably involves several duplications and losses during species evolution. Although amino acid sequence similarity is observed along the protein, with key residues conserved in almost all analyzed organisms, some differences are also consistently found. The most relevant difference is the absence of the MBD in some prokaryotic and plant VTL proteins, and the presence of a ferritin-like domain at the amino-terminus in some bacteria and archaea species (Figure C2.3). The conservation of residues involved in the discrimination between metal transition ions and iron transport implies a conserved common mechanism with some particularities in different groups.

The iron-dependent regulation of *S. cerevisiae CCC1* mRNA has been widely studied. Both transcriptional (Yap5-dependent) and post-transcriptional (Cth2-dependent) mechanisms modulate *CCC1* transcript levels according to cellular iron availability to facilitate vacuolar iron storage in high-iron conditions

and vacuolar iron mobilization during iron deficiency. Recent work has discovered that other unexpected (Snf1 and Msn2/Msn4 dependent) and unknown pathways contribute to *CCC1* expression and yeast iron resistance (Li, L. et al., 2017). An important aspect of vacuolar iron storage via Ccc1 is its close connection to mitochondrial iron transport with implications not only in iron homeostasis but also in aging (Chen, K. L. et al., 2020; Hughes et al., 2020). The regulation of Ccc1 homologs in non-Saccharomycetaceae, which includes many pathogenic fungi, seems to differ considerably from *S. cerevisiae* (Martínez-Pastor and Puig, 2020). In these fungi, CBC DNA-binding complexes associate to Hap-like CBC regulatory subunits to either positively or negatively regulate the transcription of *CCC1* homologs. Moreover, little is known about post-translational regulatory mechanisms that influence Ccc1 protein localization, stability or functionality. Further studies are needed to elucidate the intricate regulation of Ccc1 in different fungi and its connections with mitochondrial iron metabolism.

Iron is especially important for microbial virulence. As mentioned above, *Plasmodium* VIT1 and *A. fumigatus* HapX have been demonstrated to be required for pathogenicity. Interestingly, the absence of Ccc1/VIT1 transporters in animals might allow the design of specific antifungal or antiparasitic drugs that target Ccc1/VIT1 transporters with lower side effects than other current drugs. Moreover, since Ccc1/VIT1 homologs in bacteria are also involved in H_2O_2 detoxification, their inhibition could suppose a reinforcement for host defenses (Taniguchi et al., 2015). On another hand, plant VIT transporters have an important role in iron distribution in seeds, and their manipulation could represent a promising biofortification tool (Zhang, Y. et al., 2012; Narayanan et al., 2015; Connorton et al., 2017; Narayanan et al., 2019). New genome sequences are generating datasets that could be used to explore how extended these Ccc1/VIT1 homologs are through the Tree of Life. Together with functional analysis, the pathways that control these proteins might be better understood and new research lines might help to isolate or design organisms able to acquire more iron for nutritional purposes, to unravel new drug targets and to work up actions for the biocontrol of pathogenic fungi

involved in the deterioration of food (pre- and post-harvest) or in human-related diseases.

9. SUPPLEMENTARY INFORMATION

9.1. Supplementary figures

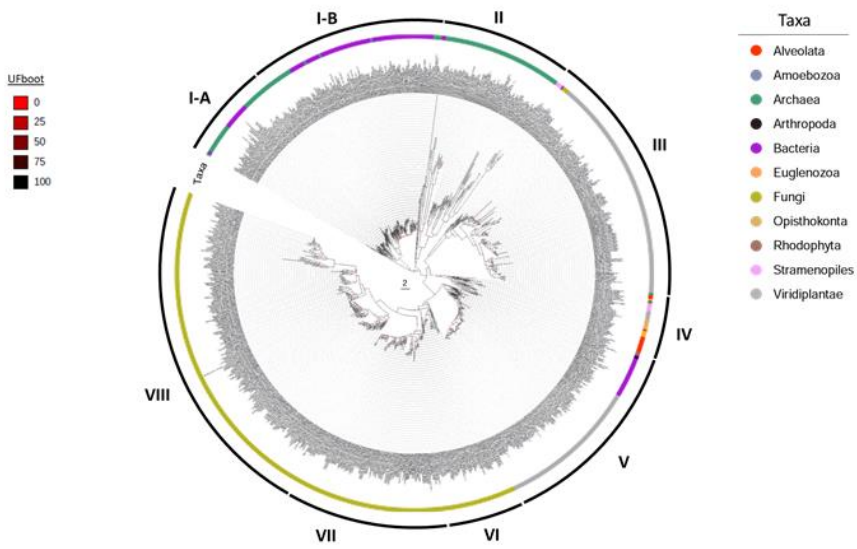

FIGURE C2.S1. DETAILED MAXIMUM LIKELIHOOD PHYLOGENETIC TREE RECONSTRUCTION OF THE IRON VACUOLAR TRANSPORTER CCC1/VIT1. A maximum likelihood phylogenetic tree reconstructed using the trimmed version of the Ccc1/VIT1 protein alignment. A more detailed circular phylogenetic tree is located in iTOL v3 (Letunic and Bork, 2016) http://itol.embl.de/shared/Peris_D. Branches were colored according to the ultrafast bootstrap branch support, with a range from 0% (red) to 100% (black). The scale bar represents the number of amino acid substitutions. Taxa designations were colored according to the legend.

9.2. Supplementary tables

Table C2.S1 is available online in the next link: https://doi.org/10.1016/j.csbj.2020.10.044.

Supplementary Materials: Supplementary data to this article can be found online at https://doi.org/10.1016/j.csbj.2020.10.044.

Author Contributions: Conceptualization, M.T.M.-P. and S.P.; Methodology, R.S.-D.. and D.P.; Investigation, R.S.-D. and D.P.; Resources, D.P. and S.P.; Data curation, R.S.-D. and D.P.;Writing—original draft preparation, R.S.-D., D.P., M.T.M.-P. and S.P.; Writing—review and editing, R.S.-D., D.P., M.T.M.-P. and S.P.; Visualization, R.S.-D. and D.P.; Supervision, M.T.M.-P. and S.P.; Project administration, S.P.; Funding acquisition, D.P. and S.P. All authors have read and agreed to the published version of the manuscript.

Funding: Work in our laboratory is supported by the Spanish Ministry of Science, Innovation and Universities (MICINN) grant BIO2017-87828-C2-1-P, the Regional Government of Valencia “Generalitat Valenciana” grant PROMETEU/2020/014 and FEDER (Fondo Europeo de Desarrollo Regional) funds to SP, and a predoctoral contract from “Generalitat Valenciana” and FEDER funds to RSD. Computations were performed on Tirant III of the Spanish Supercomputing Network (“Servei d'Informàtica de la Universitat de València”) under the project BCV-2018-2-0002 granted to DP.

Institutional Review Board Statement: Not applicable.

Informed Consent Statement: Not applicable.

Data Availability Statement: Supplementary data to this article can be found online at https://doi.org/10.1016/j.csbj.2020.10.044.

Acknowledgments: We thank all the members of the Iron Homeostasis laboratory for technical assistance and, specially Dr. Lola Peñarrubia for critically reading the manuscript.

Conflicts of Interest: The authors declare no conflict of interest. The funders had no role in the design of the study; in the collection, analyses, or interpretation of data; in the writing of the manuscript; or in the decision to publish the results.

CHAPTER 3:

Expression of a truncated Ccc1 vacuolar transporter increases environmental yeast iron extraction

Raquel Sorribes-Dauden [1], María Teresa Martínez-Pastor [1,*] and Sergi Puig [2,*]

[1]Departamento de Bioquímica y Biología Molecular, Universitat de València, Doctor Moliner 50, 46100, Burjassot, Valencia, Spain.

[2]Departamento de Biotecnología, Instituto de Agroquímica y Tecnología de Alimentos (IATA), Consejo Superior de Investigaciones Científicas (CSIC). Agustín Escardino 7, 46980, Paterna, Valencia, Spain.

* Authors to whom correspondence should be addressed.

Genes (MDPI) 12 (2021) 1120–133

(This article belongs to the Special Issue Genetic Regulation in Iron Homeostasis)

1. ABSTRACT

Iron is an essential micronutrient for all eukaryotic organisms because it participates as a redox cofactor in multiple metabolic processes. Iron bioavailability is highly restricted due to the low solubility of its oxidized form, leading frequently to iron deficiency anemia. The baker's yeast *Saccharomyces cerevisiae* is used as a model organism for iron homeostasis studies, but also as a food supplement and fermentative microorganism in the food industry. Yeast cells use the vacuolar Ccc1 transporter to detoxify and store excess iron into the vacuoles. Here, we modulate *CCC1* expression and properties to increase iron extraction from the environment. We show that constitutive expression of full-length *CCC1* is toxic, whereas deletion of its cytosolic amino-terminal (Nt) domain (*NtΔCCC1*) rescues this phenotype. Toxicity is exacerbated in cells lacking *AFT1* transcription factor. Further characterization of NtΔCcc1 protein suggests that it is a partially functional protein. Western blot analyses indicate that deletion of Ccc1 Nt domain does not significantly alter GFP-Ccc1 protein stability. A functional full-length GFP-Ccc1 protein localizes to particular regions of the vacuolar membrane, whereas GFP-NtΔCcc1 protein is evenly distributed through this endogenous membrane. Interestingly, expression of *NtΔCCC1* increases the accumulation of endogenous iron in cells cultivated under iron-sufficient conditions, a strategy that could be used to extract iron from media that are not rich in iron.

KEYWORDS: yeast; *Saccharomyces cerevisiae*; iron; Ccc1

2. INTRODUCTION

Iron is an essential micronutrient for all eukaryotic organisms. Its redox and coordination properties allow iron to participate as a cofactor in a wide range of metabolic processes including the synthesis of DNA, proteins and lipids, mitochondrial respiration and photosynthesis, and oxygen transport. Despite being one of the most abundant elements in the Earth's crust, iron bioavailability is extremely restricted in aerobic environments because it is mostly present in its oxidized from (Fe^{3+}), which is highly insoluble at physiological pH. According to the World Health Organization, iron deficiency anemia (IDA) is one of the most extended human nutritional disorders (even present in developed

countries) with high impact and fatal health consequences in children, women in fertile age, pregnant women, and elderly people (Zimmermann and Hurrell, 2007; Zimmermann, 2020). Consequences of IDA include diminished learning ability and poor physical growth of infants, fatigue and reduced work productivity in adults, greater susceptibility to infections, and increased risk of death associated with pregnancy and childbirth. Multiple strategies are used to prevent and treat IDA including a diversification of the diet, and supplementation and food fortification with particular iron forms (Sanvinsens and Puig, 2011).

The baker's yeast *Saccharomyces cerevisiae* has importantly contributed to the identification and characterization of many components of the human, plant and fungal iron homeostatic networks. Moreover, this yeast is used in multiple biotechnological applications including fermentative processes to obtain different food products (e.g. bread, wine and beer), as a nutritional supplement since it is rich in proteins, vitamins and fiber, and as a factory for the production of compounds of interest. Iron-enriched yeasts are currently being evaluated as promising sources of iron to prevent and palliate iron deficiency in humans and animals (Pas et al., 2007). In fact, iron-enriched baker's yeasts have been shown to be efficient in helping animals to recover from iron deficiency (Kyyaly et al., 2015). However, when present in excess, iron can engage into Fenton redox reactions that promote the formation of reactive oxygen species (ROS), which damage cells at the level of proteins, lipids and DNA (Eid et al., 2017). Therefore, yeast cells must coordinate iron acquisition, distribution, utilization, detoxification and storage.

Opposite to animals, yeast cells do not express ferritin; instead they accumulate iron into the vacuole for detoxification and storage purposes (Raguzzi et al., 1988). Iron can enter yeast vacuoles by endocytosis and via Ccc1, a protein that localizes to the vacuolar membrane and transports iron into its lumen (Li, L. et al., 2001; Cockrell, A. et al., 2014). Since yeast cells cannot excrete iron, Ccc1 constitutes the main yeast iron detoxification and resistance factor. Thus, yeast cells lacking *CCC1* (*ccc1Δ* mutants) are highly sensitive to elevated levels of environmental iron (Li, L. et al., 2001; Rietzschel et al., 2015). With the exception of animals, Ccc1 homologs are present in many organisms,

including bacteria, protists, fungi, and plants, where they are denoted VIT1 proteins (Sorribes-Dauden et al., 2020). The resolution of the crystal structure of *Eucalyptus grandis* VIT1 ortholog (*Eg*VIT1) has allowed the identification of essential and conserved motifs required for metal transport as well as other species-specific domains (Kato et al., 2019; Sorribes-Dauden et al., 2020). According to *Eg*VIT1 structure and protein alignments, Ccc1/VIT1 proteins including yeast Ccc1 possess five transmembrane domains (TMDs), a metal-binding loop containing three alpha helixes (H1-H3) between TMD2 and TMD3 that faces the cytosol, a cytosolic amino-terminal (Nt) region, and a vacuolar carboxyl terminus (Figure C3.1) (Kato et al., 2019). Structure-function data in *Eg*VIT1 also suggest that Ccc1/VIT1 proteins dimerize and function as H^+ antiporters for Fe^{2+} (Kato et al., 2019). Ccc1/VIT1 cytosolic Nt domain is not conserved and displays different properties depending on the species (Sorribes-Dauden et al., 2020). Yeast possesses a cytosolic Ccc1 Nt with serine and lysine residues that have been identified in proteomic studies as phosphorylated and ubiquitylated, respectively (Albuquerque et al., 2008; Swaney et al., 2013). Moreover, Malaysian wild *S. cerevisiae* strains harboring a mutation in its Nt region (G22R) are sensitive to high iron concentrations (Lee, H. N. et al., 2013). Thus, although according to conservation features, the Nt domain of yeast Ccc1 seems dispensable, it could be important for regulatory functions.

Multiple transcription factors contribute to up-regulation of *CCC1* mRNA levels in response to iron excess (Li, L. and Ward, 2018; Ramos-Alonso et al., 2020; Sorribes-Dauden et al., 2020). A member of the yeast activator protein (Yap) subfamily of transcriptional factors denoted Yap5 associates to specific *cis* elements within *CCC1* promoter and activates its transcription in response to iron excess (Li, L. et al., 2008; Li, L. et al., 2012; Pimentel et al., 2012; Rietzschel et al., 2015). Moreover, the low-glucose sensor Snf1 also contributes to *CCC1* mRNA up-regulation in high iron conditions by activating the general stress transcription factors Mns2 and Msn4 (Li, L. et al., 2017). In response to iron deficiency, yeast Aft1 and Aft2 transcription factors activate iron acquisition via Fet3-Ftr1 high-affinity iron transport system, iron mobilization from the vacuole, and a metabolic remodeling mediated by the

mRNA-binding protein Cth2 that post-transcriptionally limits *CCC1* expression (Urbanowski and Piper, 1999; Puig et al., 2005; Li, L. et al., 2008; Philpott and Protchenko, 2008; Ramos-Alonso et al., 2020).

Previous studies have shown that *CCC1* overexpression promotes iron uptake and accumulation into the vacuole (Chen, O. S. and Kaplan, J., 2000; Li, L. et al., 2001; Cockrell, A. et al., 2014). Although this strategy seems appropriate to extract iron from the environment and enrich yeast cells with iron, we show here that constitutive expression of *CCC1* is toxic to yeast cells cultivated in iron replete conditions. Interestingly, deletion of Ccc1 Nt domain rescues toxicity allowing a more efficient extraction of iron from the surrounding milieu. A potential function of Ccc1 Nt is discussed.

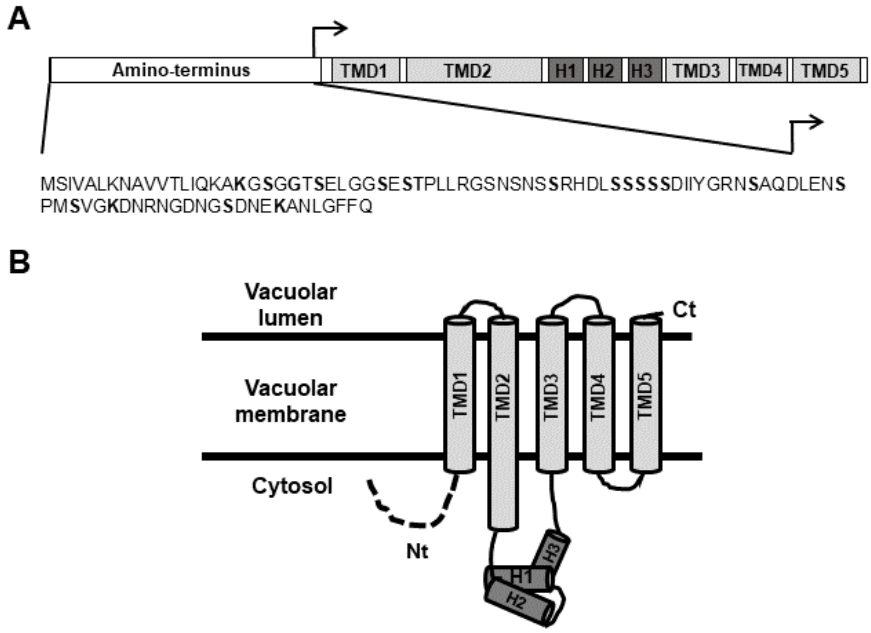

FIGURE C3.1. SCHEMATIC REPRESENTATION OF CCC1/VIT1 DOMAIN ORGANIZATION (A) AND MEMBRANE TOPOLOGY (B), based on EgVIT1 structure and protein alignments (Kato et al., 2019; Sorribes-Dauden et al., 2020). A and B: Grey rectangles/cylinders represent trans-membrane domains (TMDs); dark grey rectangles/cylinders represent three helices. A: White rectangles represent the Nt domain, which amino acid sequence is indicated below. Bold letters indicate phosphorylated and ubiquitylated residues, as well as mutation G22R in Malaysian yeast strains (Albuquerque et al., 2008; Lee, H. N. et al., 2013; Swaney et al., 2013). Black arrow indicates where NtΔCcc1 protein starts.

3. MATERIALS AND METHODS

3.1. Yeast strains

Yeast strains used in this study (Invitrogen) include BY4741 (MATa, his3Δ1, leu2Δ0, met15Δ0, ura3Δ0), BY4743 (MATa/α his3Δ1/his3Δ1 leu2Δ0/leu2Δ0 LYS2/lys2Δ0 met15Δ0/MET15 ura3Δ0/ura3Δ0), ccc1Δ (BY4741 ccc1::KanMX6), ccc1Δ (BY4743 ccc1::KanMX6/ccc1::KanMX6), fet3Δ (BY4741 fet3::KanMX6), ftr1Δ (BY4741 ftr1::KanMX6), aft1Δ (BY4741 aft1::KanMX6) and cth2Δ (BY4741 cth2::KanMX6).

3.2. Plasmids

Plasmids used in this work include empty vectors p416TEF (Mumberg et al., 1995), p416GAL and pUG36 (kindly provided by U. Güldener and J. H. Hegemann, Heinrich-Heine-University Düsseldorf, Germany), and the corresponding vectors with either *CCC1* or *NtΔCCC1* (lacking the first 87 Nt amino acids) coding sequences cloned into BamHI and XhoI. pUG36 vector expresses either *CCC1* or *NtΔCCC1* coding sequences under the control of the methionine-regulated *MET17* promoter and add a GFP tag at the Nt end.

3.3. Growth conditions

Yeasts were cultivated at 30°C in synthetic complete (SC) medium lacking uracil (SC-Ura) or lacking both uracil and methionine (SC-Ura-Met). Glucose was substituted by galactose in SC-Ura/Galactose medium. Iron was added to SC media at the indicated concentrations from a 100 mM $Fe(NH_4)_2(SO_4)_2$ (FAS; Merck-Sigma) stock solution. Stock solutions were prepared in 0.1M HCl to facilitate iron solubility and were used fresh. A control with the equivalent HCl concentration was always prepared. Fe^{2+}-specific chelator ferrozine (Fz; Merck-Sigma) was added to SC plates from a 100 mM stock solution freshly prepared in water. To grow yeast cells in liquid media, overnight SC-Ura or SC-Ura-Met precultures were reinoculated at an optical density at 600 nm (OD_{600nm}) of 0.2 and then incubated at 30°C and 190 rpm in 50-mL flasks. Alternatively, for duplication time measurements, yeast cells were inoculated in 96-well plates at an OD_{600nm} of 0.2 in 270 µL of liquid SC-Ura medium with 500 µM FAS, and

the OD_{600nm} was determined in a Spectrostar Nano absorbance microplate reader (BMGLabtech) every 30 min for 36 hours at 28°C. Duplication times were calculated using the online tool GCAT (Growth curve analysis tool) as described (Bukhman et al., 2015). To perform growth assays in solid media, cells from overnight precultures were diluted to an OD_{600nm} of 0.1 and then spotted directly and after 1:10 and 1:100 dilutions in sterile water. Plates were incubated at 28°C for 3 to 6 days and were then photographed.

3.4. Iron measurements

Yeast cells were collected and treated as previously described, and a colorimetric assay was used to determine the endogenous levels of iron (Tamarit et al., 2006; Martínez-Garay et al., 2016). To determine yeast dry weight (DW), cells corresponding to a total OD_{600nm} x mL of 30 were collected, washed, transferred to a previously weighed Eppendorf tube and dried at 50°C for 3 days. Finally, yeast DW was obtained by subtracting the total weight from the Eppendorf tube weight. To determine the iron that yeast cells extracted from the surrounding medium, endogenous iron levels were divided by the volume of medium in which these cells were growing.

3.5. RNA analyses

To determine the expression levels of particular mRNAs, total RNA was extracted and reverse transcription-quantitative PCR (RT-qPCR) was performed as previously described (Sanvisens et al., 2014). *ACT1* mRNA values were used to normalize data. Data and error bars represent the averages and standard deviations from at three independent biological experiments. Specific primer pairs for *FTR1*, *CTH2* and *ACT1* were used.

3.6. Protein analyses

To determine Ccc1 and NtΔCcc1 protein stability, exponentially growing cells were cultivated in SC-Ura-Met without (iron-sufficient conditions) or with 3 mM FAS (high-iron conditions) for 1 hour (Zhou, 2004). Then, we stopped *CCC1* synthesis by adding methionine to a final concentration of 3 mM and cells were harvested at the indicated time points. Yeast proteins were extracted with the alkali method, and processed and analyzed by Western blot as

previously detailed (Kushnirov, 2000; Romero et al., 2018). Anti-GFP (Roche) and anti-Pgk1 (Thermo Fisher Scientific) were used to detect GFP-Ccc1/GFP-NtΔCcc1 and Pgk1 proteins, respectively.

3.7. Fluorescence microscopy

Images were captured on an Eclipse 90i Nikon microscope (Nikon corporation, Japan) using a digital camera (Nikon DS-5Mc). To stain vacuolar membranes, cells were incubated for 15 min in 8 μM of FM4-64, washed and incubated for an additional hour.

3.8. Statistical analyses

Tailed t-student tests were used to determine statistical significance. Significant differences (p-value < 0.05) are indicated by different letters, whereas when there are no significant differences, at least one letter is the same.

4. RESULTS

4.1. The toxicity of a constitutively expressed *CCC1* is rescued by iron addition

Previous studies have shown that overexpression of the vacuolar iron transporter *CCC1* increases iron uptake and total iron content, leading to its accumulation into the vacuole (Chen, O. S. and Kaplan, J., 2000; Li, L. et al., 2001; Cockrell, A. et al., 2014). Given that iron is naturally detoxified and stored in the vacuole, we considered that overexpression of *CCC1* could be an appropriate strategy to increase yeast endogenous iron content. Therefore, we expressed *CCC1* coding sequence under the control of the constitutive and high-expression promoter of *TEF2* gene (P_{TEF2}-*CCC1*) in a *ccc1Δ* strain. Since *CCC1* deletion has been described to cause high cellular sensitivity to extracellular iron, we expected that *CCC1* overexpression would provide iron resistance (Li, L. et al., 2001; Rietzschel et al., 2015). To test yeast growth, we performed spot growth assays in solid media with increasing concentrations of

ferrous ammonium sulfate (FAS). We used wild-type (WT) cells and *ccc1Δ* mutants as controls. As previously described, *ccc1Δ* cells (*ccc1Δ* + vector) growth similarly to WT cells (WT + vector) under iron-sufficient conditions (SC-Ura), whereas they are more sensitive to an increase in extracellular iron, which limits *ccc1Δ* growth at 5 mM FAS and fully abrogates growth at 20 mM FAS (Figure C3.2A), (Li, L. et al., 2001). Surprisingly, we observed that overexpression of *CCC1* with *TEF2* promoter was extremely toxic under normal iron-sufficient conditions, whereas growth was recovered upon addition of iron to the growth medium, to become more resistant than *ccc1Δ* cells and only slightly less tolerant than WT cells (Figure C3.2A). These results indicate that altering the expression of *CCC1* under iron replete conditions could be detrimental to cells.

A potential explanation to the increase in iron acquisition and accumulation into the vacuole previously described for *CCC1*-overexpressing cells would be an activation of the iron regulon due to decreased cytosolic and mitochondrial iron levels. Indeed, we observed that P_{TEF2}-*CCC1* cells increase the expression of the members of the iron regulon, including the Aft1 targets *FTR1* and *CTH2*, as compared to WT cells (Figure C3.2B). Given that deletion of *FET3*, which encodes for an essential component of the cell surface Fet3-Ftr1 high-affinity iron transport complex, has been shown to fully remove iron uptake of *CCC1*-overexpressing cells, we ascertained whether deletion of either *FET3* or *FTR1* would rescue its toxicity under iron-sufficient conditions (Chen, O. S. and Kaplan, J., 2000). As shown in Figure C3.2C, none of them improved growth of P_{TEF2}-*CCC1* cells, suggesting that other reasons beyond increased iron uptake and accumulation are responsible for *CCC1* toxicity under normal conditions (see discussion). Consistent with this, decreasing extracellular bioavailability with the addition of an Fe^{2+}-specific chelator (Ferrozine, Fz) did not rescue growth of P_{TEF2}-*CCC1* cells (Figure C3.2A, Fz). Previous data have shown that increased expression of *CTH2* under normal growth conditions also leads to cellular growth defects (Thompson et al., 1996; Romero et al., 2018). Since we have observed that *CCC1* overexpression increases 7-fold *CTH2* mRNA levels (Figure C3.2B), we assessed whether deletion of *CTH2* rescued *CCC1* overexpression toxicity. As shown in Figure C3.2D, deletion of *CTH2* does not

promote growth when *CCC1* is overexpressed, which indicates that the increase levels of *CTH2* are not the reason for toxicity. Then, we explored whether deletion of *AFT1* transcription factor, which would simultaneously limit iron uptake, iron mobilization from the vacuole and *CTH2* expression, would rescue *CCC1* overexpression phenotype. Remarkably, we observed that instead of recovering growth, deletion of *AFT1* dramatically increased the toxicity of *CCC1* overexpression (Figure C3.2D). This result and the lack of rescue by *FTR1*, *FET3* and *CTH2* deletions discard that the underlying reason for *CCC1* toxicity is an increase in iron uptake, and strongly suggest that a decrease in cytosolic iron bioavailability due to higher transport of iron into the vacuole mediated by Ccc1 is the most likely reason for this phenotype.

To solve the toxicity caused by *CCC1* overexpression, we decided to test the regulatable promoters of *GAL1*, which is repressed by glucose and activated in media with galactose as the single carbon source (P_{GAL1}-*CCC1 cells*), and *MET17*, which is repressed by methionine (P_{MET17}-*GFP-CCC1 cells*). P_{GAL1}-*CCC1* cells exhibited a strong toxicity when spotted on a galactose medium (SC-Ura/Galactose) (Figure C3.3A). This phenotype was probably due to an excessive *CCC1* expression, as no growth defect was observed in SC-Ura (Figure C3.3A). Furthermore, P_{MET17}-*GFP-CCC1* cells were cultivated in methionine-containing conditions to inhibit *CCC1* expression and then spotted on SC-Ura plates lacking methionine (SC-Ura-Met), which allows *CCC1* expression. Under these conditions, we did not observe any growth defect as compared to WT cells (Figure C3.3B), probably due to lower expression levels of *MET17*-driven expression as compared to *GAL1* and *TEF2* promoters. We could notice that P_{MET17}-*GFP-CCC1* cells are as resistant to high iron concentrations as WT cells, which supports that the GFP-Ccc1 tagged protein is functional (Figure C3.3B). Interestingly, iron resistance by P_{MET17}-*GFP-Nt*Δ*CCC1* cells was lower than P_{MET17}-*GFP-CCC1* cells, suggesting that Ccc1 Nt region is important for function (Figure C.3B). Moreover, these results indicate that the promoter that drives *CCC1* expression is critical for appropriate growth.

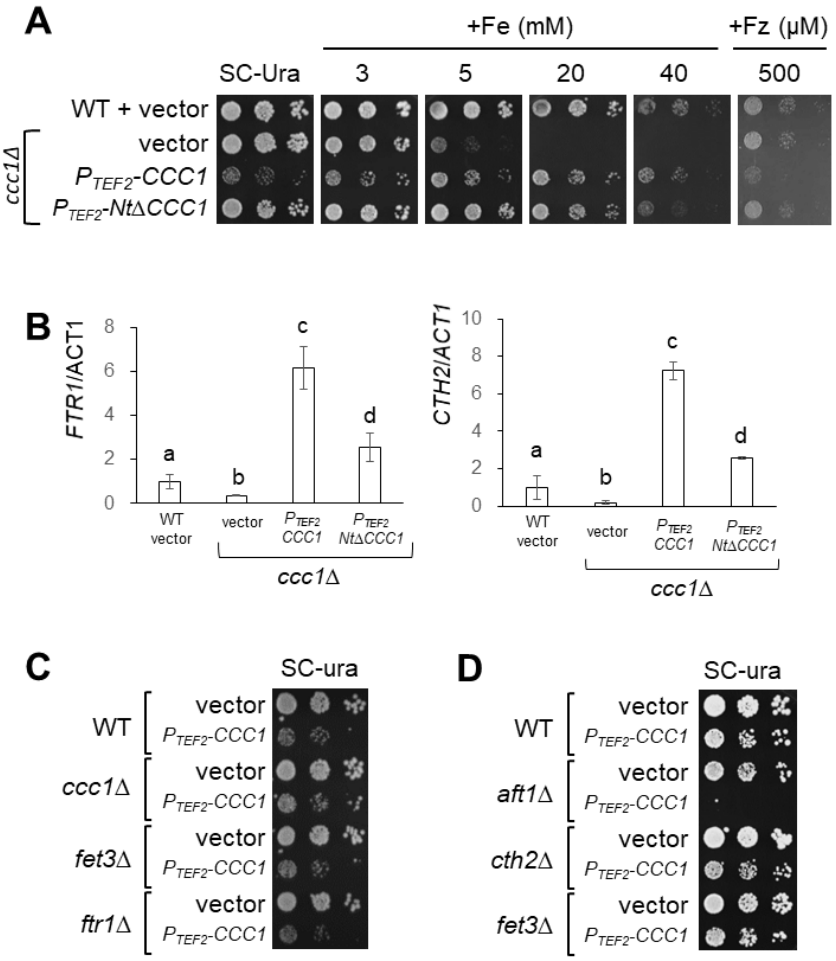

FIGURE C3.2. TOXICITY OF *CCC1* CONSTITUTIVE EXPRESSION UNDER IRON-SUFFICIENT CONDITIONS IS RESCUED BY IRON ADDITION OR BY DELETING CCC1 CYTOSOLIC AMINO-TERMINAL REGION. BY4741 (WT) cells were transformed with p416TEF (vector), and *ccc1Δ* cells were transformed with p416TEF (vector), p416TEF-*CCC1* (P_{TEF2}-*CCC1*) and p416TEF-*NtΔCCC1* (P_{TEF2}-*NtΔCCC1*) plasmids. **A)** Expression of *CCC1* alters growth in media with different iron availability. Cells were cultivated overnight in SC-Ura and then spotted on SC-Ura media containing different concentrations of FAS (Fe) or Ferrozine (Fz). **B)** *FTR1* and *CTH2* mRNA levels. Yeast cells were cultivated in SC-Ura + 500 μM FAS for 6 hours. Total RNA was extracted and the levels of particular mRNAs were determined by RT-qPCR. *ACT1* was used to normalize data. Three independent biological replicates were performed and the average and standard deviation were determined and represented relative to the WT. Different letters above the bars represent statistically significant differences (p-value < 0.05). **C)** and **D)** Deletion of the high-affinity iron uptake system does not rescue *CCC1* overexpression toxicity. BY4741 (WT), *ccc1Δ, fet3Δ, ftr1Δ, aft1Δ,* and *cth2Δ* cells transformed with p416TEF (vector) or p416TEF-*CCC1* (P_{TEF2}-*CCC1*) were spotted on SC-Ura. Plates were incubated at 30°C and photographed.

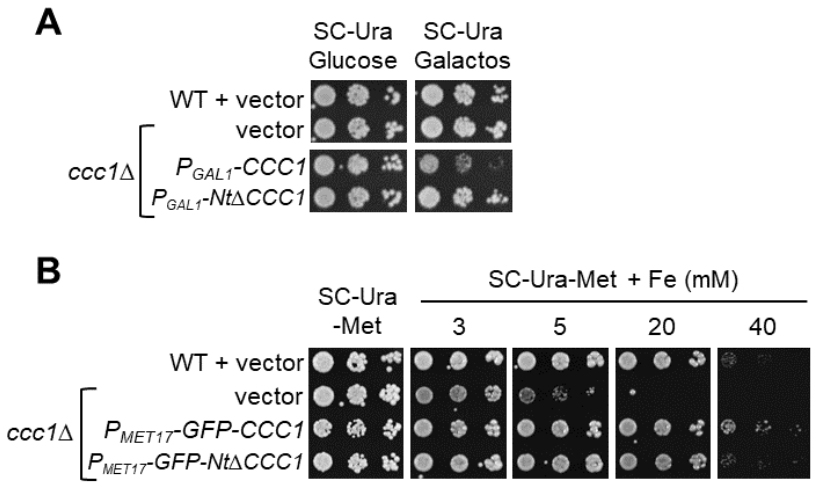

FIGURE C3.3. GROWTH OF YEAST CELLS EXPRESSING *CCC1* WITH REGULATABLE PROMOTERS. A) Expression of *CCC1*, but not *NtΔCCC1*, with *GAL1* promoter is toxic. BY4741 (WT) cells transformed with p416TEF (vector), and *ccc1Δ* cells transformed with p416TEF (vector), p416GAL-CCC1 (*PGAL1-CCC1*) and p416GAL-NtΔCCC1 were cultivated overnight in SC-Ura and then spotted on normal SC-Ura (SC-Ura Glucose) and SC-Ura without glucose but with 2% galactose (SC-Ura Galactose). **B)** Expression of *CCC1* with *MET17* promoter rescues toxicity. BY4743 (WT) cells were transformed with p416TEF (vector), and *ccc1Δ* cells were transformed with p416TEF (vector), pUG36-*CCC1* (*P_{MET17}-GFP-CCC1*) and pUG36-*NtΔCCC1* (*P_{MET17}-GFP-NtΔCCC1).* Cells were cultivated overnight in SC-Ura (which contains methionine) to inhibit *CCC1* expression, and then spotted on SC-Ura-Met media with different concentrations of FAS (Fe). Plates were incubated at 30 °C and photographed.

4.2. Deletion of *CCC1* amino-terminal region rescues toxicity by limiting iron-resistance capacity

Yeast *CCC1* protein contains an Nt region that faces the cytosol (Figure C3.1), and whose function has not been described. According to genome-wide data, this Nt domain contains multiple serine residues that are phosphorylated and lysine residues that are ubiquitylated (Albuquerque et al., 2008; Swaney et al., 2013). To test whether this region was important for Ccc1 function under high-iron conditions or contributed to its toxicity under iron-sufficient conditions, we constructed a Ccc1 protein lacking its 87 Nt amino acids (NtΔCcc1). Remarkably, expression of *NtΔCCC1* with either *TEF2, GAL1* or *MET17* promoter did not alter cell growth in iron-sufficient conditions (Figures C3.2A

and C3.3). A potential explanation for this result could be that deletion of the Nt region would fully remove Ccc1 function, but this was not the case because both *P_{TEF2}-NtΔCCC1* and *P_{MET17}-NtΔCCC1* constructs conferred an iron resistance phenotype only slightly lower than the cells expressing *CCC1* under the control of the same promoter (Figures C3.2A and C3.3B). Therefore, opposite to full-length Ccc1, overexpression of *NtΔCCC1* does not cause cellular toxicity.

4.3. Cultures of NtΔCCC1 cells are more efficient in extracting iron from media

To further study the contribution of Ccc1 Nt region to iron acquisition and growth, we first cultivated WT*, ccc1Δ,* and cells expressing either *P_{TEF2}-CCC1* or *P_{TEF2}-NtΔCCC1* for 36 hours in a microplate reader and calculated the duplication times from the resulting growth curves (Figure C3.4A and Figure C3.S1). While we observed similar duplication times for WT*, ccc1Δ* and *P_{TEF2}-NtΔCCC1* cells, *P_{TEF2}-CCC1* cells showed a 3-fold increase in duplication time, underscoring an important growth defect, in accordance with the results observed in solid media. Although *P_{TEF2}-NtΔCCC1* cells showed a growth curve similar to WT and *ccc1Δ*, a small growth defect was indicated by the lower maximum OD_{600} achieved. To further characterize this differential growth, we then cultivated WT, *ccc1Δ*, and cells expressing either *P_{TEF2}-CCC1* or *P_{TEF2}-NtΔCCC1* for six hours in a liquid medium containing 500 μM FAS. We observed that WT and *ccc1Δ* cells grew properly, whereas *P_{TEF2}-CCC1* cells again displayed a dramatic growth defect (Figure C3.4B). Remarkably, although *P_{TEF2}-NtΔCCC1* cells grew better than *P_{TEF2}-CCC1* cells, they also exhibited a significant growth decrease as compared to WT and ccc1Δ cells (Figure C3.4B). Then, we measured cellular iron accumulation and observed a 6-fold and 4-fold increase in iron accumulation in *P_{TEF2}-CCC1* and *P_{TEF2}-NtΔCCC1* cells, respectively, as compared to WT cells (Figure C3.4C). These results suggest that *CCC1*-overexpressing cells could be used to extract and accumulate iron from the environment. However, when we determined total iron

extracted per volume of medium, we observed that P_{TEF2}-*CCC1* cells did not improve the capacity of WT or *ccc1Δ* cells to remove iron from the environmental milieu, mostly due to its low growth (Figure C3.4D). Interestingly, P_{TEF2}-*NtΔCCC1* cells extracted twice as much iron from the extracellular medium as the rest of cells assayed (Figure C3.4D). These results suggest that overexpressing an Nt-truncated Ccc1 protein could be an interesting strategy to more efficiently obtain iron from media.

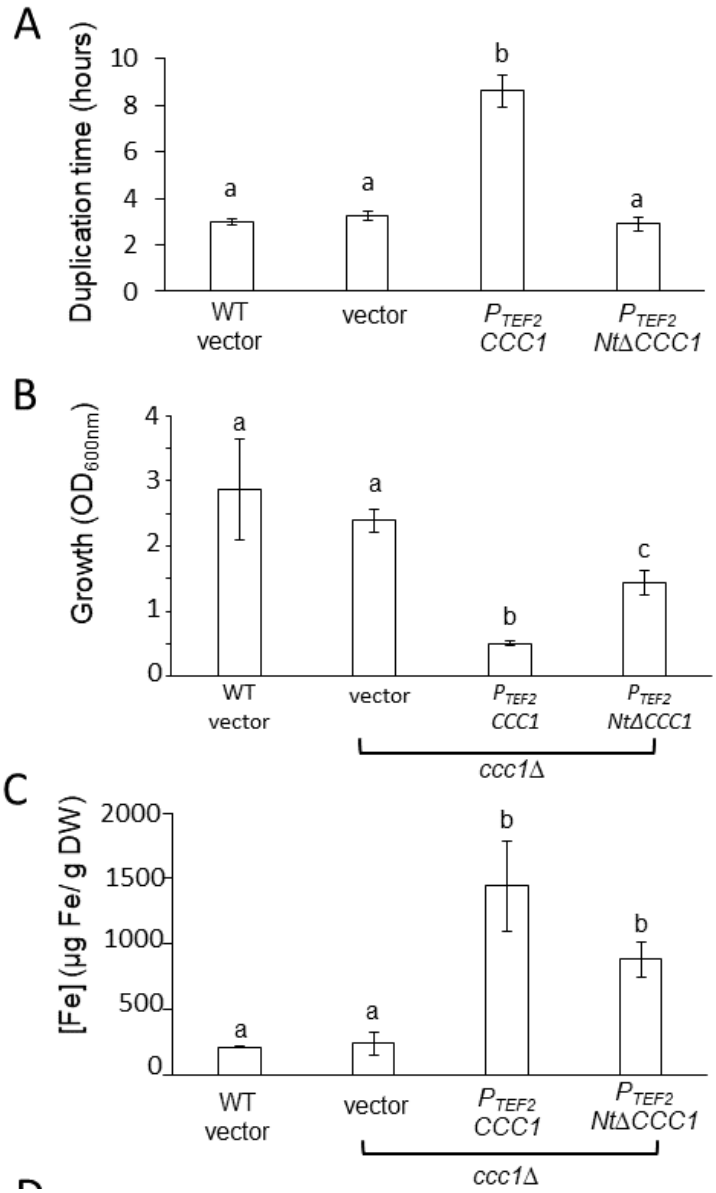

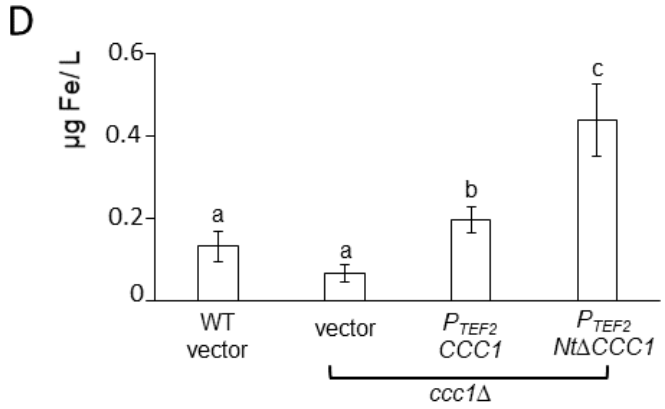

FIGURE C3.4. OVEREXPRESSION OF *NTΔCCC1* IMPROVES IRON EXTRACTION FROM MEDIA. **A)** Yeast cells described in Figure 2 were inoculated at an OD_{600} of 0.2 in SC-Ura with 500 µM FAS in a 96-well microplate reader and duplication time was calculated from the resulting growth curves as described in Materials and Methods. **B,C AND D)** Yeast cells described in Figure C3.2 were cultivated in SC-Ura + 500 µM FAS for 6 hours, and OD_{600nm} **B)**, µg Fe/g dry weight (DW) **C)**, and µg Fe/L of medium **D)** has been determined. Three independent biological replicates were carried out. The average and standard deviation were determined and represented. Different letters above the bars represent statistically significant differences (p-value <0 .05).

4.4. Ccc1 amino-terminus modulates subcellular localization

The decreased resistance to high-iron conditions of yeast cells expressing *NtΔCCC1* could be due to decreased stability or mislocalization of the truncated protein. Moreover, Ccc1 Nt contains serine and lysine residues that, according to genome-wide studies, are phosphorylated and ubiquitylated, respectively (Figure C3.1) (Albuquerque et al., 2008; Swaney et al., 2013). To ascertain if this was the case, we used yeast cells expressing GFP-tagged Ccc1 or NtΔCcc1 proteins under the control of *MET17* promoter, previously assayed for growth in iron-containing media (Figure C3.3B). It is important to highlight that incorporation of an Nt tag such as GFP removes any change in protein stability due to differences in the initial amino acids of the protein, allowing to make direct conclusions from the Nt region. Thus, we checked protein stability by stopping *CCC1* and *NtΔCCC1* expression with methione addition and determined protein levels at different time points. As shown, Ccc1 protein stability was not altered by the deletion of its Nt domain, neither under normal

growth conditions nor after addition of iron to the medium (Figure C3.5 and C3.S2). These results indicate that the deleted Nt domain does not significantly alters Ccc1 protein stability under these growth conditions.

To ascertain whether deletion of Ccc1 Nt region alters cellular distribution, we determined the subcellular localization of GFP-Ccc1 and GFP-NtΔCcc1 proteins by fluorescence microscopy in iron-sufficient and high-iron conditions (1 hour in 3 mM FAS). Differential interference contrast (DIC) was used to visualize vacuoles, since they appear as clear indentations, whereas the lipophilic dye FM4-64 selectively localized to vacuolar membranes after appropriate incubation. We observed that both full length Ccc1 protein colocalized with FM4-64 under both iron-sufficient and high-iron conditions, particularly at specific regions of the vacuolar membrane (Figure C3.6). NtΔCcc1 protein displayed a more uniform distribution through the vacuolar membrane, as compared to wild-type Ccc1 under both iron replete and excess conditions (Figure C3.6). These results suggest that Ccc1 Nt domain is important to modulate Ccc1 protein localization.

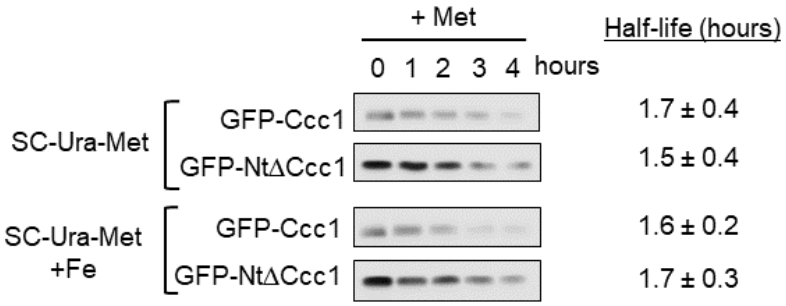

FIGURE C3.5. GFP-CCC1 AND GFP-NTΔCCC1 PROTEIN STABILITY IN NORMAL AND HIGH-IRON CONDITIONS. Yeast *ccc1Δ* cells transformed with either pUG36-*CCC1* (*P_{MET17}-GFP-CCC1*) or pUG36-*NtΔCCC1* (*P_{MET17}-GFP-NtΔCCC1*) plasmids were cultivated in SC-Ura-Met to exponential phase and 3 mM FAS was added (or not) for 1 hour. Expression was stopped by addition of 3 mM Methionine, and aliquots were isolated at the indicated time points. Total proteins were extracted, and Ccc1 protein levels were determined by immunoblotting with anti-GFP antibody. Equal amounts of total proteins were loaded in each lane. Three independent biological experiments were performed, and GFP-Ccc1 and GFP-NtΔCcc1 protein half-life was determined. The average half-life and its standard deviation is represented.

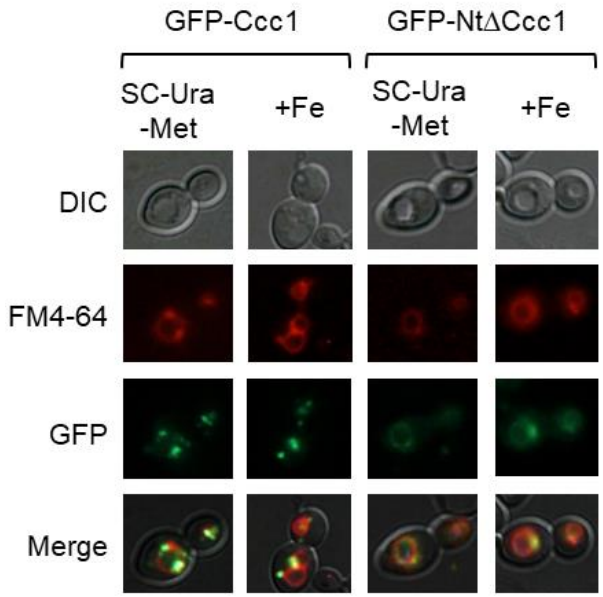

FIGURE C3.6. SUBCELLULAR LOCALIZATION OF CCC1 AND NTΔCCC1 PROTEINS IN NORMAL (SC-URA-MET) AND HIGH-IRON (+FE) CONDITIONS. Yeast cells were cultivated as described in Figure C3.5, and visualized under Nomarski (DIC) and GFP fluorescence optics. Vacuolar membranes were stained with the styryl dye FM4-64 as indicated in Materials and Methods of this section. Merge shows the overlap of the different signals**.**

5. DISCUSSION

Iron deficiency is an extended nutritional disorder whose prevention requires the development of novel strategies that increase iron intake. Baker's yeast *S. cerevisiae* is widely used in food technology to produce bakery derived products but also as a food supplement. Therefore, it seems meaningful taking advantage of the knowledge of yeast iron homeostasis to increase their capacity to acquire and store iron. An important drawback of increasing intracellular iron concentrations is the toxicity caused by ROS generation. Here, we decided to explore the potential of the main yeast iron resistance factor, Ccc1, to increase endogenous iron by storing it in an unharmful form within the vacuole. For this purpose, we overexpressed *CCC1*, and observed that it led to low growth and cellular viability when cells were cultivated in normal iron replete

media (Figures C3.2 and C3.3). Since increased expression of *CCC1* stimulates iron uptake and accumulation, due to iron regulon activation (Figure 2), we postulated that the reason for Ccc1 toxicity could be iron acquisition (Chen, O. S. and Kaplan, J., 2000; Li, L. et al., 2001; Cockrell, A. et al., 2014). In fact, previous genetic and biochemical analyses had shown that iron toxicity was due to the accumulation of cytosolic iron (Lin et al., 2011). Moreover, the toxicity caused by the expression of a constitutively active Aft1 transcription factor has been shown to be, at least partially, rescued by deletion of *FET3* (Ramos-Alonso et al., 2018). However, deletion of the components of the high-affinity iron uptake system Fet3-Ftr1 at the cell surface did not rescue the growth of *CCC1*-overexpressing cells (Figure C3.2). Then, we investigated whether the up-regulation of *CTH2*, which has been previously shown to limit growth, was responsible for *CCC1* overexpression toxicity, but no rescue was observed in a *cth2Δ* mutant (Figure C3.2), (Lin et al., 2011; Romero et al., 2018). Unexpectedly, we observed that deletion of the *AFT1* transcriptional factor increased *CCC1* overexpression toxicity (Figure C3.2). Aft1 is mainly implicated in increasing cytosolic iron levels by promoting iron uptake and mobilization from the vacuole. Therefore, these results are consistent with *CCC1* causing a decrease in the bioavailability of iron to the cytosol and other organelles, including mitochondria, whose pools are highly interconnected (Li, L. and Kaplan, 2004; Li, L. et al., 2010). Indeed, the activation of *FTR1* and *CTH2* that we observed (Figure C3.2A) is probably a consequence of decreased iron-sensing by Aft1 transcription factor. In any case, we cannot discard other non-exclusive possibilities for such toxicity. For instance, *CCC1* overexpression could cause a decrease in vacuolar lumen acidification, since Ccc1 seems to be a H^+/Fe^{2+} antiporter (Kato et al., 2019). In this sense, recent data have shown that that the loss of vacuolar acidification leads to oxidative damage of mitochondrial Fe/S cluster biosynthesis components and activities and the development of an age-related mitochondrial dysfunction (Chen, H. et al., 2020; Hughes et al., 2020). Importantly, Ccc1 overexpression toxicity was not observed in high iron media (Figures C3.2 and C3.3). This result is consistent with *CCC1* natural expression pattern, which is induced in response to elevated extracellular iron, and reinforces the hypothesis that low cytosolic and mitochondrial iron levels could be the reason for its toxicity (Li, L. et al.,

2008; Pimentel et al., 2012). However, more detailed studies would be necessary to fully elucidate the molecular reason for the toxicity of Ccc1 protein when overexpressed under iron replete conditions.

The comparison of Ccc1/VIT1 protein sequences unveiled that their cytosolic Nt domain has not been conserved during evolution and displays particular characteristics depending on the species (Sorribes-Dauden et al., 2020). In the case of fungi, including *S. cerevisiae*, Ccc1 Nt is rich in proline and serine residues (Sorribes-Dauden et al., 2020). The fact that genome-wide studies show that these serine residues could be phosphorylated prompted us to explore Ccc1 Nt function by constructing and expressing an NtΔCcc1 protein lacking its first 87 amino acids (Albuquerque et al., 2008; Swaney et al., 2013). Overexpression of *NtΔCCC1* did not confer toxicity under any of the promoters assayed (Figures C3.2 and C3.3). This was probably due a decrease in NtΔCcc1 functionality since it did not produce the same resistance to high iron media as full length Ccc1 (Figures C3.2 and C3.3). We observed that both GFP-tagged Ccc1 and NtΔCcc1 proteins localized to the vacuolar membrane, although full-length Ccc1 preferentially accumulated in small regions of the vacuolar membrane (Figure C3.6). It is tempting to speculate that phosphorylation of serine residues within Ccc1 Nt domain could modulate subcellular distribution of the protein. It has been proposed that Ccc1/VIT1 proteins dimerize, but no aggregation of such proteins has been described (Kato et al., 2019). Further studies are necessary to decipher the contribution of the Nt domain to Ccc1 function in metal transport. Importantly, NtΔCcc1-expressing cells were still able to up-regulate iron incorporation while keeping considerable growth (Figure C3.4). Consequently, NtΔCcc1 cells are able to incorporate at least 2-fold higher levels of iron from iron replete media than WT, *ccc1Δ* and *CCC1*-overexpressing cells. Overexpressing an Nt-truncated version of Ccc1 protein seems an interesting strategy to explore in order to increase the capacity of yeast cells to incorporate iron from non-iron rich media. Additional studies directed to enrich yeast cells with iron could contribute to its utilization as a tool to palliate iron deficiency.

6. CONCLUSIONS

Iron deficiency is a prevalent nutritional disorder whose prevention requires the development of novel strategies that increase iron intake. Baker's yeast *S. cerevisiae* is widely used in food technology to produce bakery derived products but also as a food supplement. Therefore, greater knowledge of yeast iron homeostasis and its ability to increase its capacity to acquire and store iron could prove meaningful. Here, we have observed that overexpression of the vacuolar iron importer Ccc1 is toxic to yeast cells. Remarkably, overexpression of an Nt-truncated version of Ccc1 (NtΔCcc1) did not alter growth and led to an increase in the extraction of iron from the environmental medium. Therefore, this truncated version of Ccc1 protein could be used to design strategies aimed to increase the capacity of yeast cells to incorporate iron from non-iron rich media. Additional studies aiming to enrich yeast cells with iron could contribute to its utilization as a tool to palliate iron deficiency.

7. SUPPLEMENTARY INFORMATION

7.1. Supplementary figures

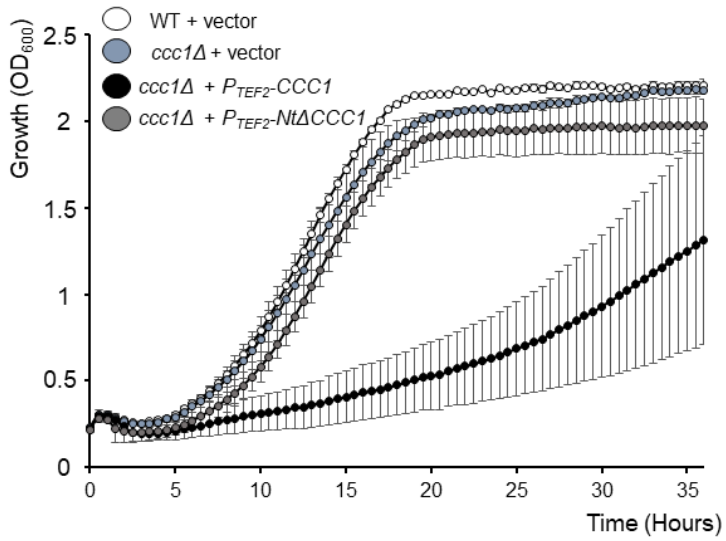

FIGURE C3.S1. OVEREXPRESSION OF *CCC1* INDUCES A DECREASE IN THE GROWTH RATE. Yeast cells described in Figure C3.2 were inoculated at an OD_{600} of 0.2 in liquid SC-Ura medium supplemented with 500 µm FAS. The OD_{600} was recorded every 30

minutes with a spectrostar nano absorbance 96-plate reader for 36 hours at 28°C. The average curve and standard deviation of at least three independent biological replicates is shown.

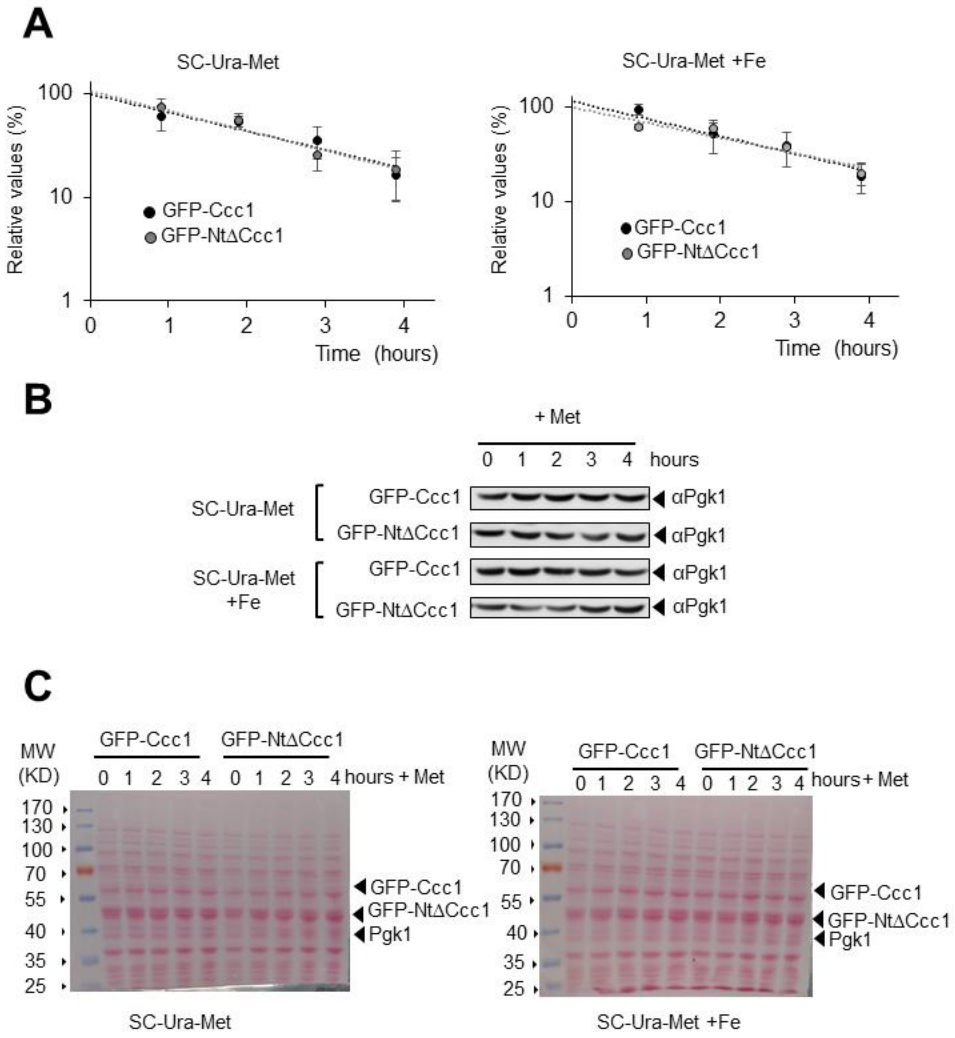

FIGURE C3.S2. GFP-CCC1 AND GFP-NTΔCCC1 PROTEIN STABILITY QUANTIFICATION AND LOADING CONTROLS. A) Quantification of GFP-Ccc1 and GFP-NtΔCcc1 protein levels. The average of three different samples and its standard deviation is represented. **B)** Western blot for Pgk1 protein levels. **C)** Ponceau staining.

Supplementary Materials: Supplementary data to this article can be found online at at https://www.mdpi.com/article/10.3390/genes12081120/s1.

Author Contributions: Conceptualization, S.P.; methodology, R.D.-S., M.T.M.-P. and S.P.; data curation, R.D.-S.; writ-ing—original draft preparation, S.P.; writing—review and editing, M.T.M.-P. and R.D.-S.; visual-ization, S.P. and R.D.-S.; supervision, M.T.M.-P. and S.P.; funding acquisition, M.T.M.-P. and S.P.. All authors have read and agreed to the published version of the manuscript.

Funding: This research was funded by a predoctoral contract ACIF/2018/077 (to R.S.-D.) and grant PRO-METEO/2020/014 from the Regional Government of Valencia (Generalitat Valenciana), grant BIO2017-87828-C2-1-P and PID2020-116940RB-I00 from the Spanish Ministry of Science, Innova-tion and Universities, and FEDER funds (ESF, European Social Fund).

Institutional Review Board Statement: Not applicable.

Informed Consent Statement: Not applicable.

Data Availability Statement: The data presented in this study are openly available in Digital.CSIC (https://digital.csic.es, accessed on 13 July 2021) at DOI: http://dx.doi.org/10.20350/digitalCSIC/13962 (accessed on 13 July 2021).

Acknowledgments: We are grateful to the members of the Iron Homeostasis laboratory for technical and scientific assistance.

Conflicts of Interest: The authors declare no conflict of interest. The funders had no role in the design of the study; in the collection, analyses, or interpretation of data; in the writing of the manuscript, or in the de-cision to publish the results.

CHAPTER 4:

Adaptation of *Saccharomyces* species to high-iron conditions

Raquel Sorribes-Dauden[1,2], Tania Jordá[2], David Peris[2,3], María Teresa Martínez-Pastor[1,*] and Sergi Puig [2,*]

[1]Departamento de Bioquímica y Biología Molecular, Universitat de València, Doctor Moliner 50, 46100 Burjassot, Spain

[2]Departamento de Biotecnología, Instituto de Agroquímica y Tecnología de Alimentos (IATA), Consejo Superior de Investigaciones Científicas (CSIC), Agustín Escardino 7, 46980 Paterna, Spain

[3]Section for Genetics and Evolutionary Biology, Department of Biosciences, University of Oslo, Blindernveien 31, 0371 Oslo, Norway

[*]Authors to whom correspondence should be addressed.

International journal of molecular sciences 23 (2022) 13965

(This article belongs to the Special Issue State-of-the-Art Molecular Microbiology in Spain)

1. ABSTRACT

Iron is an indispensable element that participates as an essential cofactor in multiple biological processes. However, when present in excess, iron can engage in redox reactions that generate reactive oxygen species that damage cells at multiple levels. In this report, we characterized the response of budding yeast species from the *Saccharomyces* genus to elevated environmental iron concentrations. We have observed that *S. cerevisiae* strains are more resistant to high-iron concentrations than *Saccharomyces* non-cerevisiae species. Liquid growth assays showed that species evolutionarily closer to *S. cerevisiae*, such as *S. paradoxus*, *S. jurei*, *S. mikatae,* and *S. arboricola,* were more resistant to high-iron levels than the more distant species *S. eubayanus* and *S. uvarum*. Remarkably, *S. kudriavzevii* strains were especially iron sensitive. Growth assays in solid media suggested that *S. cerevisiae* and *S. paradoxus* were more resistant to the oxidative stress caused by elevated iron concentrations. When comparing iron accumulation and sensitivity, different patterns were observed. As previously described for *S. cerevisiae, S. uvarum* and particular strains of *S. kudriavzevii* and *S. paradoxus* became more sensitive to iron while accumulating more intracellular iron levels. However, no remarkable changes in intracellular iron accumulation were observed for the remainder of species. These results indicate that different mechanisms of response to elevated iron concentrations exist in the different species of the genus *Saccharomyces*.

KEYWORDS: iron toxicity; yeast; *Saccharomyces* genus; adaptation; evolution; *CCC1*; oxidative stress; biodiversity

2. INTRODUCTION

Iron is a necessary redox cofactor for many key biological processes, like DNA replication and repair, amino acid and protein biosynthesis, lipid metabolism and cellular respiration (Puig et al., 2017; Jorda and Puig, 2020; Romero et al., 2021). Despite being especially abundant in the Earth's crust, in oxidative environments, iron easily switches from Fe^{2+} to Fe^{3+}, with solubility and bioavailability that are remarkably low at physiological pH. Thus, in humans, iron scarcity often leads to iron deficiency anemia, which causes

fatigue and impairs cognitive development and immunity. Iron limitation is also an agronomic problem since low iron availability decreases crop yield and quality (Sanvinsens and Puig, 2011). Moreover, competition for iron between microbial pathogens and their hosts modulates both their virulence and the host's capacity of response (Martínez-Pastor and Puig, 2020). Thus, organisms have developed different mechanisms to overcome iron shortage. In the yeast *Saccharomyces cerevisiae*, in response to iron deficiency, the transcriptional factors Aft1 and Aft2 activate a group of genes known as the iron regulon. These genes codify proteins that are involved in iron acquisition through iron-reductive uptake or the capture of siderophores, mobilization from intracellular reservoirs, such as the vacuole, recycling, and metabolism remodeling in order to optimize the use of the scarce iron (Martínez-Pastor et al., 2017). However, iron in excess is also harmful to cells since it can be involved in Fenton reactions that generate radical oxygen species (ROS), which induce damage to lipids, proteins, and nucleic acids (Winterbourn, 1995). Nonetheless, iron toxicity can even occur in anaerobic conditions, and other mechanisms, such as the mismetallation of enzymes or the activation of sphingolipid signaling have been proposed to mediate toxic iron effects in yeast (Yang, M. et al., 2006; Lin et al., 2011; Lee, Y. J. et al., 2012). In the presence of high iron levels, the *S. cerevisiae* transcriptional factor Yap5 activates the expression of *CCC1, GRX4*, and *TYW1* genes. The main factor responsible for yeast iron detoxification in Ccc1 is an iron transporter localized at the vacuole membrane that imports iron from the cytosol. Grx4 is a monothiol glutaredoxin that binds iron-sulfur (Fe-S) clusters and is involved in Aft1 deactivation. Tyw1 is a cytosolic Fe-S cluster-containing enzyme involved in the synthesis of the modified nucleoside wybutosin. Both Grx4 and Tyw1 have been described to play a key role in iron buffering in the cytosol (Li, L. et al., 2011; Pimentel et al., 2012). Iron overload also limits iron acquisition through the downregulation of the low-affinity Fet4 and high-affinity Fet3-Ftr1 cell surface iron transport systems (Martínez-Pastor et al., 2017). In addition, *S. cerevisiae* activates several genes involved in oxidative stress response, as *TRX2, SOD1, TSA1* and *YAP1*, when iron is present at high levels (Lin et al., 2011). The above-described responses to low and high iron are generally conserved in the *Saccharomyces* genus, and in a broader sense, the iron uptake and storage

systems are also conserved in fungi, with differences in the transcriptions factors involved (Aft1 vs. iron responsive GATA factors), or the ability to produce siderophores (Lee, H. N. et al., 2013; Martínez-Garay et al., 2016; Martínez-Pastor and Puig, 2020). Recent data have shed light on several biological mechanisms that have permitted the adaptation to iron scarcity in fungi, including horizontal operon transfer of bacterial genes involved in siderophore biosynthesis, loss of function of Ccc1 and Yap5, and the increase in iron uptake, which has been proposed to occur through mutations in Aft1 or the iron uptake system, or by alterations in the expression of other iron homeostasis genes (Lee, H. N. et al., 2013; Martínez-Garay et al., 2016; Eldarov et al., 2018). On the other hand, the adaptation to high iron levels requires changes in storage and energetic metabolism, upregulation of oxidative stress genes, and iron uptake avoidance (Martínez-Garay et al., 2016; Balaban et al., 2019). Furthermore, in the last two decades, the number of isolated, phenotyped, and sequenced strains among the *Saccharomyces* genus has unprecedently risen, consolidating this genus as a model to explore adaptation and evolution (Peter et al., 2018; Alsammar and Delneri, 2020; Peris et al., 2023). Previously, we analyzed the response to variations in the iron levels of a wide selection of *S. cerevisiae* strains, from a diversity of origins. In this report, we have extended the study of the response to excess iron to representative strains of the main available *Saccharomyces* populations. We characterized their growth, oxidative state, iron accumulation, and expression of iron homeostasis genes. Our results confirm that the main mechanism to avoid iron toxicity in the *Saccharomyces* genus is to diminish iron incorporation, but other mechanisms must be considered, since iron sensitivity is found in species with low iron accumulation.

3. MATERIALS AND METHODS

3.1. Yeast strains and growth conditions

All the *Saccharomyces* species strains used in this study are listed in Table C4.1. Yeast strains were stored at −80 °C in cryotubes in yeast extract-peptone-dextrose (YPD) medium and 15% glycerol. Routine cultures were maintained in YPD plus 2% agar plates at 20 °C. Unless otherwise indicated, yeasts were

grown in synthetic complete (SC) medium at 20 °C to allow for a similar comparative growth of all species (Peris et al., 2023). Iron was added at the indicated concentrations from a 100 mM ferrous ammonium sulfate (FAS, Merck-Sigma, Darmstadt, Germany) stock solution, prepared freshly in 0.1 M HCl to promote iron solubility. A control with the equivalent HCl concentration was prepared for each experiment. The redox indicator methylene blue (Merck-Sigma, Darmstadt, Germany) was added to agar plates with FAS or HCl to a 1 mM final concentration. For growth spot assays, overnight precultures were adjusted to an OD_{600} of 0.1, 0.01, and 0.001, and then spotted on SC agar plates with the indicated concentrations of FAS, H_2O_2 (Honeywell, Charlotte, NC, USA), menadione (Merck-Sigma, Darmstadt, Germany) or HCl. Plates were incubated for 7 days at 20 °C and then photographed. However, temperature spot assays were performed at 15, 20, 25, 30, and 35 °C.

3.2. Determination of non-Inhibitory and minimal inhibitory concentrations

Yeast strains were inoculated in triplicate in 96-well plates at an OD_{600} of 0.1 in SC liquid media and growth at 20 °C was registered measuring OD_{600} every 30 min with an absorbance microplate reader with a stacker microplate handling system, Spectrostar Omega (BMG Labtech, Ortenberg, Germany). The area under the curve (AUC) was obtained using Growth curve analysis tool (GCAT) online software (Bukhman et al., 2015). This value was used to calculate the fractional area ($Fa = AUC_{Fe}/AUC$). Fa was plotted versus $\log_{10}$ of FAS concentration. Non-inhibitory (NIC) and minimal inhibitory concentration (MIC) values were calculated, as previously described (Arroyo-Lopez et al., 2010), using an in-house script in R Studio 2022.07.1, version 4.2.0 (R Core Team, 2021), with “nlsLM” tool from minpack.lm package 1.2–2 (Elzhov et al., 2022). Segment representation was obtained using the “geom_segment” tool of ggplot2 package 3.3.3 (Wickham, 2016).

3.3. Endogenous iron measurements

To determine endogenous iron levels, a previously described colorimetric assay was used (Tamarit et al., 2006). First, cells were inoculated at 0.2 OD_{600} in SC medium supplemented with 4 mM FAS for 24 h. Then, 1 mL of cells at 5

OD_{600} units /mL, or an equivalent amount of cells, were harvested and washed twice with 1 mM EDTA and once with milliQ water. Cell pellets were dissolved and digested in 3% HNO_3 at 98 °C for at least 16 h. After digestion, ascorbic acid and ammonium acetate (Merck-Sigma, Darmstadt, Germany) were added to cell extracts to a final concentration of 1 M and 40 mM, respectively. Finally, 3.2 mM of the Fe^{2+}-specific chelator bathophenanthroline disulfonic acid disodium, BPS (Merck-Sigma, Darmstadt, Germany) was added and absorbance at 535 nm (A_{535}) was measured. For dry weight determination, 6 mL of cells grown in the same conditions described above were collected at 5 OD_{600} units/mL, dried at 50 °C for 3 days, and weighed. Spearman correlation coefficient between iron content and ΔMIC-NIC was obtained with “ggplot2” R Studio 2022.04.22, 4.2.0 package (R Core Team, 2021).

3.4. RNA processing and analysis

Overnight precultured cells were inoculated at an OD_{600} of 0.2 in SC liquid medium during 5 h in glass flasks. Afterwards cells were transferred to fresh medium without or with 2 mM FAS for an extra hour. Then, cells were harvested by centrifugation and frozen. Total RNA isolation and particular mRNA levels were determined by RT-qPCR, as previously described (Sanvisens et al., 2014). Specific primers used for RT-qPCR are listed in Table C4.S2. The *ACT1* mRNA values were used to normalize.

Genome assemblies. Previously published genome assemblies were downloaded from NCBI and ATCC web portal. Accession numbers or links are provided in Table C4.S1.

3.5. Phylogenetic tree

A Neighbor-joining (NJ) tree was generated based on the fast method fastANI 1.1 (Jain et al., 2018). Then, we calculated the pairwise average nucleotide identity (ANI) among genome assemblies, with a fragment length set to 400 bp. FastANI values were then converted to a percentage dissimilarity matrix by subtracting ANI from a value 100%. All calculations and matrix formatting were done in RStudio 2022.07.1, R 4.0.2 (R Core Team, 2021), using dplyr 1.0.5, stringr 1.5.3 and reshape2 1.4.4 packages. The dissimilarity

data was used as the distance to reconstruct the NJ phylogenetic tree in MEGA v5 (Tamura et al., 2011). The phylogenetic tree in newick format was rooted to the *S. eubayanus* and *S. uvarum* branch in the R using ape 5.4 (Paradis and Schliep, 2019), phytools 0.7 (Revell, 2012) and the phylogenetic tree was drawn with ggtree 2.2.4 (Yu et al., 2016).

3.6. Gene expression heatmap

The heatmap representation of log_2 fold change was obtained with the "heatmaply" tool of heatmaply 1.3.0 package (Galili et al., 2018) from R Studio 2022.04.22 4.2.0 (R Core Team, 2021).

3.7. Principal Component Analyses

The principal component analysis (PCA) of the variables was obtained in R Studio 2022.04.22 (R Core Team, 2021), 4.2.0 using the "prcomp" tool of factoextra 1.0.7 package (Kassambara and Mundt, 2020). The "fviz_pca_biplot" tool from ggfortify 0.4.14 package (Tang et al., 2016) was used to represent the two-dimensional PCA biplot of variables and individual strains.

4. RESULTS

4.1. Characterization of iron resistance and accumulation in the *Saccharomyces* genus

In a previous report, we analyzed the response of a set of *S. cerevisiae* strains, from a wide diversity of origins, to excess iron, and selected a group of strains either resistant or sensitive to elevated concentrations of iron (Martínez-Garay et al., 2016). In the present study, we aimed to expand our knowledge of how yeast cells respond to high iron to other species of the *Saccharomyces* genus, for which we selected 28 strains belonging to eight different *Saccharomyces* species (*S. cerevisiae, S. paradoxus, S. jurei, S. mikatae, S. kudriavzevii* and *S. arboricola*) and challenged them with high extracellular iron concentrations (Table C4.1 and Table C4.S1, and Figure C4.1). Nineteen *Saccharomyces* non-cerevisiae strains were selected as representative of the

genus, while nine previously characterized *S. cerevisiae* strains were used as references (Martínez-Garay et al., 2016).

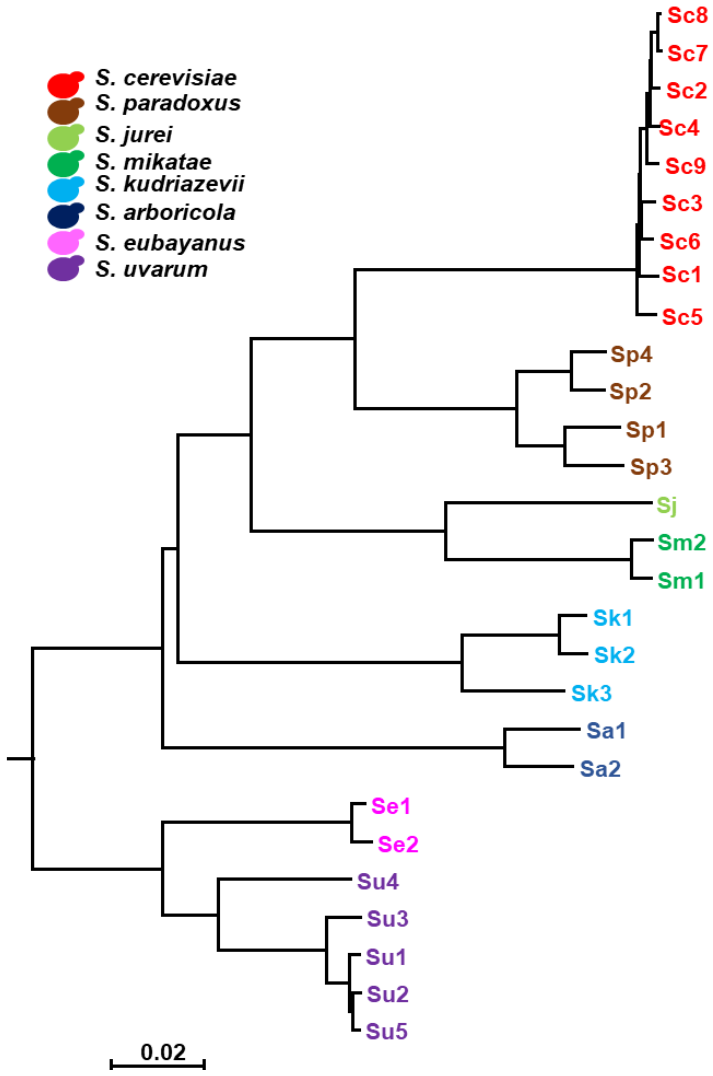

FIGURE C4.1. THE PHYLOGENETIC TREE OF THE *SACCHAROMYCES* STRAINS USED IN THIS STUDY. Neighbor-Joining (NJ) tree using the (100 − ANI)/100 values as distances for reconstruction. The scale bar represents (100 − ANI)/100. The color code assigned to each *Saccharomyces* species in this study are: *S. cerevisiae* (Sc), red; *S. paradoxus* (Sp), brown; *S. jurei* (Sj), light green; *S. mikatae* (Sm), dark green; *S. kudriavzevii* (Sk), light blue; *S. arboricola* (Sa), dark blue; *S. eubayanus* (Se), pink; and *S. uvarum* (Su), purple.

TABLE C4.1. *SACCHAROMYCES* STRAINS USED IN THIS WORK. Species are listed in order of evolutionary proximity to *S. cerevisiae*, according to the phylogenetic tree depicted in Figure C4.1. * Classification according to References (Peter et al., 2018; Peris et al., 2023).

Abbreviation	Species	Strain	Geographical Origin	Population *
Sc1	*S. cerevisiae*	UWOPS03-461.4	Asia (Malaysia)	19. Malaysian
Sc2	*S. cerevisiae*	CECT10131	Europe (Spain)	8. Mixed origin
Sc3	*S. cerevisiae*	CECT10711	Asia (Japan)	25. Sake
Sc4	*S. cerevisiae*	CECT10120	Europe (Spain)	8. Mixed origin
Sc5	*S. cerevisiae*	CLIB219-2B	Europe (Russia)	18.Far East Asia
Sc6	*S. cerevisiae*	YPS128	USA (Pennsylvania)	23. North American oak
Sc7	*S. cerevisiae*	YJM978	Europe (Italy)	1. Wine/European
Sc8	*S. cerevisiae*	CECT11032	Europe (Italy)	1. Wine/European
Sc9	*S. cerevisiae*	BY4743	-	-
Sp1	*S. paradoxus*	yHDPN24	Canada (Québec)	America C
Sp2	*S. paradoxus*	N44	Europe (Russia)	Far East
Sp3	*S. paradoxus*	YPS138	USA (Pennsylvania)	America B
Sp4	*S. paradoxus*	CBS432	Europe (Russia)	EU
Sj	*S. jurei*	NCYC3947	Europe (France)	EU
Sm1	*S. mikatae*	yHAB336	Asia (China)	Asia B

Sm2	*S. mikatae*	IFO1815	Asia (Japan)	Asia A
Sk1	*S. kudriazevii*	IFO1802	Asia (Japan)	Asia A
Sk2	*S. kudriazevii*	ZP591	Europe (Portugal)	EU
Sk3	*S. kudriazevii*	IFO1803	Asia (Japan)	Asia B
Sa1	*S. arboricola*	CBS10644	Asia (China)	Asia A
Sa2	*S. arboricola*	ZP960	Oceania (New Zealand)	Oceania
Se1	*S. eubayanus*	yHCT69	South America (Argentina)	Patagonia B/HOL
Se2	*S. eubayanus*	yHRVM107	USA (North Carolina)	Patagonia B/HOL
Su1	*S. uvarum*	yHAB60	Unknown	HOL/SA-A
Su2	*S. uvarum*	CBS7001	Europe (Spain)	HOL-EU
Su3	*S. uvarum*	yHAB521	South Ameria (Argentina)	SA-B
Su4	*S. uvarum*	ZP964	Asia (New Zealand)	Australasia
Su5	*S. uvarum*	yHCT77	USA (Oregon)	HOL-NA

To characterize how these strains respond to excess iron, we grew them at 20 °C on the SC liquid medium with increasing ferrous ammonium sulfate (FAS) concentrations, and growth was followed through OD_{600} measurements every 30 min, as described in the Materials and Methods of this section. The chosen temperature was 20 °C because it provides a similar growth rate for all the *Saccharomyces* species studied (Salvadó et al., 2011). The area under the growth curve at a particular iron concentration (AUC_{Fe}) was obtained and normalized to the AUC for the same strain when cultivated without iron to obtain the fractional area (Fa = AUC_{Fe}/AUC). Finally, Fa was plotted versus $\log_{10}$ of iron concentration (Figure C4.S1). In all cases, the representation of the Fa vs.

log_{10}[FAS] fitted to a sigmoid curve, indicating that iron-susceptibility is non-lineal in the *Saccharomyces* genus.

The non-inhibitory concentration (NIC) and the minimal inhibitory concentration (MIC) were obtained for each strain from their corresponding Fa plots (Figure C4.2). These values delimit the concentration range of iron with inhibitory effects on the growth for each particular strain. The *S. cerevisiae* strains Sc2, Sc3, Sc7, and Sc8 showed high NIC and MIC values, supporting the results of our previous study, performed in solid media at 30 °C, which characterized these strains as highly iron-resistant (Martínez-Garay et al., 2016). However, *S. cerevisiae* strains Sc6, Sc5, and Sc4, previously identified as iron-sensitive (Martínez-Garay et al., 2016), displayed lower values of NIC and MIC. The Malaysian UWOPS03-461.4 strain (Sc1), characterized as iron-sensitive (Lee, H. N. et al., 2013), presents a low value for NIC, but a MIC value higher than expected. Finally, the laboratory strain BY4743 (Sc9) displayed an intermediate iron sensitivity (Figure C4.2). A general observation shows that most strains possess NIC values around 3.5 mM, indicating that species start being affected by iron at similar iron concentrations, but only some of them are also resistant through a wider range of iron levels. Thus, ΔMIC-NIC range or MIC value could be used in most cases to classify strains according to iron sensitivity. Regarding the comparative resistance between species, the highest resistance is found in *S. cerevisiae* strains, followed by the *Saccharomyces* species that are more closely related to *S. cerevisiae*, including *S. mikatae, S. jurei*, and *S. paradoxus* (except for strain Sp4), which are highly or moderately resistant to elevated iron concentrations. Conversely, *S. eubayanus, S. uvarum*, and *S. kudriavzevii* are the most sensitive species, while *S. arboricola* behaves between those two groups of species.

In a previous characterization of various iron-resistant and iron-sensitive *S. cerevisiae* strains, we observed that the resistance to high iron was achieved by limiting the incorporation of the metal into cells, while iron-sensitive strains accumulated higher intracellular amounts of iron (Martínez-Garay et al., 2016). To determine whether this mechanism was extensive to other species of the *Saccharomyces* genus, we measured the endogenous iron levels after 24 h of incubation in SC with 4 mM FAS at 20 °C. Indeed, we observed that iron-

resistant strains, like Sc7, Sm2, Sp3, Sm1, and Sj, limit the accumulation of intracellular iron (<2 mg Fe/g DW). However, iron-sensitive strains could be separated into two groups: (i) Strains that accumulate high endogenous iron levels (3–7 mg Fe/g DW), such as Sp4, Su1–3 and Sk3, and (ii) strains that are sensitive to much lower amounts of intracellular iron (around 2 mg Fe/g DW), like Sk1–2 and Se1–2 (Figure C4.3A). According to these observations, the Spearman correlation coefficient (ρ) between iron content and ΔMIC-NIC has a value of −0.69, suggesting a fairly strong relationship, which is statistically significant (Figure C4.3B). Taken together, these results suggest that iron sensitivity in the *Saccharomyces* genus could be explained by either an excessive iron accumulation, following the same tendency observed for *S. cerevisiae* strains (Martínez-Garay et al., 2016), or by an increased sensitivity to intracellular iron.

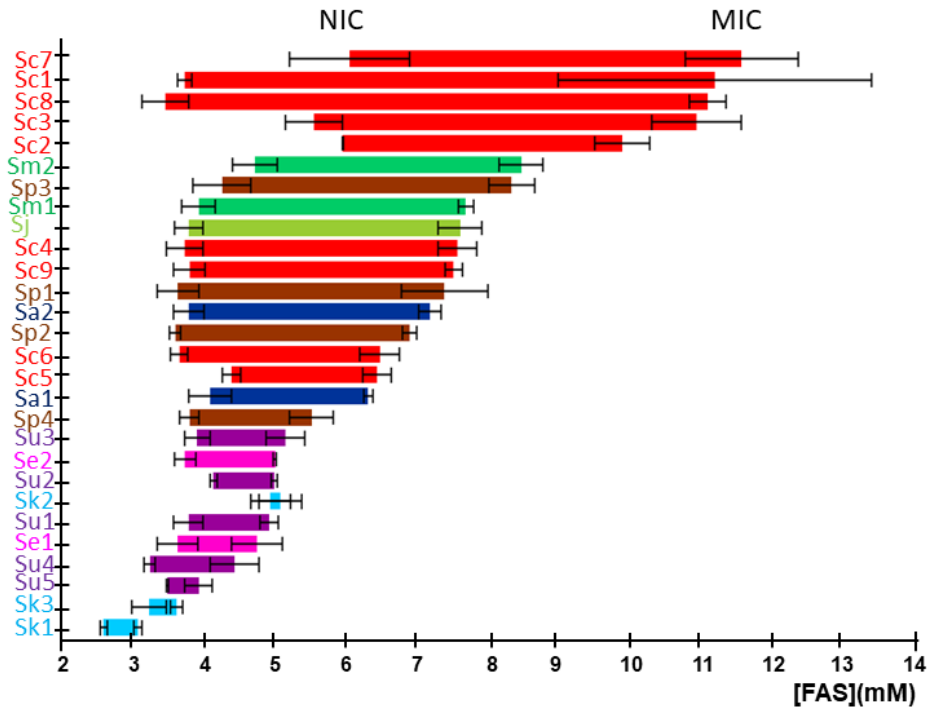

FIGURE C4.2. GROWTH INHIBITORY EFFECT OF IRON ON *SACCHAROMYCES* STRAINS. Horizontal segments represent the range of FAS concentrations between NIC (left-end) and MIC (right-end), for each yeast strain. Data and error bars represent the average and standard deviation of three independent biological replicates. The colors of segments and strain abbreviations are species-dependent according to Figure C4.1.

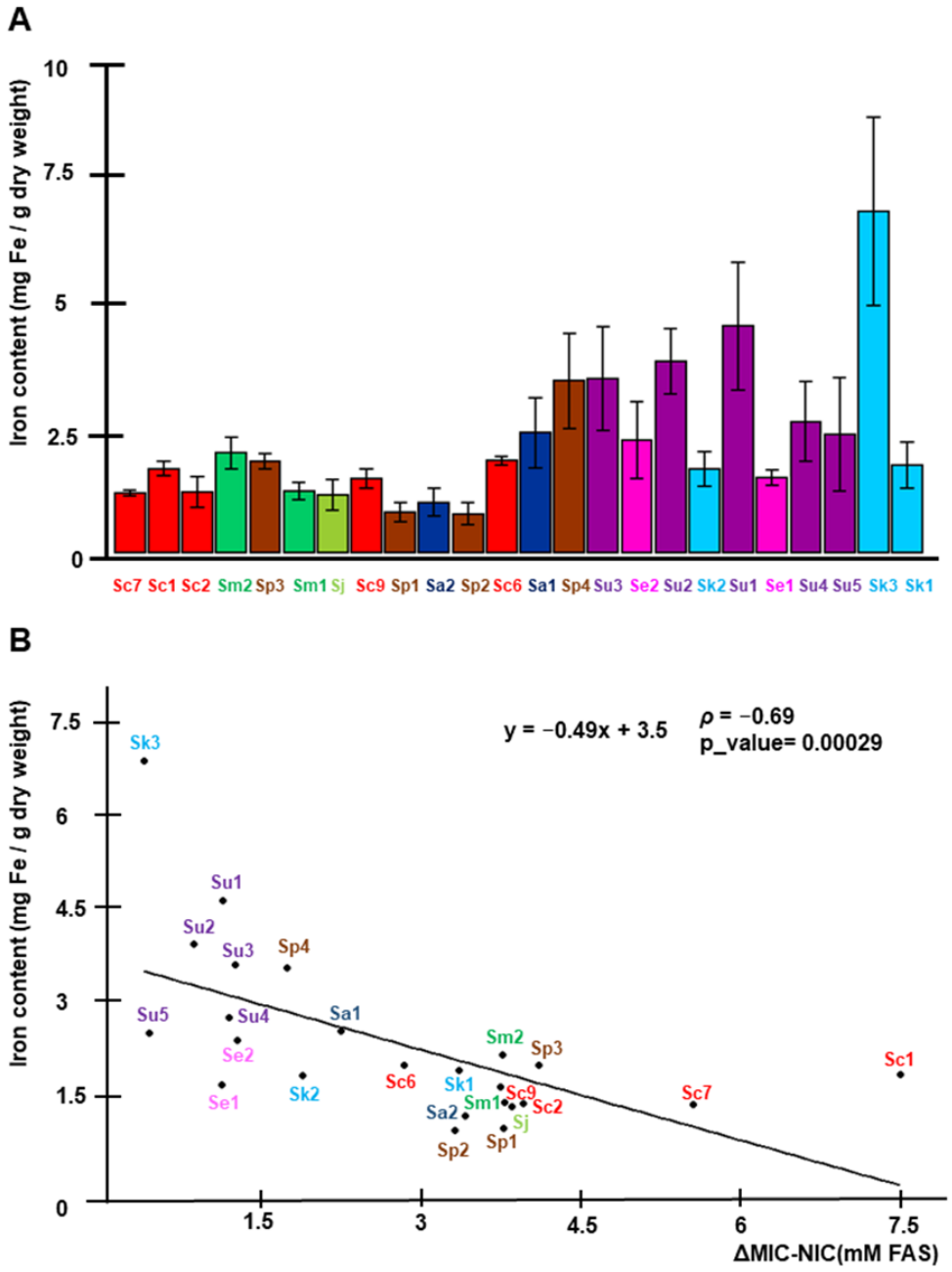

FIGURE C4.3. IRON ACCUMULATION UNDER HIGH-IRON CONDITIONS AND CORRELATION WITH IRON SENSITIVITY. A) Overnight precultures of yeast strains were reinoculated at an OD_{600} of 0.2 in liquid SC medium with 4 mM FAS and grown for 24 h. Then, cells were collected and endogenous iron (mg Fe/g dry weight) was determined as indicated in Materials and Methods. Data and error bars represent the average and standard deviation of at least three independent biological replicates. Strains are

ordered according to the MIC values depicted in Figure C4.2. **B)** Scatter plot analysis of ΔMIC-NIC (x axis) and iron content (y axis) variables. Spearman's correlation equation is shown, together with Spearman's rank coefficient (ρ) and a p_value. Colors and strain abbreviations follow the same code as in Figure C4.1.

4.2. Iron-sensitive strains show alterations in cellular redox state which are not due to a diminished response to oxidative stress

To further analyze how iron impacts the growth of different species of the *Saccharomyces* genus, we grew yeast cells in solid media containing increasing iron concentrations. For most strains, iron toxicity began to manifest at 5 mM FAS. To exclude any effects of HCl, which was used to prepare FAS stock, control plates were prepared with equivalent concentrations of HCl (Figure C4.S3). Particular strains displayed a growth defect for HCl at higher concentrations than for iron, indicating that iron effects were specific. While some exceptions are observed (e.g., Sc7 and Sc1 strains are more sensitive to iron in solid than in liquid media, and Sa1, Se2, and Sc6 strains grow better in solid media than expected by their liquid MIC values), strains with low MIC values in liquid media showed impaired growth when high-iron concentrations were present in solid conditions, whereas strains with higher liquid MIC values also grew better in plates (Figure C4.2 and Figure C4.4). Therefore, solid assays support the general conclusions made from liquid growth curves.

Iron toxicity has been attributed to the ability of this metal to participate in Fenton reactions, leading to ROS production which can cause oxidative damage to cellular components (Winterbourn, 1995). To ascertain whether the differences in the response to iron excess observed among the strains of this study could be explained by alterations in their cellular redox state, solid medium was supplemented with the biocompatible redox indicator methylene blue, which exhibits an intense blue color in its oxidized form and is colorless when reduced. Thus, blue yeast colonies are associated with a more oxidative cellular state (Nishida and Silver, 2012; Martínez-Garay et al., 2016). All *S. cerevisiae* strains, except for Sc5, exhibited white or light blue color independently of iron concentration, suggesting that, besides being more

resistant to iron, the change in their oxidative state is minimal. On the contrary, most non-cerevisiae strains, with the exception of Su2, Se1 and Sk1, showed a darker blue color after iron exposure, indicating that exposure to this metal provokes a more oxidized state. Since these observations were compatible with a general adaptation to oxidative stress, we decided to challenge these strains with two different ROS sources, H_2O_2 and menadione (Figure C4.5 and C4.6). We observed that, differently from iron resistance, non-cerevisiae species, such as *S. jurei, S. paradoxus* (Sp1–2 and 4), *S. arboricola* (Sa1) and *S. uvarum* (Su1–3, 5), were found between the most H_2O_2 resistant strains (Figure C4.5). Strikingly, *S. uvarum* strains displayed an inverse correlation between both responses, being resistant to H_2O_2, but sensitive to iron. Regarding *S. cerevisiae*, only Sc4 was among the most resistant strains, while the rest of *S. cerevisiae* strains, except Sc2, which was highly sensitive, form an intermediate resistant group, together with the evolutionarily closely related *S. mikatae* strains and Sp3 (Figure C4.5). With respect to menadione, which causes oxidative stress through the production of superoxide anions, a slightly different patron is observed, with some exchanges between the high and medium resistant groups, but still *S. cerevisiae* strains were found in the intermediate group, overcome in resistance by *S. mikatae*, Sp1–2, Se1 and Su4–5 (Figure C4.6). Finally, the most H_2O_2-sensitive strains were also sensitive to menadione, like Sc3, Sa1, Sc2, and Se2. Taken together, these results indicate that *Saccharomyces* iron sensitivity cannot be exclusively attributed to a general decrease in oxidative stress resistance.

4.3. Iron-sensitive strains are less thermotolerant

The *Saccharomyces* genus contains thermotolerant (*S. cerevisiae* and *S. paradoxus*) and cryotolerant (*S. arboricola*, *S. eubayanus* and *S. uvarum*) species. To explore a potential correlation between adaptation to high temperatures and the resistance to high iron and/or oxidative stress, we studied the growth of this particular set of *Saccharomyces* strains at different temperatures, ranging from 15 °C to 35 °C (Figure C4.7). First, we confirmed that, as reported in (Salvadó et al., 2011; Peris et al., 2023), *S. eubayanus* and *S. uvarum* are thermosensitive species, where growth at 30 °C is compromised. The *S. jurei* strains used here, *S. arboricola* and *S. kudriavzevii*, also performed

better at low temperatures and were unable to properly grow at 35 °C (Figure C4.7). However, *S. cerevisiae* and its closest relative, *S. paradoxus*, are the most thermoresistant, growing relatively well at 35 °C, but also the most cryosensitive, with growth defects at 15 °C. The remainder of the species showed an intermediate response, with variations among strains. These results show a putative link between iron resistance and thermotolerance adaptation.

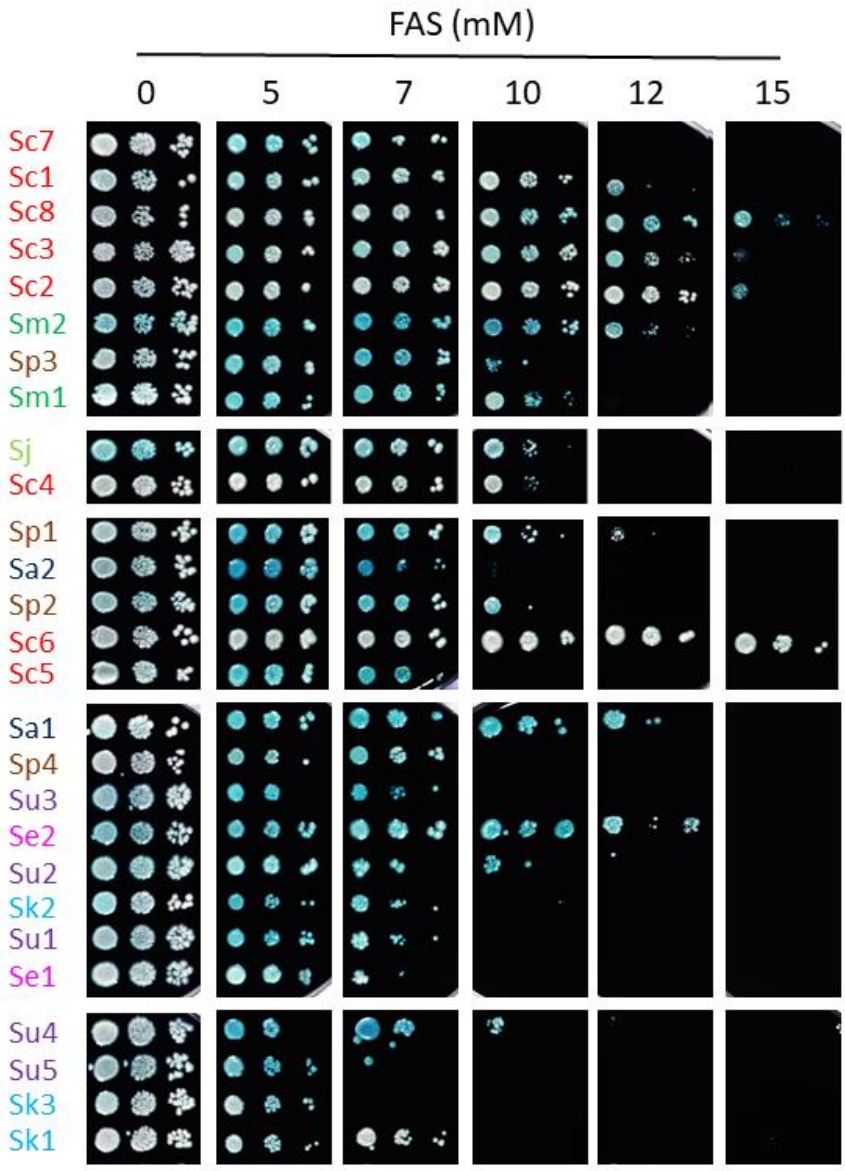

FIGURE C4.4. GROWTH OF *SACCHAROMYCES* STRAINS IN HIGH-IRON CONDITIONS. Overnight precultures were diluted to an OD_{600} of 0.1, 0.01 and 0.001 and spotted on SC + 1 mM methylene blue agar plates with the indicated range of FAS concentrations. Plates were incubated for 7 days at 20°C and then photographed. An intense blue color indicates a more oxidized state of the cells. Strains are sorted based on MIC values and species-specific colors are used as in the above figures.

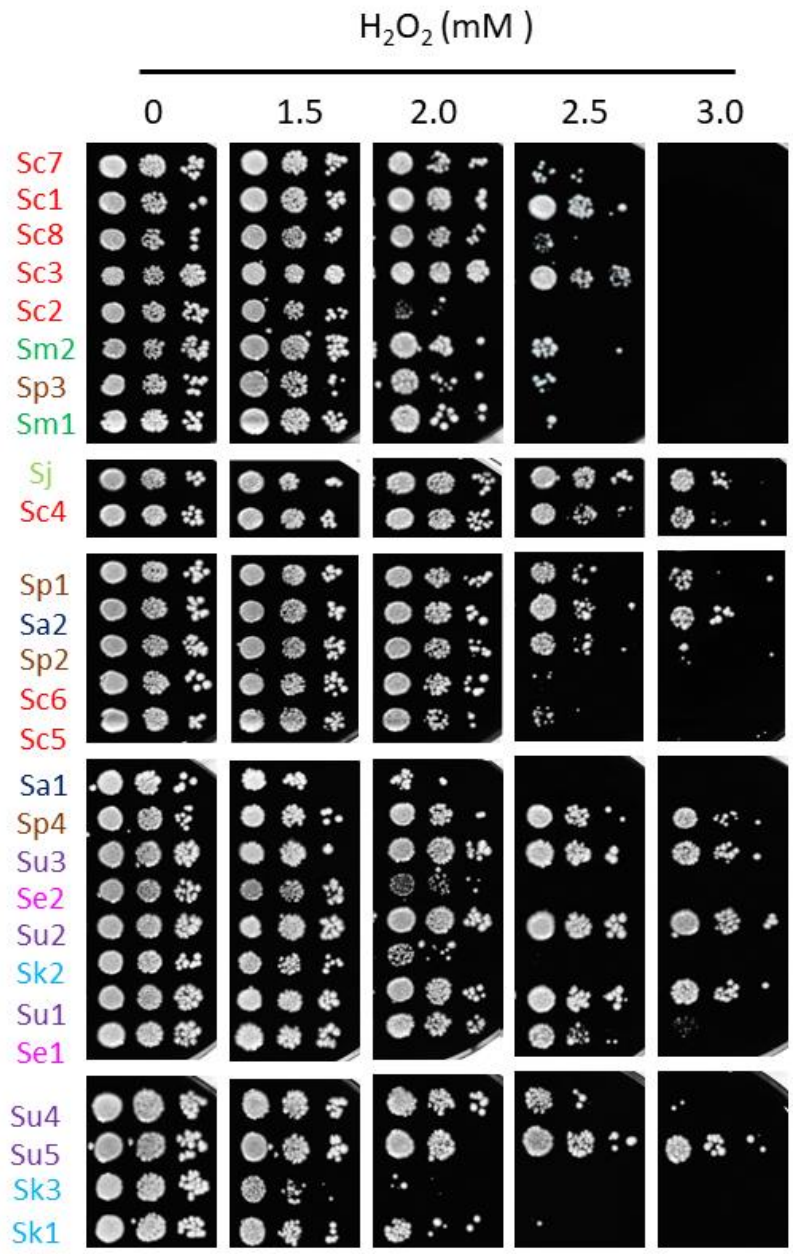

FIGURE C4.5. GROWTH OF *SACCHAROMYCES* STRAINS IN H_2O_2-CONTAINING MEDIA. Overnight precultures were diluted to an OD_{600} of 0.1, 0.01 and 0.001, and spotted in SC plates with a range of H_2O_2 concentrations. Plates were incubated during 7 days at 20°C and then photographed. Strains are sorted based on MIC values and species-specific colors are used as in the above figures.

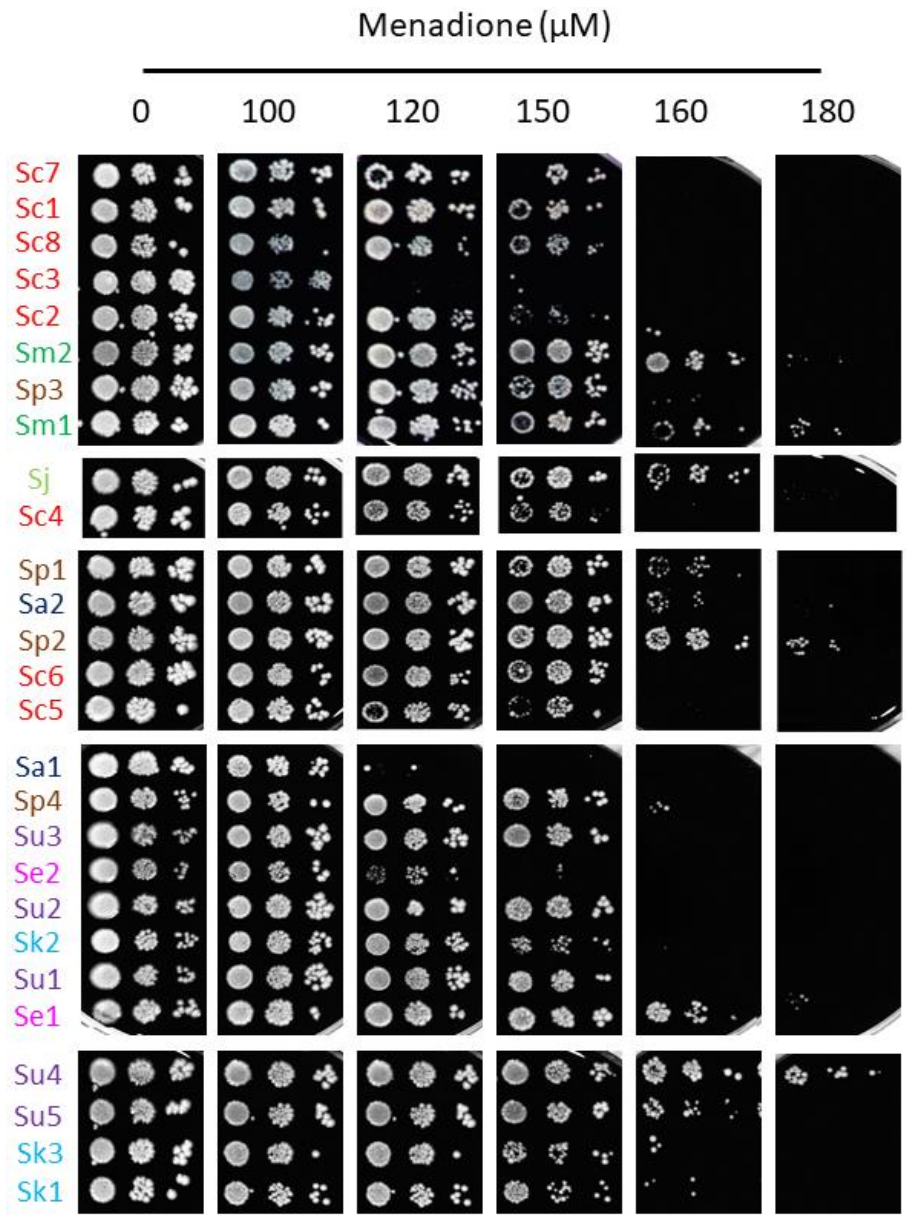

FIGURE C4.6. GROWTH OF *SACCHAROMYCES* STRAINS IN THE MENADIONE-CONTAINING MEDIA. Yeasts were cultivated and assayed for growth, as depicted in Figure C4.5, but on SC plates with the indicated range of menadione concentrations.

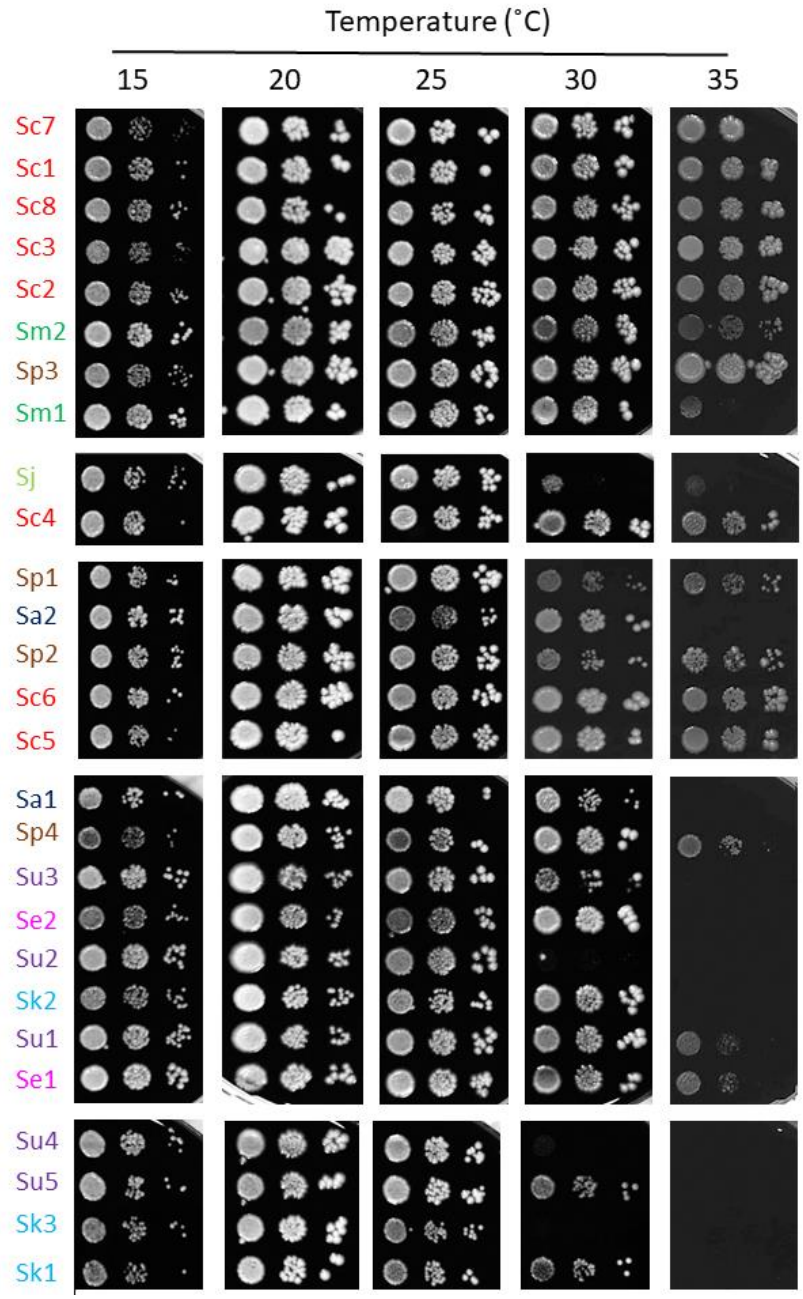

FIGURE C4.7. GROWTH OF *SACCHAROMYCES* STRAINS AT DIFFERENT TEMPERATURES. Yeasts were cultivated and assayed for growth, as indicated in Figure C4.5, but plates were incubated at 15, 20, 25, 30 and 35 °C.

4.4. Iron-sensitive strains show altered expression of iron homeostasis and oxidative response genes

In order to decipher whether genes that are regulated in response to excess iron or oxidative stress are dysregulated in the iron-sensitive strains, we grew yeast cells to the exponential phase in SC with or without 2 mM FAS and used RT-qPCR to analyze the expression of *CCC1, GRX4, TYW1, FET4*, and *TRX2* genes in the different species (Tables C4.2 and C4.S3, Figures C4.S4–S6). A hierarchical cluster heatmap was created from the $\log_2$ fold change of mRNA levels between iron addition and the control (SC) (Figure C4.8). We observed that, upon iron addition, the upregulation of Yap5 targets, *CCC1, GRX4* and *TYW1*, previously reported for *S. cerevisiae* (Li, L. et al., 2011; Pimentel et al., 2012; Park et al., 2013), was conserved in all the species of the *Saccharomyces* genus (Figure C4.S4). *GRX4* exhibited a higher increase in expression, followed by *CCC1* and *TYW1*. *TRX2* levels remained stable or lightly increased, whereas *FET4* expression decreased or was not altered, depending on the specific strain (Figure C4.S5). Hierarchical clustering of expression grouped *Saccharomyces* strains in the two main groups (Figure C4.8), with *S. uvarum* Su1 remaining unclustered. Remarkably, six out of seven components of group I (Sc1, Se1, Su4, Se2, Su5, and Su2) were iron-sensitive strains that showed the largest shutdown of *FET4* expression and high *GRX4* mRNA levels in normal conditions (Figures C4.S4 and C4.S5). However, the largest group II of strains showed a milder downregulation of *FET4* and a larger induction of *GRX4* and *CCC1*. This cluster can be divided into two different subgroups, IIa and IIb. Subgroup IIa is formed by a mixture of sensitive and resistant strains (Su3, Sa2, Sm1, Sa1, Sc6, Sc2, Sc7, Sj, and Sp4). This stands out as the highest increase in *GRX4* mRNA levels, which can be attributed to the very low expression observed without iron addition, but a low increase in *TYW1* mRNA levels

and an intermediate induction of *CCC1* (Figure C4.8 and Figure C4.S4). Subgroup IIb is composed of the resistant strains Sp3 and Sm2, the sensitive strains Sp1, Su1, Sk1–3, and the laboratory strain Sc9. The increase in *GRX4* expression is still high in these strains, and together with Sc1, Sc6 and Se1 strains, this group shows the highest induction of *CCC1* and *TYW1*. Interestingly, the most relevant downregulation of *FET4* is observed in the *S. kudriavzevii* strains. Finally, Su1 shows a divergent pattern from all other strains, mainly marked by the downregulation of *GRX4*. Regarding *TRX2* expression, as representative of the oxidative stress response, we observed only minor increases in the presence of iron, which are only remarkable in *S. cerevisiae* and *S. kudriavzevii* strains. Conversely, *TRX2* mRNA levels remain quite unchanged upon iron addition in *S. mikatae* and *S. paradoxus* strains, or even show a slight decrease in *S. jurei* or Sp4. Other genes involved in oxidative stress, such as *YAP1, SOD1* and *TSA1*, were also analyzed, but no remarkable changes were observed upon iron addition (Figure C4.S6). Taken together, these results indicate that the transcriptional response to iron excess is predominant over that of oxidative stress. While strain-specific patterns were observed, several iron-sensitive strains clustered in group I displayed a strong downregulation of the *FET4* iron transporter gene.

TABLE C4.2. LIST OF GENES INVOLVED IN IRON OVERLOAD AND OXIDATIVE STRESS ANALYZED IN THIS STUDY. Systematic and common gene names, a brief description of function, and human orthologs are indicated.

Systematic Name	Common Name	Brief Description	Human Ortholog
YLR220W	*CCC1*	Vacuolar Fe^{2+}/Mn^{2+} transporter	-
YER174C	*GRX4*	Glutathione-dependent oxidoreductase and glutathione S-transferase	*GLRX3*

YPL207W	*TYW1*	Iron-sulfur protein required for synthesis of wybutosine modified tRNA	*TYW1A* and *TYW1B*
YMR319C	*FET4*	Plasma membrane low-affinity Fe^{2+} transporter	-
YGR209C	*TRX2*	Cytoplasmic thioredoxin isoenzyme	*TXN*
YML007W	*YAP1*	Basic leucine zipper (bZIP) transcription factor	
YJR104C	*SOD1*	Cytosolic copper-zinc superoxide dismutase	*SOD1*
YML028W	*TSA1*	Thioredoxin peroxidase	*PRDX1*, *PRDX2*, *PRDX3* and *PRDX4*

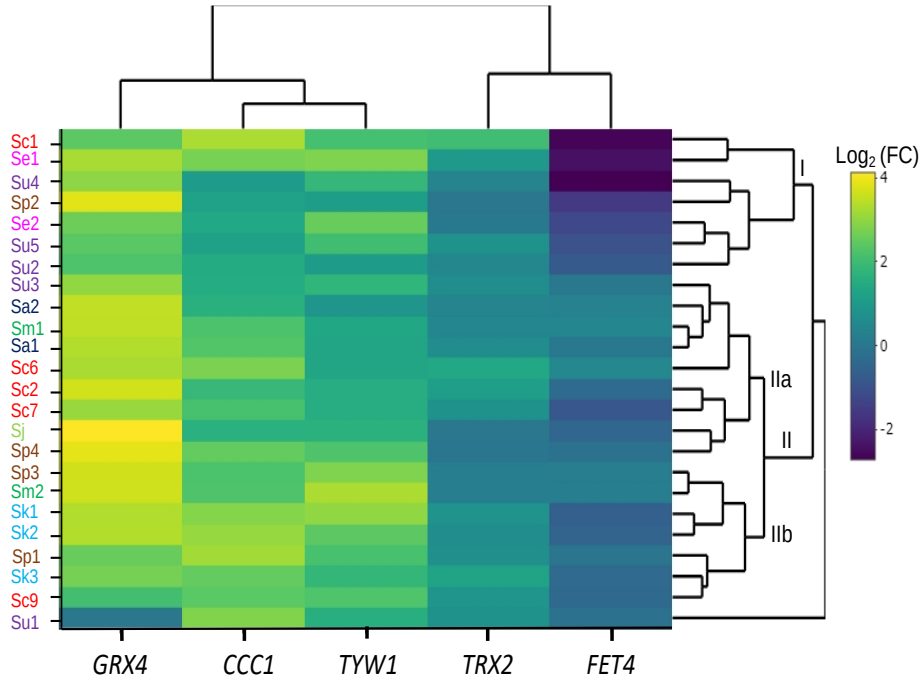

FIGURE C4.8. EFFECT OF IRON ON GENE EXPRESSION IN *SACCHAROMYCES* STRAINS. Yeast strains were exposed to 2 mM FAS for 1 h, as described in the Materials and Methods, and *GRX4, CCC1, TYW1, TRX2* and *FET4* mRNA levels were determined by RT-qPCR. The heatmap represents the $\log_2$ fold change between SC + 2 mM FAS and SC mRNA levels, with a hierarchical cluster calculated by the Euclidean distance. Higher fold changes are represented with yellow to light green and low fold changes are

depicted with light to dark blue. mRNA levels were normalized using the *ACT1* gene. Groups I, IIa and IIb are indicated. All values are the average of three independent biological replicates.

4.5. Iron-sensitive strains have impairments on iron toxicity response

To further dissect how the different variables (NIC, MIC, iron content and expression) influenced the iron performance of the *Saccharomyces* strains, we analyzed the above data (summarized in Table C4.S3) by a principal component analysis (PCA) (Figure C4.9). We identified two principal components that described 50% of the total variance. The first principal component, PC1, which explains 27.5% of the variance, shows a high positive contribution of iron content and *TRX2* expression, and a high negative component loading of NIC, MIC, *GRX4* fold-change and, in a minor way, *FET4* expression. PC2 is responsible for 22.4% of variance, and is highly contributed by *GRX4* fold changes, and shows a high negative component loading of changes in the expression of *CCC1, TRX2*, and, to a lesser extent, *TYW1*, as well as NIC and MIC. Iron content has little contribution to this component. Additionally, PC3 and PC4 represent the 15.9% and 13.9% of the variance, respectively (Figure C4.S7). However, changes in expression of *TYW1* and *CCC1* highly correlate between them, as expected for Yap5 targets, and also with changes in *TRX2*, but correlate inversely with *GRX4*, the other Yap5 target, and with *FET4* variations. *GRX4* and *FET4* mRNA changes, on the contrary, show a positive correspondence with high NIC and MIC values and inversely correlate to iron content. However, iron content only shows a small positive correlation with changes in expression of *TYW1*, but not of other genes. Strains are dispersed around the four quadrants forming small groups according to the influence of the different variables on their behavior upon iron addition. On the left, there are strains with relatively high NIC and MIC values, largely influenced by changes in *GRX4* mRNA levels. An iron-resistant group composed of Sm1, Sm2, Sp2, Sp3, Sj, and Sa2 show a negative correlation with changes in *CCC1*, *TYW1* and *TRX2*. On the right side, there are strains with low NIC and MIC values. Sc1, Se1, Sc6, Sc9 and crossing the y axis, Sp1 also present an iron content similar to the resistant strains, high positive correlation with *TYW1*,

CCC1 and *TRX2* changes and a high negative correlation with changes in *GRX4* and *FET4* expression, being Sc1 an outlier. At some distance in this quadrant we found Sk3 and Su1, which are the strains with the highest iron content. They also show a low contribution of changes in gene expression. Finally, there is a group formed by four *S. uvarum* strains, Su2–5, grouped in the above right quadrant with Se2, and close to the axis, to Sp4. They show an elevated iron content and low NIC and MIC values. In summary, PCA supports that: (i) Iron-resistant strains (high MIC values) have low iron contents, an elevated correlation with *GRX4* fold changes, and variations in *FET4* expression; (ii) iron-sensitive strains with low iron contents are more influenced by *CCC1, TYW1* and *TRX2* expression changes and by a downregulation of *FET4* expression; and (iii) iron-sensitive strains with high-iron contents are less influenced by changes in *CCC1, TYW1* and *TRX2* expression.

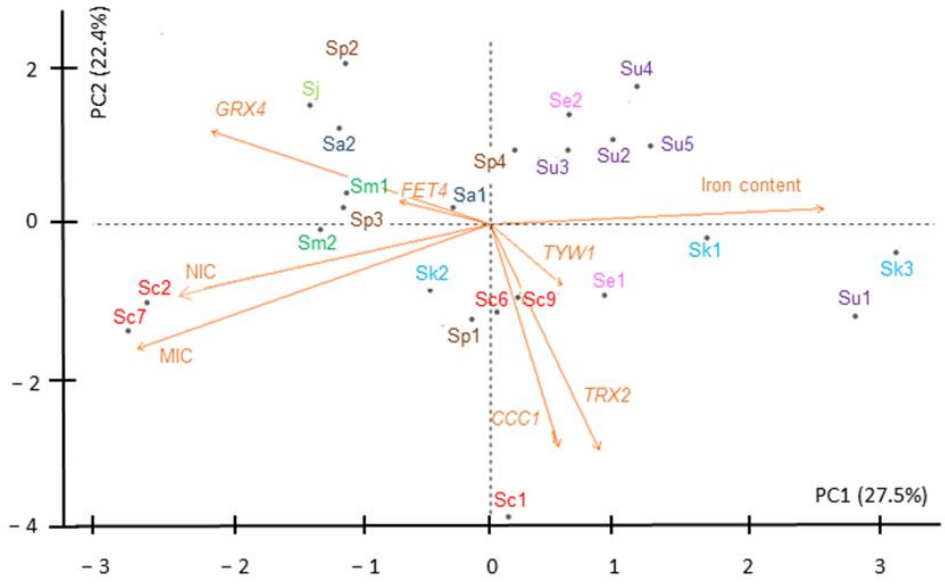

FIGURE C4.9. BEHAVIOR OF *SACCHAROMYCES* STRAINS ACCORDING TO IRON SENSITIVITY, IRON ACCUMULATION AND GENE EXPRESSION. Two-dimensional principal component analysis (PCA) biplot of NIC, MIC, iron accumulation and gene expression of *Saccharomyces* strains under high-iron exposure. Contribution of each variable to the variance is represented by the arrow length of the vectors. Strains (individuals) are depicted by the color code and abbreviations used in previous figures.

5. DISCUSSION

In the last years, we have attended to a huge increase in the sequenced genomes available of the *Saccharomyces* genus, as well as comparative genetic and phenotypic studies, elevating this genus to a eukaryotic model system to study processes of adaptation and evolution (Peter et al., 2018; Peris et al., 2023). In this work, we took advantage of this progress to expand our previous analyses on the response of *S. cerevisiae* strains from different origins to changing environmental iron levels to the *Saccharomyces* genus. For this purpose, we grew several strains from the different species in solid and liquid media supplemented with a wide range of iron concentrations. We observed differences between species regarding iron performance, with strains closely related to *S. cerevisiae* being more resistant to high-iron than the most distant ones, like *S. kudriavzevii, S. uvarum*, and *S. eubayanus*. Sc3, Sc7, and Sc8 were the most iron resistant strains, probably because they have not been isolated from wild niches, but instead are of human origin or domesticated lineages. Conversely, the rest of the strains were isolated from soils, decayed leaves, or barks from Fagales order, which are probably niches with low bioavailable iron content (Table C4.S1), (Alsammar and Delneri, 2020; Peris et al., 2023). As shown for other conditions, *S. mikatae* and *S. jurei* behaved similarly in response to iron excess, as well as *S. uvarum* and *S. eubayanus*, probably because they are the less divergent sister-species in the genus (Peris et al., 2023). *S. cerevisiae* and *S. paradoxus* strains showed a more diverse phenotype, including iron-sensitive and iron-resistant varieties.

We also determined the iron content of all strains after exposure to high-iron levels. Two different behaviors were observed in the sensitive strains: (i) strains that acquired high levels of iron from the medium and (ii) strains that were highly sensitive to low intracellular iron content. Even so, there is a quite strong inverse correlation between iron content and ΔMIC-NIC. Given that yeasts do not possess a regulated iron excretion mechanism, a higher iron accumulation indicates that cells are not able to limit iron entrance when the metal is in excess (Li, L. et al., 2012). This consideration would be in agreement with our previous observations for the *S. cerevisiae* strains, which showed that iron-sensitive strains accumulate high intracellular iron levels, whereas iron-

resistant strains had to be exposed to higher extracellular iron concentrations to become iron overloaded (Martínez-Garay et al., 2016). Moreover, Lindahl's group has demonstrated that the lack of synchronization between iron uptake and cell growth leads to iron overload (Park et al., 2013). As shown in Table C4.S4, this seems to be the case for most iron-sensitive strains analyzed in this study, which only duplicate once or twice when cultivated for 24 h at 4 mM iron. Similarly, another study has shown that *S. cerevisiae* flor strains from the Magarach collection, which are iron-sensitive, possess a codon stop in the *AFT1* gene that leads to a truncated Aft1 protein, which lacks the last 42 amino acids (Eldarov et al., 2018). The loss of Aft1 carboxy-terminal region, which may be involved in post-translational regulation of this transcriptional factor, leads to an increase in iron uptake (Eldarov et al., 2018). Siderophore-bound iron uptake is also important for adaptation to iron limitation, even for yeast species that lost the ability to synthetize these compounds, such as *S. cerevisiae*, and plays an ecological role in the competition with other microorganisms (Krause et al., 2018). Thus, particular species of budding yeasts have adapted to iron scarcity through the reacquisition of this lost ability by horizontal operon transfer from bacteria (Kominek et al., 2019). Therefore, increasing iron import efficiency from the environment seems to be a common strategy to overcome iron deficiency. On the other hand, we also found a group of strains that are highly sensitive to iron but accumulate low to moderate iron levels. It has been proposed that the two main strategies to cope with metal stress are "avoidance" or "sequestration" (Jennings, 1993). Therefore, these strains may be able to shut down iron import, in a similar manner than resistant strains, but they would be unable to detoxify iron properly once it is acquired from the medium, possibly because of defects in their sequestration machineries. Thus, Sc1 and Sc4 strains accumulate iron levels similar to the laboratory strain BY4741 at 30°C, despite they are highly iron-sensitive (Martínez-Garay et al., 2016) and, particularly, Sc1 presents loss of function mutations in *CCC1* and *YAP5* genes, which may be the molecular cause of its behavior (Lee, H. N. et al., 2013). Independently of the reason behind, we observed that iron-sensitive *Saccharomyces* strains are generally more oxidized than resistant strains at the same iron concentrations, in agreement with other studies (Lin et al., 2011; Eldarov et al., 2018; Peter et al., 2018).

Thus, iron toxicity could reside in cytosolic accumulation due to ineffective sequestration, which could lead to increased oxidative damage. Supporting this idea, overexpression of vacuolar or mitochondrial transporters has been shown to compensate the iron toxicity observed in *ccc1Δ* mutants (Li, L. et al., 2010; Li, L. et al., 2014).

To further analyze the involvement of oxidative and/or other stress responses in iron performance, we exposed strains to different oxidative sources and variations in temperature. While we could not establish a strong correlation between high-iron resistance and any other condition tested, the most iron-sensitive strains seemed to be those that performed well at low temperatures, like *S. uvarum*, *S. eubayanus*, and *S. kudriavzevii*. Further analyses will be necessary to determine a possible correlation between these two phenotypes. Finally, we also determined the effect of iron addition on the expression of genes involved in iron homeostasis and oxidative response. Generally, expression of the iron-responsive genes *CCC1, TYW1*, and *GRX4*, as well as the oxidative stress gene *TRX2* increased when iron was added. We observed a different expression pattern in a group of iron-sensitive strains, whereas other sensitive groups behaved more similarly to the iron-resistant strains. Thus, some iron-sensitive strains, such as Su2–5, Sp2 and Sa2, exhibit the lowest fold changes for *CCC1*, and in most cases, *TYW1* expression, which could match with an impaired iron sequestration or detoxification performance, as discussed above. Instead, other sensitive strains, like Sk1–2, show expression changes similar to resistant strains, such as Sm1–2 or Sp3, with moderate increases in *CCC1* as well as in *TYW1* and *GRX4* levels, and a considerable decrease in *FET4* expression, which could account for the similar intracellular iron content in these strains. These results also suggest that an insufficient upregulation of *CCC1* could lead to a rise in iron that could be compensated by *TYW1* and *GRX4*, which are shown to be involved in iron-buffering (Li, L. et al., 2011). Interestingly, some iron-sensitive strains, such as Sp2, Se1–2, and Su4 have high *FET4* mRNA levels in normal conditions, similar to the Malaysian strain Sc1. Thus, these strains seem to detect iron deficiency in normal conditions as if the threshold for iron detection was shifted towards smaller concentrations of the metal (Lee, H. N. et al., 2013). A high

expression in oxidative resistance genes has been linked to adaption to iron resistance; however, the only oxidative stress gene that presents a significant change is *TRX2*; this rise has been described as being especially important in the *S. cerevisiae* strains Sc1, Sc2, and Sc7 (Balaban et al., 2019). Moreover, it has been shown that iron toxicity is still present in anaerobiosis conditions and the overexpression or deletion of oxidative stress genes does not rescue *ccc1Δ* sensitivity to iron (Lin et al., 2011). Therefore, it is possible that other factors, such as impaired sphingolipid signaling or iron mismetallation, could also be influencing the response to iron of the yeast strains analyzed in the present work (Yang, M. et al., 2006; Lee, Y. J. et al., 2012). Further experiments should be done to decipher additional mechanisms that enable *Saccharomyces* species to survive in environments with a high-iron content.

6. CONCLUSIONS

Iron in excess is toxic for eukaryotic cells. The budding yeast *S. cerevisiae* mainly responds to excessive iron in the environment by restricting its uptake, as iron-resistant strains usually accumulate less intracellular iron than iron-sensitive ones (Martínez-Garay et al., 2016). In this work, we analyzed the response of diverse species of the *Saccharomyces* genus to elevated iron levels, and found that *S. cerevisiae* and its closer species in evolution (*S. paradoxus, S. jurei* and *S. mikatae*) generally show a higher resistance to iron than more distant species, such as *S. eubayanus* and *S. uvarum*, with *S. kudriavzevii* being especially iron-sensitive species. Two different behaviors were observed for the iron-sensitive strains. While some strains accumulated high intracellular iron levels, other strains were able to limit its incorporation, but not to properly sequester or detoxify it. Additionally, iron-sensitive strains showed a higher oxidized state, but in general, the response to iron of the *Saccharomyces* strains did not correlate with the responses to oxidative stress or variations in temperature, indicating that it is a specific response. The altered expression of iron homeostasis genes, such as the vacuolar iron importer *CCC1* or the iron transporter *FET4*, shows a certain correlation with the iron

performances of different groups of strains, while the expression of oxidative response genes, such as *TRX2*, has a lesser influence.

7. SUPPLEMENTARY INFORMATION

7.1. Supplementary figures

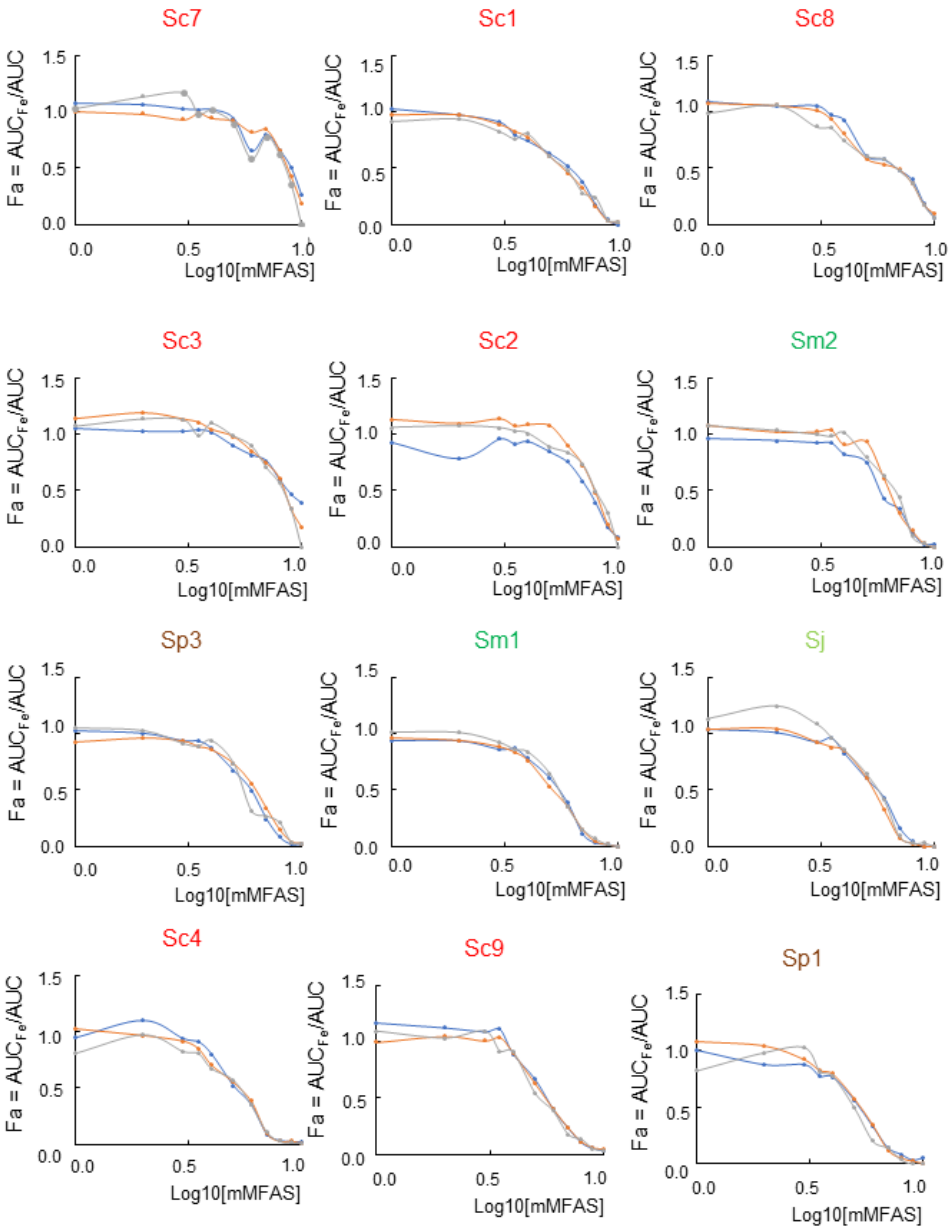

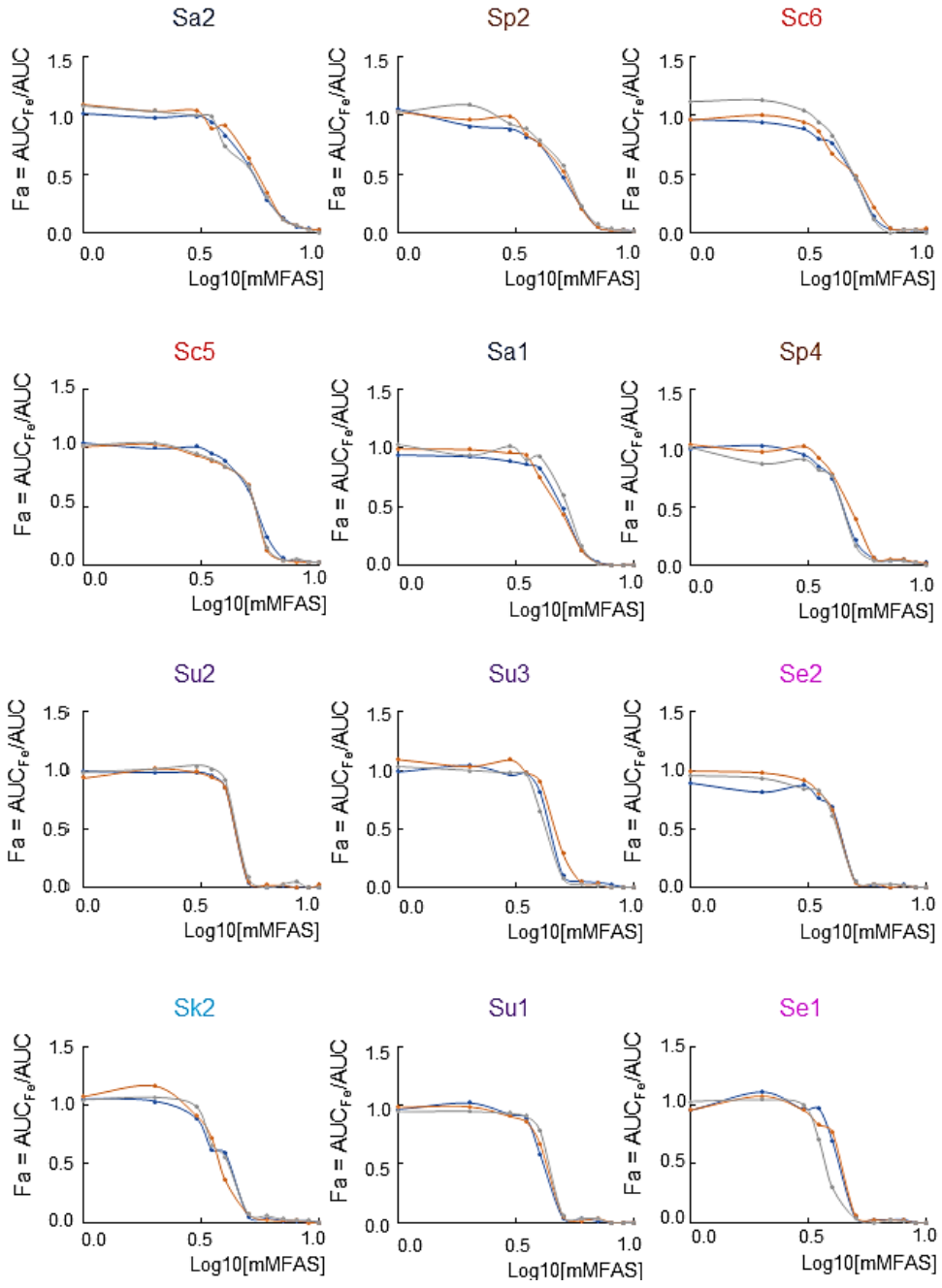
Sa2
Sp2
Sc6
Sc5
Sa1
Sp4
Su2
Su3
Se2
Sk2
Su1
Se1
Fa = AUC$_{Fe}$/AUC
Log10[mMFAS]
0.0
0.5
1.0
1.5

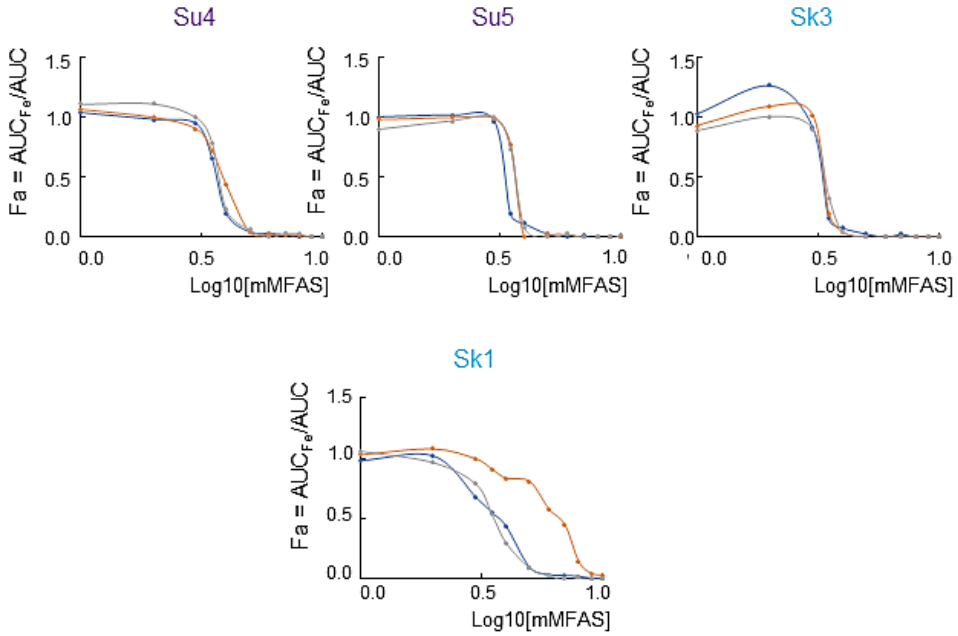

FIGURE C4.S1. REPRESENTATION OF THE FRACTIONAL AREA VS. FAS CONCENTRATION. Dots and lines represent the value of fractional area (Fa= AUC_{Fe} / AUC) against log_{10} of FAS concentration (mM) for each strain replicate. Strain names are colored as in Table C4.1 and ordered according to MIC values in Figure C4.2.

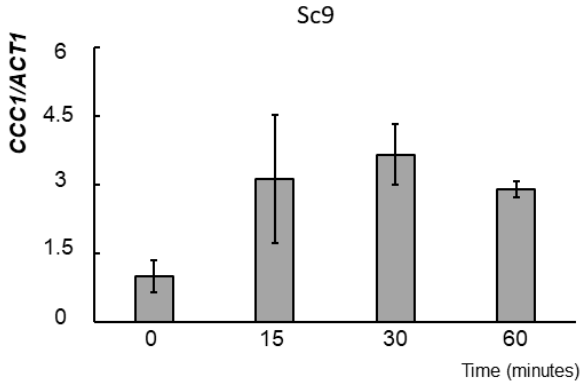

FIGURE C4.S2. EFFECT OF IRON ON *CCC1* EXPRESSION IN SC9 STRAIN AT DIFFERENT TIMES. Yeast strains were exposed to 2 mM FAS for 60 minutes, as described in Materials and Methods, and *CCC1 mR*NA levels were determined by RT-qPCR at 0, 15, 30 and 60 minutes. Bar plots represent the mRNA levels of *CCC1* gene at different points, relative to *ACT1* mRNA levels. Shown values are the average of 2 replicates and error bars constitute the standard deviation.

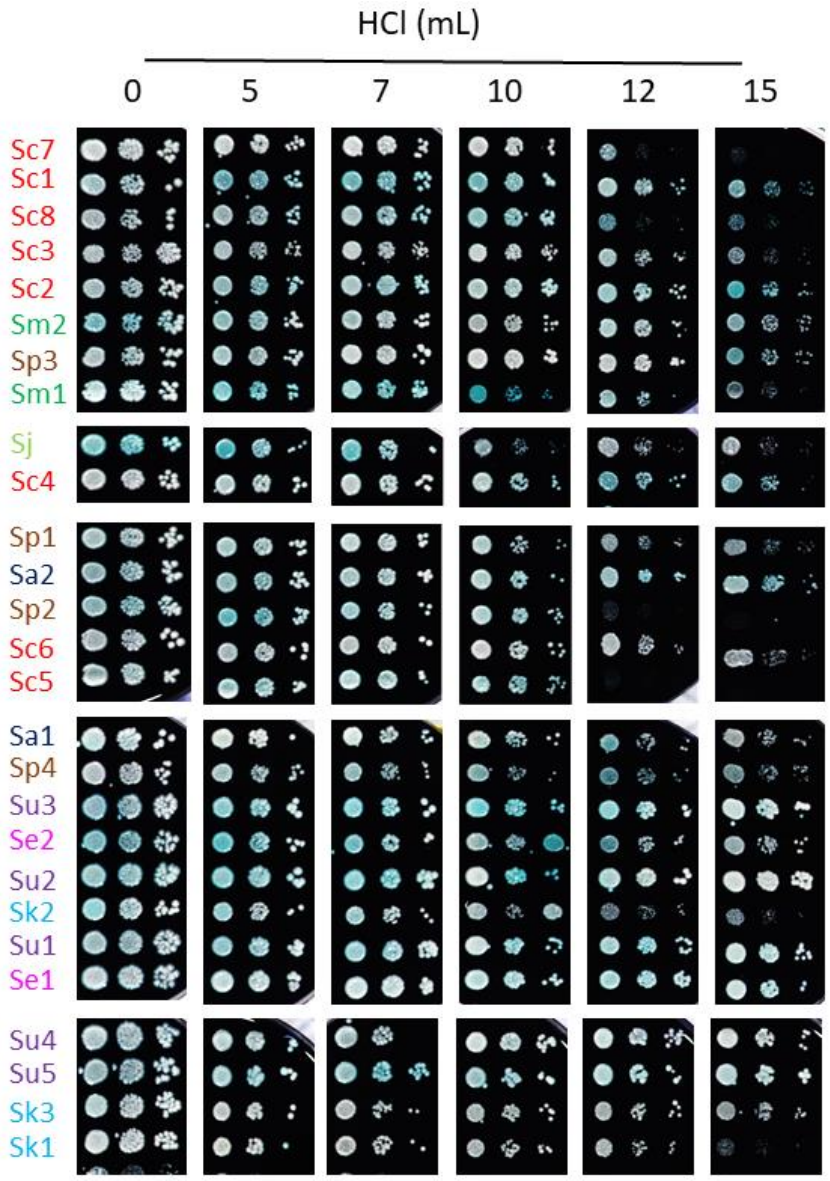

FIGURE C4.S3. GROWTH OF *SACCHAROMYCES* STRAINS IN HCL-CONTAINING MEDIA. Overnight precultures were diluted to an OD_{600} of 0.1, 0.01, and 0.001 and spotted on SC + 1 mM methylene blue agar plates with the indicated range of HCl volumes. Plates were incubated for 7 days at 20˚C and then photographed. An intense blue color indicates a more oxidized state of the cells. Strains are sorted based on MIC values and species-specific colors are used as in the above figures.

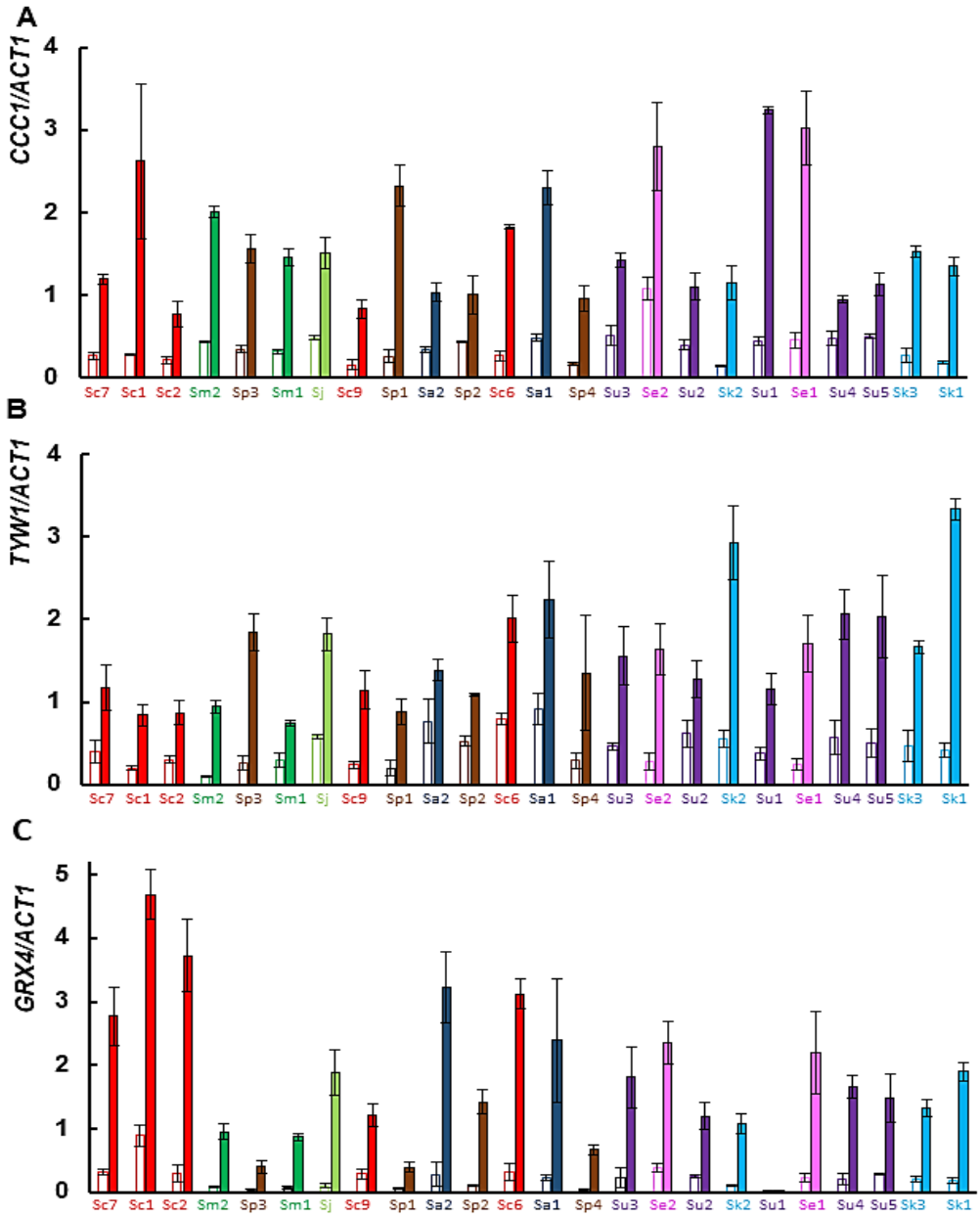

FIGURE C4.S4. EFFECT OF IRON ON YAP5 TARGETS EXPRESSION IN *SACCHAROMYCES* STRAINS. Yeast strains were exposed to 2 mM FAS for 1 h, as described in Materials and Methods, and *CCC1* (A), *TYW1* (B), *and GRX4* (C) mRNA levels were determined by RT-qPCR. Bar plots represent the mRNA levels of each gene in normal conditions (color-bordered and unfilled bars) and in 2mM FAS (black-bordered and color-filled bars), relative to *ACT1* mRNA levels and normalized to the average of all referenced mRNA levels of the same gene . Strains are sorted based on MIC values and species-specific colors are used as in the above figures. Shown values are the average of 3 replicates and error bars constitute the standard deviation.

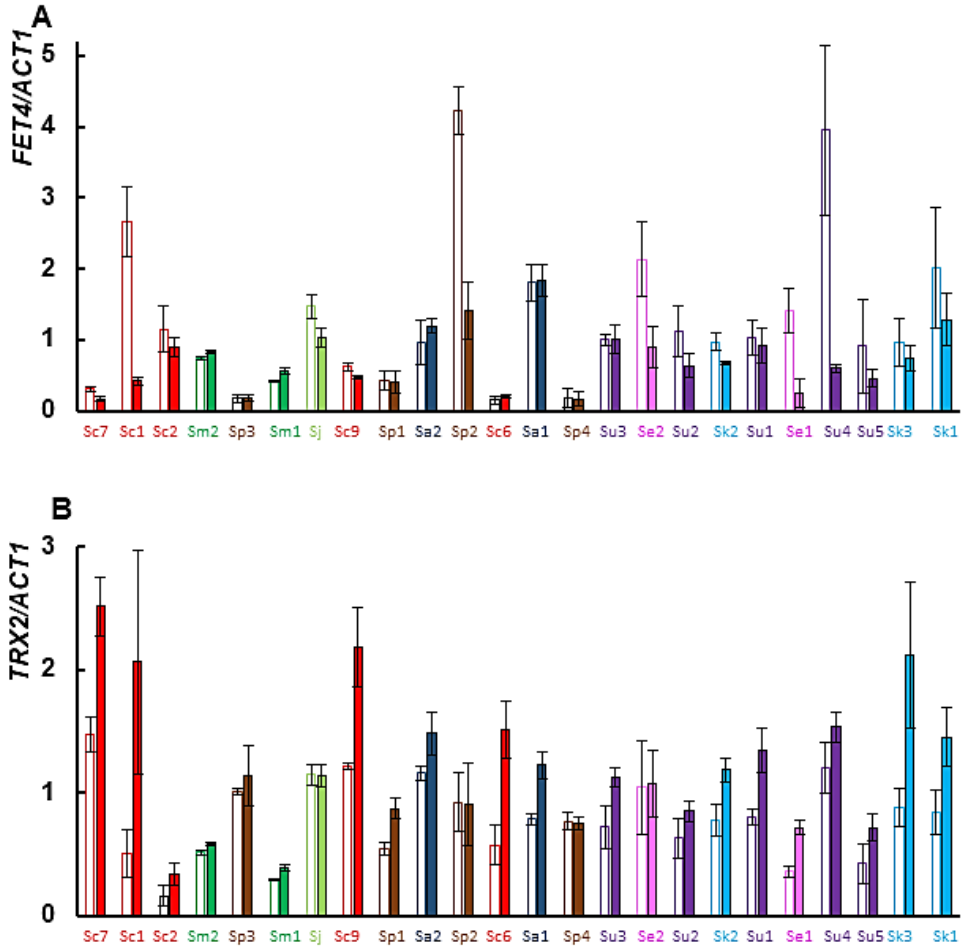

FIGURE C4.S5. EFFECT OF IRON ON *FET4* AND *TRX2* EXPRESSION IN *SACCHAROMYCES* STRAINS. Yeast strains were exposed to 2 mM FAS for 1 h, as described in Materials and Methods, and *FET4* **A)** and *TRX2* **B)** mRNA levels were determined by RT-qPCR. Bar plots represent the relative mRNA levels of each gene in normal conditions (color-bordered and unfilled bars) and in 2mM FAS (black-bordered and color-filled bars). mRNA levels of each gene are referenced to *ACT1* mRNA levels and normalized to the average of all referenced mRNA levels of the same gene. Strains are sorted based on MIC values and species-specific colors are used as in the above figures. Shown values are the average of 3 replicates and error bars constitute the standard deviation.

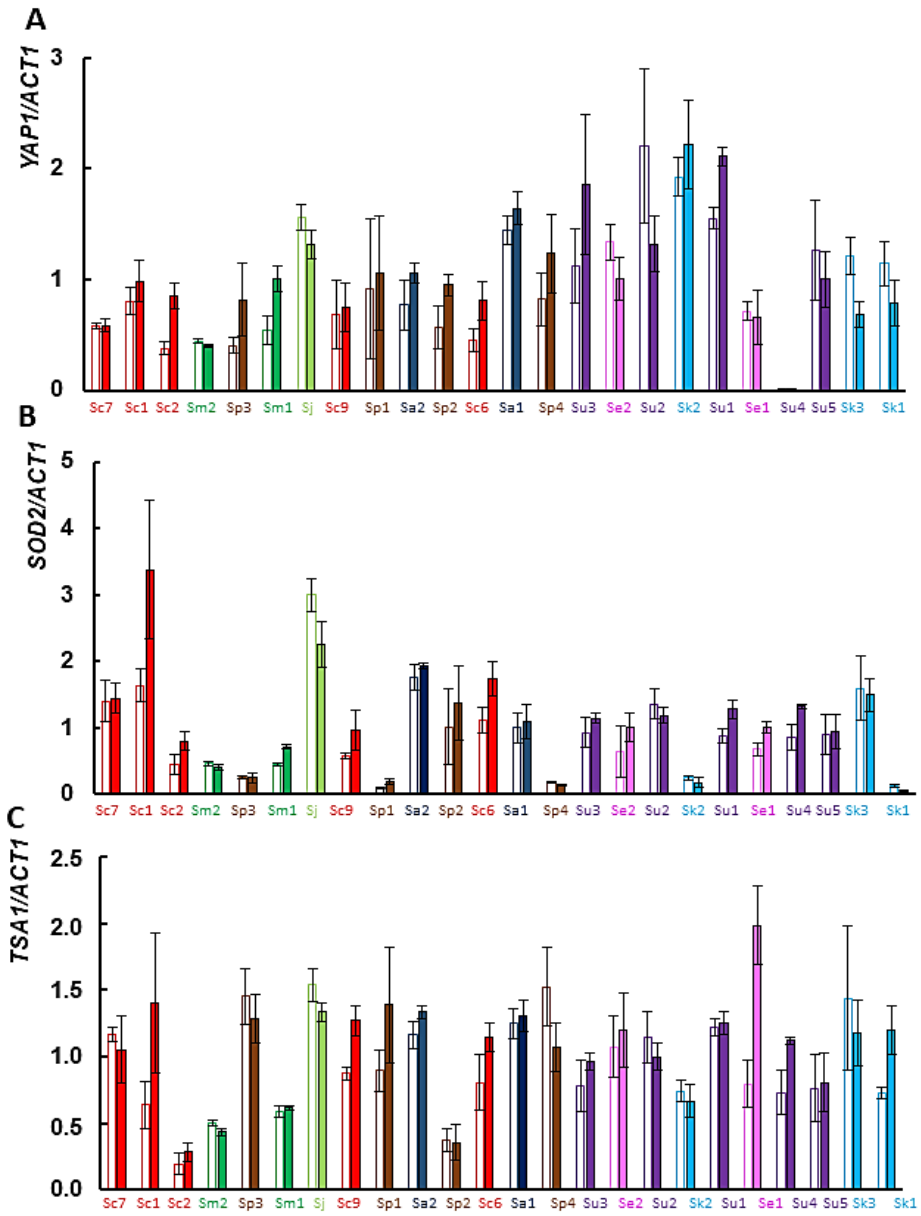

FIGURE C4.S6. EFFECT OF IRON ON *YAP1, SOD2,* AND *TSA1* EXPRESSION IN *SACCHAROMYCES* STRAINS. Yeast strains were exposed to 2 mM FAS for 1 h, as described in Materials and Methods, and *YAP1* (A), *SOD2,* and *TSA1* (C) mRNA levels were determined by RT-qPCR. Bar plots represent the relative mRNA levels of each gene in normal conditions (color-bordered and unfilled bars) and in 2mM FAS (black-bordered and color-filled bars). mRNA levels of each gene are referenced to *ACT1* mRNA levels and normalized to the average of all referenced mRNA levels of the same gene. Strains are sorted based on MIC values and species-specific colors are used as

in the above figures. Shown values are the average of 3 replicates and error bars constitute the standard deviation.

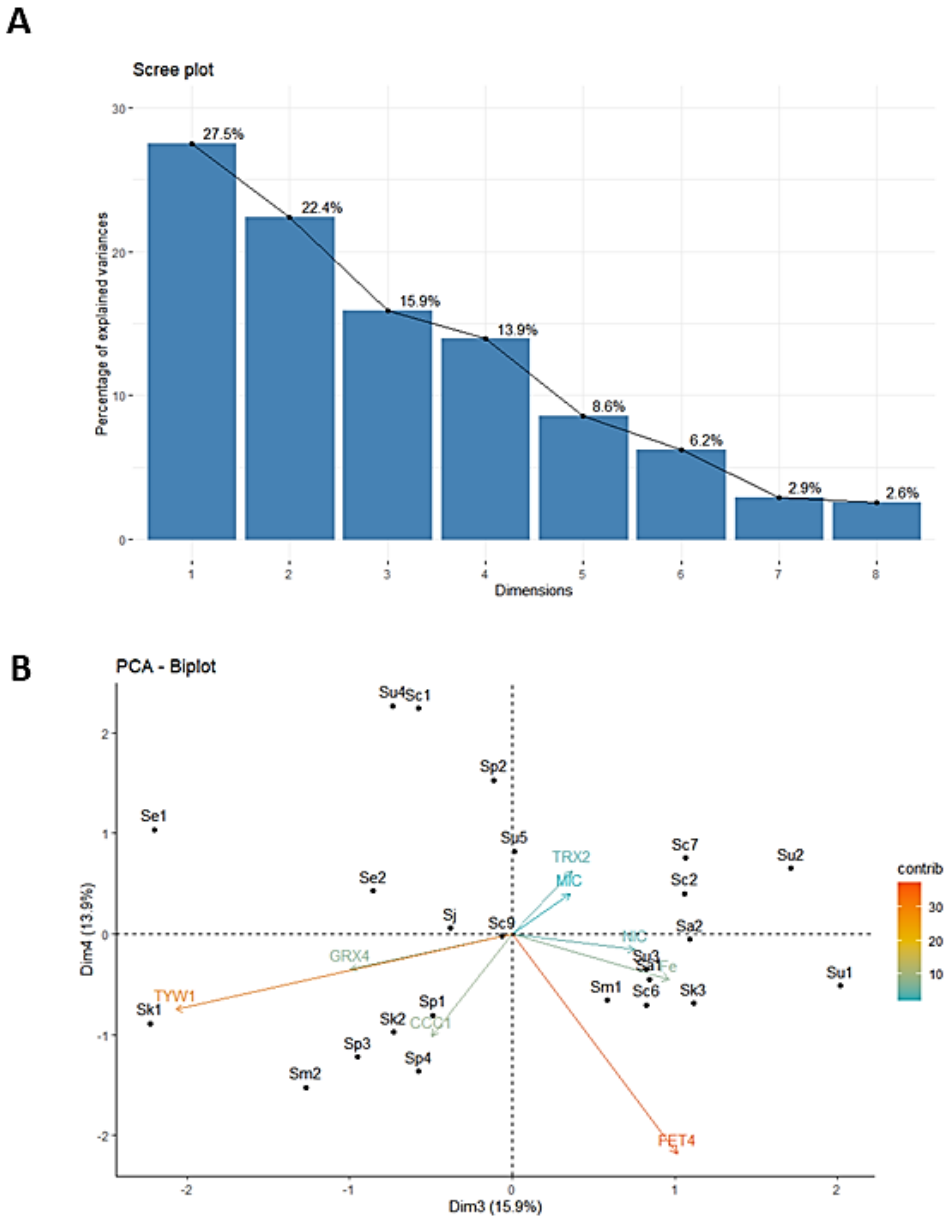

FIGURE C4.S7: PRINCIPAL COMPONENT ANALYSIS (PCA) OF IRON SENSITIVITY, IRON CONTENT, AND GENE EXPRESSION. A) Scree plot of the eigenvalues against the component number. The X-axis represents the different dimensions or principal components (PC) obtained in the analysis and Y-axis shows the percentage of data variance retained by each PC. The black line depicts the fraction of the total variance among the eight components. B) Two-dimensional PCA biplot of the principal

components PC3 and PC4. The contribution of each variable to variance is represented by the arrow length of the vectors and the color according to the legend “contrib”. Orange color describes the highest percentage of contribution to PCs and blue color the lowest. Strains (individuals) are depicted by the abbreviations used in previous figures.

7.2. Supplentary tables

Table C4.S1 is available online in the following link: https://www.mdpi.com/article/10.3390/ijms232213965/s1.

TABLE C4.S2. OLIGONUCLEOTIDES USED IN THIS WORK

ACT1-qPCR-F *Saccharomyces*	CGAAAGATTCAGAGCCCCAG
ACT1-qPCR-R *Saccharomyces*	TCCTTTTGCATTCTTTCGGC
CCC1-qPCR-F Sa	ATTATCGGGCTGAGCGATGGCT
CCC1-qPCR-F Sc	ATTATCGGGCTAAGCGACGGTT
CCC1-qPCR-F Se	ATTATTGGGCTGAGCGATGGTT
CCC1-qPCR-F Sk1	ATCATTGGGCTGAGCGATGGTT
CCC1-qPCR-F Sk2	ATCATAGGGCTGAGCGATGGTT
CCC1-qPCR-F Sm	ATTATCGGACTGAGCGATGGTT
CCC1-qPCR-F Sp	ATTATCGGGCTGAGCGACGGTT
CCC1-qPCR-F Su	ATTATCGGGCTGAGCGATGGTT
CCC1-qPCR-R Sa/Sp/Sk	AATTTTGCATCACCAAGTGAAGATAG
CCC1-qPCR-R Sc	AATTTCGCATCACCAAGTGAAGATAG
CCC1-qPCR-R Se	AATTTTGCATCACCAAGGGAAGATAA
CCC1-qPCR-R Sm	AATTTTGCATCACCAAGTGACGATAG
CCC1-qPCR-R Su	AATTTTGCATCACCAAGGGAAGATAG
FET4-qPCR F Sc, Sa y Sp	TGGATTGGTATTGGTTCGC
FET4-qPCR F Sk, Se y Su ZP964	TGGATTGGTATTGGTGCGC
FET4-qPCR F Sm IFO1815	TGGATTGGTATTGGTACGC
FET4-qPCR F Sm yHAB336 y Sj	TGGATCGGTATTGGTACGC
FET4-qPCR F Su	TGGATTGCTATTGGTGCGC
FET4-qPCR R Sa	CCAACCAAACCAGTGTATGTACC
FET4-qPCR R Se y Su	CCAACCAAACCTGTGTATGTACC
FET4-qPCR R Sj	CCAACTAAACCCGTGTATGTACC
FET4-qPCR R Sk y Sm IFO1815	CCAACTAAACCTGTGTATGTACC
FET4-qPCR R Sm yHAB336	CCAACCAAACCCGTGTATGTACC
FET4-qPCR R Sp y Sc	CCAATTAAACCTGTGTATGTACC
GRX4-qPCR F Sa y Su	AGCTAGTACAGGCTGCGCC
GRX4-qPCR F Sc	AGCTAGTACAAGCTGCACC

GRX4-qPCR F Sk	AGCTAGTACAGGCTGCTCC
GRX4-qPCR F Se	AGCTAGTACAGGCGGCGCC
GRX4-qPCR F Sj	AACTCGTGCAAGCGGCGCC
GRX4-qPCR F Sm	AGCTAGTGCAAGCAGCACC
GRX4-qPCR F Sp	AGCTAGTGCAAGCTGCGCC
GRX4-qPCR R Sa ZP960 y Se	TCAGGATCTTCTTCTATGGATTCC
GRX4-qPCR R Sc,Sp y Sa CBS10644	TCAGGATCTTCTTCTATAGATTC
GRX4-qPCR R Sj y Sm	TCAGGATCCTCTTCTATCGATTC
GRX4-qPCR R Sk	TCAGGATCCTCTTCTATAGATTCC
GRX4-qPCR R Su	TCAGAGTCTTCTTCTATGGATTC
GRX4-qPCR R Su ZP964	CAGAATCTTCTTCTATGGATTC
SOD2-qPCR F Sa, Se, Su, Sm, Sj, Sk y Sp	CAAACCTACAACCAAGACAC
SOD2-qPCR F Sc	CAAACCTACAACCAGGATAC
SOD2-qPCR R Sa, Su y Sj R	TAGTAGGCATGTTCCCAG
SOD2-qPCR R Sk, Se, Su ZP964, Sp y Sc	TAGTAGGCGTGTTCCCAG
SOD2-qPCR R Sm	TAGTAGGCATGCTCCCAG
TRX2-qPCR F Sa, Su, Sm, Sj, Sp y Se	CCACATGGTGTGGTCCAT
TRX2-qPCR F Sc y Su CBS7001	CCACATGGTGTGGGCCAT
TRX2-qPCR F Sk	CCACATGGTGCGGTCCAT
TRX2-qPCR R Sa	AGTAGGCATGGAGGAAACTTC
TRX2-qPCR R Sc	GGTAGGCATGGAAGAAACTTC
TRX2-qPCR R Se y Su	GGTAGGCATGGAGGAGACTTC
TRX2-qPCR R Sj	GGTGGGCATGGAGGAGACTTC
TRX2-qPCR R Sk	GGTAGGCATAGAGGAGACTTC
TRX2-qPCR R Sp	GGTAGGCATGGAAGAGACTTC
TSA1-qPCR F Sa	TGAAGAACAAGGTGCTCAAG
TSA1-qPCR F Sc	CGAAGAACAAGGCGCTCAAG
TSA1-qPCR F Se, Su ZP964 y yHAB521	CGAAGAACAAGGTGCGCAAG
TSA1-qPCR F Sj, Sp y Su	CGAAGAACAAGGTGCTCAAG
TSA1-qPCR F Sk	CGAAGCACAGGGTGCTCAGG
TSA1-qPCR F Sk IFO1803	CGAAGCGCAGGGTGCTCAA
TSA1-qPCR F Sm	CGAAGAGCAAGGTGCCCAA
TSA1-qPCR R-*Saccharomyces*	CCCAAACCACCTTCCTTTCTTG
TYW1-qPCR R Sa	GGTTTGTACCGTGTCTCCAACA
TYW1-qPCR F Sa, Se y Su	GATGGACCAAGAACGAACTACG
TYW1-qPCR F Sc y Sp	GATGGACTAAGAATGAACTACG
TYW1-qPCR F Sj y Sm	GATGGACCAAGAACGAACTTCG
TYW1-qPCR F Sk	GATGGACCAAGAATGAGCTACG

TYW1-qPCR F Sk IFO1803	GATGGACCAAGAACGAGCTACG
TYW1-qPCR R Se	GATTCGTACCATGTCTCCAACA
TYW1-qPCR R Sj y Sm	GATTCGTACCATGCCTCCAACA
TYW1-qPCR R Sp y Sc	GATTTGTACCATGCCTCCAACA
TYW1-qPCR R Su y Sk	GGTTCGTACCATGTCTCCAACA
YAP1-qPCR F Sc, Sp y Sa	TCGATGGATTGGTTAGATAA
YAP1-qPCR F Sj	TCGATGGATTGGCTAGATAA
YAP1-qPCR F Sk	TCCATGGATTGGCTAGATAA
YAP1-qPCR F Sm	TCAATGGATTGGCTCGATAA
YAP1-qPCR F Su	TCGATGGATTGGCTAGATAA
YAP1-qPCR F-Se	TCGATCGATTGGCTAGATAA
YAP1-qPCR R Sa	CTTGCTCATCAAACTGATTCTC
YAP1-qPCR R Sc	CTTGTTCATCAAATTGGTTTTC
YAP1-qPCR R Se	CTTGTTCATCGAACTGATTCTC
YAP1-qPCR R Sk	CCTGCTCATCAAACTGATTTTC
YAP1-qPCR R Sp	CTTGCTCATCAAACTGATTTTC
YAP1-qPCR R Su yHAB521	CTTGTTCATCAAACTGATTTTC
YAP1-qPCR R Su ZP964	CTTGTTCATCGAACTGATTTTC
YAP1-qPCR R Su, Sm y Sj	CTTGTTCATCAAACTGATTCTC

TABLE C4.S3. SUMMARY OF RESULTS OBTAINED IN THIS WORK

Species[a]	NIC (mM)	MIC (mM)	ΔMIC-NIC (mM)	Iron content	*CCC1*[e]	*GRX4*[e]	*TYW1*[e]	*TRX2*[e]	*FET4*[e]
Sc1	3.7 ± 0.3	11.2 ± 2.2	7.5	1.8 ± 0.3	3.3	2.4	2.1	2.0	-2.7
Sc2	5.9 ± 0.0	9.9 ± 0.4	4.0	1.2 ± 0.3	1.9	3.4	1.5	1.1	-0.4
Sc3	5.5 ± 0.4	10.9 ± 0.6	5.4	n.d.	n.d.	n.d.	n.d.	n.d.	n.d.
Sc4	3.7 ± 0.3	7.6 ± 0.3	3.9	n.d.	n.d.	n.d.	n.d.	n.d.	n.d.
Sc5	4.4 ± 0.1	6.4 ± 0.2	2.1	n.d.	n.d.	n.d.	n.d.	n.d.	n.d.
Sc6	3.6 ± 0.1	6.5 ± 0.3	2.8	1.8 ± 3.0	2.8	3.3	1.3	1.4	0.5
Sc7	6.0 ± 0.9	11.6 ± 0.8	5.6	1.2 ± 0.1	2.1	3.1	1.5	0.8	-0.9
Sc8	3.5 ± 0.2	11.2 ± 0.2	7.7	n.d.	n.d.	n.d.	n.d.	n.d.	n.d.
Sc9	3.8 ± 0.2	7.5 ± 0.1	3.7	1.8 ± 0.3	2.4	2.1.	2.2	0.9	-0.4
Sp1	3.6 ± 0.3	7.4 ± 0.6	3.8	1.2 ± 0.5	3.2	2.6	2.1	0.7	-0.1

Sp2	3.6 ± 0.1	6.9 ± 0.1	3.3	1.4 ± 0.1	1.2	3.8	1.1	-0.0	-1.6
Sp3	4.2 ± 0.4	8.3 ± 0.3	4.1	2.2 ± 0.1	2.2	3.6	2.8	0.2	0.1
Sp4	3.8 ± 0.1	5.5 ± 0.3	1.7	4.5 ± 1.3	2.5	3.9	2.2	-0.0	-0.2
Sj	3.8 ± 0.2	7.6 ± 0.3	3.9	1.5 ± 0.4	1.6	4.1	1.6	0.0	-0.5
Sm1	3.9 ± 0.2	7.7 ± 0.1	3.8	1.2 ± 0.2	2.2	3.5	1.4	0.4	0.4
Sm2	4.7 ± 0.3	8.5 ± 0.3	3.9	2.0 ± 0.3	2.2	3.6	3.3	0.2	0.2
Sk1	3.2 ± 1.1	6.5 ± 2.6	3.4	1.2 ± 0.3	2.9	3.3	3.0	0.8	-0.7
Sk2	3.0 ± 0.1	4.9 ± 0.3	1.9	1.8 ± 0.5	3.1	3.4	2.4	0.6	-0.5
Sk3	3.2 ± 0.2	3.6 ± 0.1	0.4	7.1 ± 2.0	2.5	2.7	3.5	1.3	-0.4
Sa1	4.1 ± 0.3	6.3 ± 0.1	2.2	2.4 ± 0.6	2.3	3.4	1.3	0.6	0.0
Sa2	3.8 ± 0.2	7.2 ± 0.2	3.4	1.2 ± 0.3	1.6	3.5	0.9	0.4	0.3
Se1	3.6 ± 0.3	4.7 ± 0.4	1.1	1.5 ± 0.2	2.7	3.2	2.8	1.0	-2.5
Se2	3.7 ± 0.2	5.0 ± 0.0	1.3	3.4 ± 1.4	1.4	2.6	2.5	0.1	-1.3
Su1	3.8 ± 0.2	4.9 ± 0.1	1.1	4.0 ± 1.5	2.8	0.0	1.6	0.7	-0.2
Su2	4.1 ± 0.1	5.0 ± 0.0	0.9	4.8 ± 0.9	1.5	2.2	1.0	0.4	-0.8
Su3	3.9 ± 0.3	5.1 ± 0.3	1.3	3.5 ± 1.0	1.5	3.0	1.8	0.6	0.0
Su4	3.2 ± 0.1	4.4 ± 0.4	1.2	2.7 ± 0.6	1.0	3.0	1.9	0.4	-2.7
Su5	3.5 ± 0.0	3.9 ± 0.2	0.4	2.2 ± 0.7	1.2	2.4	2.0	0.8	-1.0

[a] Names are abbreviated as in Table C4.1; [b] Growth in iron compared to that of Sc1, used as a control: =, similar; + and ++, levels of increased growth, -,-- and ---, levels of decreased growth; [c] n.d., not determined; [d] Iron content expressed as mg Fe/ g dry weight; [e] $\log_2$ (FC, fold change of expression).

TABLE C4.S4 REACHED OD_{600} AFTER 24 HOURS IN SC MEDIUM 4MM FAS.

Strain	OD_{600} 24h	Average	SEM
Sa1 1	1.492	1.745	0.500
Sa1 2	1.422		
Sa1 3	2.321		
Sa2 1	1.885	1.901	0.234
Sa2 2	1.675		
Sa2 3	2.143		
Sc1 1	3.918	3.388	0.485
Sc1 2	2.967		
Sc1 3	3.281		
Sc2 1	7.460	7.344	0.158
Sc2 2	7.408		
Sc2 3	7.163		
Sc6 1	8.289	8.004	0.524
Sc6 2	8.324		
Sc6 3	7.399		
Sc7 1	10.296	10.581	0.571
Sc7 2	10.208		
Sc7 3	11.238		
Sc9 1	8.620	8.876	0.224
Sc9 2	8.969		
Sc9 3	9.039		
Se1 1	1.099	1.030	0.099
Se1 2	0.960		
Se1 3			
Se2 1	0.921	0.814	0.105
Se2 2	0.810		
Se2 3	0.712		
Sj 1	2.111	2.152	0.830
Sj 2	1.344		
Sj 3	3.001		
Sk1 1	0.977	0.692	0.248
Sk1 2	0.576		
Sk1 3	0.524		
Sk2 1	1.117	1.088	0.254
Sk2 2	1.326		

Sk2 3	0.820		
Sk3 1	0.879	0.719	0.176
Sk3 2	0.530		
Sk3 3	0.747		
Sm1 1	3.124	2.908	0.233
Sm1 2	2.661		
Sm1 3	2.940		
Sm2 1	5.837	5.971	0.247
Sm2 2	5.820		
Sm2 3	6.256		
Sp1 1	3.699	3.478	0.791
Sp1 2	4.136		
Sp1 3	2.600		
Sp2 1	2.373	2.264	0.272
Sp2 2	1.954		
Sp2 3	2.464		
Sp3 1	6.087	6.114	0.190
Sp3 2	6.317		
Sp3 3	5.940		
Sp4 1	0.881	0.887	0.105
Sp4 2	0.995		
Sp4 3	0.785		
Su1 1	1.187	1.021	0.145
Su1 2	0.960		
Su1 3	0.916		
Su2 1	0.698	0.797	0.100
Su2 2	0.899		
Su2 3	0.794		
Su3 1	1.204	1.297	0.208
Su3 2	1.152		
Su3 3	1.536		
Su4 1	1.584	1.440	0.128
Su4 2	1.340		
Su4 3	1.396		
Su5 1	0.859	1.184	0.294
Su5 2	1.263		
Su5 3	1.431		

SUPPLEMENTARY MATERIALS: Supplementary data to this article can be found online at at https://www.mdpi.com/article/10.3390/ijms232213965/s1.

AUTHOR CONTRIBUTIONS: Conceptualization, M.T.M.-P. and S.P.; Methodology, R.S.-D., T.J. and D.P.; Investigation, R.S.-D., T.J. and D.P.; Resources, D.P. and S.P.; Data curation, R.S.-D., T.J. and D.P.; Writing—original draft preparation, R.S.-D., M.T.M.-P. and S.P.; Writing—review and editing, T.J. and D.P.; Visualization, R.S.-D., T.J. and D.P.; Supervision, M.T.M.-P. and S.P.; Project administration, S.P.; Funding acquisition, D.P. and S.P. All authors have read and agreed to the published version of the manuscript.

FUNDING: This research was supported by grants BIO2017-87828-C2-1-P, PID2020-116940RB-I00, and RED2018-102467-T funded by MCIN/AEI/10.13039/501100011033 and, in the case of BIO2017-87828-C2-1-P, by ERDF A way of making Europe, and by PROMETEO/2020/014 grant from the Regional Government of Valencia (Generalitat Valenciana). Some computations were performed on Tirant III of the Spanish Supercomputing Network ("Servei d'Informàtica de la Universitat de València") under the project BCV-2021-1-0001 granted to D.P., while others were performed on resources provided by UNINETT Sigma2—the National Infrastructure for High Performance Computing and Data Storage in Norway, project NN8029K. This work has also been supported by a predoctoral fellowship ACIF/2018/077 to R.S-D. and a predoctoral fellowship ACIF/2019/214 to T.J., both funded by Generalitat Valenciana and European Social Fund (ESF). D.P. is a researcher funded by the Research Council of Norway (RCN) grant Nos. RCN 324253 and Distinguished Researcher funded by Generalitat Valenciana plan GenT grant No. CIDEGENT/2021/039.

INSTITUTIONAL REVIEW BOARD STATEMENT: Not applicable.

INFORMED CONSENT STATEMENT: Not applicable.

DATA AVAILABILITY STATEMENT: The data presented in this study are openly available in Digital CSIC (https://digital.csic.es) at https://doi.org/10.20350/digitalCSIC/14763. (accessed on 6 October 2022).

ACKNOWLEDGMENTS: We thank all the members of the Iron Homeostasis laboratory for technical assistance. We acknowledge PYCC for providing strains (see Table C4.S1 for PYCC codes). We are also indebted to Drs. Daniela Delnieri, Gianni Liti and Amparo Querol for the gift of some of the *Saccharomyces* strains used in this work.

CONFLICTS OF INTEREST: The authors declare no conflict of interest. The funders had no role in the design of the study; in the collection, analyses, or interpretation of data; in the writing of the manuscript; or in the decision to publish the results.

GENERAL DISCUSSION

GENERAL DISCUSSION

S. cerevisiae, as well as other members of the *Saccharomyces* genus, have been stablished as model organisms for the study of complex traits and adaptation to certain environments. Besides, these budding yeasts have also been used as biotechnological tools for food fermentation connecting their evolution to human practices. Due to the genetic diversity present in these genera, even at an interspecies level, and the wide availability of isolated strains, genomes and data regarding growth characterization in several conditions, *Saccharomyces* genus presents an extraordinary opportunity to study iron homeostasis divergence. Moreover, exploring this diversity may allow the identification and characterization of strains that become useful as biotechnological tools to obtain iron-enriched strains.

Before starting the characterization of yeast strains behavior in iron overload, in chapter 1, we asked which would be the most appropriate iron salt for analyzing iron resistance. To address this question, we grew previously characterized *S. cerevisiae* strains in the presence of three different iron sources ($FeCl_3$, FAS and $FeSO_4$), which were added to the media from stocks prepared with and without HCl addition, an acid commonly used to increase iron salts solubility (Martínez-Garay et al., 2016). Upon our observations, $FeCl_3$ appears to be the most toxic salt, as the concentration necessary to arrest growth of the different yeast strains is lower than for the other studied salts. Apparently this occurs because of its acidic nature, which lowers the pH of the medium making iron more available for yeast cells (Figure C1.1A, C1.2A and C1.3A). However, we discarded this salt because the addition of $FeCl_3$ to the medium causes the formation of a precipitate, presumably derived from an iron compound, which interferes with the measurement of growth by absorbance (Figure C1.1B and C1.1D). It remains not clear which is the iron-derived compound responsible for the observed turbidity. Taking into account the $FeCl_3$ hydrolysis equilibrium, the observed precipitate could be $Fe(OH)_3$, which is

barely insoluble in water, and HCl addition to stock would facilitate its dissolution (Stefansson, 2007), (Figure C1.5A and C1.5B). Another possibility to consider is that a $FePO_4 \cdot 2H_2O$ precipitate is formed, since it is well documented that iron has a strong affinity for phosphate, and potassium phosphate concentration is up to 1000 mg/L in the SC medium (Pa Ho, 1976; Pierri et al., 2000; Schroder et al., 2003). In FAS and $FeSO_4$ salts, iron is present as its reduced form, Fe^{2+}, which makes these salts more soluble in water than $FeCl_3$ (Figure C1.5G). Nonetheless, when these salts were added to the medium from a Milli-Q water-prepared stock, we observed a similar effect to $FeCl_3$ addition: a precipitate was generated. These salts do not undergo hydrolysis when dissolved in water at pH<8. Instead, the formation of the aquo-complex $[Fe(H_2O)_6]^{2+}$ takes place, a compound which is highly vulnerable to oxidation and could lead to the generation of the ferric compounds $Fe(OH)_3$ or $FePO_4 \cdot 2H_2O$. When the stock of both ferrous salts is prepared with HCl, turbidity disappears and iron toxicity happens at a lower concentration. Therefore, these salts could be used for liquid growth analyses (Figure C1.2B and C1.3B). It is well-known that iron solubility can be increased almost 6 orders of magnitude when pH changes from 7 to 2 and, indeed, lowering the extracellular medium pH is a widespread strategy among organisms to increase iron uptake (Kaplan and Kaplan, 2009). Moreover, FAS is a double sulfate salt which, besides $FeSO_4$, contains ammonium sulfate, $(NH_4)_2SO_4$, in equimolar quantities. The presence of the double sulfate makes iron less susceptible to oxidation and there is no need for acid addition to prepare the stock in water (Gaensly et al., 2014) (Figure C1.5C). However, to completely avoid precipitation, it is preferred to prepare the stock in 0.1 M HCl, since a low pH makes oxidation more difficult (Greenwood and Earnshaw, 1997; Guimarães et al., 2007). Furthermore, huge evidence points out that iron is more prone to be acquired from the medium by yeasts when it is present as $FeSO_4$, FAS or conjugated with organic compounds (Pas et al., 2007; Gaensly et al., 2014). Altogether, our results indicate that all the salts analyzed in this study could be used for spot assays in solid medium, since the same tendency is observed regardless of the iron source. However, when growth in liquid medium needs to be analyzed, we propose that it is better to use $FeSO_4$ or FAS instead of $FeCl_3$, and along with an acid to make the salts fully soluble in SC medium.

Strategies used to cope with iron excess are similar among organisms and, in some cases, are conserved throughout the Tree of Life. In summary, there are two broadly used mechanisms based on: first, iron accumulation in the least toxic form, Fe^{3+}, and second, isolation from the rest of the cell. In bacteria, archaea and animals, iron is stored inside the ferritin protein complex whereas in fungi and plants iron is accumulated in the vacuole and tonoplast, respectively (Arosio et al., 2009; Kaplan and Kaplan, 2009; Sorribes-Dauden et al., 2020). In both cases, they are no watertight tanks, instead they constitute iron reservoirs from where this metal can be mobilized on demand (Arosio et al., 2017; Ramos-Alonso et al., 2020). On the other hand, plants also have ferritins, but they do not seem to play a main role in detoxification as in animals and prokaryotes (Kaplan and Kaplan, 2009; Arosio et al., 2017). In the widely used model organism *S. cerevisiae*, the main responsible for iron accumulation in the vacuole is Ccc1. Ccc1 is a Fe^{2+} and Mn^{2+} transporter located in the vacuolar membrane which imports these ions from the cytosol into the vacuole. This protein has a pivotal role since deletion of *CCC1* results in a severe growth defect phenotype when there is iron overload (Lapinskas et al., 1996; Li, L. et al., 2001). Ccc1 homologues have been found in plants (VIT1 and VTLs), diatoms, bacteria, and protists and some of them have been confirmed as functional orthologs through complementation assays in *ccc1Δ* mutants (Kim, S. A. et al., 2006; Brembu et al., 2011; Bhubhanil et al., 2014; Slavic et al., 2016). Given its important role in iron detoxification, we wanted to explore the conservation of this family of proteins. Therefore, we searched for Ccc1/VIT1 orthologs through the MetaPhORs database (Chorostecki et al., 2020). We chose MetaPhOrs because it is a public repository of phylogeny-based orthologs and paralogs that uses available phylogenetic trees from diverse sources. The growing availability of sequenced genomes in the last decades has prompted the creation of a plethora of orthology prediction methods and repositories, such as PhylomeDB, EnsemblCompara or yeast Orthogroups. Usually, these phylogenomic repositories share overlapping information, but this redundancy does not necessarily imply that the information is identical since it is usually obtained using different parameters and sources. Thus, MetaPhORs makes profit of this redundant available information increasing robustness of orthology prediction between two sequences based on more than

a single phylogenetic tree (Pryszcz et al., 2011; Chorostecki et al., 2020). Our results showed that the Ccc1/VIT1 family is widely distributed among organisms with the noticeable exception of metazoans (Figure C1.1). Curiously, Ccc1/VIT1 family is well represented in the Archaea and Bacteria domains where ferritin is the main protein involved in iron detoxification. In plants, Ccc1/VIT1 family has experimented a huge expansion via partial or full tandem duplication, since most of homologues are localized at a reduced number of chromosomes (Cao, 2019). Fungi orthologs also experimented tandem duplication but to a lesser extent (Table C2.S1). Kato et al. (2019) published the crystal structure of VIT1 transporter from the plant *Eucalyptus grandis* which consisted in a dimer structure with each oligomer composed by two domains: the transmembrane domain (TMD), which would be involved in the transport of iron itself and the metal binding domain (MBD), which could be an iron-facilitating domain. In this work, they identified key amino acid residues and proposed a transport mechanism which allowed us to expand this information to our ortholog sequences. We found that amino acid similarity is low along the sequence but the overall structure and the principal domains are deeply conserved (Figure C2.3). A huge variation is found in the amino-terminus domain (Nt), which is absent in Group II. It consists in a proline- and serine-rich domain in fungi (Group VI-VIII), while a short basic sequence is found in plants (Group III and V) and protists (Group IV). Curiously, bacteria and archaea from Group I possess a ferritin-like/Erythrin domain in the amino end probably involved in facilitating iron entrance, which has been proposed to procure protection against ROS (Andrews, S. C., 2010; Ruangkiattikul et al., 2012). The MBD also constitutes a source of remarkable diversity: for example, plants not only possess the well-known VIT1 proteins similar to the structure of *Eg*VIT1 (Group V) but also possess VTL proteins (Group III) which stand out by lacking the MBD (Gollhofer et al., 2014). Group II (mostly archaea) and Group IA also lack MBD, but not Group IB, which suggests that domain diversity appeared in these prokaryote domains. The occurrence of more than one homologue and the high diversity of domains point out to a complex evolutionary history, maybe involving HGT from bacteria and archaea during the origin of the last common eukaryote ancestor (Figure C2.1 and C2.3). Interestingly, Group I-III proteins usually localize to the plasma membrane. Such is the case of the bacteria

Agrobacterium tumefaciens, which Ccc1 othologue called membrane-bound ferritin (MbfA) acts as an iron exporter (Bhubhanil et al., 2014). Another example is constituted by some soybean VTLs located to the nodule symbiosome membrane which export iron to the rhizobia to supply the high demand for nitrogen fixation (Liu et al., 2020). On the contrary, proteins in group V-VIII are located to vacuole/tonoplast, thus maybe sequence divergence is also associated with localization and subfunctionalization. In fact, the tree topology does not change when MBD sequences are not included. The lower conservation of both these domains suggests that they are not essential and may serve as auxiliary domains adapted to each organism's needs (Bhubhanil et al., 2014; Kato et al., 2019).

Once the diversity of protein architectures of the Ccc1/Vit1 family were explored, and the domains with the greatest divergence delimited, we decided to study the overexpression of *CCC1* as a putative tool to obtain iron-enriched yeasts. Surprisingly, we observed that overexpression of a full version of *CCC1* becomes toxic for the cell in normal conditions (Figures C3.1 and C3.2A). We tried different promoters to increase *CCC1* expression: i) the constitutive promoter of *TEF2* gene, which induces expression at high levels; ii) the strong inducible *GAL1* promoter, which activates expression in the presence of galactose, and iii) the repressible *MET25* promoter, which allows the expression at low levels in the absence of methionine in the medium. We found that, although overexpression is toxic in all three cases, the toxicity is remarkably lower when *CCC1* is under the control of the *MET25* promoter, because this promoter activates expression at a lesser degree (Figures C3.2A and C3.3), (Solow et al., 2005). The main transcriptional factor that induces *CCC1* expression is Yap5, although Msn2/4 transcriptional factors regulated by Snf1 kinase are also responsible for its expression in an iron-dependent manner (Li, L. et al., 2017). It is thought that Snf1 kinase also acts on other transcriptional factors not yet identified and that other regulators may be involved in the regulation of *CCC1* (Li, L. et al., 2017). Moreover, *CYC1* gene terminator substituted native *CCC1* 3'UTR in the three constructions mentioned above, avoiding the described down-regulation by Cth2 under iron-depletion (Puig et al., 2005). Definitively, it seems that *CCC1* promoter and terminator

are essential for a proper function of Ccc1 protein and uncoupling regulation from iron concentration is detrimental in non-overload conditions.

Interestingly, we found that *CCC1* overexpression toxicity can be attributed, in part, to low iron availability, since iron regulon is highly activated and *AFT1* deletion fully abrogates growth of *CCC1*-overexpressing cells in normal conditions (Figures C3.2C and C3.2D). In addition, deleting the high-affinity iron transport (*FTR1* and *FET3*) is detrimental for cells and, on the contrary, iron addition recues the toxic phenotype (Figures C2.2C and C2.2D). Moreover, *CCC1*-overexpressing cells also accumulate high amounts of total iron when grown in slight iron excess, reinforcing the idea that iron uptake is upregulated because iron is not intracellularly available (Figures C3.2B and C3.4C). In a similar way, a previous work of our group showed that overexpressing soybean seed ferritin in yeast cells led to the transcriptional activation of *AFT1* targets, and the same occurred when the expressed ferritin was from human origin (Kim, K. S. et al., 2007; de Llanos et al., 2016). On the other hand, several studies have stablished a link between vacuole and mitochondrial iron pools in such a way that an increase in vacuolar iron content leads to a decrease in mitochondrial reservoir and the reverse (Chen, O. S. and Kaplan, J., 2000; Li, L. and Kaplan, 2004; Lin et al., 2011). For example, *CCC1* overexpression prevents mitochondrial iron accumulation in overload phenotypes and limits Fe/S cluster damage, favoring iron regulon deactivation (Chen, O. S. and Kaplan, J., 2000; Li, L. et al., 2010; Li, L. et al., 2012). In contrast, when mitochondrial iron transporters *MRS3* and *MRS4* are overexpressed in a *ccc1Δ* strain, iron toxicity is rescued by limiting cytosolic iron (Li, L. and Kaplan, 2004; Lin et al., 2011). On the other hand, transport studies on endosomes have shown that *Eg*VIT and *P. falciparum* orthologs act as H^+ antiporters (Slavic et al., 2016; Kato et al., 2019). Amino acid conservation and some evidence suggests that *S. cerevisiae* Ccc1 behaves as an H^+-antiporter. Consequently, *CCC1* activation could be unbalancing the proton gradient across the vacuolar membrane (Cockrell, A. et al., 2014; Sorribes-Dauden et al., 2020). Interestingly, deletion of any subunit of the vacuolar H^+-ATPase, V-ATPase, leads to the activation of the iron regulon due to chronic oxidative stress (Milgrom et al., 2007; Diab and Kane, 2013). The vacuole constitutes a

reservoir for several nutrients, as amino acids and other metals, besides iron. Therefore, H^+ gradient impairment may lead to cytosol nutrient accumulation which can be detrimental for cells. Specially, cytosolic cysteine accumulation has been shown to cause damage to components of the Fe/S cluster synthesis route, limiting enzyme activity and causing iron regulon activation (Hughes et al., 2020). This alteration in iron homeostasis regulation and mitochondrial dysfunction have been related to an aged phenotype (Chen, K. L. et al., 2020; Hughes et al., 2020).

As a result of the study of domain conservation in the Ccc1/VIT1 family, it was observed that Nt domain was one of the least conserved domains and with a species-specific variability. Moreover, several proteomic studies have revealed that in *S. cerevisiae* this Ccc1 domain is phosphorylated and ubiquitinated at certain serine and lysine residues, respectively (Albuquerque et al., 2008; Swaney et al., 2013). Thus, we aimed to analyze the role of this domain and its putative application in iron-enrichment of yeasts or in iron-extraction from the medium. Deletion of Ccc1 Nt domain seems to be a partial loss-of-function mutation, since at elevated iron concentrations growth of this mutant is quite impaired and the iron regulon activation is lower than when the full version is present (Figures C3.2A and C3.2B). Moreover, when cells are incubated in a slight excess of iron, *CCC1*-overexpressing cells accumulate eight times more iron compared to WT, while the increase in *NtΔCCC1*-overexpressing cells is just 4-fold (Figure C3.4C). However, when we determined the total iron extracted per volume of medium, we observed that *CCC1*-overexpressing cells did not improve the capacity of WT cells to remove iron from the medium, mostly due to their low growth (Figure C3.4D). Interestingly, NtΔCCC1-cells extracted twice as much iron from the extracellular medium as the rest of the assayed cells barely without a growth defect, becoming it in an interesting tool for iron extraction from the environment (Figure C3.4D), for example, to remove iron from wine, since it sometimes causes an unpleasant taste, rusty color and a decrease in the stability of food products (Tsuji et al., 2012). We observed that this loss-of-function is not due to lower protein stability since the half-life of GFP-tagged NtΔCcc1 protein is similar to the full version (Figure C3.5). However, it seems that the absence of

the Nt domain slightly alters the transporter distribution even though it still localizes at the vacuole membrane (Figure C3.6). Thus, it is possible that this domain is involved in the fine-tuned distribution of the Ccc1 transporter at the vacuolar membrane. On the other hand, the fact that the Nt domain possesses serine residues, which are phosphorylated, would suggest that a putative post-translational regulation of this domain could be necessary for full activation of the transporter. For example, in the case of the cadmium transporter Yeast cadmium factor 1, Ycf1, the phosphorylation of the regulatory domain (R-domain) allows the interaction with other motifs of the protein producing a conformational change responsible of complete activation (Khandelwal et al., 2022). Additionally, it cannot be ruled out that the Nt domain of Ccc1 may be subject to other regulations, since it has been demonstrated that Ccc1 increases its activity in response to ROS generation, suggesting that this protein is indeed regulated at the post-translational level, although the specific mechanism remains to be defined (Li, L. et al., 2010). Moreover, in a natural yeast population isolated from the nectar of Malaysian bertam palm tree, it has been found that a single amino acid change of a glycine for an arginine in the amino terminal end of Ccc1 causes growth impairment in excess iron (Lee, H. N. et al., 2013). On the other hand, a recent study by Amaral and colleagues (2021) showed that an internal promoter of *CCC1* leads to the translation of a truncated Ccc1 protein lacking its amino terminal domain which is less functional than the full version, in a similar line with our results. The expression of this alternative version is usually repressed and depends on the genetic background. It is possible that strains isolated from other environments with different genetic backgrounds could express different *CCC1* architectures, which would be a source of variability still unexplored. More studies have to be done in order to clarify the function of the Ccc1 Nt domain. However, the fact that *NtΔCCC1*-overexpressing cells are able to accumulate higher levels of iron compared to wild-type with a minimal growth defect already provides an interesting biotechnological tool for iron extraction from the medium, while opening a new strategy to obtain iron-enriched yeasts.

Besides *S. cerevisiae*, we took advantage of the high availability of *Saccharomyces* genus isolates and their sequenced genomes to expand our

knowledge in iron excess response to representative strains of *Saccharomyces* genus populations. The most notable result of our analysis was the observed difference in iron tolerance in a species-specific manner (Figure C4.2). Thus, we observed that species closely related to *S. cerevisiae*, such as *S. paradoxus, S. mikatae, S. jurei* or *S. arboricola*, are more resistant to high-iron than the most distant ones, *S. kudriavzevii, S. uvarum*, and *S. eubayanus*. It is well-known that temperature has been a strong selection pressure factor which had a key role in the speciation process of this genus. Some species have been described as sympatric partners, that is, species originating from a common ancestor which inhabit the same geographic region. It is thought that this co-existence depends on circadian and / or annual temperature oscillations which favor each species in turn (Gonçalves, P. et al., 2011; Peris et al., 2023). One possibility is that adaptation to temperature has conditioned iron homeostasis, for example in such a way that high temperatures will require a higher demand for iron. In fact, mtDNA which mainly encodes genes involved in mitochondrial respiration, a huge iron-consuming pathway, has been pointed out as an evolutionary hotspot linked to temperature adaptation (Li, X. C. et al., 2019). Another possibility is that *Saccharomyces* species have been forced to adopt strategies to adapt to different iron availabilities in order to co-exist in iron deficient habitats like decayed leaves or oak trunks. According to other studies, *S. mikatae* and *S. jurei* behaved similarly in response to iron excess, as well as *S. uvarum* and *S. eubayanus*, probably because they are the less divergent sister species in the genus (Figure C4.2), (Peris et al., 2023). Moreover, *S. cerevisiae* and *S. paradoxus* species present the higher intraspecific phenotypic variability (Figure C4.2). Iron-resistant strain Sc3 is Kyokai 6, which belongs to the Sake population, and Sc7 and Sc8 are YJM978 and CECT11032 both from the Wine/European population but isolated from clinical sample and grape must, respectively (Peter et al., 2018). These three strains are from human-related environments, but according to other works, it does not seem that there is a correlation between iron resistance and not sourcing from wild, since other strains closely related to Kyokai no. 6 are not as much resistant than it and a similar situation occurs in wine and clinical strains (Martínez-Garay et al., 2016). However, the number of human-related strains in this study is

reduced and they all belong to the same species, therefore, no relationship between iron resistance and the human environment can be stablished.

There is a lack of synchronization between iron uptake and cell division at post-exponential growth and it is known that the iron regulon is activated at diauxic sift in a glucose-dependent and iron-independent manner (Haurie et al., 2003; Park et al., 2013) Thus, slowly-growing or growth-arrested cells continue to import Fe through this pathway when incubated for long time. However, in a previous analysis of *S. cerevisiae* strains, iron-resistant strains were able to limit iron uptake better than iron-sensitive ones (Martínez-Garay et al., 2016). In the present study with *Saccharomyces* genus species, we observed two well-differentiated patterns in iron-sensitive strains: i) strains that accumulate high amounts of iron and ii) strains that have increased sensitivity to the interiorized iron (Figure C4.3). *Saccharomyces* species are unable to export iron and, according to the "avoidance or sequestration" theory for metal tolerance suggested by Jennings (1993), the first group seems to be unable to avoid iron entrance, while the second group would seem to have defects in detoxification machinery. As shown in Martínez-Garay and colleagues (2016), iron-sensitive strains are apparently adapted to low availability environments, since they are resistant to iron-depletion. On the other hand, a commonly observed strategy to deal with iron scarcity in natural S. cerevisiae strains is to upregulate iron uptake, through Aft1 activation (Lee, H. N. et al., 2013; Eldarov et al., 2018). Indirectly, Aft1 dysregulation has been used as a method for increasing iron entrance in bioengineered yeast strains (Ramos-Alonso et al., 2018; Gambacorta et al., 2022). Moreover, we show that iron-sensitive strains that accumulate large quantities of iron have high activation of the Yap5 targets *TYW1, CCC1* and *GRX4* upon iron addition, which would correlate to high iron accumulation (Figure C4.8). Although they are able to shut down *FET4* expression when iron is added, notably, they present expression of this gene in normal conditions as if it were perceived as iron deficiency (Figure C4.S5A). Activation of the iron regulon in normal conditions has been detected in the Malaysian iron-sensitive strain Sc1, as if the strains had adapted to severe deficiency (Lee, H. N. et al., 2013). A work from Schothorst et al. (2017) pointed out the iron permease Ftr1 as an iron transceptor which activates PKA signaling

and could be involved in shifting the threshold to which cells respond to a lower concentration range. Nonetheless, we also observed a group of strains that are highly sensitive but their iron levels are similar to resistant strains. Therefore, these strains may be able to shut down iron import, but they would not be able to detoxify iron properly. In fact, they have poor activation of *TYW1* and *CCC1* (Figure C4.8). Since a single amino acid chance in the Nt domain of Ccc1 in the Malaysian iron-sensitive Sc1 strain is behind its poor growth in iron excess, we studied the amino acid divergence in Ccc1 transporter (Lee, H. N. et al., 2013). Regarding the Ccc1/Vit1 family conservation, in the *Saccharomyces* genus barely all changes are found in the Nt domain (Figure C2.3). However, *CCC1*-overexpression toxicity makes it difficult to discern the consequence of mutations. One interesting possibility to address this analysis would be to use CRISPR, which would allow to maintain the strains genetic background without overexpression (DiCarlo et al., 2013). Additionally, we can also search for divergence in other proteins implicated in iron homeostasis, studying whether the rate of evolution is higher in these genes and if they have indeed been under selective pressure (Yang, Z., 2007). However, eventually it may be required to test if this selection has a relationship with iron or temperature. In our work, we observed that iron-sensitive yeasts are more oxidized than resistant ones at low iron concentrations but we only see an increase in *TRX2* mRNA levels, in contrast to other works which also detected *SOD1, TSA1* or *YAP1* upregulation (Lin et al., 2011; Pimentel et al., 2012). However, Lin and colleagues (2011) demonstrated that deletion of YAP1 gene or overexpression of other oxidative response genes do not have a remarkable effect on iron toxicity which is still happening even in anaerobic conditions. Thus, maybe there are other factors responsible for iron toxicity besides ROS production as mismetallation or sphingolipid signaling (Yang, M. et al., 2006; Lee, Y. J. et al., 2012).

From a biotechnological point of view, the iron-resistant strains described here seem less interesting, since apparently iron resistance is achieved by limiting iron accumulation. Iron-sensitive strains which acquired iron levels comparable to resistant ones are also not appropriated but the most compelling are the sensitive strains which are large accumulators. However, since an

excess of iron is detrimental for cell, it is crucial to achieve a balance between cell viability and iron accumulation, as in the case of NtΔCCC1 strain. On the other hand, the enhancement of metal uptake depends on the ability to increase intracellular tolerance besides the upregulation of iron uptake and vacuolar transport (Sun, G. L. et al., 2019). For example, copper tolerance has been related to the increase in the copy number of *CUP1*, which encodes a major metallothionine that sequesters copper at cytosol (Adamo et al., 2012). Regarding iron tolerance, this role is expected to be executed by *TYW1* and *GRX4*. However, it is also proven that lowering sphingolipid signaling or upregulation of oxidative damage response and mitophagy are requirements for iron tolerance (Lee, H. N. et al., 2013; Ramos-Alonso et al., 2018; Balaban et al., 2019; Kocaefe-Ozsen et al., 2022). Thus, using yeast as a tool for iron detoxification or biofortification depends on: i) upregulation of uptake, ii) upregulation of vacuolar transport and iii) increasing intracellular iron tolerance.

In this thesis work, we have shed light on the choice of the best salt to phenotype the response to excess iron, conservation of a common mechanism for iron detoxification in prokaryotes, plants, fungi and protists, development of a tool for iron extraction, and using *Saccharomyces* strains for iron biofortification.

CONCLUSIONS

CONCLUSIONS

1. $FeSO_4$ and $(NH_4)_2Fe(SO_4)_2$ are the most adequate sources of iron for iron-resistance phenotyping of *Saccharomyces cerevisiae* cells, when prepared in acidic media, as lowering pH prevents Fe^{2+} oxidation and avoids the formation of precipitates in SC medium, increasing its bioavailability. $FeCl_3$ can be used in solid plates but not in liquid media, where the formation of a precipitate makes growth recording via absorbance measurements difficult.

2. The Ccc1/Vit1 family of membrane transporter proteins is conserved along the Tree of Life, with a wide representation in plants, protists, fungi, bacteria and archaea, but not in metazoans. Amino acid similarity in Ccc1/Vit1 family is low along the sequence, but residues involved in transport and overall structure of domains are well conserved.

3. The metal-binding and amino-terminal domains of the Ccc1/Vit1 family are highly diverse among organisms, they are not essential and may serve as auxiliary domains adapted to each organism's needs. The diversity of protein architecture and the presence of multiple homologues in certain organisms points out to a complex evolutionary history.

4. *CCC1*-overexpression in normal growth conditions is detrimental for yeast cells, probably because it prevents iron from being available to mitochondria.

5. The amino-terminal domain of Ccc1 is necessary for full activity in the presence of elevated levels of iron and it is involved in fine-tuning Ccc1 subcellular localization. The deletion of the amino-terminal domain alleviates overexpression toxicity and could be used as a tool to improve iron extraction from the environment.

6. In the *Saccharomyces* genus, iron sensitivity lies either in the inability to avoid iron uptake or to tolerate the acquired iron. *S. cerevisiae* strains tend to avoid iron entrance and are generally more resistant to high-iron than *Saccharomyces* non-*cerevisiae* strains. Species evolutionarily closer to *S. cerevisiae*, such as *S. paradoxus*, *S. jurei*, *S. mikatae* and *S. arboricola* are more resistant to high-iron concentrations than more distant species, like *S. eubayanus* and *S. uvarum*, with *S. kudriavzevii* strains being especially sensitive.

7. The *S. cerevisiae* and *S. paradoxus* iron-resistant strains are less oxidized than iron-sensitive strains. This lower oxidation is specific to iron and does not occur under other stressors. Iron-sensitive strains have an altered expression pattern of iron overload response genes, such as *FET4*, and different profiles of iron accumulation are observed. While *S. cerevisiae, S. uvarum and S. kudriavzevii* sensitive strains accumulate more iron, the reminder sensitive strains show no remarkable differences in iron accumulation.

REFERENCES

REFERENCES

G. M. Adamo, M. Lotti, M. J. Tamas, and S. Brocca. (2012). Amplification of the *CUP1* gene is associated with evolution of copper tolerance in *Saccharomyces cerevisiae*. *Microbiology 158*(9), 2325-2335. doi:10.1099/mic.0.058024-0

P. C. Adams, G. Jeffrey, and J. Ryan. (2023). Haemochromatosis. *Lancet, 401*(10390), 1811-1821. doi:10.1016/S0140-6736(23)00287-8

M. Aidoo, D. J. Terlouw, M. S. Kolczak, P. D. McElroy, F. O. ter Kuile, S. Kariuki, . . . V. Udhayakumar. (2002). Protective effects of the sickle cell gene against malaria morbidity and mortality. *Lancet, 359*(9314), 1311-1312. doi:10.1016/S0140-6736(02)08273-9

C. P. Albuquerque, M. B. Smolka, S. H. Payne, V. Bafna, J. Eng, and H. Zhou. (2008). A multidimensional chromatography technology for in-depth phosphoproteome analysis. *Mol Cell Proteomics, 7*(7), 1389-1396. doi:10.1074/mcp.M700468-MCP200

H. Alsammar, and D. Delneri. (2020). An update on the diversity, ecology and biogeography of the *Saccharomyces* genus. *FEMS Yeast Res, 20*(3), 1-12. doi:10.1093/femsyr/foaa013

S. F. Altschul, W. Gish, W. Miller, E. W. Myers, and D. J. Lipman. (1990). Basic local alignment search tool. *J Mol Biol, 215*(3), 403-410. doi:10.1016/S0022-2836(05)80360-2

C. Amaral, C. T. Vicente, S. M. Caetano, A. Gaspar-Cordeiro, Y. Yang, P. Cloetens, . . . C. Pimentel. (2021). An internal promoter drives the expression of a truncated form of *CCC1* capable of protecting yeast from iron toxicity. *Microorganisms, 9*(6). doi:10.3390/microorganisms9061337

N. C. Andrews, and P. J. Schmidt. (2007). Iron homeostasis. *Annu Rev Physiol, 69*, 69-85. doi:10.1146/annurev.physiol.69.031905.164337

S. C. Andrews. (2010). The Ferritin-like superfamily: Evolution of the biological iron storeman from a rubrerythrin-like ancestor. *Biochim Biophys Acta, 1800*(8), 691-705. doi:10.1016/j.bbagen.2010.05.010

P. Arosio, L. Elia, and M. Poli. (2017). Ferritin, cellular iron storage and regulation. *IUBMB Life, 69*(6), 414-422. doi:10.1002/iub.1621

P. Arosio, R. Ingrassia, and P. Cavadini. (2009). Ferritins: a family of molecules for iron storage, antioxidation and more. *Biochim Biophys Acta, 1790*(7), 589-599. doi:10.1016/j.bbagen.2008.09.004

F. N. Arroyo-Lopez, Z. Salvado, J. Tronchoni, J. M. Guillamon, E. Barrio, and A. Querol. (2010). Susceptibility and resistance to ethanol in *Saccharomyces* strains isolated from wild and fermentative environments. *Yeast, 27*(12), 1005-1015. doi:10.1002/yea.1809

C. Askwith, A. Eide D Fau - Van Ho, P. S. Van Ho A Fau - Bernard, L. Bernard Ps Fau - Li, S. Li L Fau - Davis-Kaplan, D. M. Davis-Kaplan S Fau - Sipe, . . . J. Kaplan. (1994). The *FET3* gene of *S. cerevisiae* encodes a multicopper oxidase required for ferrous iron uptake. *Journal of Biological Chemistry, 76*(2), 403-410. doi:10.1016/0092-8674(94)90346-8

B. G. Balaban, U. Yilmaz, C. Alkim, A. Topaloglu, H. I. Kisakesen, C. Holyavkin, and Z. P. Cakar. (2019). Evolutionary engineering of an iron-resistant *Saccharomyces* cerevisiae mutant and its physiological and molecular characterization. *Microorganisms, 8*(1), 1-43. doi:10.3390/microorganisms8010043

M. F. Barber, and N. C. Elde. (2015). Buried treasure: Evolutionary perspectives on microbial iron piracy. *Trends Genet, 31*(11), 627-636. doi:10.1016/j.tig.2015.09.001

S. Bathla, and S. Arora. (2022). Prevalence and approaches to manage iron deficiency anemia (IDA). *Crit Rev Food Sci Nutr, 62*(32), 8815-8828. doi:10.1080/10408398.2021.1935442

M. Bayeva, A. Khechaduri, S. Puig, H. C. Chang, S. Patial, P. J. Blackshear, and H. Ardehali. (2012). mTOR regulates cellular iron homeostasis through tristetraprolin. *Cell Metab, 16*(5), 645-657. doi:10.1016/j.cmet.2012.10.001

S. Bhubhanil, J. Chamsing, P. Sittipo, P. Chaoprasid, R. Sukchawalit, and S. Mongkolsuk. (2014). Roles of *Agrobacterium tumefaciens* membrane-bound ferritin (MbfA) in iron transport and resistance to iron under acidic conditions. *Microbiology (Reading), 160*(5), 863-871. doi:10.1099/mic.0.076802-0

M. R. Bleackley, B. P. Young, C. J. Loewen, and R. T. MacGillivray. (2011). High density array screening to identify the genetic requirements for transition metal tolerance in *Saccharomyces cerevisiae*. *Metallomics, 3*(2), 195-205. doi:10.1039/c0mt00035c

H. E. Bouis, and A. Saltzman. (2017). Improving nutrition through biofortification: A review of evidence from HarvestPlus, 2003 through 2016. *Glob Food Sec, 12*, 49-58. doi:10.1016/j.gfs.2017.01.009

P. J. Boynton, and D. Greig. (2014). The ecology and evolution of non-domesticated *Saccharomyces* species. *Yeast, 31*(12), 449-462. doi:10.1002/yea.3040

J. J. Braymer, and R. Lill. (2017). Iron-sulfur cluster biogenesis and trafficking in mitochondria. *J Biol Chem, 292*(31), 12754-12763. doi:10.1074/jbc.R117.787101

E. M. Brear, F. Bedon, A. Gavrin, I. S. Kryvoruchko, I. Torres-Jerez, M. K. Udvardi, . . . P. M. C. Smith. (2020). *Gm*VTL1a is an iron transporter on the symbiosome membrane of soybean with an important role in nitrogen fixation. *New Phytol, 228*(2), 667-681. doi:10.1111/nph.16734

T. Brembu, M. Jorstad, P. Winge, K. C. Valle, and A. M. Bones. (2011). Genome-wide profiling of responses to cadmium in the diatom *Phaeodactylum tricornutum*. *Environ Sci Technol, 45*(18), 7640-7647. doi:10.1021/es2002259

J. F. Briat, C. Duc, K. Ravet, and F. Gaymard. (2010). Ferritins and iron storage in plants. *Biochim Biophys Acta, 1800*(8), 806-814. doi:10.1016/j.bbagen.2009.12.003

K. Brzóska, M. Meczyńska S Fau - Kruszewski, and M. Kruszewski. (2006). Iron-sulfur cluster proteins: electron transfer and beyond. *Acta biochimica Polonica, 53*(4), 685-691 doi:10.18388/ABP.2006_3296

Y. V. Bukhman, N. W. DiPiazza, J. Piotrowski, J. Shao, A. G. W. Halstead, M. D. Bui, . . . T. K. Sato. (2015). Modeling microbial growth curves with GCAT. *BioEnergy Research, 8*(3), 1022-1030. doi:10.1007/s12155-015-9584-3

M. L. Caldas Nogueira, A. J. Pastore, and V. L. Davidson. (2021). Diversity of structures and functions of oxo-bridged non-heme diiron proteins. *Arch Biochem Biophys, 705*, 108917-108934. doi:10.1016/j.abb.2021.108917

C. Camaschella. (2019). Iron deficiency. *Blood, 133*(1), 30-39. doi:10.1182/blood-2018-05-815944

J. Cao. (2019). Molecular evolution of the Vacuolar Iron Transporter (VIT) family genes in 14 Plant Species. *Genes (Basel), 10*(2), 144-160. doi:10.3390/genes10020144

F. Capozzi, S. Ciurli, and C. Luchinat. (1998). Coordination sphere versus protein environment as determinants of electronic and functional properties of iron-sulfur proteins. In H. A. O. Hill, P. J. Sadler, and A. J. Thomson (Eds.), *Metal sites in proteins and models redox centres* (pp. 127-160). Berlin, Heidelberg: Springer Berlin Heidelberg.

I. G. Chambers, M. M. Willoughby, I. Hamza, and A. R. Reddi. (2021). One ring to bring them all and in the darkness bind them: The trafficking of heme

without deliverers. *Biochim Biophys Acta Mol Cell Res, 1868*(1), 118881-118921. doi:10.1016/j.bbamcr.2020.118881

C. Chen, K. Pande, S. D. French, B. B. Tuch, and S. M. Noble. (2011). An iron homeostasis regulatory circuit with reciprocal roles in *Candida albicans* commensalism and pathogenesis. *Cell Host Microbe, 10*(2), 118-135. doi:10.1016/j.chom.2011.07.005

H. Chen, P. W. Miller, D. L. Johnson, and R. N. Laribee. (2020). The Ccr4-Not complex regulates TORC1 signaling and mitochondrial metabolism by promoting vacuole V-ATPase activity. *PLoS Genet, 16*(10), e1009046-1009076. doi:10.1371/journal.pgen.1009046

K. L. Chen, T. N. Ven, M. M. Crane, M. L. C. Brunner, A. K. Pun, K. L. Helget, . . . B. M. Wasko. (2020). Loss of vacuolar acidity results in iron-sulfur cluster defects and divergent homeostatic responses during aging in *Saccharomyces cerevisiae*. *Geroscience, 42*(2), 749-764. doi:10.1007/s11357-020-00159-3

O. S. Chen, R. J. Crisp, M. Valachovic, M. Bard, D. R. Winge, and J. Kaplan. (2004). Transcription of the yeast iron regulon does not respond directly to iron but rather to iron-sulfur cluster biosynthesis. *J Biol Chem, 279*(28), 29513-29518. doi:10.1074/jbc.M403209200

O. S. Chen, and J. Kaplan. (2000). *CCC1* suppresses mitochondrial damage in the yeast model of Friedreich's ataxia by limiting mitochondrial iron accumulation. *J Biol Chem, 275*(11), 7626-7632. doi:10.1074/jbc.275.11.7626

J. Choi, P. Masaratana, G. O. Latunde-Dada, M. Arno, R. J. Simpson, and A. T. McKie. (2012). Duodenal reductase activity and spleen iron stores are reduced and erythropoiesis is abnormal in Dcytb knockout mice exposed to hypoxic conditions. *J Nutr, 142*(11), 1929-1934. doi:10.3945/jn.112.160358

U. Chorostecki, M. Molina, L. P. Pryszcz, and T. Gabaldon. (2020). MetaPhOrs 2.0: integrative, phylogeny-based inference of orthology and paralogy across the tree of life. *Nucleic Acids Res, 48*(1), 553-557. doi:10.1093/nar/gkaa282

A. Cockrell, S. P. McCormick, M. J. Moore, M. Chakrabarti, and P. A. Lindahl. (2014). Mossbauer, EPR, and modeling study of iron trafficking and regulation in Deltaccc1 and *CCC1*-up *Saccharomyces cerevisiae*. *Biochemistry, 53*(18), 2926-2940. doi:10.1021/bi500002n

A. L. Cockrell, G. P. Holmes-Hampton, S. P. McCormick, M. Chakrabarti, and P. A. Lindahl. (2011). Mossbauer and EPR study of iron in vacuoles from fermenting *Saccharomyces cerevisiae*. *Biochemistry, 50*(47), 10275-10283. doi:10.1021/bi2014954

A. Cohen, H. Nelson, and N. Nelson. (2000). The family of SMF metal ion transporters in yeast cells. *J Biol Chem, 275*(43), 33388-33394. doi:10.1074/jbc.M004611200

J. M. Connorton, J. Balk, and J. Rodriguez-Celma. (2017). Iron homeostasis in plants - a brief overview. *Metallomics, 9*(7), 813-823. doi:10.1039/c7mt00136c

M. Courel, S. Lallet, J. M. Camadro, and P. L. Blaiseau. (2005). Direct activation of genes involved in intracellular iron use by the yeast iron-responsive transcription factor Aft2 without its paralog Aft1. *Mol Cell Biol, 25*(15), 6760-6771. doi:10.1128/MCB.25.15.6760-6771.2005

R. de Llanos, C. A. Martinez-Garay, J. Fita-Torro, A. M. Romero, M. T. Martinez-Pastor, and S. Puig. (2016). Soybean ferritin expression in *Saccharomyces cerevisiae* modulates iron accumulation and resistance to elevated iron concentrations. *Appl Environ Microbiol, 82*(10), 3052-3060. doi:10.1128/AEM.00305-16

H. I. Diab, and P. M. Kane. (2013). Loss of vacuolar H^+-ATPase (V-ATPase) activity in yeast generates an iron deprivation signal that is moderated by induction of the peroxiredoxin *TSA2*. *J Biol Chem, 288*(16), 11366-11377. doi:10.1074/jbc.M112.419259

J. E. DiCarlo, J. E. Norville, P. Mali, X. Rios, J. Aach, and G. M. Church. (2013). Genome engineering in *Saccharomyces cerevisiae* using CRISPR-Cas systems. *Nucleic Acids Res, 41*(7), 4336-4343. doi:10.1093/nar/gkt135

S. J. Dixon, K. M. Lemberg, M. R. Lamprecht, R. Skouta, E. M. Zaitsev, C. E. Gleason, . . . B. R. Stockwell. (2012). Ferroptosis: an iron-dependent form of nonapoptotic cell death. *Cell, 149*(5), 1060-1072. doi:10.1016/j.cell.2012.03.042

S. J. Dixon, and B. R. Stockwell. (2014). The role of iron and reactive oxygen species in cell death. *Nat Chem Biol, 10*(1), 9-17. doi:10.1038/nchembio.1416

A. E. Donker, H. van der Staaij, and D. W. Swinkels. (2021). The critical roles of iron during the journey from fetus to adolescent: Developmental aspects of iron homeostasis. *Blood Rev, 50*, 100866-100886. doi:10.1016/j.blre.2021.100866

B. Dresow, D. Petersen, R. Fischer, and P. Nielsen. (2008). Non-transferrin-bound iron in plasma following administration of oral iron drugs. *Biometals, 21*(3), 273-276. doi:10.1007/s10534-007-9116-5

Y. Du, W. Cheng, and W. F. Li. (2012). Expression profiling reveals an unexpected growth-stimulating effect of surplus iron on the yeast *Saccharomyces cerevisiae*. *Mol Cells, 34*(2), 127-132. doi:10.1007/s10059-012-2242-0

C. L. Dupont, A. Butcher, R. E. Valas, P. E. Bourne, and G. Caetano-Anolles. (2010). History of biological metal utilization inferred through phylogenomic analysis of protein structures. *Proc Natl Acad Sci U S A, 107*(23), 10567-10572. doi:10.1073/pnas.0912491107

C. L. Dupont, S. Yang, B. Palenik, and P. E. Bourne. (2006). Modern proteomes contain putative imprints of ancient shifts in trace metal geochemistry. *Proc Natl Acad Sci U S A, 103*(47), 17822-17827. doi:10.1073/pnas.0605798103

I. A. Ehrnstorfer, C. Manatschal, F. M. Arnold, J. Laederach, and R. Dutzler. (2017). Structural and mechanistic basis of proton-coupled metal ion transport in the SLC11/NRAMP family. *Nat Commun, 8*(14033), 1-11. doi:10.1038/ncomms14033

R. Eid, N. T. Arab, and M. T. Greenwood. (2017). Iron mediated toxicity and programmed cell death: A review and a re-examination of existing paradigms. *Biochim Biophys Acta Mol Cell Res, 1864*(2), 399-430. doi:10.1016/j.bbamcr.2016.12.002

M. A. Eldarov, A. V. Beletsky, T. N. Tanashchuk, S. A. Kishkovskaya, N. V. Ravin, and A. V. Mardanov. (2018). Whole-genome analysis of three yeast strains used for production of sherry-like wines revealed genetic traits specific to flor yeasts. *Front Microbiol, 9*, 965-978. doi:10.3389/fmicb.2018.00965

T. V. Elzhov, K. M. Mullen, A.-N. Spiess, and B. Bolker. (2022). R interface to the Levenberg-Marquardt nonlinear least-squares algorithm found in MINPACK, plus support for bounds (Version 1.2-2): CRAN repository. Retrieved from https://CRAN.R-project.org/package=minpack.lm (accessed on 20 September 2022).

S. Eroglu, N. Karaca, K. Vogel-Mikus, A. Kavcic, E. Filiz, and B. Tanyolac. (2019). The conservation of VIT1-dependent iron distribution in seeds. *Front Plant Sci, 10*, 907-920. doi:10.3389/fpls.2019.00907

T. H. Flo, K. D. Smith, S. Sato, D. J. Rodriguez, M. A. Holmes, R. K. Strong, . . . A. Aderem. (2004). Lipocalin 2 mediates an innate immune response to bacterial infection by sequestrating iron. *Nature, 432*(7019), 917-921. doi:10.1038/nature03104

E. M. Froschauer, R. J. Schweyen, and G. Wiesenberger. (2009). The yeast mitochondrial carrier proteins Mrs3p/Mrs4p mediate iron transport across the inner mitochondrial membrane. *Biochim Biophys Acta, 1788*(5), 1044-1050. doi:10.1016/j.bbamem.2009.03.004

T. Furukawa, M. T. Scheven, M. Misslinger, C. Zhao, S. Hoefgen, F. Gsaller, . . . P. Hortschansky. (2020). The fungal CCAAT-binding complex and HapX display highly variable but evolutionary conserved synergetic

promoter-specific DNA recognition. *Nucleic Acids Res, 48*(7), 3567-3590. doi:10.1093/nar/gkaa109

F. Gaensly, G. Picheth, D. Brand, and T. M. Bonfim. (2014). The uptake of different iron salts by the yeast *Saccharomyces cerevisiae*. *Brazilian journal of microbiology, 45*(2), 491–494. doi:10.1590/s1517-83822014000200016

T. Galili, A. O'Callaghan, J. Sidi, and C. Sievert. (2018). heatmaply: an R package for creating interactive cluster heatmaps for online publishing. *Bioinformatics, 34*(9), 1600-1602. doi:10.1093/bioinformatics/btx657

F. V. Gambacorta, E. R. Wagner, T. B. Jacobson, M. Tremaine, L. K. Muehlbauer, M. A. McGee, . . . B. F. Pfleger. (2022). Comparative functional genomics identifies an iron-limited bottleneck in a *Saccharomyces cerevisiae* strain with a cytosolic-localized isobutanol pathway. *Synth Syst Biotechnol, 7*(2), 738-749. doi:10.1016/j.synbio.2022.02.007

G. Gani, B. Gulzar, O. Bashir, T. Ah Bhat, B. Naseer, T. Qadri, and N. Jan. (2018). Hidden hunger and its prevention by food processing: A review. *International Journal of Unani and Integrative Medicine, 2*(3), 01-10.

T. Ganz, and E. Nemeth. (2012). Hepcidin and iron homeostasis. *Biochim Biophys Acta, 1823*(9), 1434-1443. doi:10.1016/j.bbamcr.2012.01.014

A. P. Gasch, B. A. Payseur, and J. E. Pool. (2016). The power of natural variation for model organism Biology. *Trends Genet, 32*(3), 147-154. doi:10.1016/j.tig.2015.12.003

F. Gerwien, A. Safyan, S. Wisgott, F. Hille, P. Kaemmer, J. Linde, . . . B. Hube. (2016). A novel hybrid iron regulation network combines features from pathogenic and nonpathogenic yeasts. *mBio, 7*(5), e01782-01716. doi:10.1128/mBio.01782-16

K. Giannakou, M. Cotterrell, and D. Delneri. (2020). Genomic adaptation of *Saccharomyces* species to industrial environments. *Front Genet, 11*, 916-926. doi:10.3389/fgene.2020.00916

J. Gollhofer, R. Timofeev, P. Lan, W. Schmidt, and T. J. Buckhout. (2014). Vacuolar-Iron-Transporter1-Like proteins mediate iron homeostasis in Arabidopsis. *PLoS One, 9*(10), e110468-110476. doi:10.1371/journal.pone.0110468

I. R. Gonçalves, N. Conde e Silva, C. L. Garay, E. Lesuisse, J. M. Camadro, and P. L. Blaiseau. (2014). The basis for evolution of DNA-binding specificity of the Aft1 transcription factor in yeasts. *Genetics, 196*(1), 149-160. doi:10.1534/genetics.113.157693

P. Gonçalves, E. Valerio, C. Correia, J. M. de Almeida, and J. P. Sampaio. (2011). Evidence for divergent evolution of growth temperature

preference in sympatric *Saccharomyces* species. *PLoS One, 6*(6), e20739-20750. doi:10.1371/journal.pone.0020739

N. N. Greenwood, and A. Earnshaw. (1997). *Chemistry of elements*. Oxford (United Kingdom): Butterworth-Heinemann.

F. Gsaller, M. Eisendle, B. E. Lechner, M. Schrettl, H. Lindner, D. Muller, . . . H. Haas. (2012). The interplay between vacuolar and siderophore-mediated iron storage in *Aspergillus fumigatus*. *Metallomics, 4*(12), 1262-1270. doi:10.1039/c2mt20179h

F. Gsaller, P. Hortschansky, S. R. Beattie, V. Klammer, K. Tuppatsch, B. E. Lechner, . . . H. Haas. (2014). The Janus transcription factor HapX controls fungal adaptation to both iron starvation and iron excess. *EMBO J, 33*(19), 2261-2276. doi:10.15252/embj.201489468

L. Guimarães, H. A. de Abreu, and H. A. Duarte. (2007). Fe(II) hydrolysis in aqueous solution: A DFT study. *Chemical Physics, 333*(1), 10-17. doi:10.1016/j.chemphys.2006.12.023

A. Hagman, T. Sall, C. Compagno, and J. Piskur. (2013). Yeast "make-accumulate-consume" life strategy evolved as a multi-step process that predates the whole genome duplication. *PLoS One, 8*(7), e68734-68746. doi:10.1371/journal.pone.0068734

T. Hakoyama, K. Niimi, T. Yamamoto, S. Isobe, S. Sato, Y. Nakamura, . . . N. Suganuma. (2012). The integral membrane protein SEN1 is required for symbiotic nitrogen fixation in *Lotus japonicus* nodules. *Plant Cell Physiol, 53*(1), 225-236. doi:10.1093/pcp/pcr167

R. Hassett, D. J. Dix Dr Fau - Eide, D. J. Eide Dj Fau - Kosman, and D. J. Kosman. (2000). The Fe(II) permease Fet4p functions as a low affinity copper transporter and supports normal copper trafficking in *Saccharomyces cerevisiae*. *Biochemical Journal, 351* (2), 477–484.

V. Haurie, H. Boucherie, and F. Sagliocco. (2003). The Snf1 protein kinase controls the induction of genes of the iron uptake pathway at the diauxic shift in *Saccharomyces cerevisiae*. *J Biol Chem, 278*(46), 45391-45396. doi:10.1074/jbc.M307447200

S. Y. Hess, A. Owais, M. E. D. Jefferds, M. F. Young, A. Cahill, and L. M. Rogers. (2023). Accelerating action to reduce anemia: Review of causes and risk factors and related data needs. *Ann N Y Acad Sci, 1523*(1), 11-23. doi:10.1111/nyas.14985

G. P. Holmes-Hampton, N. D. Jhurry, S. P. McCormick, and P. A. Lindahl. (2013). Iron content of *Saccharomyces cerevisiae* cells grown under iron-deficient and iron-overload conditions. *Biochemistry, 52*(1), 105-114. doi:10.1021/bi3015339

M. I. Hood, and E. P. Skaar. (2012). Nutritional immunity: transition metals at the pathogen-host interface. *Nat Rev Microbiol, 10*(8), 525-537. doi:10.1038/nrmicro2836

G. Huang, P. N. Ulrich, M. Storey, D. Johnson, J. Tischer, J. A. Tovar, . . . R. Docampo. (2014). Proteomic analysis of the acidocalcisome, an organelle conserved from bacteria to human cells. *PLoS Pathog, 10*(12), e1004555-1004572. doi:10.1371/journal.ppat.1004555

C. E. Hughes, T. K. Coody, M. Y. Jeong, J. A. Berg, D. R. Winge, and A. L. Hughes. (2020). Cysteine toxicity drives age-related mitochondrial decline by altering iron homeostasis. *Cell, 180*(2), 296-310. doi:10.1016/j.cell.2019.12.035

C. Jain, R. L. Rodriguez, A. M. Phillippy, K. T. Konstantinidis, and S. Aluru. (2018). High throughput ANI analysis of 90K prokaryotic genomes reveals clear species boundaries. *Nat Commun, 9*(1), 5114-5122. doi:10.1038/s41467-018-07641-9

D. H. Jennings. (1993). *Stress tolerance of Fungi* (Vol. 10). New York, USA: Taylor and Francis Group.

L. T. Jensen, and V. C. Culotta. (2002). Regulation of *Saccharomyces cerevisiae FET4* by oxygen and iron. *J Mol Biol, 318*(2), 251-260. doi:10.1016/S0022-2836(02)00093-1

T. Jorda, and S. Puig. (2020). Regulation of ergosterol biosynthesis in *Saccharomyces cerevisiae*. *Genes (Basel), 11*(7), 795-813. doi:10.3390/genes11070795

S. Kalyaanamoorthy, B. Q. Minh, T. K. F. Wong, A. von Haeseler, and L. S. Jermiin. (2017). ModelFinder: fast model selection for accurate phylogenetic estimates. *Nat Methods, 14*(6), 587-589. doi:10.1038/nmeth.4285

C. D. Kaplan, and J. Kaplan. (2009). Iron acquisition and transcriptional regulation. *Chem Rev, 109*(10), 4536-4552. doi:10.1021/cr9001676

A. Kassambara, and F. Mundt. (2020). Factoextra: Extract and visualize the results of multivariate data analyses. (Version 1.0.7). Retrieved from https://CRAN.R-project.org/package=factoextra (accessed on 20 September 2022).

T. Kato, K. Kumazaki, M. Wada, R. Taniguchi, T. Nakane, K. Yamashita, . . . O. Nureki. (2019). Crystal structure of plant vacuolar iron transporter VIT1. *Nature plants, 5*(3), 308–315. doi:10.1038/s41477-019-0367-2

K. Katoh, and D. M. Standley. (2013). MAFFT multiple sequence alignment software version 7: improvements in performance and usability. *Mol Biol Evol, 30*(4), 772-780. doi:10.1093/molbev/mst010

M. Kearse, R. Moir, A. Wilson, S. Stones-Havas, M. Cheung, S. Sturrock, . . . A. Drummond. (2012). Geneious Basic: an integrated and extendable desktop software platform for the organization and analysis of sequence data. *Bioinformatics, 28*(12), 1647-1649. doi:10.1093/bioinformatics/bts199

N. K. Khandelwal, C. R. Millan, S. I. Zangari, S. Avila, D. Williams, T. M. Thaker, and T. M. Tomasiak. (2022). The structural basis for regulation of the glutathione transporter Ycf1 by regulatory domain phosphorylation. *Nat Commun, 13*(1), 1278-1289. doi:10.1038/s41467-022-28811-w

K. S. Kim, Y. J. Chang, Y. J. Chung, C. U. Park, and H. Y. Seo. (2007). Enhanced expression of high-affinity iron transporters via H-ferritin production in yeast. *J Biochem Mol Biol, 40*(1), 82-87. doi:10.5483/bmbrep.2007.40.1.082

S. A. Kim, T. Punshon, A. Lanzirotti, L. Li, J. M. Alonso, J. R. Ecker, . . . M. L. Guerinot. (2006). Localization of iron in *Arabidopsis* seed requires the vacuolar membrane transporter VIT1. *Science, 314*(5803), 1295-1298. doi:10.1126/science.1132563

N. Kocaefe-Ozsen, B. Yilmaz, C. Alkim, M. Arslan, A. Topaloglu, H. L. B. Kisakesen, . . . Z. P. Cakar. (2022). Physiological and molecular characterization of an oxidative stress-resistant Saccharomyces cerevisiae strain obtained by evolutionary engineering. *Front Microbiol, 13*, 822864-822884. doi:10.3389/fmicb.2022.822864

N. Koleini, J. S. Shapiro, J. Geier, and H. Ardehali. (2021). Ironing out mechanisms of iron homeostasis and disorders of iron deficiency. *J Clin Invest, 131*(11), e148671-148682. doi:10.1172/JCI148671

J. Kominek, D. T. Doering, D. A. Opulente, X. X. Shen, X. Zhou, J. DeVirgilio, . . . C. T. Hittinger. (2019). Eukaryotic acquisition of a bacterial operon. *Cell, 176*(6), 1356-1366. doi:10.1016/j.cell.2019.01.034

D. J. Kosman. (2013). Iron metabolism in aerobes: managing ferric iron hydrolysis and ferrous iron autoxidation. *Coord Chem Rev, 257*(1), 210-217. doi:10.1016/j.ccr.2012.06.030

J. Kramer, O. Ozkaya, and R. Kummerli. (2020). Bacterial siderophores in community and host interactions. *Nat Rev Microbiol, 18*(3), 152-163. doi:10.1038/s41579-019-0284-4

D. J. Krause, J. Kominek, D. A. Opulente, X. X. Shen, X. Zhou, Q. K. Langdon, . . . C. T. Hittinger. (2018). Functional and evolutionary characterization of a secondary metabolite gene cluster in budding yeasts. *Proc Natl Acad Sci U S A, 115*(43), 11030-11035. doi:10.1073/pnas.1806268115

A. Kumanovics, O. S. Chen, L. Li, D. Bagley, E. M. Adkins, H. Lin, . . . J. Kaplan. (2008). Identification of *FRA1* and *FRA2* as genes involved in regulating the yeast iron regulon in response to decreased

mitochondrial iron-sulfur cluster synthesis. *J Biol Chem, 283*(16), 10276-10286. doi:10.1074/jbc.M801160200

T. Kurz, J. W. Eaton, and U. T. Brunk. (2011). The role of lysosomes in iron metabolism and recycling. *Int J Biochem Cell Biol, 43*(12), 1686-1697. doi:10.1016/j.biocel.2011.08.016

V. V. Kushnirov. (2000). Rapid and reliable protein extraction from yeast. *Yeast, 16*(9), 857-860. doi:10.1002/1097-0061(20000630)16:9<857::AID-YEA561>3.0.CO;2-B

M. A. Kyyaly, C. Powell, and E. Ramadan. (2015). Preparation of iron-enriched baker's yeast and its efficiency in recovery of rats from dietary iron deficiency. *Nutrition, 31*(9), 1155-1164. doi:10.1016/j.nut.2015.04.017

S. Labbe, M. G. Khan, and J. F. Jacques. (2013). Iron uptake and regulation in *Schizosaccharomyces pombe*. *Curr Opin Microbiol, 16*(6), 669-676. doi:10.1016/j.mib.2013.07.007

P. J. Lapinskas, S. J. Lin, and V. C. Culotta. (1996). The role of the *Saccharomyces cerevisiae CCC1* gene in the homeostasis of manganese ions. *Mol Microbiol, 21*(3), 519-528. doi:10.1111/j.1365-2958.1996.tb02561.x

G. O. Latunde-Dada, K. Takeuchi, R. J. Simpson, and A. T. McKie. (2006). Haem carrier protein 1 (HCP1): Expression and functional studies in cultured cells. *FEBS Lett, 580*(30), 6865-6870. doi:10.1016/j.febslet.2006.11.048

H. N. Lee, Y. Mostovoy, T. Y. Hsu, A. H. Chang, and R. B. Brem. (2013). Divergence of iron metabolism in wild Malaysian yeast. *G3 (Bethesda), 3*(12), 2187-2194. doi:10.1534/g3.113.008011

T. J. Lee, Y. C. Liu, W. A. Liu, Y. F. Lin, H. H. Lee, H. M. Ke, . . . I. J. Tsai. (2022). Extensive sampling of *Saccharomyces cerevisiae* in Taiwan reveals ecology and evolution of predomesticated lineages. *Genome Res, 32*(5), 864-877. doi:10.1101/gr.276286.121

Y. J. Lee, X. Huang, J. Kropat, A. Henras, S. S. Merchant, R. C. Dickson, and G. F. Chanfreau. (2012). Sphingolipid signaling mediates iron toxicity. *Cell Metab, 16*(1), 90-96. doi:10.1016/j.cmet.2012.06.004

I. Letunic, and P. Bork. (2016). Interactive tree of life (iTOL) v3: an online tool for the display and annotation of phylogenetic and other trees. *Nucleic Acids Res, 44*(1), 242-245. doi:10.1093/nar/gkw290

H. Li, D. T. Mapolelo, N. N. Dingra, S. G. Naik, N. S. Lees, B. M. Hoffman, . . . C. E. Outten. (2009). The yeast iron regulatory proteins Grx3/4 and Fra2 form heterodimeric complexes containing a [2Fe-2S] cluster with cysteinyl and histidyl ligation. *Biochemistry, 48*(40), 9569-9581. doi:10.1021/bi901182w

H. Li, and C. E. Outten. (2019). The conserved CDC motif in the yeast iron regulator Aft2 mediates iron-sulfur cluster exchange and protein-protein interactions with Grx3 and Bol2. *J Biol Inorg Chem, 24*(6), 809-815. doi:10.1007/s00775-019-01705-x

L. Li, D. Bagley, D. M. Ward, and J. Kaplan. (2008). Yap5 is an iron-responsive transcriptional activator that regulates vacuolar iron storage in yeast. *Mol Cell Biol, 28*(4), 1326-1337. doi:10.1128/MCB.01219-07

L. Li, O. S. Chen, D. McVey Ward, and J. Kaplan. (2001). *CCC1* is a transporter that mediates vacuolar iron storage in yeast. *J Biol Chem, 276*(31), 29515-29519. doi:10.1074/jbc.M103944200

L. Li, X. Jia, D. M. Ward, and J. Kaplan. (2011). Yap5 protein-regulated transcription of the *TYW1* gene protects yeast from high iron toxicity. *J Biol Chem, 286*(44), 38488-38497. doi:10.1074/jbc.M111.286666

L. Li, and J. Kaplan. (2004). A mitochondrial-vacuolar signaling pathway in yeast that affects iron and copper metabolism. *J Biol Chem, 279*(32), 33653-33661. doi:10.1074/jbc.M403146200

L. Li, J. Kaplan, and D. M. Ward. (2017). The glucose sensor Snf1 and the transcription factors Msn2 and Msn4 regulate transcription of the vacuolar iron importer gene *CCC1* and iron resistance in yeast. *J Biol Chem, 292*(37), 15577-15586. doi:10.1074/jbc.M117.802504

L. Li, R. Miao, S. Bertram, X. Jia, D. M. Ward, and J. Kaplan. (2012). A role for iron-sulfur clusters in the regulation of transcription factor Yap5-dependent high iron transcriptional responses in yeast. *J Biol Chem, 287*(42), 35709-35721. doi:10.1074/jbc.M112.395533

L. Li, R. Miao, X. Jia, D. M. Ward, and J. Kaplan. (2014). Expression of the yeast cation diffusion facilitators Mmt1 and Mmt2 affects mitochondrial and cellular iron homeostasis: evidence for mitochondrial iron export. *J Biol Chem, 289*(24), 17132-17141. doi:10.1074/jbc.M114.574723

L. Li, G. Murdock, D. Bagley, X. Jia, D. M. Ward, and J. Kaplan. (2010). Genetic dissection of a mitochondria-vacuole signaling pathway in yeast reveals a link between chronic oxidative stress and vacuolar iron transport. *J Biol Chem, 285*(14), 10232-10242. doi:10.1074/jbc.M109.096859

L. Li, and D. M. Ward. (2018). Iron toxicity in yeast: transcriptional regulation of the vacuolar iron importer Ccc1. *Curr Genet, 64*(2), 413-416. doi:10.1007/s00294-017-0767-7

X. C. Li, D. Peris, C. T. Hittinger, E. A. Sia, and J. C. Fay. (2019). Mitochondria-encoded genes contribute to evolution of heat and cold tolerance in yeast. *Sci Adv, 5*(1), 1848-1858. doi:10.1126/sciadv.aav1848

Y. Li, J. L. Steenwyk, Y. Chang, Y. Wang, T. Y. James, J. E. Stajich, . . . A. Rokas. (2021). A genome-scale phylogeny of the kingdom Fungi. *Curr Biol, 31*(8), 1653-1665. doi:10.1016/j.cub.2021.01.074

R. Lill, and S. A. Freibert. (2020). Mechanisms of Mitochondrial Iron-Sulfur Protein Biogenesis. *Annu Rev Biochem, 89*, 471-499. doi:10.1146/annurev-biochem-013118-111540

H. Lin, L. Li, X. Jia, D. M. Ward, and J. Kaplan. (2011). Genetic and biochemical analysis of high iron toxicity in yeast: iron toxicity is due to the accumulation of cytosolic iron and occurs under both aerobic and anaerobic conditions. *J Biol Chem, 286*(5), 3851-3862. doi:10.1074/jbc.M110.190959

S. Liu, L. L. Liao, M. M. Nie, W. T. Peng, M. S. Zhang, J. N. Lei, . . . Z. C. Chen. (2020). A VIT-like transporter facilitates iron transport into nodule symbiosomes for nitrogen fixation in soybean. *New Phytol, 226*(5), 1413-1428. doi:10.1111/nph.16506

N. M. Lowe. (2021). The global challenge of hidden hunger: perspectives from the field. *Proc Nutr Soc, 80*(3), 283-289. doi:10.1017/S0029665121000902

A. N. Luck, and A. B. Mason. (2012). Transferrin-mediated cellular iron delivery. *Curr Top Membr, 69*, 3-35. doi:10.1016/B978-0-12-394390-3.00001-X

B. Mackenzie, M. L. Ujwal, M. H. Chang, M. F. Romero, and M. A. Hediger. (2006). Divalent metal-ion transporter DMT1 mediates both H+ -coupled Fe2+ transport and uncoupled fluxes. *Pflugers Arch, 451*(4), 544-558. doi:10.1007/s00424-005-1494-3

C. A. Martínez-Garay, R. de Llanos, A. M. Romero, M. T. Martínez-Pastor, and S. Puig. (2016). Responses of *Saccharomyces cerevisiae* strains from different origins to elevated iron concentrations. *Appl Environ Microbiol, 82*(6), 1906-1916. doi:10.1128/AEM.03464-15

M. T. Martínez-Pastor, A. Perea-García, and S. Puig. (2017). Mechanisms of iron sensing and regulation in the yeast *Saccharomyces cerevisiae*. *World J Microbiol Biotechnol, 33*(4), 75-84. doi:10.1007/s11274-017-2215-8

M. T. Martínez-Pastor, and S. Puig. (2020). Adaptation to iron deficiency in human pathogenic fungi. *Biochim Biophys Acta Mol Cell Res, 1867*(10), 118797-118811. doi:10.1016/j.bbamcr.2020.118797

L. J. Martins, L. T. Jensen, J. R. Simon, G. L. Keller, and D. R. Winge. (1998). Metalloregulation of *FRE1* and *FRE2* homologs in *Saccharomyces cerevisiae*. *J Biol Chem, 273*(37), 23716-23721. doi:10.1074/jbc.273.37.23716

T. S. Martins, C. Pereira, D. Canadell, R. Vilaça, V. Teixeira, P. Moradas-Ferreira, . . . V. Costa. (2018). The Hog1p kinase regulates Aft1p transcription factor to control iron accumulation. *Biochimica et biophysica acta. Molecular and cell biology of lipids*, 1863(1), 61–70. doi:10.1016/j.bbalip.2017.10.001.

A. Mercier, B. Pelletier, and S. Labbé. (2006). A transcription factor cascade involving Fep1 and the CCAAT-binding factor Php4 regulates gene expression in response to iron deficiency in the fission yeast *Schizosaccharomyces pombe*. *Eukaryot Cell, 5*(11), 1866-1881. doi:10.1128/EC.00199-06

A. Merico, P. Sulo, J. Piskur, and C. Compagno. (2007). Fermentative lifestyle in yeasts belonging to the *Saccharomyces* complex. *FEBS J, 274*(4), 976-989. doi:10.1111/j.1742-4658.2007.05645.x

E. Milgrom, H. Diab, F. Middleton, and P. M. Kane. (2007). Loss of vacuolar proton-translocating ATPase activity in yeast results in chronic oxidative stress. *J Biol Chem, 282*(10), 7125-7136. doi:10.1074/jbc.M608293200

B. Q. Minh, H. A. Schmidt, O. Chernomor, D. Schrempf, M. D. Woodhams, A. von Haeseler, and R. Lanfear. (2020). IQ-TREE 2: New models and efficient methods for phylogenetic inference in the genomic era. *Mol Biol Evol, 37*(5), 1530-1534. doi:10.1093/molbev/msaa015

P. Mkambula, M. N. N. Mbuya, L. A. Rowe, M. Sablah, V. M. Friesen, M. Chadha, . . . J. Gorstein. (2020). The unfinished agenda for food fortification in low- and middle-income countries: Quantifying progress, gaps and potential opportunities. *Nutrients, 12*(2), 354-373. doi:10.3390/nu12020354

K. Momonoi, K. Yoshida, S. Mano, H. Takahashi, C. Nakamori, K. Shoji, . . . M. Nishimura. (2009). A vacuolar iron transporter in tulip, *Tg*Vit1, is responsible for blue coloration in petal cells through iron accumulation. *Plant J, 59*(3), 437-447. doi:10.1111/j.1365-313X.2009.03879.x

D. Moretti, J. S. Goede, C. Zeder, M. Jiskra, V. Chatzinakou, H. Tjalsma, . . . M. B. Zimmermann. (2015). Oral iron supplements increase hepcidin and decrease iron absorption from daily or twice-daily doses in iron-depleted young women. *Blood, 126*(17), 1981-1989. doi:10.1182/blood-2015-05-642223

U. Muhlenhoff, J. A. Stadler, N. Richhardt, A. Seubert, T. Eickhorst, R. J. Schweyen, . . . G. Wiesenberger. (2003). A specific role of the yeast mitochondrial carriers MRS3/4p in mitochondrial iron acquisition under iron-limiting conditions. *J Biol Chem, 278*(42), 40612-40620. doi:10.1074/jbc.M307847200

D. Mumberg, R. Muller, and M. Funk. (1995). Yeast vectors for the controlled expression of heterologous proteins in different genetic backgrounds. *Gene, 156*(1), 119-122. doi:10.1016/0378-1119(95)00037-7

M. K. Nair, L. F. Augustine, and A. Konapur. (2015). Food-based interventions to modify diet quality and diversity to address multiple micronutrient deficiency. *Front Public Health, 3*, 277-291. doi:10.3389/fpubh.2015.00277

N. Narayanan, G. Beyene, R. D. Chauhan, E. Gaitan-Solis, J. Gehan, P. Butts, . . . N. J. Taylor. (2019). Biofortification of field-grown cassava by engineering expression of an iron transporter and ferritin. *Nat Biotechnol, 37*(2), 144-151. doi:10.1038/s41587-018-0002-1

N. Narayanan, G. Beyene, R. D. Chauhan, E. Gaitan-Solis, M. A. Grusak, N. Taylor, and P. Anderson. (2015). Overexpression of *Arabidopsis* VIT1 increases accumulation of iron in cassava roots and stems. *Plant Sci, 240*, 170-181. doi:10.1016/j.plantsci.2015.09.007

C. M. Ngou, A. N. Bayibeki, L. Abate, O. S. Makinde, L. B. Feufack-Donfack, E. M. Sarah-Matio, . . . I. Morlais. (2023). Influence of the sickle cell trait on *Plasmodium falciparum* infectivity from naturally infected gametocyte carriers. *BMC Infect Dis, 23*(1), 317-328. doi:10.1186/s12879-023-08134-x

K. Nishida, and P. A. Silver. (2012). Induction of biogenic magnetization and redox control by a component of the target of rapamycin complex 1 signaling pathway. *PLoS Biol, 10*(2), e1001269-1001279. doi:10.1371/journal.pbio.1001269

K. Nowosad, M. Sujka, U. Pankiewicz, D. Miklavcic, and M. Arczewska. (2021). Pulsed Electric Field (PEF) enhances iron uptake by the yeast *Saccharomyces cerevisiae*. *Biomolecules, 11*(6), 850-869. doi:10.3390/biom11060850

K. F. Ofori, S. Antoniello, M. M. English, and A. N. A. Aryee. (2022). Improving nutrition through biofortification-A systematic review. *Front Nutr, 9*, 1043655-1043675. doi:10.3389/fnut.2022.1043655

R. Olson, B. Gavin-Smith, C. Ferraboschi, and K. Kraemer. (2021). Food fortification: The advantages, disadvantages and lessons from sight and life programs. *Nutrients, 13*(4), 1118-1130. doi:10.3390/nu13041118

J. Ono, D. Greig, and P. J. Boynton. (2020). Defining and disrupting species boundaries in *Saccharomyces. Annu Rev Microbiol, 74*, 477-495. doi:10.1146/annurev-micro-021320-014036

D. A. Opulente, A. Leavitt LaBella, M. C. Harrison, J. F. Wolters, C. Liu, Y. Li, . . . C. T. Hittinger. (2023). Genomic and ecological factors shaping

specialism and generalism across an entire subphylum. *bioRxiv : the preprint server for biology*. doi:10.1101/2023.06.19.545611

D. A. Opulente, E. J. Rollinson, C. Bernick-Roehr, A. B. Hulfachor, A. Rokas, C. P. Kurtzman, and C. T. Hittinger. (2018). Factors driving metabolic diversity in the budding yeast subphylum. *BMC Biol, 16*(1), 26-41. doi:10.1186/s12915-018-0498-3

H. Pa Ho. (1976). Comparison of iron(III) and aluminum in precipitation of phosphate from solution. *Water Research, 10*(10), 903-907. doi:10.1016/0043-1354(76)90026-9

E. Paradis, and K. Schliep. (2019). ape 5.0: an environment for modern phylogenetics and evolutionary analyses in R. *Bioinformatics, 35*(3), 526-528. doi:10.1093/bioinformatics/bty633

J. Park, S. P. McCormick, M. Chakrabarti, and P. A. Lindahl. (2013). The lack of synchronization between iron uptake and cell growth leads to iron overload in *Saccharomyces cerevisiae* during post-exponential growth modes. *Biochemistry, 52*(52), 9413-9425. doi:10.1021/bi4010304

M. Pas, B. Piskur, M. Sustaric, and P. Raspor. (2007). Iron enriched yeast biomass-a promising mineral feed supplement. *Bioresour Technol, 98*(8), 1622-1628. doi:10.1016/j.biortech.2006.06.002

E. Pedro-Segura, S. V. Vergara, S. Rodriguez-Navarro, R. Parker, D. J. Thiele, and S. Puig. (2008). The Cth2 ARE-binding protein recruits the Dhh1 helicase to promote the decay of succinate dehydrogenase *SDH4* mRNA in response to iron deficiency. *J Biol Chem, 283*(42), 28527-28535. doi:10.1074/jbc.M804910200

D. Peris, E. J. Ubbelohde, M. C. Kuang, J. Kominek, Q. K. Langdon, M. Adams, . . . C. T. Hittinger. (2023). Macroevolutionary diversity of traits and genomes in the model yeast genus *Saccharomyces*. *Nat Commun, 14*(1), 690-709. doi:10.1038/s41467-023-36139-2

J. Peter, M. De Chiara, A. Friedrich, J. X. Yue, D. Pflieger, A. Bergstrom, . . . J. Schacherer. (2018). Genome evolution across 1,011 *Saccharomyces cerevisiae* isolates. *Nature, 556*(7701), 339-344. doi:10.1038/s41586-018-0030-5

C. C. Philpott. (2006). Iron uptake in fungi: a system for every source. *Biochimica et biophysica acta, 1763*(7), 636–645. doi:10.1016/j.bbamcr.2006.05.008

C. C. Philpott, and O. Protchenko. (2008). Response to iron deprivation in *Saccharomyces cerevisiae*. *Eukaryot Cell, 7*(1), 20-27. doi:10.1128/EC.00354-07

C. C. Philpott, Y. W. Protchenko O Fau - Kim, Y. Kim Yw Fau - Boretsky, M. Boretsky Y Fau - Shakoury-Elizeh, and M. Shakoury-Elizeh. (2002).

The response to iron deprivation in *Saccharomyces cerevisiae*: expression of siderophore-based systems of iron uptake. *Biochemical Society transactions, 30*(4). doi:10.1042/bst0300698

C. C. Philpott, O. Protchenko, Y. Wang, L. Novoa-Aponte, A. Leon-Torres, S. Grounds, and A. J. Tietgens. (2023). Iron-tracking strategies: Chaperones capture iron in the cytosolic labile iron pool. *Front Mol Biosci, 10*, 1127690-1127703. doi:10.3389/fmolb.2023.1127690

R. B. Piel, 3rd, H. A. Dailey, Jr., and A. E. Medlock. (2019). The mitochondrial heme metabolon: Insights into the complex(ity) of heme synthesis and distribution. *Mol Genet Metab, 128*(3), 198-203. doi:10.1016/j.ymgme.2019.01.006

E. Pierri, D. Tsamouras, and E. Dalas. (2000). Ferric phosphate precipitation in aqueous media. *Journal of Crystal Growth, 213*(1), 93-98. doi:10.1016/S0022-0248(00)00336-5

C. Pimentel, C. Vicente, R. A. Menezes, S. Caetano, L. Carreto, and C. Rodrigues-Pousada. (2012). The role of the Yap5 transcription factor in remodeling gene expression in response to Fe bioavailability. *PLoS One, 7*(5), e37434-37445. doi:10.1371/journal.pone.0037434

T. Pirman, and A. Oresnik. (2012). Fe bioavailability from Fe-enriched yeast biomass in growing rats. *Animal, 6*(2), 221-226. doi:10.1017/S1751731111001546

C. B. Poor, S. V. Wegner, H. Li, A. C. Dlouhy, J. P. Schuermann, R. Sanishvili, . . . C. He. (2014). Molecular mechanism and structure of the *Saccharomyces cerevisiae* iron regulator Aft2. *Proc Natl Acad Sci U S A, 111*(11), 4043-4048. doi:10.1073/pnas.1318869111

J. B. Porter, T. de Witte, M. D. Cappellini, and N. Gattermann. (2016). New insights into transfusion-related iron toxicity: Implications for the oncologist. *Crit Rev Oncol Hematol, 99*, 261-271. doi:10.1016/j.critrevonc.2015.11.017

M. E. Portnoy, X. F. Liu, and V. C. Culotta. (2000). *Saccharomyces cerevisiae* expresses three functionally distinct homologues of the nramp family of metal transporters. *Mol Cell Biol, 20*(21), 7893-7902. doi:10.1128/MCB.20.21.7893-7902.2000

T. L. Poulos. (2014). Heme enzyme structure and function. *Chem Rev, 114*(7), 3919-3962. doi:10.1021/cr400415k

O. Protchenko, and C. C. Philpott. (2003). Regulation of intracellular heme levels by HMX1, a homologue of heme oxygenase, in *Saccharomyces cerevisiae*. *J Biol Chem, 278*(38), 36582-36587. doi:10.1074/jbc.M306584200

M. Prouteau, M. C. Daugeron, and B. Seraphin. (2008). Regulation of ARE transcript 3' end processing by the yeast Cth2 mRNA decay factor. *EMBO J, 27*(22), 2966-2976. doi:10.1038/emboj.2008.212

L. P. Pryszcz, J. Huerta-Cepas, and T. Gabaldon. (2011). MetaPhOrs: orthology and paralogy predictions from multiple phylogenetic evidence using a consistency-based confidence score. *Nucleic Acids Res, 39*(5), 32-40. doi:10.1093/nar/gkq953

S. Puig, E. Askeland, and D. J. Thiele. (2005). Coordinated remodeling of cellular metabolism during iron deficiency through targeted mRNA degradation. *Cell, 120*(1), 99-110. doi:10.1016/j.cell.2004.11.032

S. Puig, L. Ramos-Alonso, A. M. Romero, and M. T. Martinez-Pastor. (2017). The elemental role of iron in DNA synthesis and repair. *Metallomics, 9*(11), 1483-1500. doi:10.1039/c7mt00116a

S. Puig, S. V. Vergara, and D. J. Thiele. (2008). Cooperation of two mRNA-binding proteins drives metabolic adaptation to iron deficiency. *Cell Metab, 7*(6), 555-564. doi:10.1016/j.cmet.2008.04.010

R Core Team. (2021). R: A language and environment for statistical computing. (Version 4.2.0). Vienna, Austria: R Foundation for Statistical Computing. Retrieved from https://www.R-project.org/ (accessed on 20 Setember 2022)

F. Raguzzi, E. Lesuisse, and R. R. Crichton. (1988). Iron storage in *Saccharomyces cerevisiae*. *FEBS Lett, 231*(1), 253-258. doi:10.1016/0014-5793(88)80742-7

L. Ramos-Alonso, A. M. Romero, M. T. Martínez-Pastor, and S. Puig. (2020). Iron regulatory mechanisms in *Saccharomyces cerevisiae*. *Front Microbiol, 11*, 582830-582838. doi:10.3389/fmicb.2020.582830

L. Ramos-Alonso, A. M. Romero, J. Polaina, S. Puig, and M. T. Martínez-Pastor. (2019). Dissecting mRNA decay and translation inhibition during iron deficiency. *Curr Genet, 65*(1), 139-145. doi:10.1007/s00294-018-0880-2

L. Ramos-Alonso, N. Wittmaack, I. Mulet, C. A. Martínez-Garay, J. Fita-Torro, M. J. Lozano, . . . S. Puig. (2018). Molecular strategies to increase yeast iron accumulation and resistance. *Metallomics, 10*(9), 1245-1256. doi:10.1039/c8mt00124c

L. J. Revell. (2012). phytools: an R package for phylogenetic comparative biology (and other things). *Methods in Ecology and Evolution, 3*(2), 217-223. doi:10.1111/j.2041-210X.2011.00169.x

N. Rietzschel, A. J. Pierik, E. Bill, R. Lill, and U. Mühlenhoff. (2015). The basic leucine zipper stress response regulator Yap5 senses high-iron

conditions by coordination of [2Fe-2S] clusters. *Mol Cell Biol, 35*(2), 370-378. doi:10.1128/MCB.01033-14

C. Rodrigues-Pousada, F. Devaux, S. M. Caetano, C. Pimentel, S. da Silva, A. C. Cordeiro, and C. Amaral. (2019). Yeast AP-1 like transcription factors (Yap) and stress response: a current overview. *Microb Cell, 6*(6), 267-285. doi:10.15698/mic2019.06.679

A. M. Romero, M. Martínez-Pastor, G. Du, C. Sole, M. Carlos, S. V. Vergara, . . . S. Puig. (2018). Phosphorylation and proteasome recognition of the mRNA-binding protein Cth2 facilitates yeast adaptation to iron deficiency. *mBio, 9*(5), 01694-01618. doi:10.1128/mBio.01694-18

A. M. Romero, M. T. Martínez-Pastor, and S. Puig. (2021). Iron in translation: From the beginning to the end. *Microorganisms, 9*(5), 1058-1080. doi:10.3390/microorganisms9051058

N. Ruangkiattikul, S. Bhubhanil, J. Chamsing, P. Niamyim, R. Sukchawalit, and S. Mongkolsuk. (2012). *Agrobacterium tumefaciens* membrane-bound ferritin plays a role in protection against hydrogen peroxide toxicity and is negatively regulated by the iron response regulator. *FEMS Microbiol Lett, 329*(1), 87-92. doi:10.1111/j.1574-6968.2012.02509.x

J. C. Rutherford, S. Jaron, E. Ray, P. O. Brown, and D. R. Winge. (2001). A second iron-regulatory system in yeast independent of Aft1p. *Proc Natl Acad Sci U S A, 98*(25), 14322-14327. doi:10.1073/pnas.261381198

J. C. Rutherford, S. Jaron, and D. R. Winge. (2003). Aft1p and Aft2p mediate iron-responsive gene expression in yeast through related promoter elements. *J Biol Chem, 278*(30), 27636-27643. doi:10.1074/jbc.M300076200

M. Sabatier, I. Egli, R. Hurrell, M. Hoppler, C. Gysler, S. Georgeon, . . . C. Schaffer-Lequart. (2017). Iron bioavailability from fresh cheese fortified with iron-enriched yeast. *Eur J Nutr, 56*(4), 1551-1560. doi:10.1007/s00394-016-1200-6

Z. Salvadó, F. N. Arroyo-López, J. M. Guillamón, G. Salazar, A. Querol, and E. Barrio. (2011). Temperature adaptation markedly determines evolution within the genus *Saccharomyces*. *Appl Environ Microbiol, 77*(7), 2292-2302. doi:10.1128/AEM.01861-10

S. Sankari, and M. R. O'Brian. (2014). A bacterial iron exporter for maintenance of iron homeostasis. *J Biol Chem, 289*(23), 16498-16507. doi:10.1074/jbc.M114.571562

S. Sankari, and M. R. O'Brian. (2016). Synthetic lethality of the bfr and mbfA genes reveals a functional relationship between iron storage and iron export in managing stress responses in *Bradyrhizobium japonicum*. *PLoS One, 11*(6), 0157250-0157265. doi:10.1371/journal.pone.0157250

N. Sanvinsens, and S. Puig. (2011). Causes and consequences of nutritional iron deficiency in living organisms. . In H. D. Perkins (Ed.), *Biology of Starvation in Humans and Other Organisms.* (pp. 1-30). New York, USA: Nova Science Publishers, Inc.

N. Sanvisens, A. M. Romero, X. An, C. Zhang, R. de Llanos, M. T. Martínez-Pastor, . . . S. Puig. (2014). Yeast Dun1 kinase regulates ribonucleotide reductase inhibitor Sml1 in response to iron deficiency. *Mol Cell Biol, 34*(17), 3259-3271. doi:10.1128/MCB.00472-14

J. Schothorst, G. V. Zeebroeck, and J. M. Thevelein. (2017). Identification of Ftr1 and Zrt1 as iron and zinc micronutrient transceptors for activation of the PKA pathway in *Saccharomyces cerevisiae*. *Microb Cell, 4*(3), 74-89. doi:10.15698/mic2017.03.561

M. Schrettl, N. Beckmann, J. Varga, T. Heinekamp, I. D. Jacobsen, C. Jöchl, . . . H. Haas. (2010). HapX-mediated adaption to iron starvation is crucial for virulence of *Aspergillus fumigatus*. *PLoS Pathog, 6*(9), e1001124-1001136. doi:10.1371/journal.ppat.1001124

M. Schrettl, E. Bignell, C. Kragl, Y. Sabiha, O. Loss, M. Eisendle, . . . H. Haas. (2007). Distinct roles for intra- and extracellular siderophores during Aspergillus fumigatus infection. *PLoS Pathog, 3*(9), 1195-1207. doi:10.1371/journal.ppat.0030128

I. Schroder, E. Johnson, and S. de Vries. (2003). Microbial ferric iron reductases. *FEMS Microbiol Rev, 27*(2-3), 427-447. doi:10.1016/S0168-6445(03)00043-3

A. Sfera, K. Bullock, A. Price, L. Inderias, and C. Osorio. (2018). Ferrosenescence: The iron age of neurodegeneration? *Mech Ageing Dev, 174*, 63-75. doi:10.1016/j.mad.2017.11.012

M. Shakoury-Elizeh, J. Tiedeman, J. Rashford, T. Ferea, J. Demeter, E. García, . . . C. C. Philpott. (2004). Transcriptional remodeling in response to iron deprivation in *Saccharomyces cerevisiae*. *Mol Biol Cell, 15*(3), 1233-1243. doi:10.1091/mbc.e03-09-0642

S. S. Sharma, K. J. Dietz, and T. Mimura. (2016). Vacuolar compartmentalization as indispensable component of heavy metal detoxification in plants. *Plant Cell Environ, 39*(5), 1112-1126. doi:10.1111/pce.12706

X. X. Shen, J. L. Steenwyk, A. L. LaBella, D. A. Opulente, X. Zhou, J. Kominek, . . . A. Rokas. (2020). Genome-scale phylogeny and contrasting modes of genome evolution in the fungal phylum Ascomycota. *Sci Adv, 6*(45), 79-91. doi:10.1126/sciadv.abd0079

A. Singh, N. Kaur, and D. J. Kosman. (2007). The metalloreductase Fre6p in Fe-efflux from the yeast vacuole. *J Biol Chem, 282*(39), 28619-28626. doi:10.1074/jbc.M703398200

R. P. Singh, H. K. Prasad, I. Sinha, N. Agarwal, and K. Natarajan. (2011). Cap2-HAP complex is a critical transcriptional regulator that has dual but contrasting roles in regulation of iron homeostasis in *Candida albicans*. *J Biol Chem, 286*(28), 25154-25170. doi:10.1074/jbc.M111.233569

K. Slavic, S. Krishna, A. Lahree, G. Bouyer, K. K. Hanson, I. Vera, . . . M. M. Mota. (2016). A vacuolar iron-transporter homologue acts as a detoxifier in Plasmodium. *Nat Commun, 7*(10403), 1-10. doi:10.1038/ncomms10403

S. P. Solow, J. Sengbusch, and M. W. Laird. (2005). Heterologous protein production from the inducible *MET25* promoter in *Saccharomyces cerevisiae*. *Biotechnol Prog, 21*(2), 617-620. doi:10.1021/bp049916q

R. Sorribes-Dauden, T. Jordá, D. Peris, M. T. Martínez-Pastor, and S. Puig. (2022). Adaptation of *Saccharomyces* species to high-iron conditions. *Int J Mol Sci, 23*(22), 13965-13985. doi:10.3390/ijms232213965

R. Sorribes-Dauden, M. T. Martínez-Pastor, and S. Puig. (2021). Expression of a truncated yeast Ccc1 vacuolar transporter increases the accumulation of endogenous iron. *Genes (Basel), 18*, 3712–3722. doi:10.3390/genes12081120

R. Sorribes-Dauden, D. Peris, M. T. Martínez-Pastor, and S. Puig. (2020). Structure and function of the vacuolar Ccc1/VIT1 family of iron transporters and its regulation in fungi. *Comput Struct Biotechnol J, 18*, 3712-3722. doi:10.1016/j.csbj.2020.10.044

W. J. Spurley, K. J. Fisher, Q. K. Langdon, K. V. Buh, M. Jarzyna, M. A. B. Haase, . . . C. T. Hittinger. (2022). Substrate, temperature, and geographical patterns among nearly 2000 natural yeast isolates. *Yeast, 39*(1-2), 55-68. doi:10.1002/yea.3679

J. L. Steenwyk, T. J. Buida, 3rd, Y. Li, X. X. Shen, and A. Rokas. (2020). ClipKIT: A multiple sequence alignment trimming software for accurate phylogenomic inference. *PLoS Biol, 18*(12), e3001007-3001024. doi:10.1371/journal.pbio.3001007

A. Stefansson. (2007). Iron (III) hydrolysis and solubility at 25 ºC. *Environ Sci Technol, 41*(17), 6117-6123. doi:10.1021/es070174h

G. Stelitano, M. Cocorullo, M. Mori, S. Villa, F. Meneghetti, and L. R. Chiarelli. (2023). Iron acquisition and metabolism as a promising target for antimicrobials (Bottlenecks and opportunities): Where do we stand? *Int J Mol Sci, 24*(7), 6181-6200. doi:10.3390/ijms24076181

G. L. Sun, E. E. Reynolds, and A. M. Belcher. (2019). Designing yeast as plant-like hyperaccumulators for heavy metals. *Nat Commun, 10*(1), 5080-5092. doi:10.1038/s41467-019-13093-6

J. Sun, S. Xu, Y. Du, K. Yu, Y. Jiang, H. Weng, and W. Yuan. (2022). Accumulation and enrichment of trace elements by yeast cells and their applications: A critical review. *Microorganisms, 10*(9). doi:10.3390/microorganisms10091746

D. L. Swaney, P. Beltrao, L. Starita, A. Guo, J. Rush, S. Fields, . . . J. Villen. (2013). Global analysis of phosphorylation and ubiquitylation cross-talk in protein degradation. *Nat Methods, 10*(7), 676-682. doi:10.1038/nmeth.2519

J. Tamarit, V. Irazusta, A. Moreno-Cermeno, and J. Ros. (2006). Colorimetric assay for the quantitation of iron in yeast. *Anal Biochem, 351*(1), 149-151. doi:10.1016/j.ab.2005.12.001

K. Tamura, D. Peterson, N. Peterson, G. Stecher, M. Nei, and S. Kumar. (2011). MEGA5: molecular evolutionary genetics analysis using maximum likelihood, evolutionary distance, and maximum parsimony methods. *Mol Biol Evol, 28*(10), 2731-2739. doi:10.1093/molbev/msr121

Y. Tang, M. Horikoshi, and W. Li. (2016). ggfortify: Unified interface to visualize statistical results of popular R packages. *The R Journal, 8*, 474-485. doi:10.32614/RJ-2016-060

R. Taniguchi, H. E. Kato, J. Font, C. N. Deshpande, M. Wada, K. Ito, . . . O. Nureki. (2015). Outward- and inward-facing structures of a putative bacterial transition-metal transporter with homology to ferroportin. *Nat Commun, 6*, 8545-8555. doi:10.1038/ncomms9545

A. Thiébaut, T. Delaveau, M. Benchouaia, J. Boeri, M. Garcia, G. Lelandais, and F. Devaux. (2017). The CCAAT-binding complex controls respiratory gene expression and iron homeostasis in *Candida Glabrata*. *Sci Rep, 7*(1), 3531-3541. doi:10.1038/s41598-017-03750-5

M. J. Thompson, W. S. Lai, G. A. Taylor, and P. J. Blackshear. (1996). Cloning and characterization of two yeast genes encoding members of the CCCH class of zinc finger proteins: zinc finger-mediated impairment of cell growth. *Gene, 174*(2), 225-233. doi:10.1016/0378-1119(96)00084-4

Y. Tian, Y. Tian, Z. Yuan, Y. Zeng, S. Wang, X. Fan, . . . M. Yang. (2022). Iron metabolism in aging and age-related diseases. *Int J Mol Sci, 23*(7), 3612-3633. doi:10.3390/ijms23073612

T. Tsuji, K. Kanai, A. Yokoyama, T. Tamura, K. Hanamure, K. Sasaki, . . . S. Yoshida. (2012). Novel method to reduce fishy aftertaste in wine and seafood pairing using alcohol-treated yeast cells. *J Agric Food Chem, 60*(24), 6197-6203. doi:10.1021/jf300265x

R. Ueta, N. Fujiwara, K. Iwai, and Y. Yamaguchi-Iwai. (2012). Iron-induced dissociation of the Aft1p transcriptional regulator from target gene promoters is an initial event in iron-dependent gene suppression. *Mol Cell Biol, 32*(24), 4998-5008. doi:10.1128/MCB.00726-12

R. Ueta, A. Fukunaka, and Y. Yamaguchi-Iwai. (2003). Pse1p mediates the nuclear import of the iron-responsive transcription factor Aft1p in *Saccharomyces cerevisiae*. *J Biol Chem, 278*(50), 50120-50127. doi:10.1074/jbc.M305046200

J. L. Urbanowski, and R. C. Piper. (1999). The iron transporter Fth1p forms a complex with the Fet5 iron oxidase and resides on the vacuolar membrane. *The Journal of Biochemical Chemistry, 274*(53), 38061–38070. doi:10.1074/jbc.274.53.38061

S. V. Vergara, S. Puig, and D. J. Thiele. (2011). Early recruitment of AU-rich element-containing mRNAs determines their cytosolic fate during iron deficiency. *Mol Cell Biol, 31*(3), 417-429. doi:10.1128/MCB.00754-10

S. von Haehling, N. Ebner, R. Evertz, P. Ponikowski, and S. D. Anker. (2019). Iron deficiency in heart failure: An overview. *JACC Heart Fail, 7*(1), 36-46. doi:10.1016/j.jchf.2018.07.015

J. Wade, D. J. Byrne, C. J. Ballentine, and H. Drakesmith. (2021). Temporal variation of planetary iron as a driver of evolution. *Proc Natl Acad Sci U S A, 118*(51), 2109865118-2109865126. doi:10.1073/pnas.2109865118

J. H. Walton, G. Kontra-Kovats, R. T. Green, A. Domonkos, B. Horvath, E. M. Brear, . . . J. Balk. (2020). The *Medicago truncatula* Vacuolar Iron Transporter-Like proteins VTL4 and VTL8 deliver iron to symbiotic bacteria at different stages of the infection process. *New Phytol, 228*(2), 651-666. doi:10.1111/nph.16735

L. G. Wang, T. T. Lam, S. Xu, Z. Dai, L. Zhou, T. Feng, . . . G. Yu. (2020). Treeio: An R package for phylogenetic tree input and output with Richly annotated and associated data. *Mol Biol Evol, 37*(2), 599-603. doi:10.1093/molbev/msz240

T. P. Wang, L. Quintanar, S. Severance, E. I. Solomon, and D. J. Kosman. (2003). Targeted suppression of the ferroxidase and iron trafficking activities of the multicopper oxidase Fet3p from *Saccharomyces cerevisiae*. *J Biol Inorg Chem, 8*(6), 611-620. doi:10.1007/s00775-003-0456-5

B. M. Waters, and D. J. Eide. (2002). Combinatorial control of yeast FET4 gene expression by iron, zinc, and oxygen. *J Biol Chem, 277*(37), 33749-33757. doi:10.1074/jbc.M206214200

J. Weiner, and T. W. Kooij. (2016). Phylogenetic profiles of all membrane transport proteins of the malaria parasite highlight new drug targets. *Microb Cell, 3*(10), 511-521. doi:10.15698/mic2016.10.534

H. Wickham. (2016). ggplot2: Elegant graphics for data analysis (Version 3.3.3). New York (USA): Springer-Verlag New York. Retrieved from https://ggplot2.tidyverse.org (accessed on 20 September 2022)

N. Wilkinson, and K. Pantopoulos. (2014). The IRP/IRE system in vivo: insights from mouse models. *Front Pharmacol, 5*, 176-191. doi:10.3389/fphar.2014.00176

T. A. Williams, C. J. Cox, P. G. Foster, G. J. Szollosi, and T. M. Embley. (2020). Phylogenomics provides robust support for a two-domains tree of life. *Nat Ecol Evol, 4*(11), 138–147. doi:10.1038/s41559-020-01347-2

C. C. Winterbourn. (1995). Toxicity of iron and hydrogen peroxide: the Fenton reaction. *Toxicology Letters, 82-83*, 969-974. doi:10.1016/0378-4274(95)03532-X

N. Xu, X. Cheng, Q. Yu, B. Zhang, X. Ding, L. Xing, and M. Li. (2012). Identification and functional characterization of mitochondrial carrier Mrs4 in Candida albicans. *FEMS Yeast Res, 12*(7), 844-858. doi:10.1111/j.1567-1364.2012.00835.x

N. Xu, Y. Dong, X. Cheng, Q. Yu, K. Qian, J. Mao, . . . M. Li. (2014). Cellular iron homeostasis mediated by the Mrs4-Ccc1-Smf3 pathway is essential for mitochondrial function, morphogenesis and virulence in *Candida albicans*. *Biochim Biophys Acta, 1843*(3), 629-639. doi:10.1016/j.bbamcr.2013.12.009

Y. Yamaguchi-Iwai, A. Dancis, and R. D. Klausner. (1995). *AFT1*: a mediator of iron regulated transcriptional control in *Saccharomyces cerevisiae*. *EMBO J, 14*(6), 1231-1239. doi:10.1002/j.1460-2075.1995.tb07106.x

M. Yang, P. A. Cobine, S. Molik, A. Naranuntarat, R. Lill, D. R. Winge, and V. C. Culotta. (2006). The effects of mitochondrial iron homeostasis on cofactor specificity of superoxide dismutase 2. *EMBO J, 25*(8), 1775-1783. doi:10.1038/sj.emboj.7601064

Z. Yang. (2007). PAML 4: phylogenetic analysis by maximum likelihood. *Mol Biol Evol, 24*(8), 1586-1591. doi:10.1093/molbev/msm088

G. Yu, D. K. Smith, H. Zhu, Y. Guan, T. T. Y. Lam, and G. McInerny. (2016). ggtree: an r package for visualization and annotation of phylogenetic trees with their covariates and other associated data. *Methods in Ecology and Evolution, 8*(1), 28-36. doi:10.1111/2041-210x.12628

J. X. Yue, J. Li, L. Aigrain, J. Hallin, K. Persson, K. Oliver, . . . G. Liti. (2017). Contrasting evolutionary genome dynamics between domesticated and wild yeasts. *Nat Genet, 49*(6), 913-924. doi:10.1038/ng.3847

C. W. Yun, M. Bauler, R. E. Moore, P. E. Klebba, and C. C. Philpott. (2001). The role of the FRE family of plasma membrane reductases in the uptake of siderophore-iron in *Saccharomyces cerevisiae*. *J Biol Chem, 276*(13), 10218-10223. doi:10.1074/jbc.M010065200

R. Zhang, J. Chen, S. Wang, W. Zhang, Q. Zheng, and R. Cai. (2023). Ferroptosis in Cancer Progression. *Cells, 12*(14), 1820-1834. doi:10.3390/cells12141820

Y. Zhang, Y. H. Xu, H. Y. Yi, and J. M. Gong. (2012). Vacuolar membrane transporters OsVIT1 and OsVIT2 modulate iron translocation between flag leaves and seeds in rice. *Plant J, 72*(3), 400-410. doi:10.1111/j.1365-313X.2012.05088.x

P. Zhou. (2004). Determining protein half-lives. In R. C. Dickson, Mendenhall, M.D. (Ed.), *Signal Transduction Protocols. Methods in Molecular Biology* (Vol. 284, pp. 67–77). Clifton, N.J: Humana Press.

M. B. Zimmermann. (2020). Global look at nutritional and functional iron deficiency in infancy. *Hematology Am Soc Hematol Educ Program, 2020*(1), 471-477. doi:10.1182/hematology.2020000131

M. B. Zimmermann, and R. F. Hurrell. (2007). Nutritional iron deficiency. *Lancet, 370*(9586), 511-520. doi:10.1016/S0140-6736(07)61235-5

ANNEX 1: PUBLICATIONS

Computational and Structural Biotechnology Journal 18 (2020) 3712–3722

ELSEVIER

COMPUTATIONAL AND STRUCTURAL BIOTECHNOLOGY JOURNAL

journal homepage: www.elsevier.com/locate/csbj

Structure and function of the vacuolar Ccc1/VIT1 family of iron transporters and its regulation in fungi

Raquel Sorribes-Dauden [a], David Peris [b,1], María Teresa Martínez-Pastor [a], Sergi Puig [b,*]

[a] Departamento de Bioquímica y Biología Molecular, Universitat de València, Burjassot, Valencia, Spain
[b] Departamento de Biotecnología, Instituto de Agroquímica y Tecnología de Alimentos (IATA), Consejo Superior de Investigaciones Científicas (CSIC), Paterna, Valencia, Spain

ARTICLE INFO

Article history:
Received 10 September 2020
Received in revised form 28 October 2020
Accepted 31 October 2020
Available online 23 November 2020

Keywords:
Iron detoxification
Iron regulation
Iron transport
Yeast
Fungi
Plants
Vacuole
Ccc1
VIT1

ABSTRACT

Iron is an essential micronutrient for most living beings since it participates as a redox active cofactor in many biological processes including cellular respiration, lipid biosynthesis, DNA replication and repair, and ribosome biogenesis and recycling. However, when present in excess, iron can participate in Fenton reactions and generate reactive oxygen species that damage cells at the level of proteins, lipids and nucleic acids. Organisms have developed different molecular strategies to protect themselves against the harmful effects of high concentrations of iron. In the case of fungi and plants, detoxification mainly occurs by importing cytosolic iron into the vacuole through the Ccc1/VIT1 iron transporter. New sequenced genomes and bioinformatic tools are facilitating the functional characterization, evolution and ecological relevance of metabolic pathways and homeostatic networks across the Tree of Life. Sequence analysis shows that Ccc1/VIT1 homologs are widely distributed among organisms with the exception of animals. The recent elucidation of the crystal structure of a Ccc1/VIT1 plant ortholog has enabled the identification of both conserved and species-specific motifs required for its metal transport mechanism. Moreover, recent studies in the yeast *Saccharomyces cerevisiae* have also revealed that multiple transcription factors including Yap5 and Msn2/Msn4 contribute to the expression of *CCC1* in high-iron conditions. Interestingly, Malaysian *S. cerevisiae* strains express a partially functional Ccc1 protein that renders them sensitive to iron. Different regulatory mechanisms have been described for non-Saccharomycetaceae Ccc1 homologs. The characterization of Ccc1/VIT1 proteins is of high interest in the development of biofortified crops and the protection against microbial-derived diseases.

Contents

Abbreviations: BLOSUM, BLOcks SUbstitution Matrix; bZIP, basic leucine-zipper; CBC, CCAAT-binding core complex; *Cg*, *Candida glabrata*; CRD, Cysteine-rich domain; CS, Consistency score; *Eg*, *Eucalyptus grandis*; Fe, Iron; H, Helix; Hap, Heme activator protein; ISC, Iron-sulfur luster; MAFFT, Multiple Alignment using Fast Fourier Transform; MBD, Metal-binding domain; ML, Maximum-likelihood; NRAMP, Natural Resistance-Associated Macrophage Protein; ROS, Reactive oxygen species; TMD, Transmembrane domain; VIT, Vacuolar iron transporter; VTL, Vacuolar iron transporter-like; YRE, Yap response elements.

* Corresponding author at: Dept. Biotecnología, IATA-CSIC, Agustín Escardino 7, 46980, Paterna, Valencia, Spain.
E-mail address: spuig@iata.csic.es (S. Puig).
[1] Present address: Department of Biosciences, University of Oslo, Oslo, Norway.

https://doi.org/10.1016/j.csbj.2020.10.044

genes

MDPI

Article

Expression of a Truncated Yeast Ccc1 Vacuolar Transporter Increases the Accumulation of Endogenous Iron

Raquel Sorribes-Dauden [1], María Teresa Martínez-Pastor [1,*] and Sergi Puig [2,*]

[1] Departamento de Bioquímica y Biología Molecular, Universitat de València, Doctor Moliner 50, 46100 Burjassot, Valencia, Spain; Raquel.Sorribes@uv.es
[2] Departamento de Biotecnología, Instituto de Agroquímica y Tecnología de Alimentos (IATA), Consejo Superior de Investigaciones Científicas (CSIC), Agustín Escardino 7, 46980 Paterna, Valencia, Spain
* Correspondence: maria.teresa.martinez@uv.es (M.T.M.-P.); spuig@iata.csic.es (S.P.)

Abstract: Iron is an essential micronutrient for all eukaryotic organisms because it participates as a redox cofactor in multiple metabolic processes. Iron bioavailability is highly restricted due to the low solubility of its oxidized form, frequently leading to iron deficiency anemia. The baker's yeast *Saccharomyces cerevisiae* is used as a model organism for iron homeostasis studies, but also as a food supplement and fermentative microorganism in the food industry. Yeast cells use the vacuolar Ccc1 transporter to detoxify and store excess iron in the vacuoles. Here, we modulate *CCC1* expression and properties to increase iron extraction from the environment. We show that constitutive expression of full-length *CCC1* is toxic, whereas deletion of its cytosolic amino-terminal (Nt) domain (*NtΔCCC1*) rescues this phenotype. Toxicity is exacerbated in cells lacking *AFT1* transcription factor. Further characterization of NtΔCcc1 protein suggests that it is a partially functional protein. Western blot analyses indicate that deletion of Ccc1 Nt domain does not significantly alter GFP-Ccc1 protein stability. A functional full-length GFP-Ccc1 protein localized to particular regions of the vacuolar membrane, whereas GFP-NtΔCcc1 protein was evenly distributed throughout this endogenous membrane. Interestingly, expression of *NtΔCCC1* increased the accumulation of endogenous iron in cells cultivated under iron-sufficient conditions, a strategy that could be used to extract iron from media that are not rich in iron.

Keywords: yeast; *Saccharomyces cerevisiae*; iron; Ccc1

Citation: Sorribes-Dauden, R.; Martínez-Pastor, M.T.; Puig, S. Expression of a Truncated Yeast Ccc1 Vacuolar Transporter Increases the Accumulation of Endogenous Iron. *Genes* **2021**, *12*, 1120. https://doi.org/10.3390/genes12081120

Academic Editor: Paweł Lipiński

Received: 7 June 2021
Accepted: 15 July 2021
Published: 23 July 2021

1. Introduction

Iron is an essential micronutrient for all eukaryotic organisms. Its redox and coordination properties allow iron to participate as a cofactor in a wide range of metabolic processes including the synthesis of DNA, proteins, and lipids, mitochondrial respiration and photosynthesis, and oxygen transport. Despite being one of the most abundant elements in the Earth's crust, iron bioavailability is extremely restricted in aerobic environments as it is mostly present in its oxidized from (Fe^{3+}), which is highly insoluble at physiological pH. According to the World Health Organization, iron deficiency anemia (IDA) is one of the most prevalent human nutritional disorders (even present in developed countries) with high impact and potentially fatal health consequences in children, women of fertile age, pregnant women, and the elderly (reviewed in [1,2]). Consequences of IDA include diminished learning ability and poor physical growth of infants, fatigue and reduced work productivity in adults, greater susceptibility to infections, and increased risk of death associated with pregnancy and childbirth. Multiple strategies are used to prevent and treat IDA including diversification of the diet and supplementation or food fortification with particular iron forms (reviewed in [3]).

The baker's yeast *Saccharomyces cerevisiae* contributed significantly to the identification and characterization of many components of the human, plant, and fungal iron homeostatic networks. Moreover, this yeast is used in multiple biotechnological applications including

International Journal of
Molecular Sciences

MDPI

Article

Adaptation of *Saccharomyces* Species to High-Iron Conditions

Raquel Sorribes-Dauden [1,2], Tania Jordá [2], David Peris [2,3], María Teresa Martínez-Pastor [1,*] and Sergi Puig [2,*]

[1] Departamento de Bioquímica y Biología Molecular, Universitat de València, Doctor Moliner 50, 46100 Burjassot, Spain
[2] Departamento de Biotecnología, Instituto de Agroquímica y Tecnología de Alimentos (IATA), Consejo Superior de Investigaciones Científicas (CSIC), Agustín Escardino 7, 46980 Paterna, Spain
[3] Section for Genetics and Evolutionary Biology, Department of Biosciences, University of Oslo, Blindernveien 31, 0371 Oslo, Norway
* Correspondence: maria.teresa.martinez@uv.es (M.T.M.-P.); spuig@iata.csic.es (S.P.)

Abstract: Iron is an indispensable element that participates as an essential cofactor in multiple biological processes. However, when present in excess, iron can engage in redox reactions that generate reactive oxygen species that damage cells at multiple levels. In this report, we characterized the response of budding yeast species from the *Saccharomyces* genus to elevated environmental iron concentrations. We have observed that *S. cerevisiae* strains are more resistant to high-iron concentrations than *Saccharomyces* non-*cerevisiae* species. Liquid growth assays showed that species evolutionarily closer to *S. cerevisiae*, such as *S. paradoxus*, *S. jurei*, *S. mikatae*, and *S. arboricola*, were more resistant to high-iron levels than the more distant species *S. eubayanus* and *S. uvarum*. Remarkably, *S. kudriavzevii* strains were especially iron sensitive. Growth assays in solid media suggested that *S. cerevisiae* and *S. paradoxus* were more resistant to the oxidative stress caused by elevated iron concentrations. When comparing iron accumulation and sensitivity, different patterns were observed. As previously described for *S. cerevisiae*, *S. uvarum* and particular strains of *S. kudriavzevii* and *S. paradoxus* became more sensitive to iron while accumulating more intracellular iron levels. However, no remarkable changes in intracellular iron accumulation were observed for the remainder of species. These results indicate that different mechanisms of response to elevated iron concentrations exist in the different species of the genus *Saccharomyces*.

Keywords: iron toxicity; yeast; *Saccharomyces* genus; adaptation; evolution; *CCC1*; oxidative stress; biodiversity

Citation: Sorribes-Dauden, R.; Jordá, T.; Peris, D.; Martínez-Pastor, M.T.; Puig, S. Adaptation of *Saccharomyces* Species to High-Iron Conditions. *Int. J. Mol. Sci.* **2022**, *23*, 13965. https://doi.org/10.3390/ijms232213965

Academic Editor: Joaquin Arino

Received: 7 October 2022
Accepted: 9 November 2022
Published: 12 November 2022

1. Introduction

Iron is a necessary redox cofactor for many key biological processes, like DNA replication and repair, amino acid and protein biosynthesis, lipid metabolism and cellular respiration (reviewed in References [1–3]). Despite being especially abundant in the Earth's crust, in oxidative environments, iron easily switches from Fe^{2+} to Fe^{3+}, with solubility and bioavailability that are remarkably low at physiological pH. Thus, in humans, iron scarcity often leads to iron deficiency anemia, which causes fatigue and impairs cognitive development and immunity. Iron limitation is also an agronomic problem since low iron availability decreases crop yield and quality (reviewed in Reference [4]). Moreover, competition for iron between microbial pathogens and their hosts modulates both their virulence and the host's capacity of response (reviewed in Reference [5]). Thus, organisms have developed different mechanisms to overcome iron shortage. In the yeast *Saccharomyces cerevisiae*, in response to iron deficiency, the transcriptional factors Aft1 and Aft2 activate a group of genes known as the iron regulon. These genes codify proteins that are involved in iron acquisition through iron-reductive uptake or the capture of siderophores, mobilization from intracellular reservoirs, such as the vacuole, recycling, and metabolism remodeling in order to optimize the use of the scarce iron (reviewed in Reference [6]). However, iron